

INVESTIGATIONS ON AURONES AS MODULATORS OF  
ABCG2

SIM HONG MAY

*(B. Sc. (Pharmacy) (Hons.), NUS)*

A THESIS SUBMITTED

FOR THE DEGREE OF DOCTOR OF PHILOSOPHY

DEPARTMENT OF PHARMACY

NATIONAL UNIVERSITY OF SINGAPORE

2010

## **Acknowledgements**

First and foremost, I would like to express my heartfelt gratitude to my supervisor Assoc. Prof. Go Mei Lin for her unwavering support and encouragement throughout the whole course of my research. This piece of thesis work would not be possible without her advice and insights into the research topic.

I would also like to thank Dr Rachel Ee Pui Lai for her advice in my research and the offer of cell lines (MDA-MB-231/V and R) as well as the opportunity to carry out biological assays (Western Blotting) in her laboratory in the Department of Pharmacy.

Special thanks to my senior, Dr Lee Chong Yew for the contribution of his auronones to my research work as well as the constant help in bench work and the encouragement rendered especially in the early years of my graduate studies.

Many thanks to the past and present members of the Medicinal Chemistry Laboratory at the Department of Pharmacy for their camaraderie and sharing of knowledge and research experiences: Dr. Liu Xiao Ling, Dr. Suresh Kumar Gorla, Dr Zhang Wei, Dr Leow Jolene, Mr Yeo Wee Kiang, Ms Nguyen Thi Hanh Thuy, Mr Wee Xi Kai, Mr Pondy Murgappan Ramanujulu, Dr Yang Tian Ming, Ms Tan Kheng Lin and Ms Chen Xiao. Appreciation also goes out to the past research assistants and final year students: Ms Tee Hui Wearn, Ms Audrey Chan Xie Wah, and Ms Loh Ker Yun for their help in my project. I would also like to thank Dr Han Yi, Dr Tian Quan, Ms Leow Pay Chin and Ms Ong Zhan Yuin from Dr Rachel Ee's laboratory for their advice and assistance in biological work.

Appreciation goes to Mdm Oh Tang Booy, Ms. Ng Sek Eng and the rest of the technical staff at the Department of Pharmacy. Research is made easier with their help in the purchasing of chemicals/biologicals and trouble-shooting of machines.

I would like to acknowledge the financial support for my graduate studies from the National University of Singapore Research Scholarship.

Last but not least, I would like to thank my parents and family for their constant support, understanding and concern throughout the course of my graduate studies.

## **Conferences and Publications**

- 1) Hong-May Sim, Pui-Lai Rachel Ee and Mei-Lin Go, 4, 6-Dimethoxyaurones as Dual Modulators of P-glycoprotein (P-gp) and Breast Cancer Resistance Protein (BCRP), European School of Medicinal Chemistry (ESMEC), 6<sup>th</sup> to 11<sup>th</sup> July 2008, Urbino, Italy.
- 2) Hong-May Sim and Mei-Lin Go, Structurally Modified Aurones as Inhibitors of the ATP Binding Cassette Transport Protein ABCG2 (Breast Cancer Resistance Protein), 10<sup>th</sup> Asia Pacific Rim Universities Doctoral Students Conference (APRU DSC), 6<sup>th</sup> to 10<sup>th</sup> July 2009, Kyoto, Japan.
- 3) Hong-May Sim and Mei-Lin Go, Structurally Modified Aurones: Inhibitors of the ATP Binding Cassette Transport Proteins Breast Cancer Resistance Protein (ABCG2) and P-glycoprotein (ABCB1), 7<sup>th</sup> International Symposium for Chinese Medicinal Chemists (ISCMC), 1<sup>st</sup> to 5<sup>th</sup> Feb 2010, Kaoshiung, Taiwan.
- 4) Sim. H.M., Lee, C.Y., Ee, P.L.R., Go, M.L., Dimethoxyaurones: Potent inhibitors of ABCG2 (breast cancer resistance protein) *European Journal of Pharmaceutical Sciences*, **2008**, 293-306.

## **Manuscripts in preparation:**

- 1) Sim. H.M., Lee, C.Y., Yeo, W.K., Loh, K.Y., Ee, P.L.R., Go, M.L., Structurally modified aurones as modulators of ABCG2: Structure-activity relationships and pharmacophore modeling.
- 2) Sim. H.M., Wu. C.P., Ee, P.L.R., Ambudkar. S., Go, M.L., *In vitro* and *in vivo* evaluations of structurally modified aurones as modulators of ABCG2

## Table of Contents

Acknowledgements.....	ii
Conferences and Publications.....	iv
Table of contents.....	v
Summary.....	vi
List of Tables.....	viii
List of Figures.....	x
List of Schemes.....	xv
List of Abbreviations.....	xvi
<b>Chapter 1: Introduction.....</b>	<b>1</b>
1.1. Multidrug resistance (MDR) and ATP-Binding Cassette (ABC) transporters.....	1
1.2. Structural features of ABCB1 and ABCG2.....	2
1.3. Functions of ABCB1 and ABCG2.....	4
1.4. Substrates and Inhibitors of ABCB1 and ABCG2.....	6
1.5. Flavonoids as MDR reversal agents.....	12
1.6. Aurones as modulators of ABC transporter proteins.....	16
1.7. Statement of Purpose.....	18
<b>Chapter 2: Design and Synthesis of Target Compounds.....</b>	<b>21</b>
2.1. Introduction.....	21
2.2. Rationale of design.....	22
2.2.1. Series 1-5.....	23
2.2.2. Series 6-12.....	29
2.3. Chemical considerations.....	37
2.3.1. Aurones (Series 1, 2, 5) and Dehydroaurones (Series 8).....	37
2.3.2. Indanones (Series 6).....	42

2.3.3.	Aza-aurones (Series 7).....	43
2.3.4.	Chalcones (Series 11).....	47
2.3.5.	Flavones (Series 12).....	47
2.4.	Assignment of configurations.....	49
2.4.1.	Aurones (Series 1, 2, 5) and dehydroaurones (Series 8).....	49
2.4.2.	Indanones (Series 6).....	51
2.4.3.	4, 6-Dimethoxy aza-aurones (Series 7).....	52
2.4.4.	2'-Hydroxy, 4'6'-dimethoxy chalcones (Series 11).....	55
2.5.	Experimental methods.....	57
2.5.1.	General details.....	57
2.5.2.	General procedure for the synthesis of series 1, 2, 6 and 8 (4, 6-dimethoxy-aurones, 4, 5, 6-trimethoxy-aurones, unsubstituted (Ring A) aurones and 4, 5, 6-trimethoxy dehydro aurone).....	58
2.5.2.1.	4, 6-Dimethoxy-aurones.....	58
2.5.2.1.1.	3, 5-Dimethoxyphenoxyacetic acid (A-1).....	58
2.5.2.1.2.	4, 6-Dimethoxybenzofuran-3(2H)-one (A-3).....	59
2.5.2.2.	4, 5, 6-Trimethoxy-aurones.....	59
2.5.2.2.1.	3, 4, 5-Trimethoxyphenoxyacetic acid (A-2).....	59
2.5.2.2.2.	4, 5, 6-Dimethoxybenzofuran-3(2H)-one (A-4).....	59
2.5.2.3	General procedure for the synthesis of 4, 6-dimethoxyaurones and 4, 5, 6-trimethoxyaurones (Compounds <b>1-1</b> to <b>1-28</b> , <b>2-1</b> to <b>2-10</b> ).....	60
2.5.2.4	Procedure for synthesis of (Z)-2-(cyclohexylmethylene)-4, 5, 6-trimethoxybenzofuran-3(2H)-one ( <b>2-11</b> ).....	61
2.5.2.5	General procedure for the synthesis of unsubstituted aurones (Compounds <b>5-1</b> to <b>5-8</b> ).....	61

2.5.2.6 General procedure for the synthesis of 4, 5, 6-trimethoxydehydroaurone (Compound <b>8-3</b> ).....	62
2.5.3 General procedure for the synthesis of 4, 6-dimethoxy-indanones (Compounds <b>6-1</b> to <b>6-2</b> ).....	62
2.5.3.1. 3, 5-Dimethoxypropanoic acid (I-1).....	62
2.5.3.2. 5, 7-Dimethoxy-2, 3-dihydro-1H-inden-1-one (I-2).....	63
2.5.3.3. Condensation of I-2 with substituted benzaldehydes.....	64
2.5.4 General procedure for the synthesis of 4, 6-dimethoxy-aza-aurones (Compounds <b>7-1</b> to <b>7-8</b> ).....	64
2.5.4.1. 2-Amino-4,6-dimethoxy- $\alpha$ -chloroacetophenone (AZ-1).....	64
2.5.4.2. 1-Acetyl-4,6-dimethoxy-2,3-dihydro-1H-indole-3-one (AZ-2).....	65
2.5.4.3. Condensation of AZ-2 with substituted benzaldehydes.....	66
2.5.5. General procedure for the synthesis of 2'-hydroxy-4', 6'-dimethoxychalcones (Compounds <b>11-1</b> to <b>11-5</b> ).....	66
2.5.6. General procedure for the synthesis of 5, 7-dimethoxy flavones (Compounds <b>12-1</b> to <b>12-5</b> ).....	67
2.5.7. Protection and deprotection of phenolic hydroxyl groups on 3-hydroxybenzaldehyde, 4-hydroxybenzaldehyde, 3, 4-dihydroxybenzaldehyde, 3, 5-dihydroxybenzaldehyde, 3-hydroxy-4-methoxybenzaldehyde and 4-hydroxy-3-methoxybenzaldehyde.....	67
2.5.8. X-ray crystallography of compounds <b>1-2</b> and <b>6-20</b> .....	68
2.5.9 High pressure liquid chromatography (HPLC) analyses.....	68
2.6 Summary.....	69
<b>Chapter 3: Effects of aurones and related compounds on the efflux of pheophorbide a (PhA) by ABCG2 over-expressing human breast cancer (MDA-MB-231/R) cells and calcein-AM (CAM) by ABCB1 over-expressing Mardin-Darby canine kidney (MDCK) cells.....</b>	<b>70</b>
3.1. Introduction.....	70
3.2. Experimental.....	70
3.2.1. Cell lines and materials for biological assay.....	70

3.2.2. Procedure for western blot analysis.....	71
3.2.3. Procedure for PhA accumulation assay.....	71
3.2.4. Procedure for calcein-AM (CAM) accumulation assay.....	73
3.2.5. Statistical Analysis.....	75
3. 3. Results.....	76
3.3.1. Determination of EC <sub>50</sub> from PhA assay.....	76
3.3.2. Determination of EC <sub>50</sub> from CAM assay.....	78
3.3.3. Effect of structural modifications on efflux of PhA by ABCG2 over-expressing human breast cancer (MDA-MB-231/R) cells.....	81
3.3.3.1. Series 1-5 compounds with mono-substituted ring B.....	88
3.3.3.2. Series 1-5 compounds with di-substituted ring B.....	90
3.3.3.3. Ring C modifications that result in no activity.....	91
3.3.3.4. Ring C modifications: Replacement of O with CH <sub>2</sub> or NH.....	91
3.3.3.5. Ring C modifications: Cleavage of ring C.....	92
3.3.3.6. Ring C modifications: Expansion of ring C.....	92
3.3.4. Effect of structural modifications on efflux of calcein-AM (CAM) by ABCB1 over-expressing MDCKII/MDR1 cells.....	93
3.4. Discussion.....	104
3.5. Conclusions.....	110
<b>Chapter 4: Efflux of pheophorbide a (PhA) by ABCG2 over-expressing human breast cancer (MDA-MB-231/R) cells and calcein-AM (CAM) by ABCB1 over-expressing Mardin-Darby canine kidney (MDCK) cells by aurones and related compounds: Quantitative Structure-Activity Relationships (QSAR) and Derivation of Pharmacophore.....</b>	<b>112</b>
4.1. Introduction.....	112
4.2. Experimental.....	112
4.2.1. Modified Free Wilson Analysis.....	112
4.2.2. Auto-QSAR by MOE.....	115



4.3. Results.....	117
4.3.1. Modified Free Wilson Analysis.....	117
4.3.1.1. Analysis of compounds with EC <sub>50</sub> values for inhibition of PhA efflux.....	117
4.3.1.2. Analysis on selected compounds with EC <sub>50</sub> values for inhibition of PhA efflux and CAM efflux.....	121
4.3.2. QSAR for inhibition of PhA efflux by ABCG2-overexpressing cell lines using AutoQuaSAR from MOE.....	127
4.3.3. Establishing a pharmacophore model for inhibition of PhA efflux.....	130
4.4. Discussion.....	138
4.5. Conclusion.....	143
<b>Chapter 5: Investigations into the effects of aurones and related compounds on the efflux activity of ABCG2 over-expressing MDA-MB-231 cells.....</b>	<b>144</b>
5.1. Introduction.....	144
5.2. Experimental.....	145
5.2.1. Cell lines and materials for biological assay.....	145
5.2.2. Mitoxantrone Sensitization.....	146
5.2.3. Mitoxantrone accumulation studies.....	147
5.2.4. ATPase assay.....	148
5.2.5. Photoaffinity labeling of ABCG2 with [ <sup>125</sup> I]Iodoarylazidoprazosin (IAAP).....	149
5.2.6. Western blot analysis.....	149
5.2.7. Cytotoxicity Studies.....	150
5.2.8. Statistical analysis.....	150
5.3. Results.....	150
5.3.1. Mitoxantrone Sensitization.....	150
5.3.2. Cellular accumulation of mitoxantrone in MDA-MB-231/R cells.....	155

5.3.3. Photoaffinity labeling of ABCG2/BCRP with [ <sup>125</sup> I]Iodoarylazidoprazosin ([ <sup>125</sup> I]-IAAP).....	163
5.3.4. Western blot analysis.....	164
5.3.5. Growth inhibitory effects on MDA-MB-231/R and MDA-MB-231/V cells.....	166
5.4. Discussion.....	172
5.5. Conclusion.....	177
<b>Chapter 6: <i>In vivo</i> evaluation of a 4,6-dimethoxyaurone analog (1-26) in mice bearing human breast cancer cells (MDA-MB-231) xenografts.....</b>	<b>179</b>
6.1. Introduction.....	179
6.2 Experimental.....	180
6.2.1 Materials.....	180
6.2.2. Cell Lines.....	180
6.2.3 <i>In vivo</i> studies.....	181
6.2.4. Statistical analysis.....	183
6.3. Results.....	183
6.4. Discussion.....	191
6.5. Conclusion.....	193
<b>Chapter 7: Conclusions and Future Work.....</b>	<b>194</b>
<b>Bibliography.....</b>	<b>200</b>
<b>Appendix 2-1: Characterization of synthesized analogues.....</b>	<b>214</b>
<b>Appendix 4-1: Assignment of 19 substructures to test compounds.....</b>	<b>244</b>
<b>Appendix 4-2: Assignment of 13 substructures to test compounds.....</b>	<b>246</b>
<b>Appendix 4-3: Descriptors for Auto-QSAR.....</b>	<b>247</b>
<b>Appendix 4-4: Structures of 27 compounds in the external database.....</b>	<b>256</b>

**Appendix 5-1:** Effects of selected test compounds on beryllium fluoride-sensitive ATPase activity in High Five insect cell crude membranes.....261

**Appendix 5-2:** Photoaffinity labelling of ABCG2 with [<sup>125</sup>I]-IAAP in the absence (C, control) or presence of test compounds evaluated at 5 μM in crude membranes of MCF-7 FLV1000 cells.....265

## Summary

The aim of the thesis was to test the hypothesis that aurones interacted with the ATP-Binding Cassette (ABC) protein ABCG2 to modulate its efflux activity. ABCG2 is associated with multi-drug resistance to cancer chemotherapy and modulation of ABCG2 by aurones would underscore the potential of this template for the design of multi-drug reversal agents.

Twelve series of compounds comprising 112 functionalized aurones and related analogs were synthesized and screened for inhibition of Pheophorbide a (PhA) efflux in MDA-MB-231/R cells. Several dimethoxyaurones, benzylideneindanones, dimethoxyflavones were found to have micromolar modulatory potencies that were comparable to an established ABCG2 inhibitor, Fumitremorgin C (FTC).

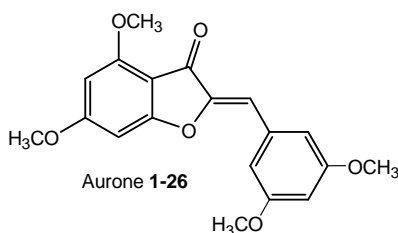
A qualitative assessment of the structural features required for modulatory activity highlighted important roles for (i) a methoxylated ring A but not a hydroxylated or unsubstituted ring A; (ii) an intact exocyclic double bond attached to a 5-membered ring C (iii) the location of the double bond on ring C. Activity is retained when O in aurone is replaced by a methylene CH<sub>2</sub> but not by a NH. A dimethoxylated ring A together with a disubstituted ring B, particularly with dimethoxy groups at 3',4' or 3',5'-positions yielded the most potent inhibitors among the aurones, indanones and flavones (EC<sub>50</sub>: 0.91 to 2.45 μM). QSAR approach based on the modified Free-Wilson method identified methoxy groups on ring A as significant contributors to activity, functioning as hydrogen bond acceptors and hydrophobic features in a pharmacophore model.

Mitoxantrone (MX) sensitization assay showed that potent analogs completely restored sensitivity to MX in MDA-MB-231/R cells at 0.5 μM which can be attributed to the increase in the accumulation of intracellular MX. Direct interaction between ABCG2 and selected flavonoidic compounds were investigated with the ABCG2 ATPase assay which

showed the most potent inhibitors stimulating ATPase activity at nanomolar  $K_m$  values. Photoaffinity-labeling of ABCG2 by [ $^{125}$  I]-IAAP was reduced in the presence of several potent members, pointing to competition for IAAP binding site on ABCG2. Likelihood of the compounds interfering with upstream cellular processes involved in the synthesis of the ABCG2 protein was excluded by Western blot analysis. The *in vivo* efficacy of a representative dimethoxyaurone (**1-26**) in sensitizing a MDA-MB-231/R xenograft induced in Balb/c mice to the cytotoxic effects of MX was also demonstrated. The combination of **1-26** and MX significantly increased the life span of the treated mice, illustrating the translation of *in vitro* results to xenograft-bearing animals.

In conclusion, the findings of this thesis supported the hypothesis that aurones was a promising template with modulatory properties on the ABCG2. Well-defined structural requirements were needed for interaction with ABCG2. Aurone **1-26** was identified as a promising lead for further advancement to preclinical evaluation as a non-toxic and potent modulator of ABCG2.

(445 words)



## List of Tables

Table 1-1: List of representative substrates of ABCB1 and ABCG2.....	7
Table 2-1: Structures and estimated lipophilicities (SlogP <sup>a</sup> , LogP(o/w) <sup>b</sup> , ClogP <sup>b</sup> ) of unsubstituted ring B compounds for Series 1-5.....	25
Table 2-2: Structures and estimated lipophilicities (SlogP) of Series 1-5 compounds.....	27
Table 2-3: Structures, SlogP, logP and ClogP of unsubstituted ring B compounds in Series 6-12.....	30
Table 2-4: Structures and SlogP values of Series 6-12 compounds.....	33
Table 3-1: EC <sub>50</sub> (μM) values of compounds obtained from Pheophorbide a (PhA).....	82
Table 3-2: Accumulation of calcein-AM in MDCKII/MDR1 cells in the presence of test compounds.....	94
Table 3-3: EC <sub>50</sub> (μM) for PhA accumulation and CAM accumulation of selected compounds.....	102
Table 4-1: Independent variables (substructure features) used in the modified Free-Wilson analysis for inhibition of PhA efflux for 110 compounds.....	113
Table 4-2: Independent variables (substructure features) used in the modified Free-Wilson analysis for inhibition of PhA and CAM for 20 compounds.....	114
Table 4-3: Descriptors used to generate QSAR model by AutoQuaSAR by MOE.....	116
Table 4-4: Modified Free Wilson Analysis of pEC <sub>50</sub> PhA of 110 compounds by Linear Regression (Stepwise and Backward).....	119

Table 4-5: Modified Free Wilson Analysis of pEC <sub>50</sub> PhA and pEC <sub>50</sub> CAM of 20 compounds Linear Regression (Stepwise).....	122
Table 4-6: Modified Free Wilson Analysis of pEC <sub>50</sub> PhA and pEC <sub>50</sub> CAM of 20 compounds Linear Regression (Backward).....	124
Table 4-7: Confusion matrix for test set of 22 compounds.....	133
Table 4-8: Confusion matrix for external database of 27 compounds.....	135
Table 5-1: Effects of selected test compounds on IC <sub>50</sub> of mitoxantrone in MDA-MD-231 /R cells.....	152
Table 5-2: Accumulation of MX in MDA-MB-231/R cells in presence of test compounds ( <b>1-1</b> <b>1-15</b> ).....	158
Table 5-3: Accumulation of MX in MDA-MB-231/V cells in the presence of test compounds ( <b>1-1</b> to <b>1-15</b> ) at 5 μM.....	160
Table 5-4: Km (μM) of selected compounds for ABCG2 ATPase activity in High Five insect cell crude membranes and EC <sub>50</sub> (μM) values for increasing PhA accumulation in MDA-MB-231/R cells.....	161
Table 5-5: Effects of selected compounds on percentage cell survival in MDA-MB-231/R and MDA-MB-231/V cells.....	168
Table 5-6: Effects of selected compounds on percentage cell survival in HCT 116 and IMR 90 cells.....	171
Table 6-1: Kaplan-Meier analysis <sup>a</sup> for comparison between treatment schemes in mice with MDA-MB-231/V induced xenografts and MDA-MB-231/R induced xenografts.....	183
Table 6-2: Estimates of variables in experimental model by Cox regression.....	187

## List of Figures

Figure 1-1: Schematic representation of ABCB1 (Pgp) and ABCG2 (BCRP).....	3
Figure 1-2: Structure of ABCB1 (A) front and (B) back stereo views of ABCB1.....	4
Figure 1-3: Structures of above-named flavonoids.....	14
Figure 1-4: Structural features of a flavone required for interaction with ABCB1.....	15
Figure 1-5: Structures of 6-prenylchrysin, 7,8-benzoflavone, 2'-hydroxy- $\alpha$ -naphthoflavone.....	16
Figure 1-6: (A) Common requirements for both ABCB1 and ABCG2; (B) Requirements for ABCG2 but not ABCB1.....	16
Figure 1-7: (A) Structure of aurone (B) Halogenated 4,6-dimethoxyaurones and 4-hydroxy-6-methoxyaurones.....	17
Figure 2-1: Summary of modifications made to rings A and B of functionalized aurones.....	21
Figure 2-2: Summary of modifications made to ring C of the aurone template.....	21
Figure 2-3: Conformation of the $\alpha\beta$ -unsaturated enone: (A) Aurone: s-cis; (B) Chalcone: s-cis; (C) Chalcone: s-trans.....	32
Figure 2-4: Formation of 3,5-dimethoxyphenoxyacetic acid (A-1) and 3,4,5-trimethoxyphenoxyacetic acid (A-2).....	38



Figure 2-5: Intramolecular Friedel-Craft acylation to form (A-3) and (A-4).....	38
Figure 2-6: Aldol condensation of benzofuranone with benzaldehydes.....	39
Figure 2-7: Proposed mechanism for the synthesis of <b>2-11</b> .....	40
Figure 2-8: Proposed boronium cationic species stabilized by tetrachloroaluminate.....	44
Figure 2-9: Reaction of 3,5-dimethoxyaniline with chloroacetonitrile by a Friedel Crafts reaction followed by acid hydrolysis of imine intermediate to give 2-amino-4,6-dimethoxy- $\alpha$ -chloroacetophenone, AZ-1.....	45
Figure 2-10: Acetylation of AZ-1 followed by ring closure to give AZ-2.....	46
Figure 2-11: Reaction of <i>s-cis</i> chalcone with iodine to form freely rotating addition product.....	66
Figure 2-12: Proposed mechanism of ring closure involving replacement of $\beta$ -iodine by phenolic OH.....	49
Figure 2-13: <i>E</i> and <i>Z</i> aurones.....	49
Figure 2-14: X-ray structure of (a) <b>1-2</b> and (b) 5-hydroxy-2-(4'-methoxybenzylidene)-benzofuran-3(2H)-one.....	51
Figure 2-15: <i>E</i> and <i>Z</i> benzylidene indanones.....	51
Figure 2-16: Chemical shifts of methine CH of <i>E</i> and <i>Z</i> isomers of 2-(phenylmethylene)-3,3,-dimethyl-1-indanone.....	51

Figure 2-17: X-ray structure of indanone <b>6-20</b> .....	52
Figure 2-18: <i>Z</i> and <i>E</i> aza-aurones.....	52
Figure 2-19: Assignment of <sup>1</sup> H chemical shifts of compound <b>7-1</b> .....	53
Figure 2-20: Proposed nuclear Overhauser (NOE) effects in the <i>Z</i> and <i>E</i> isomers of <b>7-1</b> .....	54
Figure 2.21: 2D-NOESY spectrum of Compound <b>7-1</b> .....	55
Figure 2-22: Chalcone represented in its <i>E</i> and <i>Z</i> configuration. Both <i>E</i> and <i>Z</i> isomers are represented in the <i>s-cis</i> conformation.....	56
Figure 3-1: Dose response curve of PhA accumulation (% of control) against concentration of FTC (μM).....	77
Figure 3-2: Dose response curves of % PhA accumulation versus varying concentrations of FTC (μM) and compound <b>1-25</b> (μM).....	77
Figure 3-3: Fluorescence readings of accumulated calcein over time (up to 60 min of incubation time after addition of calcein-AM) in parental MDCKII/WT and the Pgp over-expressing MDCKII/MDR1 cells .....	79
Figures 3-4: Fluorescence-time curves of (A) cyclosporin A and (B) compound <b>1-26</b> at various concentrations.....	80
Figure 3-5: Dose response curve for the % accumulation of calcein-AM versus concentration of compound <b>1-26</b> in MDCKII/MDR1 cells.....	81
Figure 3-6: Chalcones reported to increase mitoxantrone accumulation in MDA-MB-231 /R cells.....	107

Figure 3-7: Summary of SAR requirements for aurone-ABCG2 interaction.....	111
Figure 3-8: Summary of common SAR requirements for aurone-ABCG2 and aurone-ABCB1 interactions.....	111
Figure 4-1: Summary of QSAR requirements for aurone-ABCG2 interaction.....	120
Figure 4-2: Summary of common QSAR requirements for aurone-ABCG2 and aurone-ABCB1 interactions.....	124
Figure 4-3: Plot of actual versus predicted/calculated pEC <sub>50</sub> values based on the model given in Equation 4-7 (n = 61). No outliers were identified in this model.....	128
Figure 4-4: Pharmacophore model of ABCG2 modulators.....	131
Figure 4-5: Distances (Å) between pharmacophoric features in the model.....	132
Figure 4-6: Alignment of structure of FTC to the pharmacophore model.....	135
Figure 4-7: Alignment of gefitinib to the pharmacophore model.....	136
Figure 4-8: Alignment of structure of Novobiocin to the pharmacophore model.....	137
Figure 4-9: Distances between features found in the pharmacophore models reported by (A) Mattson et al and (B) in this chapter.....	142

Figures 5-1: Dose response curves of MX determined in the presence of (A) **1-26** and (B) **6-15** on MDA-MB-231/R cells.....153

Figure 5-2. Representative FACS histograms of MX Accumulation in (A) MDA-MB-231/V cells; (B) MDA-MB-231/R cells; (C) MDA-MB-231/R cells + MX; (D) test compound **1-3** (5  $\mu$ M) + MX in MDA-MB-231/R cells; (E) MDA-MB-231/V cells + MX.....155

Figures 5-3: Effect of increasing concentration of representative compounds **1-26** and **8-1** on BeFx-sensitive ABCG2 ATPase activity.....161

Figure 5-4: Photoaffinity labelling of ABCG2 with [<sup>125</sup>I]-IAAP in the absence (C, control) or presence of test compounds evaluated at 5  $\mu$ M.....164

Figure 5-5: Western blot analyses showing the effects of compound **1-26** (alone or in combination with MX) on ABCG2 expression in MDA-MB-231/R and V cells.....165

Figure 5-6: Structures of test compounds associated with lower % cell survival values on MDA-MB-231/R cells than MDA-MB-231/V cells at 10  $\mu$ M.....171

Figures 6-1(a) and 6-1(b): Survival plots of Balb/c nude mice inoculated with (A) parental MDA-MB-231/V and (B) ABCG2-overexpressing MDA-MB-231/R cells and subjected to different treatment schedules (i) Control (DMSO + saline); (ii) **1-26** (0.2 mg/kg); (iii) MX (4 mg/kg) (iv) **1-26** (0.2 mg/kg) + MX (4 mg/kg).....184

Figures 6-2(a-d): Weight changes of mice bearing MDA-MB-231/V xenografts over time.....189

Figures 6-3(a-d): Weight changes (grams) of mice bearing MDA-MB-231/R xenografts over time.....190

## List of Schemes

Scheme 2-1: Synthesis of 5,6,7-trimethoxybenzofuran-(2H)-3-one .....	24
Scheme 2-2: Synthesis of <b>1-1 to 1-28, 2-1 to 2-10</b> .....	37
Scheme 2-3: Synthesis of <b>2-11, 5-1, 5-3, 5-5 to 5-8</b> .....	40
Scheme 2-4: Synthesis of <b>1-6</b> .....	41
Scheme 2-5: Synthesis of <b>6-1 to 6-20</b> .....	42
Scheme 2-6: Synthesis of <b>7-1 to 7-8</b> .....	43
Scheme 2-7: Synthesis of <b>7-1 to 7-8</b> .....	47
Scheme 2-8: Synthesis of <b>12-1 to 12-5</b> .....	47

## Abbreviations

$^{13}\text{C}$ NMR	Carbon-13 nuclear magnetic resonance spectrum
$^1\text{H}$ NMR	Proton nuclear magnetic resonance spectrum
3D-QSAR	Three dimensional quantitative structure activity relationship
ABC	ATP-Binding Cassette
ADMET	Absorption, distribution, metabolism, excretion, toxicity
APCI	Atomic pressure chemical ionization
BCRP	Breast cancer resistance protein
CAM	calcein acetyoxymethyl ester, calcein-AM
CDK2	Cyclin-dependent kinase 2
DMF	Dimethylformamide
DMSO	Dimethyl sulfoxide
EMEM	Eagle's Minimal Essential Medium
FTC	Fumitremorgin C
HBSS	Hank's Buffered Saline Solution
HCT116	Human colon carcinoma
HRMS	High resolution mass spectroscopy
IAAP	[ $^{125}\text{I}$ ] Iodoarylazidoprazosin
IMR-90	Normal human diploid embryonic lung fibroblasts
log P	Lipophilicity
MDA-MB-231/V	Human breast cancer cells (parental cells)
MDCKII/MDR1	ABCB1-overexpressing Mardin-Darby canine kidney cells
MDCKII/WT cells	Mardin-Darby canine kidney wild type cells
MDR	Multi-drug resistance

MOE	Molecular Operating Environment
MRP-1	multidrug resistance-associated protein-1
MRP-2	multidrug resistance-associated protein-2
MTT	3-(4,5-Dimethylthiazol-2-yl)-2,5-diphenyltetrazolium bromide
MX	Mitoxantrone
NBDs	Nucleotide-binding domains
2D NOESY	2-Dimensional Nuclear Overhauser Effect
PBS	Phosphate Buffer Saline
PCR	Principal Component Regression
PhA	Pheophorbide a
PLS	Partial Least Squares Projection to Latent Structures
Pgp	P-glycoprotein
RMSE	Root mean square error
SAR	Structure activity relationships
SDS-PAGE	Sodium dodecyl sulphate-polyacrylamide gel
SEM	Standard error of the mean
TKIs	Receptor tyrosine kinase inhibitors
TMDs	Transmembrane domains
TMS	Tetramethylsilane

## Chapter 1: Introduction

### 1.1. Multidrug resistance (MDR) and ATP-Binding Cassette (ABC) transporters

Multidrug resistance (MDR) is a phenomenon associated with the resistance of tumor cells to the cytostatic or cytotoxic actions of multiple, structurally dissimilar and functionally divergent drugs commonly used in cancer chemotherapy<sup>1</sup>. When a disease is refractory to chemotherapy from the onset, MDR is described as “intrinsic” whereas it is considered to be “acquired” if the disease becomes insensitive to treatment following a relapse<sup>1</sup>. There are three major mechanisms of drug resistance in cells, namely (i) decreased uptake of water-soluble drugs which requires the role of uptake transporters; (ii) altered cell cycle, increased repair of DNA damage, reduced apoptosis which affects the capacity of cytotoxic drugs to kill cells; and (iii) increased efflux of hydrophobic drugs that can easily enter the cells by diffusion through the plasma membrane. Of these, considerable attention has been paid to the last mechanism in which cancer cells acquire resistance through the over-expression of ATP-binding cassette (ABC) transporters which utilize the energy of cellular ATP to move anti-cancer drugs out of cells<sup>2</sup>. ABC transporters are large membrane-bound proteins with evolutionary conserved structure-function features. Characteristic structural domains common to all ABC transporters are the cytoplasmic globular ATP-binding cassette domain (also called the nucleotide-binding domains, NBDs) and the helical transmembrane domains (TMDs). The NBD is the catalytic unit that serves to bind and hydrolyze ATP, thus providing the energy required to transport substrates across the biological membrane. The NBD comprises Walker A and Walker B motifs which are involved in the binding of ATP, and the intervening signature motif which couples ATP hydrolysis with transport of substrate<sup>3</sup>. The substrate binding site(s) are located within the TMD. The molecular link responsible for ensuring communication and signal transmission between the two domains has yet to be fully understood<sup>4</sup>. For functional integrity, ABC transporters need at least two



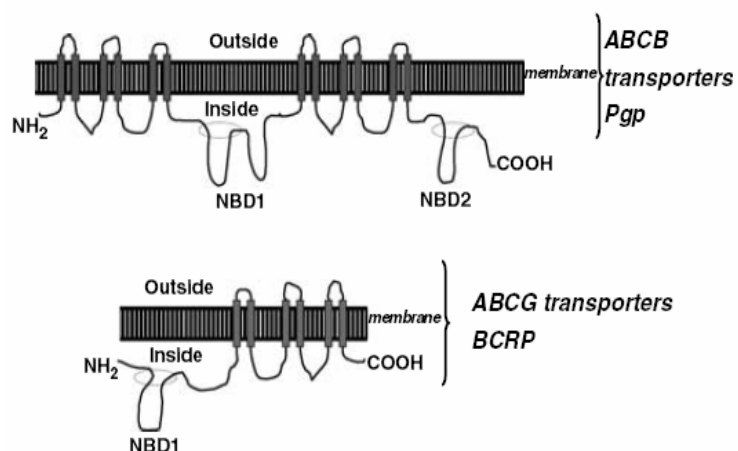
NBDs and two TMDs. In “full transporters”, these domains are present in a single polypeptide chain whereas in “half transporters”, only a single NBD and a single TMD are present. Homo- or heterodimerization is then required to generate the fully functional transporter<sup>2</sup>.

The three most common human ABC transporters associated with MDR are the multidrug resistance protein P-glycoprotein (Pgp or ABCB1) encoded by the *ABCB1* (or *MDR-1*) gene; the multidrug resistance-associated protein-1 (MRP-1) encoded by the *ABCC1* (or *MRP-1*) gene and the breast cancer resistance protein (BCRP or ABCG2) encoded by the *ABCG2* gene<sup>5</sup>. The role of these transporters in the failure of chemotherapy in cancer patients have been widely discussed and reviewed<sup>2, 6</sup>. As the focus of this thesis is on ABCG2 and ABCB1, key features (structure, function, role in multidrug resistance) of these transporters are discussed in the following sections.

## 1.2. Structural features of ABCB1 and ABCG2

ABCB1 is the best characterized of the ABC transporters. It has been intensively studied since its discovery in 1976<sup>7</sup>. Structurally, ABCB1 is a 170kDa phospho-glycoprotein with 12 transmembrane domains (TMDs) and two ATP-binding sites. It is a “full transporter” made up of two nucleotide-binding domains (NBDs) and two membrane spanning domains, each comprising of six TMDs (Fig 1-1).

Figure 1-1: Schematic representation of ABCB1 (Pgp) and ABCG2 (BCRP)<sup>8</sup>

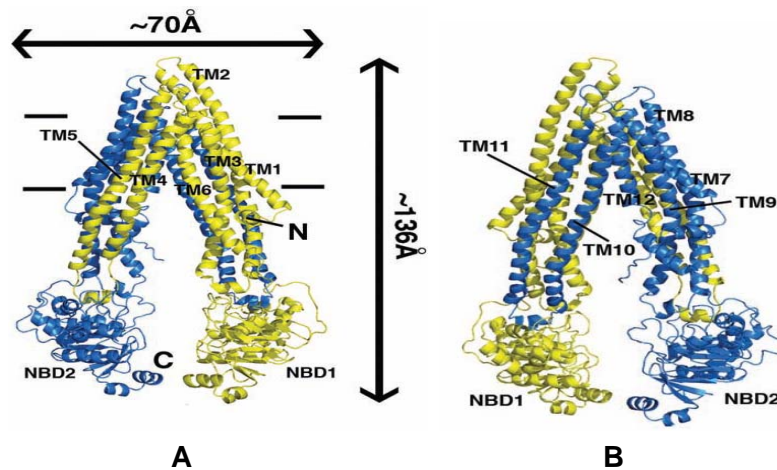


ABCG2 is the most recent ABC transport protein to be linked to multi-drug resistance. It was independently isolated in three laboratories in 1998<sup>9, 10, 11</sup>. It is called ABCP for its abundance in placenta, MXR for its ability to confer cell-growth resistance to mitoxantrone (MX) and BCRP for its identification from resistant breast cancer cells<sup>1</sup>. Structurally, ABCG2 is a 72kDa ABC protein comprising a single NH<sub>2</sub>-terminal cytosolic nucleotide-binding domain (NBD1) and six transmembrane domains (TMDs) (Figure 1-1). Unlike ABCB1, it is a half transporter. The domain arrangement in ABCG2 is also different from ABCB1 in that the NBD is located closer to the amino terminal, as illustrated in Figure 1-1<sup>12, 13</sup>. Hence, ABCG2 requires homodimerization to exert its activity and a homotetrameric configuration of the protein has been proposed<sup>14, 15, 16</sup>. Rosenberg and co-workers<sup>14</sup> purified human ABCG2 from the yeast *Pichia Pastoris* and found that the protein structure underwent significant conformational changes in the presence of the substrate mitoxantrone. This phenomenon of conformational change on ligand binding may be common to other ABC transporters as well.

Aller and co-workers reported the x-ray crystal structure of mouse apo-ABCB1 (crystallized at 3.8 Å resolution) in a drug-binding competent state<sup>17</sup>. The structure of

ABCB1 was reported to have a nucleotide-free inward-facing conformation arranged as two “halves” with pseudo two-fold molecular symmetry. (Figure 1-2) Each of the two bundles of six transmembrane helices were composed of portions from both the N-terminal and C-terminal halves of the protein and they lined a large cavity (6000 Å<sup>3</sup>) within the lipid bilayer which was able to accommodate at least two compounds simultaneously<sup>17, 18</sup>. The upper half of the drug binding pocket of ABCB1 comprised predominantly hydrophobic and aromatic residues while the lower half of the chamber had polar and charged residues, thus allowing hydrophobic and/or positively charged substrates to gain access to the binding pocket<sup>17</sup>. Mouse ABCB1 has a 87% sequence identity to human ABCB1 and the availability of this structure is anticipated to facilitate structure-based drug design efforts which have hitherto been hampered by the lack of mammalian structures with acceptable resolution.

Figure 1-2: Structure of ABCB1 (A) front and (B) back stereo views of ABCB1<sup>17</sup>. TMs = transmembrane and NBDs = nucleotide binding domains are labeled. The N- and C-terminal half of ABCB1 is colored yellow and blue respectively. Horizontal bars represent the approximate positioning of the lipid bilayer.



### 1.3. Functions of ABCB1 and ABCG2

ABCB1 and ABCG2, along with other ABC transporters, are found at important pharmacological barriers like the pregnant uterus, blood brain barrier, small and large

intestines, kidney, liver and skin. There, they play an important role as gate-keeper proteins, controlling the entry of potentially noxious substances into the body. By extension, they also influence the absorption, distribution, metabolism, excretion (ADME) profiles of therapeutic agents and contribute to clinical drug-drug interactions. For this reason, the transport activities of ABCB1 and ABCG2 at the luminal surface of gastrointestinal epithelial cells reduce the oral bioavailability of drugs that are substrates of these proteins. In the same way, their presence in the epithelial cells that make up the blood-brain barrier limits the access of drugs targeted for activity at the central nervous system.

Efflux by transporters is reported to have a relatively greater effect when the drug/substrate concentration at the luminal surface is low and when the substrate has a slow rate of passive diffusion<sup>19</sup>. This is because there is a finite number of transporter molecules on the cell surface and when they are saturated as would be the case when the substrate concentration is high, the rate of efflux levels off. On the other hand, passive diffusion is not hampered by a saturation phenomenon and in a case where efflux activity has leveled off, passive diffusion into the cell continues. Under these circumstances, a highly permeable substrate will gain access into the cell faster than one with lower permeability. The implication is that high oral dosing of a drug substrate may reduce the deleterious effect of transporters on its oral bioavailability but is less likely to overcome the limited distribution of substrates in the brain due to the generally lower concentrations of the drug substrate at the blood brain barrier<sup>19</sup>.

ABCB1 and ABCG2 are most frequently over-expressed in cancer cell lines cultured under selective drug pressure and their roles in *in vitro* MDR is beyond dispute<sup>2</sup>. In contrast, the role of these transporters in clinical anticancer resistance has been difficult to assess. There is more evidence linking ABCB1 expression with poor clinical outcomes for many cancers including breast cancer<sup>20</sup>, sarcomas<sup>21</sup> and certain leukemias<sup>22, 23, 24</sup>. Studies

correlating the expression of ABCG2 in cancerous tissues and clinical outcomes have not been conclusive<sup>25</sup>. ABCG2 is expressed in hematological malignancies and solid tumors, particularly those derived from the digestive tract, endometrium and melanoma<sup>26</sup>.

ABCB1 and more frequently, ABCG2 have been detected in a side population of established cancer cells and tumor biopsies<sup>27, 28, 29, 30</sup>. These cells are slow-growing and capable of long-term self renewal. They may contribute to treatment failures in cancer chemotherapy because of their slow proliferation and transporter - mediated drug resistance. Specific targeting of this side population of stem-cell like cancer cells may be a promising approach in cancer therapy.

#### 1.4. Substrates and Inhibitors of ABCB1 and ABCG2

A hallmark of ABCB1 and ABCG2 is their ability to recognize a large number of structurally diverse ligands. The polyspecificity (“promiscuity”) in ligand recognition is likely due to the conformational flexibility of the protein which allows it to reconfigure its binding pocket to accommodate diverse ligands<sup>31, 32</sup>. Alternatively, a ligand may adopt different poses (“differential ligand positioning”) when it binds at different sites on the same protein<sup>33</sup>.

There is also considerable overlap in the substrate profiles of the different ABC transporters. Pedersen et al found 37-44% substrate overlap for ABCB1, ABCG2 and MRP2<sup>34</sup>. There is less agreement on the extent of overlap among inhibitors, with some sources citing a high overlap (67%) for ABCB1, ABCG2 and MRP2<sup>34</sup> while others have proposed a limited overlap in the inhibitor profile of ABCG2 and ABCB1<sup>2</sup>. Table 1-1<sup>2</sup> provides a list of representative substrates of ABCB1 and ABCG2, including those that are common to both transporters.

Table 1-1: List of representative substrates of ABCB1 and ABCG2.

Substrates		ABC transporters	
Drug class	Drug	ABCB1	ABCG2
Vinca alkaloids	Vinblastine	+ <sup>a</sup>	
	Vincristine	+	
Anthracyclines	Daunorubicin	+	+
	Doxorubicin	+	+
	Epirubicin	+	+
Epipodophyllotoxins	Etoposide	+	+
	Teniposide	+	+
Taxanes	Docetaxel	+	
	Paclitaxel	+	
Kinase inhibitors	Imatinib	+	+
	Flavopiridol		+
Camptothecins	Irinotecan	+	+
	SN-38	+	+
	Topotecan		+
Other	Bisantrene	+	+
	Colchicine	+	
	Methotrexate	+	+
	Mitoxantrone	+	+
	Saquinivir	+	
	Actinomycin D	+	
	Azidothymidine		+

<sup>a</sup> (+) indicates drug is a substrate of the ABC transporter

Computational methods have been widely used to investigate recognition patterns for substrates of ABC transporters based on their structural features or physicochemical

properties. More work has been done with ABCB1 substrates. The pioneering work of Seelig<sup>35</sup> proposed that interaction with ABCB1 required two electron donor groups with a spatial separation of 2.5 Å (Type I) or 4.6 Å (Type II). Alternatively, three electron donor groups with a Type II spatial separation for its outer two groups may be involved. Didziapetris and co-workers<sup>36</sup> proposed a “rule of four” for ABCB1 substrates, characterized by hydrogen (H) bond acceptor atoms (N + O) > 8, molecular weight > 400 and acid pKa < 4. 3D QSAR using pharmacophore-based descriptors identified a model comprising of two hydrophobic groups 16.5 Å apart and two H bond acceptor groups 11.5 Å apart<sup>37</sup>. The general consensus is that substrates of ABCB1 are lipophilic, of large size, amphipathic, sometimes cationic and with electronegative groups as H bond acceptors<sup>38</sup>. Raub<sup>38</sup> proposed that the minimum requirement for a ABCB1 substrate was the presence of one or two hydrophobic centres (usually at aromatic rings), one to three H bond acceptors and one H bond donor. The results of another study on ADMET relevant ABC transporters (ABCB1, ABCC1, ABCG2) showed broad similarities in the substrate profile of each transporter but noted that non-substrates had fewer rotatable bonds and were significantly more rigid<sup>39</sup>.

ABCG2 but not ABCB1 is able to efflux large, lipophilic molecules which are both positively and negatively charged and with amphiphilic character<sup>40</sup>. H bond donor features were also more prevalent among ABCG2 substrates<sup>40, 41, 42</sup>.

The list of substrates and inhibitors of ABCG2 has been steadily expanding since the discovery of the protein. The earliest substrates were anti-cancer agents like mitoxantrone, flavopiridol, camptothecins, methotrexate, many of which are substrates of ABCB1. Several other classes have since been included like antivirals, antibiotics, calcium channel blockers, HMG-CoA reductase inhibitors<sup>12, 43</sup>. Several receptor tyrosine kinase inhibitors (TKIs) have been reported to interact with high affinity to ABCB1 and ABCG2<sup>44, 45</sup>. There are concerns that this may be a class effect, in which case there would be significant consequences on

treatment outcomes as well as the disposition and toxicity of these drugs in cancer therapy<sup>46</sup>. The question as to whether the TKIs are substrates or inhibitors of ABCG2 and other transport proteins has yet to be resolved. Imatinib was reported to be an ABCG2 substrate at low concentrations but had the characteristics of an inhibitor at higher concentrations<sup>45</sup>. The same profile has been noted for gefitinib<sup>47</sup>.

The substrate specificity of ABCG2 is known to be affected by mutation at position 482 which is occupied by arginine (R) in the wild-type protein. Drug selected human tumor cell lines were found to express different ABCG2 variants, in which R482 was replaced by glycine (G) or threonine (T)<sup>48</sup>. The R482T and R482G variants were proposed to be gain-of-function mutations acquired during the course of drug selection. These variants exhibited altered drug resistance profile and substrate specificity. For example, doxorubicin and rhodamine 123 were transported by the ABCG2 variants but not the wild type ABCG2<sup>48, 49, 50, 51</sup>. On the other hand, methotrexate binds to variant forms but was not transported. The present evidence suggests that the residue 482 played an important role in substrate transport but not binding, since mutations at this site did not modify the binding affinity for a given substrate<sup>52</sup>. Quite unusually, mutation at this site caused a gain-of-function of ATPase activity by increasing both the maximal rate of hydrolysis and affinity for ATP<sup>49, 53</sup>.

To circumvent or resolve the reduced intracellular accumulation of anticancer drugs that are substrates of ABCB1 and ABCG2, modulators (also called “inhibitors”) of these efflux proteins have been developed. The earliest agents targeted ABCB1 and were clinical drugs already approved for other medical indications and whose modulating properties were discovered fortuitously. They included calcium channel blockers (e.g. verapamil), immunosuppressants (e.g. cyclosporine A) and antibiotics (e.g. erythromycin)<sup>1, 54</sup>. They were hampered by their ability to function concurrently as substrates and thus compete with the cytotoxic drug for efflux by the protein. This often led to unpredictable pharmacokinetics<sup>1</sup>.



Moreover, they lacked potency and the high doses required for clinical efficacy resulted in off-target effects. Second generation modulators addressed some but not all of these shortcomings. Compounds like dexverapamil, dexniguldipine and valsopodar were more potent and less toxic but induced pharmacokinetic interactions because they were also substrates of cytochrome P450 3A (CYP3A)<sup>2</sup>. Through repeated extrusion and reabsorption, ABCB1 prolonged the exposure of the drug substrate to the metabolizing enzymes. Hence, inhibition of ABCB1 would interfere with CYP3A mediated metabolism and decrease the systemic clearance of the drug substrate. The third generation of modulators like LY335979 /zosuquidar and CBT-1<sup>55</sup> were designed specifically for high transport affinity and low pharmacokinetic interaction<sup>6</sup>. Some of them inhibited multiple ABC transporters and this might extend the scope of possible side effects associated with these drugs. Despite the clear rationale for the use of inhibitors of ABCB1 to address MDR, results from recent clinical trials have not been encouraging<sup>56</sup>.

There are several reports in the literature describing the design of selective ABCG2 or ABCB1 inhibitors. Kuhnle and co-workers obtained a potent and selective ABCG2 inhibitor by introducing minor changes to the structure of tariquidar, a dual ABCG2/ABCB1 inhibitor<sup>57</sup>. Relatively simple modifications of the antiarrhythmic agent propafenone gave compounds that were either selective for ABCG2 or ABCB1<sup>58</sup>. It has been argued that specific inhibitors were desirable because they could be used to probe transporter function and thus advance the understanding of its function. They were anticipated to cause fewer unwelcomed effects as inhibition was targeted at a specific transporter. On the other hand, the multidrug resistance associated with tumors and malignancies are usually due to the over-expression of several transporters and the overlapping substrate specificities of the clinically relevant transporters would mean that most anticancer drugs are substrates of several

transporters<sup>59</sup>. Under these circumstances, a multi-targeting inhibitor would have greater clinical relevance.

In spite of divided opinions over the merits of a multi-targeting versus specific inhibitor, considerable effort has been directed towards investigating the structural features or physicochemical properties that characterize inhibitors of ABCB1 or ABCG2. Nicolle and co-workers have provided a comprehensive review on this topic<sup>41</sup>. Considerable work has been done in this area, particularly for ABCB1 inhibitors, but a caveat is that most of these investigations focused on congeneric series and results drawn from them may not be applicable to a structurally different class. Moreover, it is difficult to unambiguously assign a ligand as either a substrate of the transporter or an inhibitor of transport activity. Many compounds inhibit ABCB1 at high concentrations but function as substrates at lower concentrations<sup>36</sup>. The dual behavior of imatinib and gefitinib as substrate/ inhibitor of ABCG2 was mentioned earlier.

These limitations notwithstanding, some interesting results have emerged from QSAR and molecular modeling approaches. One study based on a database of diverse structures proposed that ABCB1 inhibitors were characterized by a lipophilicity (log P) value of  $\geq 2.92$ , length of the molecule (molecular axis)  $\geq 18$  atoms and the presence of a tertiary N atom<sup>60</sup>. SAR studies have been reported for several structural classes of ABCG2 inhibitors like fumitremorgin C (FTC) analogues<sup>61</sup>, taxanes<sup>62</sup>, tamoxifen analogues<sup>63</sup> and flavonoids<sup>64, 65, 66, 67, 68</sup>. Descriptors associated with most but not all inhibitors were lipophilicity<sup>69, 70</sup>, presence of a planar structure<sup>69</sup>, presence of groups for H bonding and  $\pi$ - $\pi$  interactions (molecular polarizability)<sup>70</sup> and abundance of N atoms<sup>70</sup>. The requirement for lipophilicity reflected the need for the inhibitor to reach the substrate binding site embedded within the lipid bilayer while the emphasis on interactions involving H bonds and  $\pi$  electron systems

was attributed to the abundance of aromatic and H bond donor side chains in the transmembrane domain of ABCG2<sup>70</sup>.

### 1.5. Flavonoids as MDR reversal agents

Flavonoids are a large class of polyphenolic compounds found abundantly present in dietary vegetables, fruits and plant-derived beverages<sup>64</sup>. They are associated with varied pharmacological properties like antioxidant, anti-inflammatory, antiproliferative, antiangiogenic and chemopreventive effects<sup>54, 71, 72</sup> and this has led to the widely held view that flavonoids play a preventive role against cancer, cardiovascular diseases and age-related diseases.

Flavonoids were reported to interact with clinically relevant ABC transporters like ABCB1 and ABCG2 as substrates and inhibitors. An early study by Conseil et al<sup>73</sup> proposed that flavonoids interacted with ABCB1 at two sites – the ATP binding site and a hydrophobic steroid binding domain adjacent to the ATP binding site. The affinity of the 4H-chromen-4-one ring, present in common flavonoids like flavones, isoflavones and flavonols, for the ATP binding site was anticipated in view of its structural resemblance to the adenine of ATP. Indeed, flavonoids are known to interact with various ATP binding proteins such as mitochondrial ATPase<sup>74</sup>, plasma membrane ATPases<sup>75, 76</sup> serine threonine kinases<sup>77</sup> and tyrosine protein kinase<sup>78</sup>. The interaction of the flavonoid with the ATP binding site of the transport protein would inhibit or stimulate transport activity. As a caveat, inhibition of ATPase activity does not necessarily mean that the flavonoid inhibits transporter activity and stimulation of ATPase activity does not always imply it is a substrate. For example, verapamil stimulated ABCB1-associated ATPase activity but inhibited transport activity<sup>79</sup>. In other instances, a flavonoid may compete with another substrate for binding, thus resulting in

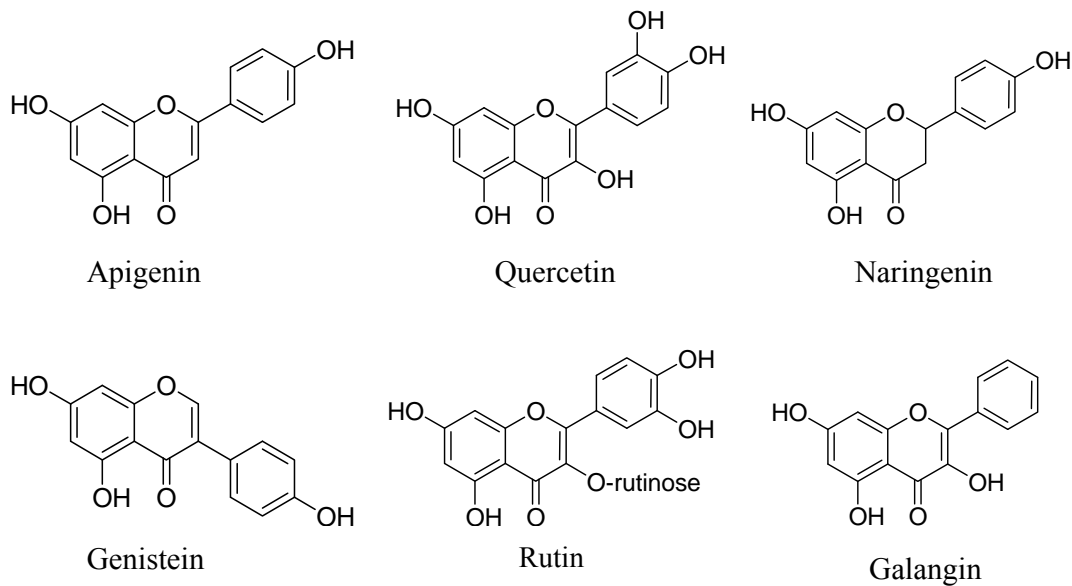
a diminished rate (“inhibition”) at which the affected substrate is effluxed by the transporter. The situation is further complicated by the presence of multiple binding sites on the transporter. It has been proposed that ABCB1 has at least two positively cooperative sites for drug binding and that binding to one site stimulated binding to the other site and its transport activity<sup>80</sup>. Concentration effects must also be considered. Quercetin and kaempferol were reported to have a biphasic effect on vincristine efflux, causing inhibition or enhancement depending on the test concentration employed<sup>81</sup>.

Considerable scientific effort has been invested to understand the modulatory properties of flavonoids on clinically relevant transporters. Flavonoids have the advantage of being relatively non-toxic compounds but their modulatory potencies were generally weak to moderate. In spite of their low toxicities, high doses were likely to cause a range of side effects in view of the broad spectrum of their biological activities. However, they serve as good lead structures and for this reason, considerable effort has been made to elucidate the structural requirements for interaction at specific transport proteins, in particular ABCB1 and ABCG2.

The interaction of flavonoids with ABCB1 has been extensively reviewed<sup>82, 83</sup>. In an investigation on the binding affinities of various flavonoids with the C-terminal nucleotide-binding domain (NBD2) of ABCB1, flavones (apigenin) and flavonols (quercetin) exhibited the strongest affinities, followed by other flavonoids which included flavonones (naringenin), isoflavones (genistein) and glycosylated derivatives (rutin)<sup>73</sup>. Starting from 3,4,5-trihydroxyflavone (galangin), it was found that introducing a 4'-iodo or 4'-n-octyl substituent to ring C enhanced binding affinities by 6- and 93-fold respectively<sup>84</sup>. The importance of lipophilic substituents was further emphasized in a series of flavonoid dimers where analogs with methyl groups at positions 3, 6 or 7 (but not 5) were more active than those with

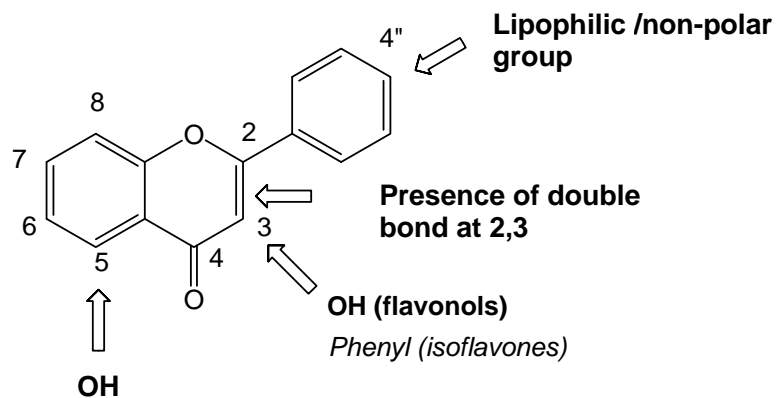
hydroxyl groups at the same positions<sup>85</sup>. Structures of the above-named flavonoids are given in Figure 1-3.

Figure 1-3: Structures of above-named flavonoids.



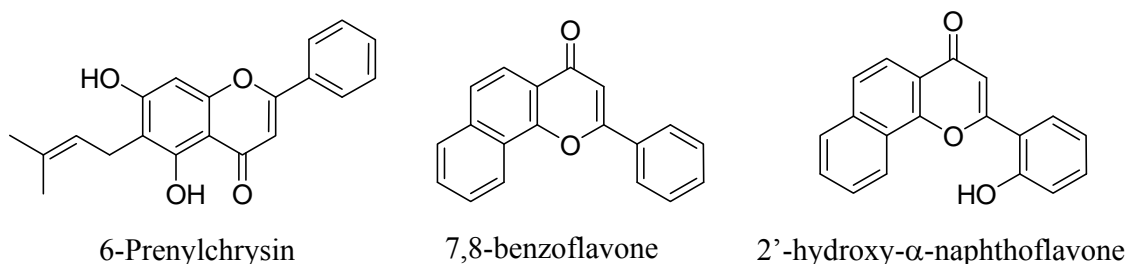
A general SAR profile was deduced from these investigations and key features are summarized in Figure 1-4. Desirable features were a phenyl group at C2 but not C3, a double bond at C2-C3, OH group at C3 and C5 and a lipophilic group at C4'.

Figure 1-4: Structural features of a flavone required for interaction with ABCB1. Features favorable for activities are depicted in bold, unfavourable features are in italicized fonts.



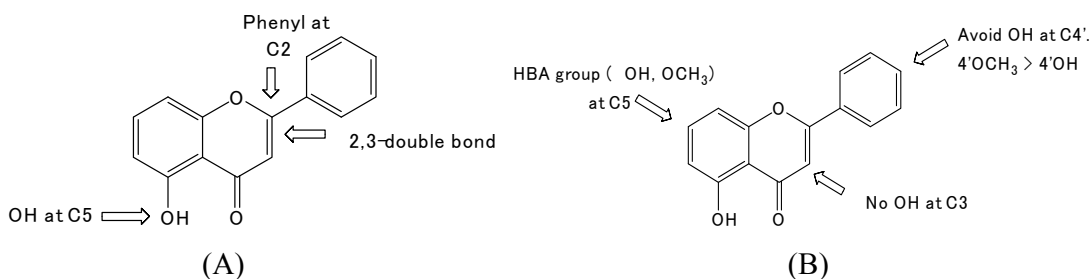
In spite of the late recognition as a clinically relevant transport protein, the SAR for flavonoid interaction with ABCG2 has been widely investigated and comprehensively reviewed<sup>41, 69, 83</sup>. Important structure activity relationships were derived by Zhang et al<sup>64, 86</sup> and Ahmed-Belkacem et al<sup>65</sup> from different flavonoid series employing related methods (accumulation of mitoxantrone and/or Hoechst 33342 in ABCG2-overexpressing human cancer cell lines) for quantifying affinity. Their studies highlighted the following structural features that were important for affinity: (i) Presence of 2,3-double bond, indicating the importance of maintaining a planar ring C; (ii) Phenyl at C2 and not C3 which would explain the poor affinity of isoflavones (genistein, daidzein) for ABCG2; (iii) OH groups at C5 and C7, with C5-OH proposed to have an important H bond donor role. Thus, replacement of C5-OH with C5-OCH<sub>3</sub> sharply reduced affinity whereas the same change at the C7-OH had marginal effects; (iv) Non-polar, lipophilic groups at C6, C7 and C8 of ring A greatly enhanced affinity, as seen from the active compounds (6-prenylchrysin, 7,8-benzoflavone, 2'-hydroxy- $\alpha$ -naphthoflavone) identified in these studies (Figure 1-5); (v) A methoxy group at C4' of ring B is preferred to a 4'-OH group or an unsubstituted ring.

Figure 1-5: Structures of 6-prenylchrysin, 7,8-benzoflavone, 2'-hydroxy- $\alpha$ -naphthoflavone.



While there are many similarities in the structural requirements for good affinities to ABCB1 and ABCG2, significant differences are also evident. These are (i) C3-OH which is favorable for ABCB1 but not ABCG2; (ii) A hydrophilic group like OH at C4' of ring C is better tolerated for ABCB1 than ABCG2 interaction; (iii) The presence of C7-OH favors ABCG2 interaction to a greater degree than ABCB1 interaction. It was proposed that the role of C7-OH was that of a H bond acceptor. When replaced by a C7-OCH<sub>3</sub>, improved activity was observed. Figure 1-6 summarizes the (A) shared features required for interactions at both proteins and (B) key features required for ABCG2 but not ABCB1 interaction.

Figure 1-6: (A) Common requirements for both ABCB1 and ABCG2; (B) Requirements for ABCG2 but not ABCB1.

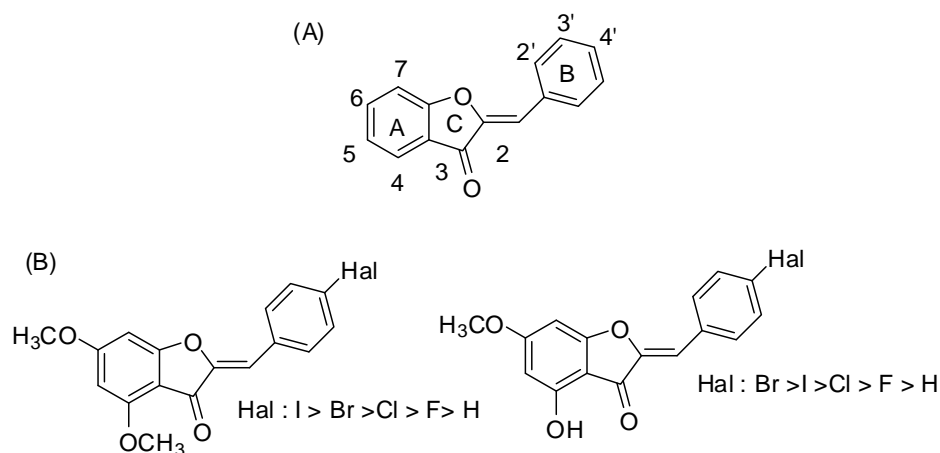


### 1.6. Aurones as modulators of ABC transporter proteins

Aurones are a subset of flavonoids and are structural isomers of flavones (Figure 1-7). They possess a variety of biological activities such as chemoprevention, anti-bacterial, anti-cancer, anti-parasitic activities and modulation of P-gp activity<sup>87, 88</sup>. Boumendjel and co workers were the first to report that aurones bind to the C-terminal cytosolic domain of

mouse ABCB1<sup>89</sup>. By applying the structural criteria previously found to enhance binding of flavones to ABCB1, they obtained B-ring halogenated aurones with improved binding affinities. The C-terminal cytosolic domain comprised a steroid-interacting hydrophobic region in close proximity to the ATP binding site and the authors proposed that ring B of the aurones overlapped with the hydrophobic site while the rings A and C interacted with the ATP binding site.

Figure 1-7: (A) Structure of aurone (B) Halogenated 4,6-dimethoxyaurones and 4-hydroxy-6-methoxyaurones identified by Boumendjel et al<sup>89</sup> to have strong binding affinities to the C-terminal cytosolic domain of ABCB1.



In another investigation, nanomolar concentrations of 4,6-dimethoxyaurone were found to increase the uptake of the rhodamine 123 into an ABCB1-overexpressing cancer cell line (K562)<sup>54</sup>. The authors commented that it was unusual for a non-nitrogen containing compound to exhibit this level of reversal activity and compared the aurone with the inactivity of its flavone analog (5,7-dimethoxyflavone). 4,6-Dimethoxyaurones with halogens on ring B were subsequently reported to increase the uptake of paclitaxel into ABCB1-overexpressing breast cancer cells<sup>90</sup>. They were found to be more active than other flavonoids (flavones, chalcones, flavonols) that were concurrently investigated. The authors also concluded there was no correlation between binding affinities of these compounds for the C-



terminal cytosolic domain of ABCB1 and their ability to increase paclitaxel transport into cells with high ABCB1 content.

In spite of the interesting reversal properties of aurones in ABCB1 over-expressing cell lines, no follow up investigation was carried out to expand the number of analogs investigated or to determine the structural features that contributed to their promising activity. Neither were they investigated to determine if they had similar effects on other clinically relevant ABC transport proteins.

### 1.7. Statement of Purpose

The preceding sections (1.5, 1.6) have provided an overview of the propensity of flavonoids to interact with the clinically relevant ABC transport proteins ABCB1 and ABCG2. Of particular interest were the reports on the activity of a lesser known group of flavonoids (methoxylated aurones) to increase the uptake of ABCB1 substrates (rhodamine 123, paclitaxel) into human cancer cell lines that over-express ABCB1 and their greater potencies compared to other flavonoids that were concurrently investigated<sup>54, 90</sup>. There is a strong likelihood that the modulatory activity of aurones observed with ABCB1 may be extended to ABCG2, as observed for other flavonoids like chalcones<sup>91</sup> and flavones<sup>65</sup>. The structural similarity between the benzofuranone ring of the aurone and adenine of ATP may lead to an interaction at the nucleotide binding domains of these transporters. A related interaction has been proposed for a functionalized 4,6-dihydroxyaurone with the ATP binding site of cyclin-dependent kinase 2 (CDK2)<sup>92</sup>. Additional interactions with the substrate binding site of the transport proteins, depending on other pendant groups attached to the scaffold, cannot be discounted.

To examine this hypothesis, a series of functionalized aurones were synthesized and evaluated for their ability to interact with ABCG2 in functional assays. These in vitro assays

were (i) the accumulation of the ABCG2 substrates pheophorbide A and mitoxantrone in ABCG2-overexpressing human breast cancer MDA-MB-231/R cells; (ii) re-sensitization of the same cells to the growth inhibitory effects of mitoxantrone and (iii) effects on ABCG2 ATPase activity and photoaffinity labeling of ABCG2 with [<sup>125</sup>I] Iodoarylazidoprazosin (IAAP). The latter experiments were carried out by a collaborator. A preliminary in vivo evaluation was performed to determine if a representative aurone could prolong the survival of mitoxantrone-treated mice bearing an ABCG2-overexpressing tumor xenograft. These investigations would provide insight into the nature of the interactions induced by aurones at ABCG2 as well as the structural features that promoted these interactions.

Clinical multi-drug resistance is normally mediated by the expression of multiple drug efflux pumps in the tumor or malignancy<sup>93</sup>. Hence, modulators that target more than one ABC transport protein are clinically more useful, notwithstanding concerns over a likely expanded list of drug-drug interactions and side effects associated with such agents. Although aurones have been reported to interact with ABCB1, little is known of the structure-activity relationships involved in this interaction. It is also not known if there are overlapping structural requirements for activity at ABCB1 and ABCG2 for this scaffold. The availability of this information would help to “design in” or “design out” appropriate features to give specific or dual targeting modulators of ABCB1 and ABCG2, as the need arises. For this reason, the synthesized aurones were also investigated for their effects on the uptake of calcein acetyoxymethyl ester (calcein-AM, CAM) by Mardin-Darby canine kidney (MDCK) cells that over-express the ABCB1 protein. In this way, comparative structure-activity relationships for aurones at these two clinically relevant transport proteins could be deduced to guide future lead-optimization.

The potential of the aurones as modulators of ABCB1 and ABCG2 activities is clearly under-explored, in terms of the structural features required for interaction, the

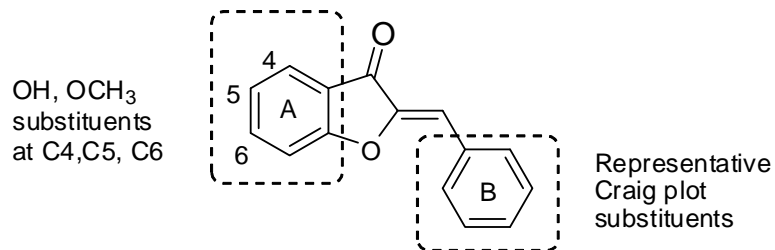
mechanisms involved and the clinical potential of these interactions. The objective of this thesis is to address some of these issues and provide insight that will stimulate and drive further research in this promising class of compounds.

## Chapter 2: Design and Synthesis of Target Compounds

### 2.1. Introduction

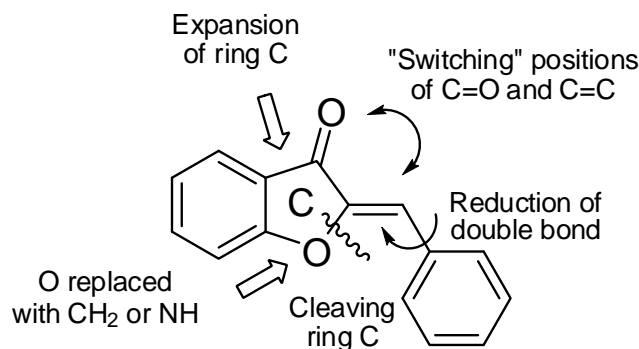
This chapter describes the design and synthesis of compounds targeted for interaction with the ATP-binding cassette (ABC) transport proteins ABCB1 (P-glycoprotein, P-gp) and ABCG2 (breast cancer resistance protein, BCRP). In total, 112 compounds were investigated, of which more than half bear the aurone template in keeping with the focus of the thesis. Variations among these compounds were restricted to rings A and B (Figure 2-1), with more modifications at ring B than ring A.

Figure 2-1: Summary of modifications made to rings A and B of functionalized aurones.



The remaining compounds were obtained by changing ring C of the aurone template. The variations made to ring C are summarized in Figure 2-2. As these compounds no longer retain the aurone scaffold, they served the purpose of injecting chemical diversity into the target compounds.

Figure 2-2: Summary of modifications made to ring C of the aurone template.



Of the 112 compounds, 65 (58%) were synthesized by the author while the remaining were synthesized by previous graduate students of the laboratory. The synthesis and characterization of the latter compounds were not presented in this chapter as they had been reported in the literature. However, the rationale for their inclusion would be discussed. The sources of these previously synthesized compounds are : 4,6-dimethoxyaurones (**1-1** to **1-11**, **1-13**, **1-15** to **1-19**, **1-22**, **1-23**); aurones (**5-2**, **5-4**), 4,6-dimethoxydehydroaurones (**8-1**,**8-2**), hydroxyaurones (Series **3** and **4**), 4,6-dimethoxyisaurones and 5-hydroxyisaurones (Series **9**) from Dr Lee CY<sup>71</sup>; azaaurones (**7-9**, **7-10**), benzylideneindolinones (**10-1** to **10-3**) from Dr Zhang W<sup>94</sup> and chalcones (**11-6** to **11-8**) from Dr Liu M<sup>95</sup>. These compounds which were of at least 95% purity and stored in their crystalline states at  $\leq 25^{\circ}\text{C}$ , were used as received from the respective sources.

## 2.2. Rationale of design

There were 8 distinct scaffolds among the 112 compounds. They were 2-benzylidenebenzofuran-3(2H)-ones (aurones), 3-benzylidenebenzofuran-2(3H)-ones (isaurones), 2-benzyl-benzofuran-3-ones (dehydroaurones), 2-benzylidene-2,3-dihydro-1H-inden-1-ones (referred to as “indanones” in this chapter), 2-benzylidene indolin-3-one (aza-aurones), 3-benzylidene indolin-2-ones (referred to as “indolinones” in this chapter), chalcones and flavones. The lead scaffold in this thesis was the aurone and it was selected for structural manipulation for the following reasons:

(i) Dimethoxyaurones were reported to have potent reversal effects on the uptake of ABCB1 substrates into ABCB1 over-expressing human cancer cell lines<sup>54,90</sup>. Four 4,6-dimethoxyaurones were identified in these two reports and their reversal effects exceeded that of other flavonoids like flavones, flavonols and chalcones investigated under similar experimental conditions.

(ii) A bifunctional interaction was proposed to account for the submicromolar binding affinities of ring B halogenated 4,6-dimethoxyaurones and 4-hydroxy-6-methoxyaurones with the C-terminal cytosolic domain of mouse ABCB1<sup>89</sup>. The interaction involved the overlap of the benzofuranone ring (rings A/C) of the aurone with the ATP binding site, and the non-polar halogenated ring B with a proposed “steroid-interacting” hydrophobic domain close to the ATP binding site. The structural mimicry of the benzofuranone template with adenine of ATP was alluded in another report<sup>92</sup>. The same mimicry was proposed for the chromenone ring of flavones to explain their binding affinities for the C-terminal cytosolic domain of ABCB1<sup>82</sup>.

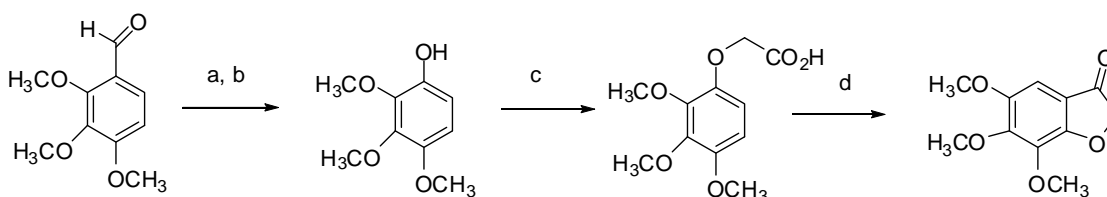
#### 2.2.1. Series 1-5

Functionalization of the aurone template was carried out to give a comprehensive series of compounds (Series 1-5) from which useful structure-activity relationships could be extracted to delineate requirements for the modulation of ABCB1 and ABCG2 activities.

Modifications on ring A were limited to the introduction of methoxy or hydroxyl groups, or to leave the ring in an unsubstituted state. The choice of 4,6-dimethoxy groups (Series 1) was prompted by the presence of these groups in all four aurones reported to have excellent modulatory properties on ABCB1<sup>54, 90</sup>. 4,6-Dihydroxyaurones (Series 3) were included because hydroxyl groups were proposed to play a critical role in the ABCG2 modulatory properties of flavones<sup>64, 65, 66</sup>. On the flavone, the C5-OH group (corresponding to C4-OH in aurone) was reported to be involved as a H bond donor, the C7-OH (corresponding to C6-OH in aurone) as a H bond acceptor and a non-polar group was recommended at position 6 (corresponding to C5 in aurone). Thus, two series of hydroxylated aurones are prepared: Series 3 (4,6-dihydroxyaurones) and Series 4 (5-hydroxyaurones and 6-hydroxyaurones). If the SAR for hydroxylated flavones held true for the aurones, then the 5-hydroxyaurones were anticipated to be less active than the 6-

hydroxyaurones. Ideally, a series of 4-hydroxyaurones would provide interesting comparisons to 6-hydroxyaurones and 4,6-dihydroxyaurones but this series was not synthesized.

A small number of 4,5,6-trimethoxyaurones (Series 2) were included to investigate the effect of added bulk and an additional H bond acceptor on ring A. The original plan was to investigate the regioisomeric 5,6,7-trimethoxyaurones because these compounds were reported to have significant growth inhibitory properties on cancer cells<sup>88</sup>. A compound that combined potent growth inhibition with the ability to increase transport of affected drug-substrates into resistant tumors was an attractive proposition. Unfortunately, the synthesis of 5,6,7-trimethoxybenzofuran-(2H)-3-one which involved the Baeyer-Villiger oxidation of the benzaldehyde to give a phenol, reaction with chloroacetic acid and then ring closure, proceeded with very low yields (Scheme 2-1). Hence, the decision was made to concentrate on the synthetically more tractable 4,5,6-trimethoxyaurones.



Scheme 2-1<sup>88</sup> Reagents and conditions: (a) m-CPBA, DCM, rt, 18 h. (b) NaOMe, MeOH, rt, 4 h. (c) Chloroacetic acid, NaH, DMF, rt, overnight. (d) Polyphosphoric acid, 80° C, 8 h.

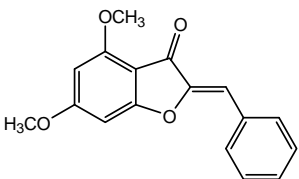
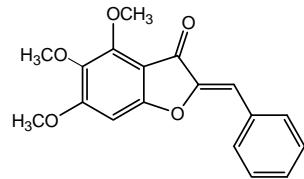
The scaffolds in Series 1-5 were of varying lipophilicities. Taking the unsubstituted ring B analog of each series as an example, estimated lipophilicities ranged from 2.7 to 3.3 (SlogP from MOE 2008.10, Chemical Computing Group), 2.5 to 4.0 (ClogP, ChemDrawUltra Ver 7) and 3.2 to 3.7 (LogPo/w, MOE 2008.10, Chemical Computing Group) (Table 2-1). Based on SlogP values, the trimethoxy and dimethoxyaurones (**1-1**, **2-1**) were the most lipophilic, followed by the ring A unsubstituted aurone (**5-1**),

monohydroxyaurones (**4-1**, **4-4**) and dihydroxyaurone (**3-1**). Therefore, the activities of Series 1-5 would provide insight as to how lipophilicity affected the interaction with ABCG2.

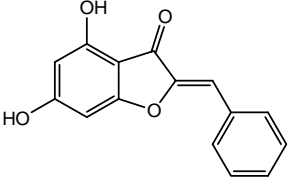
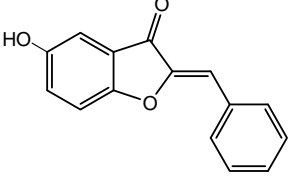
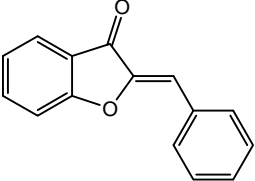
Three different estimated lipophilicity parameters were obtained for the compounds and as seen from Table 2-1, they differed quantitatively and also gave distinct rankings to compounds based on these values. In general, it is preferred that the same lipophilicity measure be used in a report and here, SlogP was selected because some of the compounds had ionizable groups (Series 7) and their lipophilicities would be better represented by SlogP than the other estimates. SlogP originated from an atomic contribution model (ca 7000 compounds in the training set) that calculated the partition coefficient (logP) of compounds in their correct protonation states (“washed structures”)<sup>96</sup>.

Different substituents were introduced on the ring B of each series. Substitutions were selected primarily to give a broad coverage of lipophilicity (Hansch  $\pi$ ) and electron-withdrawing/-donating (Hammett  $\sigma$ ) properties, as defined by the Craig Plot<sup>97</sup>. Substitution on ring B was expected to influence the physicochemical profile, and depending on its bulk and position on ring B, the conformational orientation of the final compound.

Table 2-1: Structures and estimated lipophilicities (SlogP<sup>a</sup>, LogP(o/w)<sup>b</sup>, ClogP<sup>b</sup>) of unsubstituted ring B compounds for Series 1-5.

Compound	Structure	SlogP	LogP	ClogP
1-1		3.320	3.768	4.034
2-1		3.329	3.187	3.264



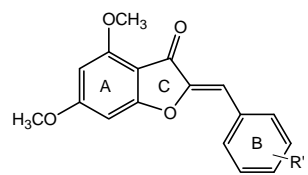
3-1		2.714	3.240	3.688
4-1		3.008	3.513	2.475
5-1		3.303	3.784	4.051

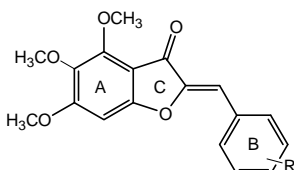
<sup>a</sup> SlogP is the estimated lipophilicity in octanol/water of the compound in its protonated state.

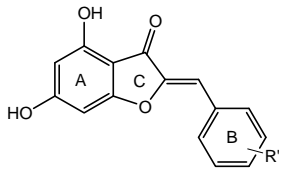
<sup>b</sup> LogP and ClogP are estimated lipophilicities in octanol/water of the compound in its neutral /non-protonated state.

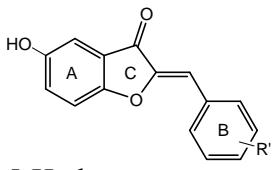
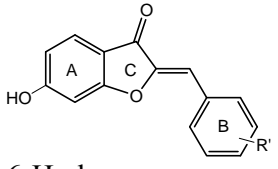
The larger number of ring B substituents in Series 1 was prompted by the findings of preliminary investigations on some compounds (**1-1** to **1-15**) and their effects on the accumulation of mitoxantrone by ABCG2 overexpressing breast cancer cells. It was observed that greater activity was associated with groups at 3' position of ring B, regardless of the electron donating/withdrawing character of the group. To confirm these findings, more groups (trifluoromethyl, fluoro, dimethoxy, dihydroxy, methoxy-hydroxy) were introduced on ring B, and where possible, at 2', 3' and 4' positions to determine if the 3' position was consistently advantageous. The structures of compounds in Series 1-5 and their SlogP values are given in Table 2-2.

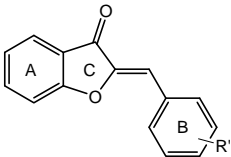
Table 2-2: Structures and estimated lipophilicities (SlogP) of Series 1-5 compounds

Compound	R'	SlogP <sup>a</sup>	
 <p>4,6-Dimethoxy aurones (Series 1)</p>	1-1	H	3.320
	1-2	2'-OCH <sub>3</sub>	3.329
	1-3	3'-OCH <sub>3</sub>	3.329
	1-4	4'-OCH <sub>3</sub>	3.329
	1-5	2'-OH	3.026
	1-6	3'-OH	3.026
	1-7	4'-OH	3.026
	1-8	2'-Cl	3.973
	1-9	3'-Cl	3.973
	1-10	4'-Cl	3.973
	1-11	2'-CH <sub>3</sub>	3.628
	1-12	3'-CH <sub>3</sub>	3.628
	1-13	4'-CH <sub>3</sub>	3.628
	1-14	3'-CN	3.192
	1-15	4'-CN	3.192
	1-16	2'-F	3.459
	1-17	3'-F	3.459
	1-18	4'-F	3.459
	1-19	4'-CF <sub>3</sub>	4.650
	1-20	3'-OH, 4'-OCH <sub>3</sub>	3.034
	1-21	3'-OCH <sub>3</sub> , 4'-OH	3.034
	1-22	2', 3'-(OH) <sub>2</sub>	2.731
	1-23	2', 4'-(OH) <sub>2</sub>	2.731
	1-24	3', 4'-(OH) <sub>2</sub>	2.731
	1-25	3', 4'-(OCH <sub>3</sub> ) <sub>2</sub>	3.337
	1-26	3', 5'-(OCH <sub>3</sub> ) <sub>2</sub>	3.337
	1-27	3', 4'-F <sub>2</sub>	3.598
	1-28	3', 5'-F <sub>2</sub>	3.598

	Compound	R'	SlogP
	2-1	H	3.329
	2-2	2'-Cl	3.982
	2-3	3'-Cl	3.982
	2-4	4'-Cl	3.982
	2-5	2'-OCH <sub>3</sub>	3.337
	2-6	3'-OCH <sub>3</sub>	3.337
4,5,6-Trimethoxy aurones (Series 2)	2-7	4'-OCH <sub>3</sub>	3.337
	2-8	3'-CN	3.200
	2-9	3'-OH	3.034
	2-10	3'-CH <sub>3</sub>	3.637
	2-11	cyclohexane <sup>b</sup>	3.752

	Compound	R'	SlogP
	3-1	H	2.714
	3-2	2'-OCH <sub>3</sub>	2.723
	3-3	3'-OCH <sub>3</sub>	2.723
4,6-Dihydroxy aurones (Series 3)	3-4	4'-Cl	3.367
	3-5	3'-OCH <sub>3</sub> , 4'-OH	2.428

	Compound	R'	SlogP
	4-1	H	3.008
	4-2	2'-OCH <sub>3</sub>	3.017
	4-3	4'-Cl	3.662
5-Hydroxy aurones (Series 4)			
	4-4	H	3.008
	4-5	2'-OCH <sub>3</sub>	3.017
	4-6	4'-Cl	3.662
6-Hydroxy aurones (Series 4)			

	Compound	R'	SlogP
 Unsubstituted aurones (Series 5)	5-1	H	3.303
	5-2	2'-OH	3.008
	5-3	3'-OH	3.008
	5-4	2'-Cl	3.956
	5-5	3'-Cl	3.956
	5-6	3'-OCH <sub>3</sub>	3.311
	5-7	3'-CN	3.175
	5-8	3'-CH <sub>3</sub>	3.611

<sup>a</sup> SlogP is the estimated lipophilicity in octanol/water of the compound in its protonated state.

<sup>b</sup> Phenyl ring B is replaced by a cyclohexyl ring

#### 2.2.2. Series 6-12

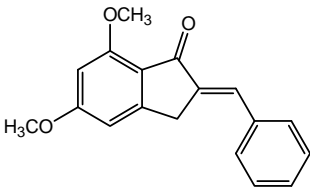
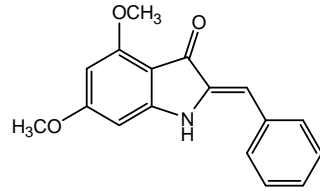
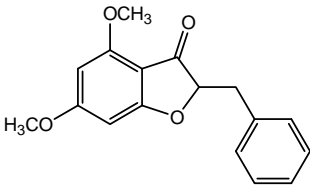
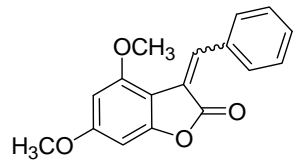
Thus far, changes had been limited to varying the type of groups at rings A and B to give the functionalized aurones of Series 1-5. In Series 6-12, the focus was on modifying ring C to give chemically more diverse ring templates.

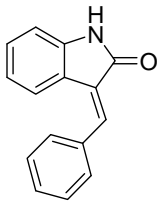
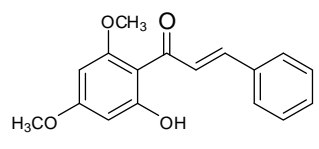
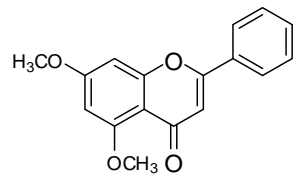
The oxygen atom of ring C was replaced by a methylene (CH<sub>2</sub>) group to give the benzylideneindanones (“indanones”) of Series 3 or nitrogen (NH) to give azaaurones of Series 4. The consequences of these changes were as follows:

(i) Loss of a H bond acceptor moiety when oxygen was replaced with methylene (CH<sub>2</sub>) in indanones. The H bond acceptor property of NH in azaaurones was anticipated to be poor because the lone pair of electrons on NH would be mesomerically withdrawn by the adjacent exocyclic double bond on ring A. Hence, the azaaurones were anticipated to be weak bases with pK<sub>a</sub> estimated to be less than 6. On the other hand, the NH in azaaurone is a H bond donor and this may influence its permeability /solubility properties.

(ii) Change in lipophilicity. For the same groups on rings A and B, the indanone analog was expected to be more lipophilic than the aurone and azaaurone analogs. As seen from the unsubstituted ring B analogs **1-1**, **6-1** and **7-1** as representative compounds, SlogP values were 3.32, 3.53 and 3.35 respectively. The SlogP of the azaaurone **7-1** should be for the protonated state, in which case the non-protonated azaaurone should have a higher SlogP and apparently more lipophilic than the aurone **1-1** (SlogP 3.320). However when the ClogP and LogP values of azaaurone (**7-1**) and aurone (**1-1**) were compared (these are for the neutral state of compound), the azaaurone was seen to be less lipophilic (Tables 2-3)

Table 2-3: Structures, SlogP, logP and ClogP of unsubstituted ring B compounds in Series 6-12.

Compound	Structure	SlogP <sup>a</sup>	LogP <sup>b</sup>	ClogP <sup>b</sup>
6-1		3.526	3.873	3.847
7-1		3.353	3.540	3.478
8-1		2.890	3.216	3.278
9-1		3.163	3.865	3.751

10-1		3.179	3.239	3.230
11-1		3.306	3.739	4.004
12-1		3.320	3.370	3.621

<sup>a</sup> SlogP is the estimated lipophilicity in octanol/water of the compound in its protonated state.

<sup>b</sup> LogP and ClogP are estimated lipophilicities in octanol/water of the compound in its neutral /non-protonated state.

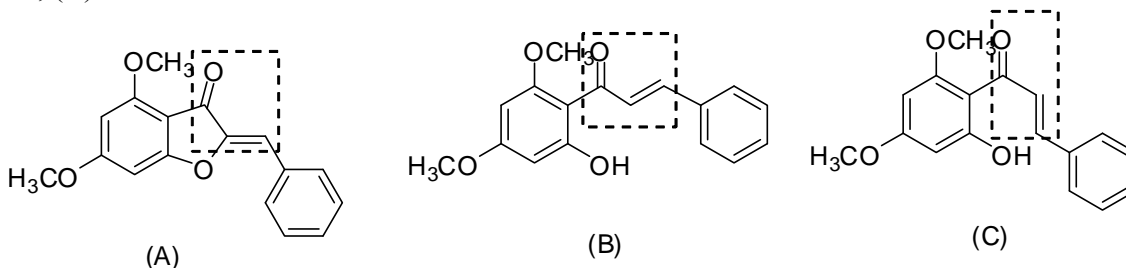
Rings A of the indanones (Series 6) and the majority of azaaurones (Series 7) were substituted with 4,6-dimethoxy groups to facilitate comparison to 4,6-dimethoxyaurones (Series 1). The same substitution pattern was retained for other compound series (8, 9, 11, 12) for the same reason.

The exocyclic double bond of the aurone was reduced to give dehydro analogs (Series 8). The consequences of this modification were the loss of the Michael acceptor moiety ( $\alpha\beta$ -unsaturated ketone) and the *E-Z* isomerism associated with the double bond. There was now a chiral carbon at C2 and ring B was attached to ring C by a more flexible carbon chain which had 2 rotatable bonds, compared to one rotatable bond in the aurone. The dehydroaurones were less lipophilic than the aurones.

The location of the carbonyl and exocyclic bonds in aurones were “switched” to give the regioisomeric isoaurones (Series 9). Interestingly, in spite of their structural similarity to aurones, the isoaurones were not as lipophilic as the corresponding aurones (SlogP of **1-1** = 3.320; **9-1** = 3.163). A similar “switch” was made for the carbonyl and exocyclic double bonds of azaaurones to give the indolinones of Series 10. A similar decrease in lipophilicity was observed (SlogP of **7-9** = 3.345; **10-1** = 3.179).

Cleavage of the bond between the oxygen and C2 of the aurone template gave the chalcones of Series 11. Ring A of the chalcone had the same dimethoxy groups as the Series 1 aurones. In addition, a C2 OH from the oxygen atom of the cleaved ring C was present. Also included in Series 11 were chalcones (**11-6** to **11-8**) with only a C2 OH on ring A. Comparisons with the chalcones would report on the importance of the following features for activity: (i) the planar benzofuranone ring (rings A/C) and in particular, the retention of ring C and (ii) the number of rotatable bonds in the scaffold as the chalcones were more flexible due to a greater number (3) of rotatable bonds linking rings A and B. Conformationally, the Michael acceptor moiety in chalcones could assume an *s-cis* or *s-trans* conformation<sup>98</sup>. Most chalcones were *s-cis* but one report showed that substituting the carbon adjacent to the carbonyl (C $\alpha$ ) favored the *s-trans* conformation<sup>99</sup> (Figure 2-3). The chalcone **11-1** was of comparable lipophilicity to the aurone **1-1**.

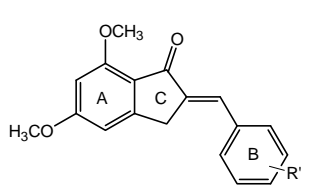
Figure 2-3: Conformation of the  $\alpha\beta$ -unsaturated enone: (A) Aurone: *s-cis*; (B) Chalcone: *s-cis*; (C) Chalcone: *s-trans*.



Series 12 comprise 5,7-dimethoxyflavones and they are investigated because of their isomeric relationship to Series 1 aurones. Increasing the size of ring C of the aurone by an additional carbon atom and changing the double bond from an exocyclic to an endocyclic position gave ring C of the flavone. Both rings retained the Michael acceptor moiety but with an *s-trans* conformation in flavone compared to *s-cis* in aurone. Lipophilicities of the two templates, based on SlogP values, were well matched. Flavones were recognized for their ability to modulate ABCG2 activity<sup>65, 66, 100</sup> and it would be of interest to compare their activities with the aurones.

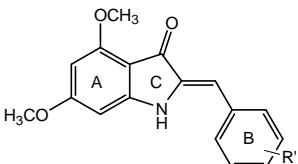
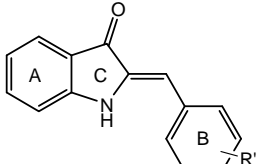
The structures of compounds in Series 6-12 and their SlogP values are given in Table 2-4. Groups on ring B of these series were mostly those associated with promising activity in Series 1.

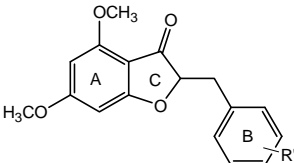
Table 2-4: Structures and SlogP values of Series 6-12 compounds

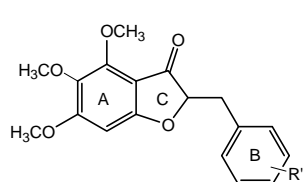
	Compound	R'	SlogP
 <p>4,6-Dimethoxy indanonones (Series 6)</p>	6-1	H	3.526
	6-2	2'-OCH <sub>3</sub>	3.535
	6-3	3'-OCH <sub>3</sub>	3.535
	6-4	4'-OCH <sub>3</sub>	3.535
	6-5	3'-OH	3.232
	6-6	4'-OH	3.232
	6-7	2'-Cl	4.180
	6-8	3'-Cl	4.180
	6-9	4'-Cl	4.180
	6-10	3'-CN	3.398
	6-11	4'-CN	3.398
	6-12	2'-CH <sub>3</sub>	3.835
	6-13	3'-CH <sub>3</sub>	3.835
	6-14	4'-CH <sub>3</sub>	3.835
	6-15	3', 5'-(OCH <sub>3</sub> ) <sub>2</sub>	3.543



6-16	3', 5'-(OH) <sub>2</sub>	2.937
6-17	3'-OCH <sub>3</sub> , 4'-OH	3.240
6-18	3'-OH, 4'-OCH <sub>3</sub>	3.240
6-19	3', 4'-(OH) <sub>2</sub>	2.937
6-20	3', 4'-(OCH <sub>3</sub> ) <sub>2</sub>	3.543

	Compound	R'	SlogP
 <p>4,6-Dimethoxy azaaurones (Series 7)</p>	7-1	H	3.353
	7-2	3'-OCH <sub>3</sub>	3.362
	7-3	4'-OCH <sub>3</sub>	3.362
	7-4	3'-Cl	4.007
	7-5	4'-Cl	4.007
	7-6	3'-CN	3.225
	7-7	3'-CH <sub>3</sub>	3.662
	7-8	3'-OH	3.059
	7-9	3'-OCH <sub>3</sub>	3.345
7-10	3'-OH, 4'-OCH <sub>3</sub>	3.050	
 <p>Unsubstituted azaaurones (Series 7)</p>			

	Compound	R'	SlogP
 <p>4,6-Dimethoxy dehydroaurones (Series 8)</p>	8-1	H	2.890
	8-2	2'-OH	2.596



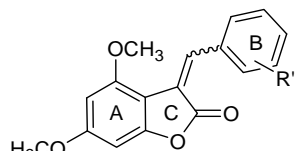
8-3

4'-OCH<sub>3</sub>

2.907

4,5,6-Trimethoxy  
dehydro aurones  
(Series 8)

Compound	R'	SlogP
----------	----	-------



9-1

H

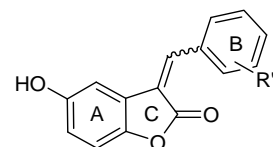
3.163

9-2

4'-Cl

3.817

4,6-Dimethoxy  
isoaurones (Series 9)



9-3

H

2.852

9-4

2'-OCH<sub>3</sub>

2.860

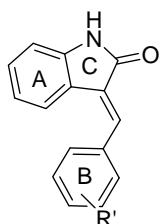
9-5

4'-Cl

3.505

5-Hydroxy  
isoaurones (Series 9)

Compound	R'	SlogP
----------	----	-------



10-1

H

3.179

10-2

3'-Cl

3.833

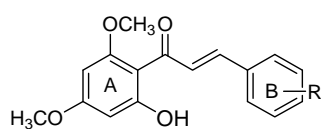
10-3

3', 5'-(OCH<sub>3</sub>)<sub>2</sub>

3.197

Unsubstituted  
indolinones  
(Series 10)

Compound	R	SlogP
----------	---	-------



11-1

H

3.306

11-2

3-OCH<sub>3</sub>

3.314

11-3

4-OCH<sub>3</sub>

3.314

2'-Hydroxy,4',6'-  
dimethoxy chalcones  
(Series 11)

11-4

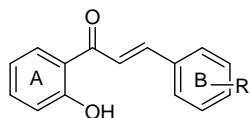
3, 4-(OCH<sub>3</sub>)<sub>2</sub>

3.323

11-5

3, 5-(OCH<sub>3</sub>)<sub>2</sub>

3.323



	11-6	4-Cl	3.942
	11-7	4-CH <sub>3</sub>	3.597
2'-Hydroxy chalcones (Series 11)	11-8	4-OCH <sub>3</sub>	3.297

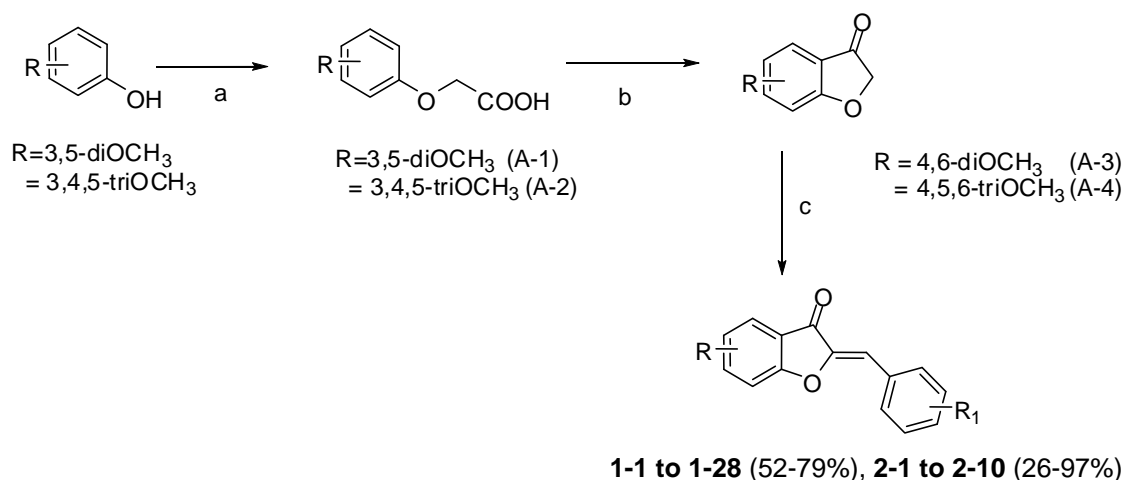
	Compound	R'	SlogP
	12-1	H	3.320
	12-2	3'-OCH <sub>3</sub>	3.329
	12-3	4'-OCH <sub>3</sub>	3.329
	12-4	3', 4'-(OCH <sub>3</sub> ) <sub>2</sub>	3.337
	12-5	3', 5'-(OCH <sub>3</sub> ) <sub>2</sub>	3.337

5,7-Dimethoxy flavones  
(Series 12)

## 2.3. Chemical considerations

### 2.3.1. Aurones (Series 1, 2, 5) and Dehydroaurones (Series 8)

4,6-Dimethoxyaurones (Series 1) and 4, 5, 6-trimethoxyaurones (Series 2) were synthesized by reported methods<sup>88, 101</sup>. As shown in Scheme 2-2, the reaction involved the condensation of 3, 5-dimethoxyphenol or 3, 4, 5-trimethoxyphenol with chloroacetic acid in the presence of sodium hydride to give the corresponding phenoxyacetic acid (Step a). This was followed by an intra-molecular Friedel-Craft acylation in the presence of polyphosphoric acid to form the benzofuranone ring (Step b). Base-catalysed aldol condensation of the benzofuranone with a substituted benzaldehyde gave the desired aurone (Step c).

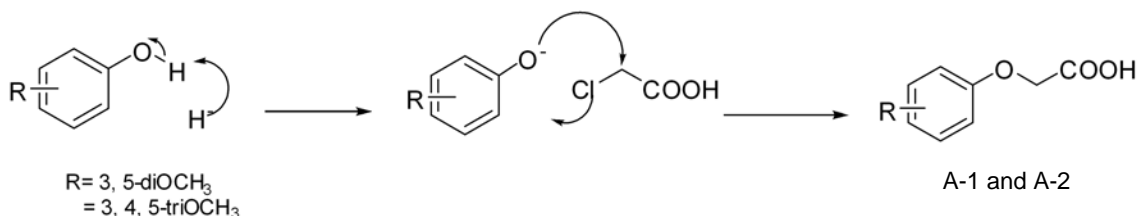


Scheme 2-2 Reagents and conditions: (a) Chloroacetic acid (1.1 eq), NaH, DMF, r.t., 12 h. (b) Polyphosphoric acid, 80° C, 8 h. (c) R-substituted benzaldehyde, 50% KOH in MeOH/H<sub>2</sub>O, r.t., 3 h.

In Step (a), sodium hydride deprotonated the reacting phenol to give the phenoxide anion which then attacked the electron deficient  $\alpha$  carbon of chloroacetic acid with displacement of the chloride ion to give the methoxylated phenoxyacetic acid (Figure 2-4). To ensure that deprotonation of phenol was not hampered by the presence of chloroacetic

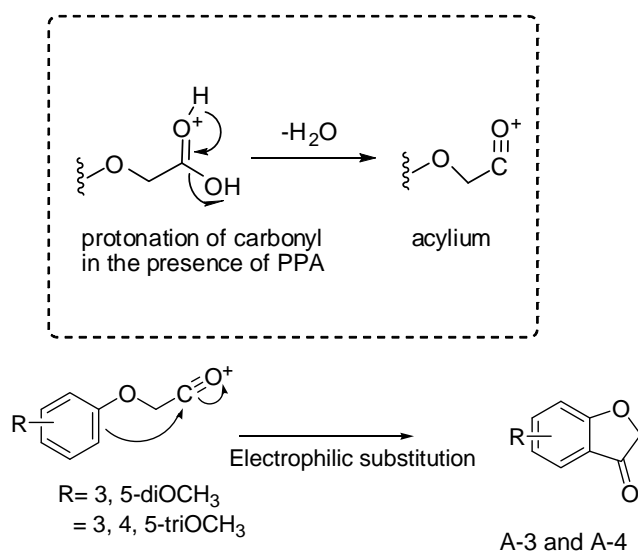
acid, the phenol and sodium hydride were stirred together before the dropwise addition of chloroacetic acid.

Figure 2-4: Formation of 3, 5-dimethoxyphenoxyacetic acid (A-1) and 3, 4, 5-trimethoxyphenoxyacetic acid (A-2).



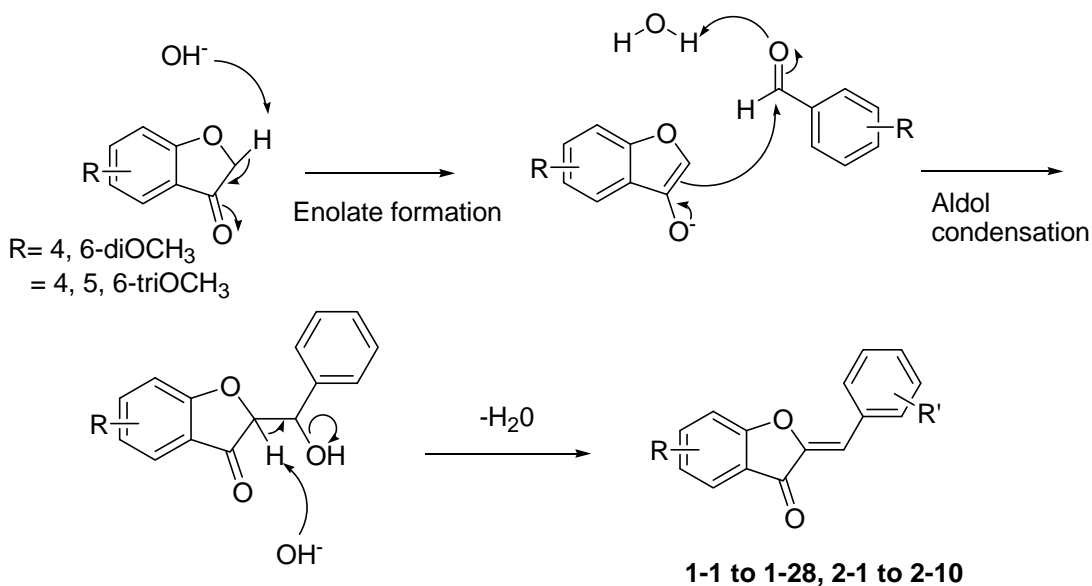
In Step (b), polyphosphoric acid served as the Lewis acid and protonated the carbonyl oxygen of the phenoxyacetic acid, thereby promoting the loss of water and formation of the electron deficient acylium ion (Figure 2-5). The latter acted as an electrophile in the ensuing Friedel-Craft reaction, resulting in intramolecular cyclization and formation of the benzofuran-3-one ring. The phenyl ring was activated for electrophilic attack by the electron donating methoxy groups which were ortho or para to the carbon atom involved in the cyclization reaction.

Figure 2-5: Intramolecular Friedel-Craft acylation to form (A-3) and (A-4).

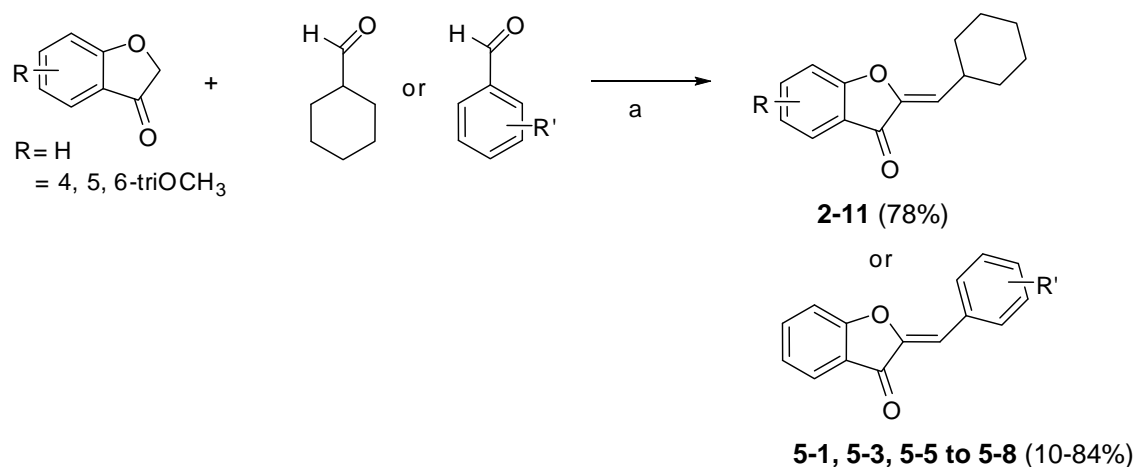


In the final step (c) of Scheme 2-2, the benzofuranone reacted with the benzaldehyde in a base-catalyzed aldol reaction (Figure 2-6). Loss of  $H^+$  from C2 under the basic conditions of the reaction gave an enolate which reacted with the electron deficient carbonyl carbon of benzaldehyde with loss of water to yield the desired aurone.

Figure 2-6: Aldol condensation of benzofuranone with benzaldehydes.



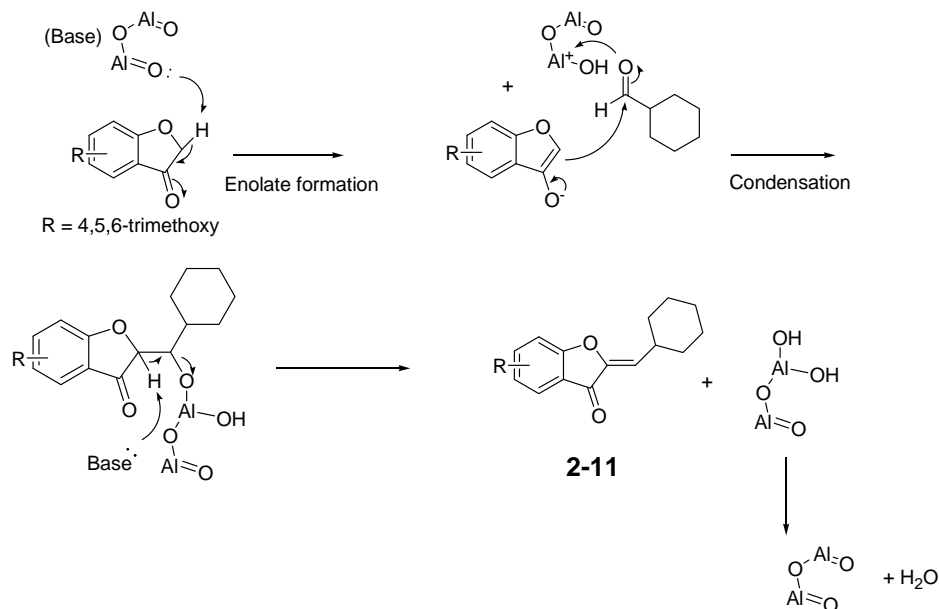
An alternative to the base catalyzed aldol reaction was to react the benzofuranone and aldehyde in the presence of aluminium oxide (alumina)<sup>102</sup>. This method was found to work well for the syntheses of **2-11** and **5-1, 5-3, 5-5 to 5-8** (Scheme 2-3). It involved vigorously stirring the aldehyde, benzofuranone and alumina in methylene chloride for 3 hours to 8 hours (overnight)



Scheme 2-3 Reagents and conditions: (a) activated basic  $\text{Al}_2\text{O}_3$ , DCM, r.t., 3h to overnight.

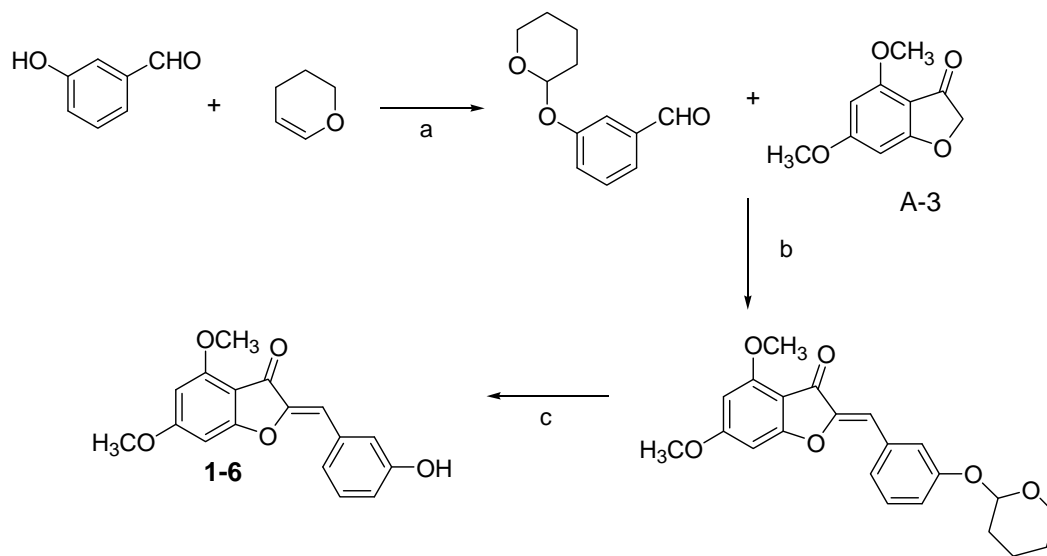
Figure 2-7 depicts the proposed mechanism for the alumina-mediated condensation leading to the formation of **2-11** (as an example). Alumina acted as a base to promote the formation of the enolate. It was also an electrophile and accepted electrons from the carbonyl oxygen of the aldehyde to form an aluminium hydroxy intermediate. The last step involved the elimination of the aluminium hydroxy moiety and loss of water to give the desired aurone.

Figure 2-7: Proposed mechanism for the synthesis of **2-11**.



Most of the dehydroaurones (Series 8) had been synthesized and only one member (**8-3**) was prepared by a reported method<sup>71</sup> which involved low pressure hydrogenation of the corresponding aurone with palladium/charcoal as catalyst.

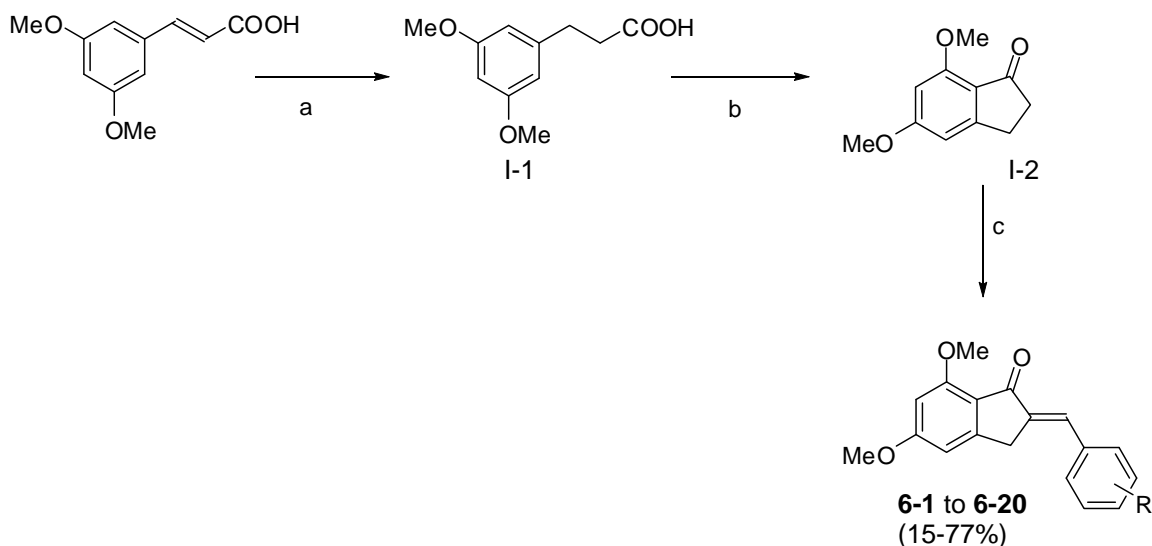
In aldol condensations involving benzaldehydes with phenolic hydroxyl groups as reagents, the OH groups were first converted to tetrahydropyranyl ethers with 2H-3,4-dihydropyran in the presence of pyridinium p-toluenesulphonate. The protecting group was then removed by acid hydrolysis of the condensation product (Scheme 2-4 with **1-6** as an example). The protection and deprotection steps were carried out on all phenolic OH groups except those attached to the ortho position(s) of the benzaldehyde.



Scheme 2-4 Reagents and conditions: (a) Pyridinium p-toluenesulphonate (0.2 mmol), CH<sub>2</sub>Cl<sub>2</sub>, r.t., 4h. (b) 50% KOH in MeOH/H<sub>2</sub>O, r.t., 3 h.(c) 4M HCl, rt, 4h.



### 2.3.2. Indanones (Series 6)



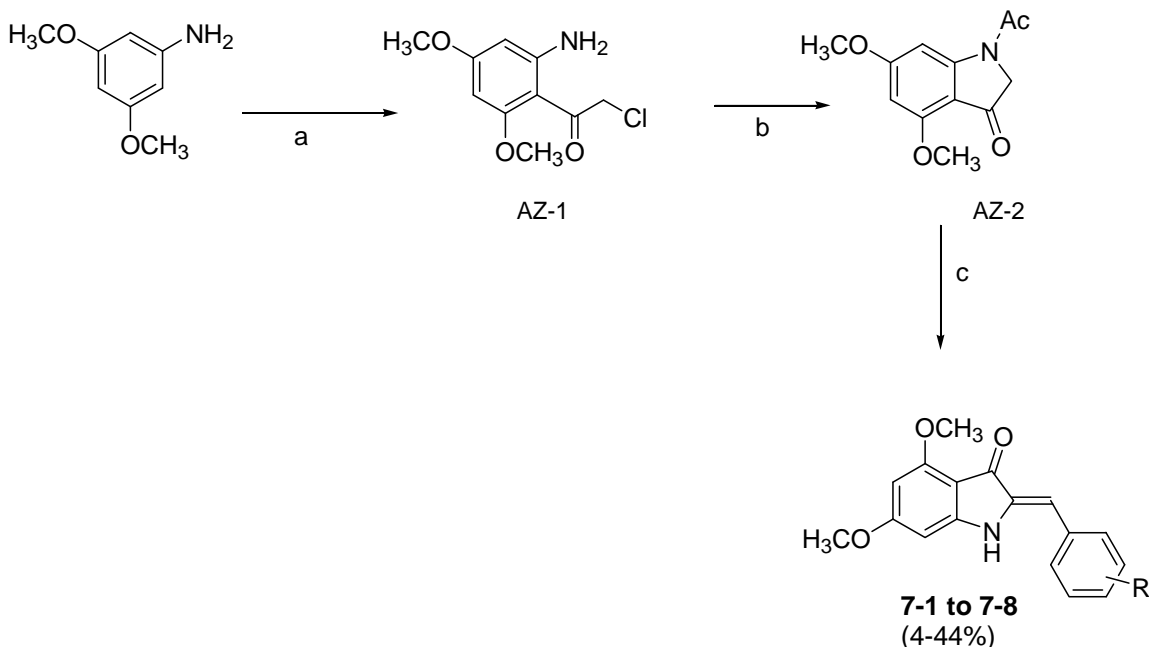
Scheme 2-5 Reagents and conditions: (a) H<sub>2</sub>, 10% Pd/C, HCO<sub>2</sub>NH<sub>4</sub>, MeOH, r.t., 16 h. (b) Methane sulfonic acid, 95<sup>0</sup>C, 6 h. (c) R'-substituted benzaldehyde, 50% KOH, r.t., 3 h.

The 2-benzylidene-5, 7-dimethoxy-2, 3-dihydro-1H-inden-1-ones (“indanones”) **6-1** to **6-20** were synthesized according to Scheme 2-5. First, 3, 5-dimethoxycinnamic acid was subjected to low pressure catalytic hydrogenation to give 3, 5-dimethoxypropanoic acid (I-1). Ring closure was effected in the presence of methane sulfonic acid to give the 2,3-dihydro-1H-inden-1-one (I-2)<sup>103</sup> which was condensed with an appropriately substituted benzaldehyde to give the desired product. Polyphosphoric acid had been used for the cyclization of the propanoic acid side chain of I-2<sup>104</sup> but methane sulphonic acid was employed here because of the difficulty in handling the highly viscous polyphosphoric acid.

The mechanism of ring closure to give I-1 proceeded by a similar mechanism as that described for the benzofuranones (Figure 2-5). Protonation of the carbonyl oxygen was effected by methanesulfonic acid, followed by the loss of water, generation of the electrophilic acylium ion and Friedel-Craft acylation to give I-2. Base-catalysed aldol

condensation of I-2 with appropriately substituted benzaldehydes yielded the benzylidene-dimethoxy-indanones **6-1** to **6-20** via enolate formation.

### 2.3.3 Aza-aurones (Series 7)



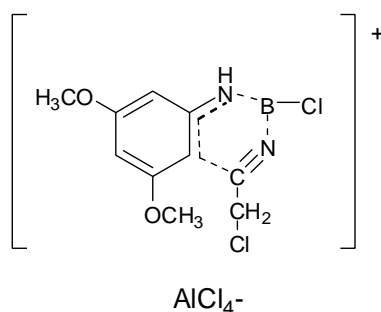
Scheme 2-6 Reagents and conditions: (a) (i)  $\text{ClCH}_2\text{CN}$ ,  $\text{BCl}_3$  /DCM,  $\text{AlCl}_3$ , dry benzene, reflux, 6h, (ii) 1M HCl, reflux, 30 mins (b) (i)  $(\text{CH}_3\text{CO})_2\text{O}$ , 80 - 85°C, 1h (ii)  $\text{K}_2\text{CO}_3$ , KI, dry acetone, reflux (iii) microwave (mw), 150°C, 12 mins (c) Substituted benzaldehyde, 50% KOH in MeOH/ $\text{H}_2\text{O}$ , 50°C, 3-4h or mw, 110°C, 5 mins.

Scheme 2-6 provides an overview of the reactions involved in the synthesis of the 4,6-dimethoxyaza-aurones. 3,5-Dimethoxyaniline was chloroacetylated at the ortho position, followed by acetylation of the aniline nitrogen and concurrent cyclization to give 1-acetyl-4,6-dimethoxy-2,3-dihydro-1H-indole (AZ-2)<sup>105, 106</sup>. The latter was reacted under basic conditions with substituted benzaldehydes to give the desired azaaurones.

In Step (a) of Scheme 2-6, 3,5-dimethoxyaniline was reacted with chloroacetonitrile in the presence of Lewis acids boron trichloride and aluminium trichloride. This was a Friedel-Crafts acylation reaction except that the acyl side chain was not directly introduced but obtained via the hydrolysis of the iminium intermediate. Following the method of

Sugasawa et al (1979)<sup>106</sup>, two Lewis acids were used in the reaction, namely aluminium chloride and boron trichloride. In terms of reactivity, aluminium chloride is generally viewed as the more reactive<sup>107</sup>. It may be necessary to use two Lewis acids here because the amino group in the reagent (3,5-dimethoxyaniline) may undergo co-ordination with the Lewis acid (in particular, the more reactive aluminium chloride) and thus prevent the reaction from proceeding further. To reduce the likelihood of its occurrence, the literature<sup>106</sup> suggested stirring the reagent (3,5-dimethoxyaniline) with boron trichloride prior to the addition of aluminium chloride. This was to promote complex formation between boron trichloride and the amino group in the reactant. On addition of chloroacetonitrile and aluminium trichloride, a boronium cationic species that was stabilized by tetrachloroaluminate would then be formed<sup>106</sup> (Figure 2-8).

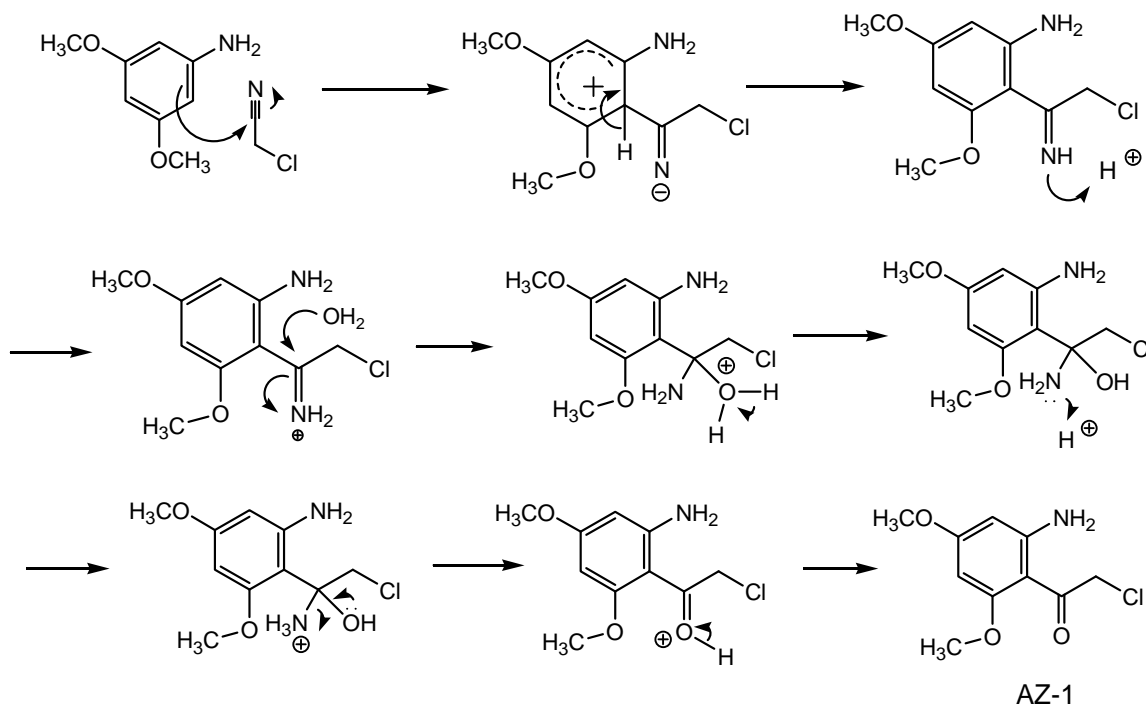
Figure 2-8: Proposed boronium cationic species stabilized by tetrachloroaluminate.



It may be that as boron trichloride was a “softer” acid (compared to aluminium chloride) and the aniline was a hard base, the resulting complex dissociate readily and would not adversely affect the course of the reaction. Moreover, the complex served to position the electrophilic carbon in chloroacetonitrile for reaction at the desired ortho (C2) position of the ring. It should be noted that the carbon in the nitrile was a weak electrophile (compared to a carbonyl carbon) and complex formation served to enhance its electrophilicity by converting the nitrile nitrogen to its quaternary state. Figure 2-9 shows the electrophilic substitution of

3,5-dimethoxyaniline by chloroacetonitrile. Once introduced, the iminium side chain was hydrolyzed in the presence of acid to give the ketone AZ-1.

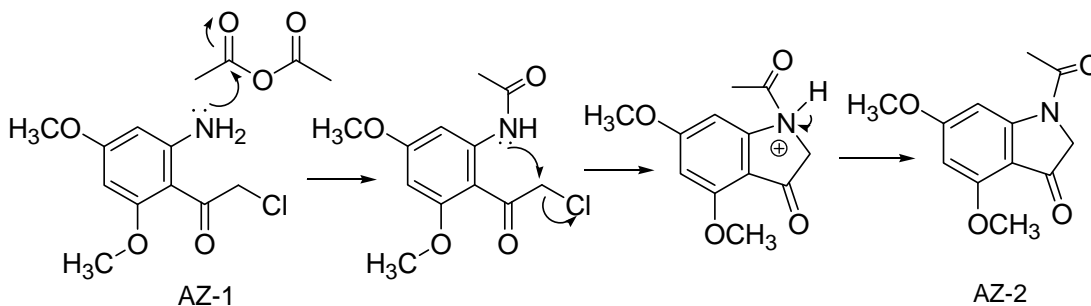
Figure 2-9: Reaction of 3,5-dimethoxyaniline with chloroacetonitrile by a Friedel Crafts reaction followed by acid hydrolysis of imine intermediate to give 2-amino-4,6-dimethoxy- $\alpha$ -chloroacetophenone, AZ-1.



In the next step, the amino group of (AZ-1) was acetylated with acetic anhydride in good yield. Ring closure was then initiated by reaction of the weakly nucleophilic amide nitrogen with the electron deficient  $\alpha$ -carbon on the adjacent side chain. To facilitate the reaction, iodide was added to displace the chlorine atom from the side chain. Iodide is a better leaving group than chloride and this would aid the attack by the weakly nucleophilic amide nitrogen. In the original method described by Sagasawa et al, the cyclization was carried out in the presence of sodium hydride as base but in a later report, Lawson et al accomplished the cyclization in the presence of potassium carbonate. However, in Lawson's method<sup>105</sup>, the amino function was not acetylated prior to ring closure, most likely to

maintain the nitrogen in its more nucleophilic state as an amino N compared to an amide N. This method was followed initially but gave a low yield (15%). Noting that Sagasawa et al had used the amide and not the amine for the reaction, the reaction was carried out with the amide using the conditions described by Lawson (K<sub>2</sub>CO<sub>3</sub>/KI). Surprisingly, the reaction proceeded to give the product AZ-2 at almost the same yield (21%) as Lawson's method using the amine. To improve the yield, the method of refluxing in acetone for 2 days<sup>105</sup> was set aside in favor of a shorter reaction period (12 min) by microwave heating at 150°C. The 2-day refluxing method gave a mixture with multiple side products (detected on thin layer chromatography) which were difficult to work up and probably contributed to the low yield. In contrast, the microwave method gave fewer side products and AZ-2 was obtained at a significantly improved yield of 66%. The reaction mechanism involved in the synthesis of AZ-2 from AZ-1 is given in Figure 2-10.

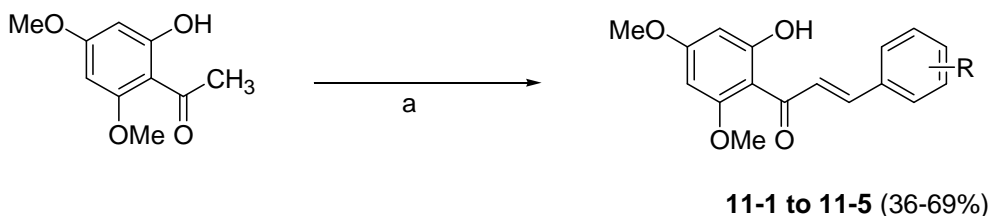
Figure 2-10: Acetylation of AZ-1 followed by ring closure to give AZ-2.



Synthesis of aza-aurones **7-1** to **7-8** was carried by condensing AZ-2 with substituted benzaldehydes following the method of Gerby et al. This was an aldol condensation like that described for the aurones and indanones. Mechanistically, it involved deprotonation of C2-H in the presence of base, formation of an enol anion which attacked the electrophilic carbonyl carbon of the benzaldehyde to give the desired azaaurone on dehydration. In this instance, the base (KOH) served a dual purpose of promoting the formation of the enol anion as well as

removing the N-acetyl group. The condensation was carried out by refluxing in methanol (ca 4 h). For some compounds (**7-2**, **7-6**, **7-7**), microwave heating (110°C, 5 min) was attempted but no improvement in yield was noted.

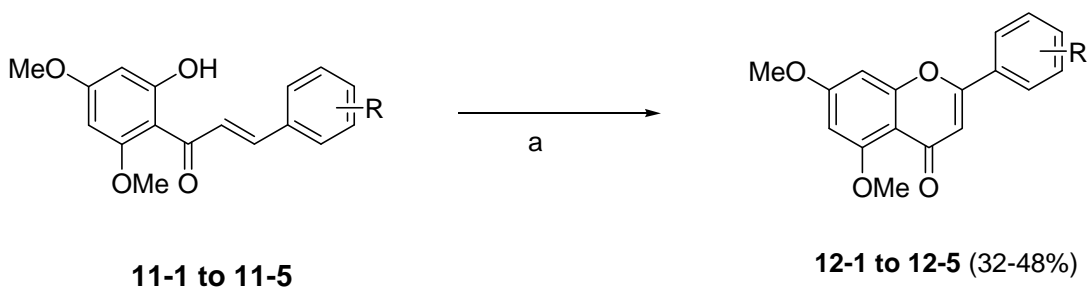
#### 2.3.4. Chalcones (Series 11)



Scheme 2-7 Reagents and conditions: (a) substituted benzaldehyde, 50% KOH, r.t., overnight.

The 2'-hydroxy-4',6'-dimethoxychalcones of Series 11 were readily synthesized from commercially available 2'-hydroxy-4',6'-dimethoxyacetophenone. A straight forward base catalyzed aldol condensation of the acetophenone with a suitably substituted benzaldehyde gave the desired chalcone in reasonable yields (36 to 69%) (Scheme 2-7). Protection of the 2'-OH of the acetophenone was not found to be necessary.

#### 2.3.5. Flavones (Series 12)

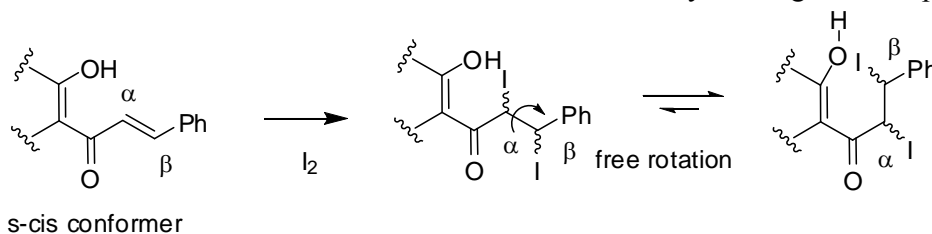


Scheme 2-8 Reagents and conditions: (a) I<sub>2</sub> (cat), DMSO, 180°C, 1.5-2 hours.

5, 7-Dimethoxyflavones (**12-1** to **12-5**) were synthesized from the corresponding chalcones **11-1** to **11-5**. The reaction involved refluxing the chalcone in the presence of a catalytic amount of iodine in DMSO (Scheme 2-8)<sup>108</sup>. The final products **12-1** to **12-5** were obtained in moderate yields (32% to 48% purified yields).

Iodine is known to equilibrate alkenes to the thermodynamically more stable (*E*) isomer<sup>109</sup>. As mentioned earlier, the Michael acceptor moiety of chalcones could assume two conformations (*s-cis* and *s-trans*), with a preference for *s-cis*<sup>98</sup>. The mechanism was proposed to involve the initial electrophilic addition of iodine to the double bond of the Michael acceptor to give an addition product which rotated freely about the C $\alpha$ -C $\beta$  bond<sup>110</sup>. Presumably, the conformation that was better placed for reaction with the nucleophilic phenolic OH would predominate (Figure 2-11).

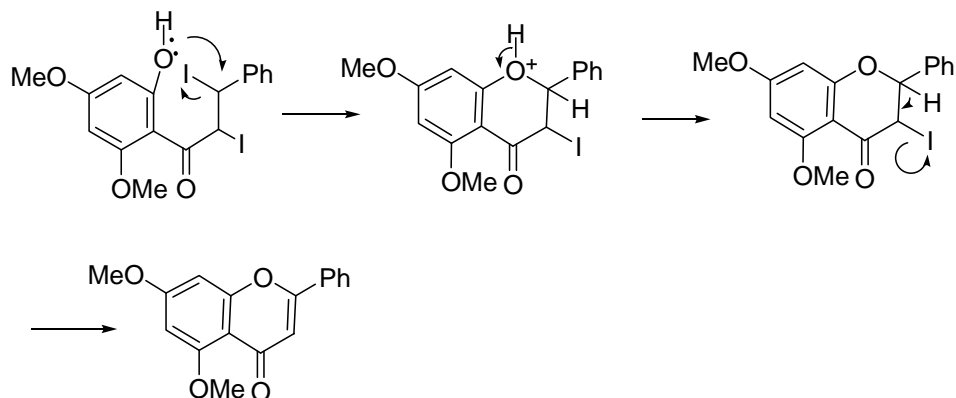
Figure 2-11: Reaction of *s-cis* chalcone with iodine to form freely rotating addition product.



The mechanism of ring closure was discussed by Miyake and workers<sup>111</sup>. They proposed elimination of HI, followed by conjugate addition by the phenolic hydroxyl group to give the chromanone intermediate and  $\beta$ -elimination of the second HI molecule to give the flavone.

Alternately, ring closure could proceed by replacement of the iodine on the  $\beta$ -C by the phenolic OH, followed by elimination of the second molecule of HI to give the flavone (Figure 2-12).

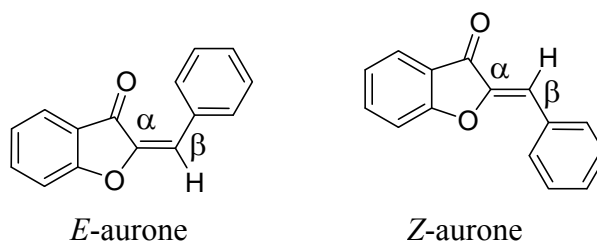
Figure 2-12: Proposed mechanism of ring closure involving replacement of  $\beta$ -iodine by phenolic OH<sup>111</sup>.



## 2.4. Assignment of configurations

### 2.4.1. Aurones (Series 1, 2, 5) and dehydroaurones (Series 8)

Figure 2-13: *E* and *Z* aurones.



Aurones exist as the *E* or *Z* isomers (Figure 2-13), with the *Z* isomer considered to be the thermodynamically more stable form<sup>112</sup>. *E/Z* assignment of double bond in aurones had been made on the basis of the <sup>1</sup>H chemical shift of the methine (olefinic) proton (C $\beta$ -H)<sup>101, 113, 114</sup>. A chemical shift of  $\delta$  6.70 ppm was cited for the C $\beta$ -H in the *Z* isomer and  $\delta$  7.01 ppm for the C $\beta$ -H in the *E* isomer<sup>101</sup>. This assignment could be explained by the anisotropic diamagnetic shielding of the methine proton by the circulating  $\pi$  electrons of the carbonyl bond. In the *Z* isomer, C $\beta$ -H was shielded because it was found in a region where the induced magnetic field arising from the circulating  $\pi$  electrons of the carbonyl bond opposed the applied magnetic field. Therefore, it was found at a lower  $\delta$  value. In the *E* isomer, C $\beta$ -H lies

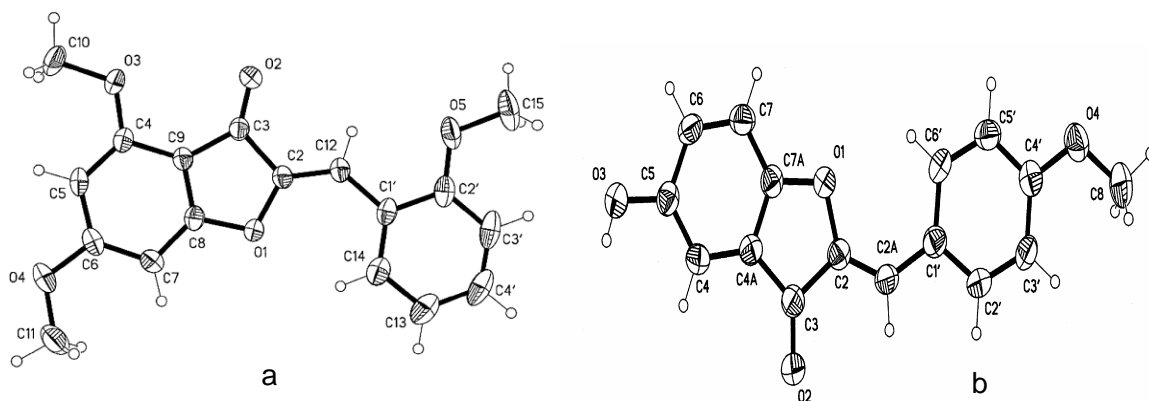


in the plane of the double bond and was therefore deshielded<sup>115</sup>. Assignment of *E/Z* configuration of aurones could also be made by considering the <sup>13</sup>C chemical shifts of the exocyclic carbon C $\beta$ <sup>116</sup>. The <sup>13</sup>C chemical shifts of C $\beta$  were reported at  $\delta$  111 ppm and  $\delta$ 120 - 130 ppm for the *Z* and *E* isomers respectively.

Both <sup>13</sup>C and <sup>1</sup>H chemical shifts were used to assign the *E/Z* configuration of the synthesized aurones. The <sup>13</sup>C chemical shifts of C $\beta$  in all the aurones were found at  $\delta$ 105-111ppm, which implied a *Z* configuration for the exocyclic double bond. The <sup>1</sup>H chemical shifts of C $\beta$ -H of these aurones were found over the range of  $\delta$  6.27-6.90 ppm which was again more indicative of a *Z* isomer (C $\beta$ -H  $\delta$  6.70 ppm)<sup>101</sup> than an *E* isomer (C $\beta$ -H  $\delta$  7.01 ppm)<sup>101</sup>. However for aurones with 2'-substituents, the <sup>1</sup>H chemical shifts of C $\beta$ -H were observed downfield at  $\delta$  7.00 - 7.38 ppm, which might indicate an *E* configuration for these compounds. Fortunately, the solid state x-ray structure of a 2'-substituted aurone (**1-2**, with 2'-methoxy on ring B) was obtained (Figure 2-14) and it showed the *Z* configuration for the double bond. The downfield shift of the C $\beta$ -H in 2'-substituted aurones was attributed to the anomalous "ortho effect" often associated with these positional isomers.

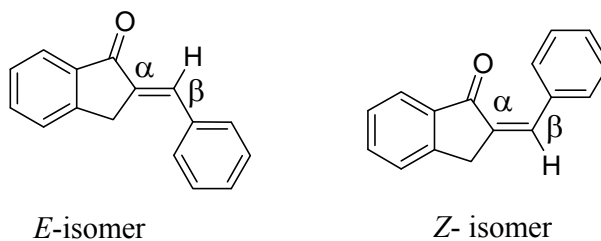
The x-ray structure of another aurone (**4-5**, 5-hydroxy-2-(4'-methoxybenzylidene)-benzofuran-3(2H)-one) was also obtained (Figure 2-14) and it showed a *Z* configuration. The C $\beta$ -H of **4-5** showed a <sup>1</sup>H chemical shift at  $\delta$  6.87 ppm<sup>71</sup> and in view of its association with a *Z* configuration, gave added confidence to the use of C $\beta$ -H chemical shifts for assigning *E/Z* configuration of the other aurones. Therefore, the *Z* configuration was assigned to aurones in Series 1-5.

Figure 2-14: X-ray structure of (a) **1-2** and (b) 5-hydroxy-2-(4'-methoxybenzylidene)-benzofuran-3(2H)-one.



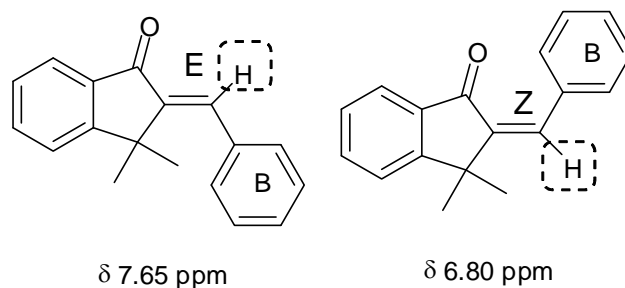
#### 2.4.2. Indanones (Series 6)

Figure 2-15: *E* and *Z* benzylidene indanones.



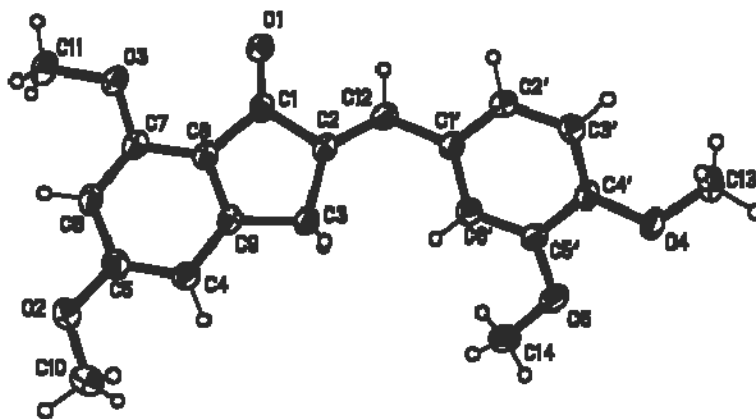
Like the aurones, the indanones of Series 6 existed in *Z* or *E* forms (Figure 2-15). The chemical shifts of the methine proton of the *E* and *Z* isomers of 2-(phenylmethylene)-3,3,-dimethyl-1-indanone were reported at 7.65 and 6.80 ppm respectively<sup>117</sup> (Figure 2-16).

Figure 2-16: Chemical shifts of methine CH of *E* and *Z* isomers of 2-(phenylmethylene)-3,3,-dimethyl-1-indanone: Methine CH is encircled.



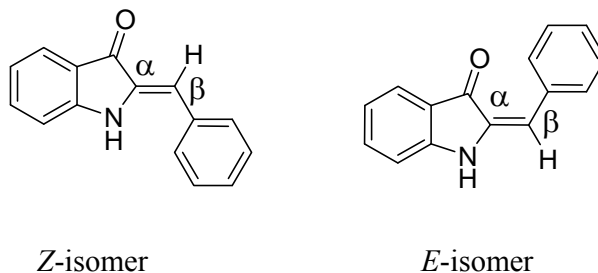
The deshielding effect arising from the diamagnetic anisotropy of the carbonyl group caused the methine CH signal in the *E* isomer to be shifted downfield. Thus, it had a larger chemical shift than the *Z* isomer. Dimmock and coworkers reported the methine CH signals of the *E* isomers in their series of benzylidene-2,3-dihydro-indenones at 7.15 - 7.95 ppm and noted that they frequently overlapped with the peaks of the aromatic protons. Of the two isomers, the *Z* isomer was less favored due to steric interactions between the phenyl ring B and the carbonyl group<sup>118</sup>. In the case of the Series 6 indanones, the <sup>1</sup>H chemical shift of the methine proton was found as a singlet at  $\delta$  6.21-7.89 ppm or as a multiplet due to overlaps with the aromatic protons. The x-ray crystal structure of **6-20** which had 3',4'-dimethoxy groups on ring B was obtained and found to have the *E* configuration. On this basis, the other Series 6 indanones were proposed to have the *E* configuration.

Figure 2-17: X-ray structure of indanone **6-20**.



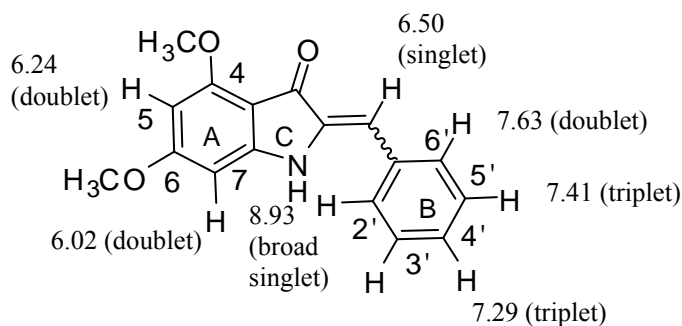
#### 2.4.3. 4, 6-Dimethoxy aza-aurones (Series 7)

Figure 2-18: *Z* and *E* aza-aurones.



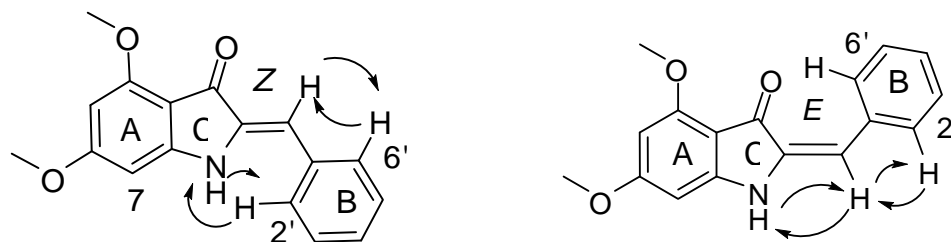
*E/Z* isomerism is also present in the 4, 6-dimethoxyaza-aurones of Series 7 (Figure 2-18). The 4, 6-dimethoxyaza-aurones synthesized by Lawson et al<sup>105</sup> were reported to be *Z* isomers and the <sup>1</sup>H chemical shifts of the methine CH in these compounds appeared at δ 6.4 to 6.7 ppm. In the present series of azaaurones, the <sup>1</sup>H chemical shifts of the methine CH groups were found over a narrower range of δ 6.40 to 6.50 ppm. As they were synthesized using the same method reported by Lawson, they were likely to be *Z* isomers. For confirmation, a representative compound (**7-1**, unsubstituted ring B) was examined by 2D Nuclear Overhauser effect spectroscopy (NOESY). The <sup>1</sup>H chemical shifts of **7-1** are assigned as follows:

Figure 2-19: Assignment of <sup>1</sup>H chemical shifts of compound **7-1**.



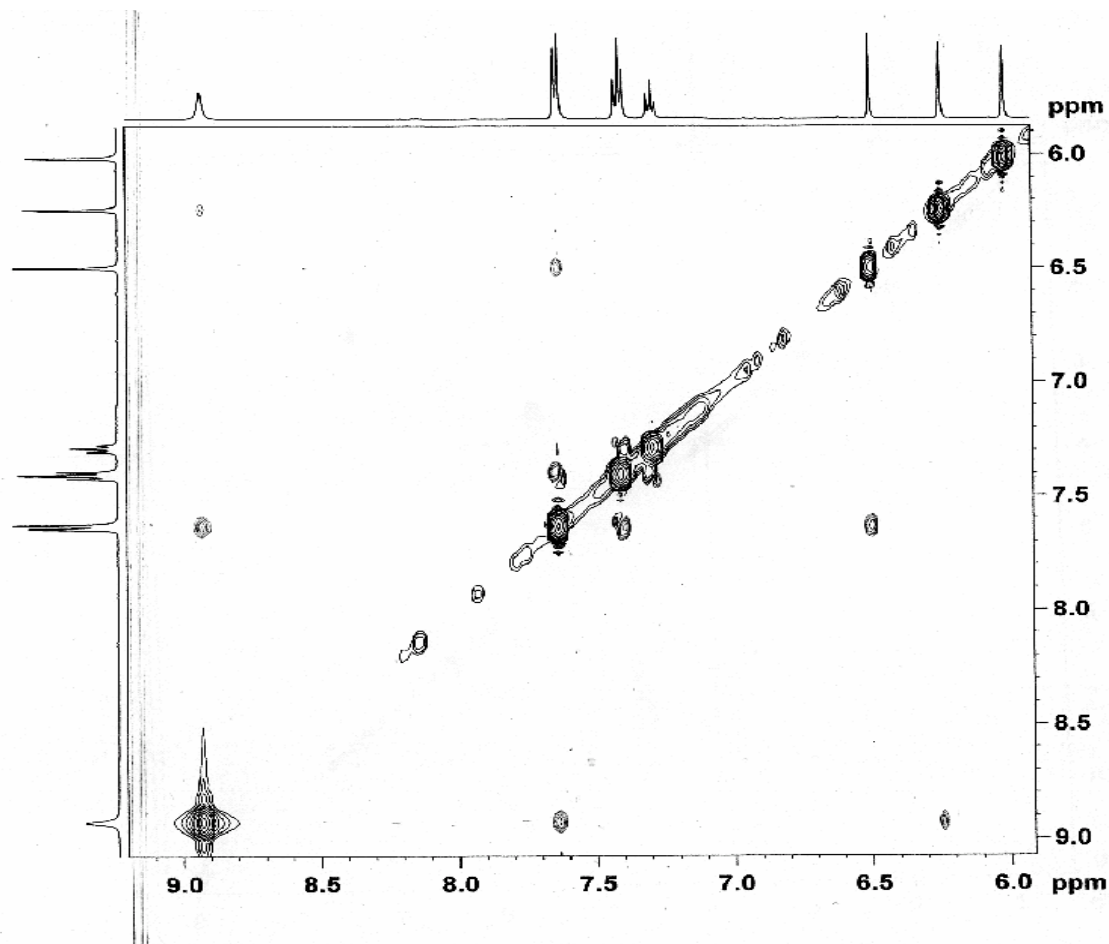
The *E* and *Z* isomers of an azaaurone were readily distinguished by their NOESY spectra. If it was a *Z* isomer, irradiation of the proton at nitrogen (NH) on ring C would result in the Nuclear Overhauser enhancement of the signals attributed to the aromatic protons of ring B (in particular, the ortho proton). If it was an *E* isomer, irradiation of the proton at nitrogen (NH) of ring C would enhance the signal attributed to the methine (CH) proton. The proposed NOE interactions are shown in Figure 2-20:

Figure 2-20: Proposed nuclear Overhauser (NOE) effects in the *Z* and *E* isomers of **7-1**.



The 2D NOESY spectrum of compound **7-1** is shown in Figure 2-21. The methine proton was assigned to the singlet at 6.50ppm and the N-H was assigned to the broad singlet at 8.93ppm. The ortho (2' and 6') protons of ring B were represented by a doublet at 7.63 ppm. From the spectrum, an interaction between the methine proton and the NH proton was not evident, thus ruling out the *E* configuration for **7-1**. Instead, interactions between the methine proton and the ortho proton of ring B, as well as that between the NH proton and the other ortho proton of ring B were clearly observed. Hence, it was concluded that **7-1** existed as the *Z* isomer and this was likely to be the configuration of the other azaaurones of Series 7.

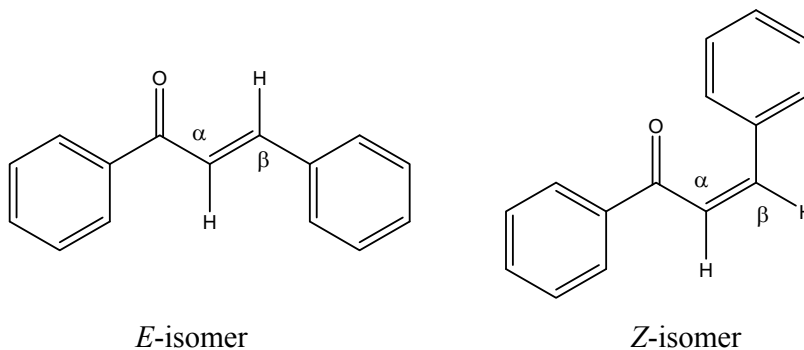
Figure 2.21: 2D-NOESY spectrum of Compound 7-1.



#### 2.4.4. 2'-Hydroxy, 4'6'-dimethoxy chalcones (Series 11)

*E/Z* isomerism was present in the  $\alpha$ ,  $\beta$ -unsaturated double bond of chalcones (Figure 2-22). In addition, the orientation of the double bond with respect to the carbonyl bond may be *s-cis* or *s-trans*, as described earlier. The *s-cis* conformation was reportedly the favored conformation. Ducki et al obtained the x ray crystal structure of the chalcone 3-(4-hydroxy-3-methoxyphenyl)-1-(3,4,5-trimethoxyphenyl)-propenone which was structurally related to the present series of chalcones, and showed that it was present in the *s-cis* conformation<sup>99</sup>. The *s-trans* conformation was reported in a chalcone that was substituted at  $C\alpha$  with a methyl group<sup>99</sup>.

Figure 2-22: Chalcone represented in its *E* and *Z* configuration. Both *E* and *Z* isomers are represented in the *s-cis* conformation.



The *E* and *Z* isomers were readily distinguished by the coupling constants of the vicinal methine protons. These protons were seen as two characteristic doublets with chemical shifts of  $\delta$  7 to 8 ppm on the  $^1\text{H}$  NMR spectrum. The *E* isomer had a larger coupling constant ( $J_{\text{Ha, Hb}} = 15\text{-}16$  Hz) because of the larger dihedral angle between the protons. In the *Z* isomer, the coupling constant was considerably smaller ( $J_{\text{Ha, Hb}} = 5\text{-}10$  Hz). For the 2'-hydroxy, 4'6'-dimethoxy chalcones of Series 11, the coupling constants of the vicinal methine protons were found in the range of 15.6 – 16.2 Hz, indicating that they were present as *E* isomers and most likely in the *s-cis* conformation.

## 2.5. Experimental methods

### 2.5.1. General details

Reagents (synthetic grade or better) were obtained from Sigma-Aldrich Chemical Company Inc (Singapore) and used without further purification. Melting points were determined on a Gallenkamp melting point apparatus and reported as uncorrected values. Mass spectra were captured on an LCQ Finnigan MAT equipped with a chemical ionization (APCI) probe and  $m/z$  values for the molecular ion were reported. HRMS were taken using a Q-TOF Premier (Waters Corp., Milford, USA).  $^1\text{H}$  spectra were determined on a Bruker Spectrospin 300 Ultrashield spectrometer and referenced to TMS or residual  $\text{CDCl}_3$  ( $\delta$  7.25) and DMSO ( $\delta$  2.49) as internal standards.  $^{13}\text{C}$  NMR spectra (75 MHz) were determined on the same instrument and reported in ppm ( $\delta$ ) relative to residual  $\text{CDCl}_3$  ( $\delta$  77.0) and DMSO ( $\delta$  39.5). Coupling constants (J) were reported in hertz (Hz). Proton ( $^1\text{H}$ ) NMR spectral information is tabulated in the following format: multiplicity, coupling constant, number of protons. Multiplicities are reported as follows: s=singlet, d=doublet, t=triplet, q=quartet, dd=doublet of doublets, m=multiplet. Two-dimensional NOESY spectra were recorded on Bruker (DRX-500) 500MHz spectrophotometer with DMSO- $d_6$  ( $\delta$  2.49 ppm) solvent and internal standard. Microwave heating was carried out on a Biotage Initiator  $\text{\textcircled{R}}$  instrument. Merck silica 60 F254 sheets and Merck 45 silica gel (0.040-0.063 mm) were used for thin layer chromatography (TLC) and flash chromatography respectively. Purity of final compounds was verified by combustion analysis (C, H) on a Perkin Elmer PRE-2400 Elemental Analyzer or by HPLC on two different solvent systems (Section 2.5.9). For compounds analyzed by combustion analysis, %C and %H values must be no less than 95% of theoretical %C and %H values to be deemed pure while for compounds analyzed by HPLC, peak area must be no less than 95% of total peak area on two different solvent



systems. Spectroscopic data, melting points, yields and purities of individual compounds are listed in Appendix 2-1. Compound **12-4** (97% purity) was purchased from Alfa Aesar (Ward Hill, MA 01835, USA) and used without further purification. The melting points, nominal mass and NMR data of intermediates and final compounds are presented in the subsections of 2.5 and Appendix 2-1.

2.5.2. General procedure for the synthesis of series 1, 2, 6 and 8 (4, 6-dimethoxy-aurones, 4, 5, 6-trimethoxy-aurones, unsubstituted (Ring A) aurones and 4, 5, 6-trimethoxy dehydroaurone)

2.5.2.1. 4, 6-Dimethoxy-aurones

2.5.2.1.1. 3, 5-Dimethoxyphenoxyacetic acid (A-1)

The method of Lawrence et al<sup>88</sup> was followed. To a solution of 3, 5-dimethoxyphenol (0.83 g, 5.44 mmol) in anhydrous DMF (10 ml) was added sodium hydride (0.33 g, 13.6 mmol). Chloroacetic acid (0.51 g, 5.44 mmol) in DMF (10 ml) was added dropwise and the mixture stirred under cover of nitrogen gas at room temperature (30°C) for 12 h. After this time, the mixture was quenched with 4M HCl (100 ml) and extracted with dichloromethane (3 × 50 ml). The organic phase was washed with brine, dried with anhydrous Na<sub>2</sub>SO<sub>4</sub> and evaporated in vacuo to give brownish oil which solidified to a white solid on cooling in an ice-bath. Recrystallisation in chloroform–hexane gave A-1 in 60-70 % yield. White needle-like crystalline solid; mp 148–149 °C (lit: 146-147°C)<sup>119</sup>; <sup>1</sup>H NMR (CDCl<sub>3</sub>, 300 MHz): δ 6.14 (t, 1H, J = 2.0 Hz), 6.11 (d, 2H, J = 2.1 Hz), 4.65 (s, 2H), 3.74 (s, 6H); MS (APCI) m/z [M+1]<sup>+</sup> 212.5.

#### 2.5.2.1.2. 4, 6-Dimethoxybenzofuran-3(2H)-one (A-3)

The method of Lawrence et al<sup>88</sup> was followed. Polyphosphoric acid (20 g) was heated to 80 °C on an oil bath, after which was added 0.5 g of compound A-1. The mixture was stirred at 90 °C for 8 h and then poured into ice-water (100 ml) and subsequently extracted with dichloromethane (4×50 ml). The combined organic phase was washed with brine, dried with anhydrous Na<sub>2</sub>SO<sub>4</sub> and evaporated in vacuo. The residue was purified by column chromatography, with hexane: ethyl acetate 2:1 as eluting solvent. A-3 was obtained as a pale yellow solid, yield: 56%; mp 137-139 °C (lit: 132-136°C)<sup>120</sup>; <sup>1</sup>H NMR (CDCl<sub>3</sub>, 300 MHz): δ 6.16 (d, 1H, J = 1.5 Hz), 6.02 (d, 1H, J = 1.1 Hz), 4.60 (s, 2H), 3.91 (s, 3H), 3.87 (s, 3H); <sup>13</sup>C NMR (CDCl<sub>3</sub>, 75 MHz): δ 55.8, 56.2, 75.2, 89.4, 92.8, 104.8, 158.2, 169.2, 176.2, 194.0; MS (APCI) m/z 195.1 [M+1]<sup>+</sup>.

#### 2.5.2.2. 4, 5, 6-Trimethoxy-aurones

##### 2.5.2.2.1. 3, 4, 5-Trimethoxyphenoxyacetic acid (A-2)

The method of Lawrence et al<sup>88</sup> was followed. To a solution of 3, 4, 5-trimethoxyphenol (1.00 g, 5.43 mmol) in anhydrous DMF (10 ml) was added sodium hydride (0.39 g, 16.3 mmol). Chloroacetic acid (0.77 g, 8.21 mmol) in DMF (10 ml) was added dropwise and the mixture reacted and worked up in the same way as described for A-1. Recrystallisation in chloroform gave 3, 4, 5-trimethoxyphenoxyacetic acid in 57% yield; mp 95-96°C (lit: 96-99°C)<sup>121</sup>; White solid; <sup>1</sup>H NMR (CDCl<sub>3</sub>, 300 MHz): 3.79 (s, 3H), 3.84 (s, 6H), 4.66 (s, 2H), 6.19 (s, 2H); MS (APCI): m/z 243.0 [M+1]<sup>+</sup>.

##### 2.5.2.2.2. 4, 5, 6-Dimethoxybenzofuran-3(2H)-one (A-4)

The method of Lawrence et al<sup>88</sup> was followed. A-2 (0.3 g) was reacted with polyphosphoric acid (20 g) as described for A-3. The crude compound was purified by

column chromatography, with hexane/ethyl acetate (1:1) as eluting solvent. A-4 was obtained as a brown solid, yield: 59%; mp 142-143°C (lit: 143-144°C)<sup>122</sup>; <sup>1</sup>H NMR (CDCl<sub>3</sub>, 300MHz): δ 3.79 (s, 3H), 3.93 (s, 3H), 4.16 (s, 3H), 4.58 (s, 2H), 6.32 (s, 1H); <sup>13</sup>C NMR (CDCl<sub>3</sub>, 75MHz): δ 56.5, 61.6, 62.0, 75.4, 90.6, 106.7, 135.7, 150.6, 162.6, 172.1, 195.3; MS (APCI): m/z 225.3 [M+1]<sup>+</sup>.

### 2.5.2.3 General procedure for the synthesis of 4, 6-dimethoxyaurones and 4, 5, 6-trimethoxyaurones (Compounds **1-1** to **1-28**, **2-1** to **2-10**)

The method of Lawrence et al<sup>88</sup> was followed. To a solution of A-3 or A-4 in methanol (10 ml) was added the substituted benzaldehyde (1.1 to 1.5 equiv), followed by a solution of KOH (500 mg, 8.92 mmol) in distilled water (1 ml). The solution was stirred at room temperature for 3 h. The desired compound was obtained as a precipitate, removed by suction filtration, washed with cold methanol and crystallized in ethanol or methanol to give the desired aurones. If no precipitate was formed after 3h, 4M HCl was added to the reaction mixture to effect precipitation. If no precipitation occurred, the reaction mixture was evaporated under reduced pressure to remove the solvent (methanol), after which H<sub>2</sub>O (30ml) was added and the mixture extracted with CH<sub>2</sub>Cl<sub>2</sub> (3 x 50ml). The combined organic layers were washed with brine (2 x 50ml), dried over anhydrous Na<sub>2</sub>SO<sub>4</sub>, filtered and evaporated under reduced pressure to give crude residue. The latter was purified by column chromatography using hexane/ethyl acetate (3:1) or 100% CH<sub>2</sub>Cl<sub>2</sub> as eluting solvent. In the case of aurones **1-5** to **1-7**, **1-20**, **1-21**, **1-24** and **2-9**, additional protection and deprotection of the phenolic hydroxyl group(s) on the benzaldehydes were required and this is described in Section 2.5.7.

#### 2.5.2.4 Procedure for synthesis of (Z)-2-(cyclohexylmethylene)-4, 5, 6-trimethoxybenzofuran-3(2H)-one (**2-11**)

The method of Wallez et al<sup>123</sup> was followed. Cyclohexaldehyde (0.36g, 0.321mmol) and activated basic aluminium oxide (0.98g) were added to a vigorously stirred solution of A-4 in 10ml of methylene chloride and allowed to stir overnight. The aluminium oxide was then removed by filtration and washed abundantly with methylene chloride. The filtrate was concentrated in vacuo to give crude **2-11**, which was purified by column chromatography (hexane/ethyl acetate (4:1)) to give pure **2-11**; yellow solid, 78% yield; mp: 86-88°C; <sup>1</sup>H NMR (CDCl<sub>3</sub>, 300MHz): δ 1.20 -1.43 (m, 5H), 1.65 -1.80 (m, 5H), 2.61- 2.71 (m, 1H), 3.80 (s, 3H), 3.94 (s, 3H), 4.21(s, 3H), 5.92 (d, 1H, J= 9.6Hz), 6.42 (s, 1H); <sup>13</sup>C NMR (CDCl<sub>3</sub>, 75MHz): δ 25.4, 25.7, 32.1, 35.1, 56.4, 61.5, 62.2, 90.2, 107.6, 120.1, 136.2, 148.0, 151.5, 161.6, 164.0, 180.8; MS (APCI): m/z 319.4 [M+1]<sup>+</sup>; Anal. calcd for C<sub>18</sub>H<sub>22</sub>O<sub>5</sub>: C, 67.91; H, 6.97; Found: C, 67.68; H, 6.46.

#### 2.5.2.5 General procedure for the synthesis of unsubstituted auronones (Compounds **5-1** to **5-8**)

The method of Wallez et al<sup>123</sup> was followed. Substituted benzaldehydes (1.1 equiv) and activated basic aluminium oxide (36 equiv) were added to a vigorously stirred solution of benzofuran-3(2H)-one (0.15g, 1.13mmol) in 10ml of methylene chloride and allowed to stir for 3 hours. Aluminium oxide was then removed by filtration and washed abundantly with methylene chloride. The filtrate was concentrated in vacuo to give the crude product, which was purified by either column chromatography hexane/ethyl acetate (95:5) or re-crystallisation in methanol to give purified **5-1** to **5-8**.

### 2.5.2.6 General procedure for the synthesis of 4, 5, 6-trimethoxydehydroaurone

#### (Compound **8-3**)

A solution of 4, 5, 6-trimethoxyaurone (0.03g, 0.09mmol) in 50ml of methanol was hydrogenated over 10% Pd-C at 50 psi and allowed to stir overnight for 15 hours. The reaction mixture was then filtered through a layer of celite and the solvent was evaporated in vacuo. The residue was purified by column chromatography hexane/ethyl acetate (4:1) to give **8-3** as an off-white solid (50% yield); mp: 89-92°C; <sup>1</sup>H NMR (CDCl<sub>3</sub>, 300MHz): δ 2.88 – 2.96 (m, 1H), 3.27 (dd, 1H, J= 3.3, 3.6 Hz), 3.76 (s, 3H), 3.77 (s, 3H), 3.90 (s, 3H), 4.12 (s, 3H), 4.69 (dd, 1H, J= 3.6, 3.6 Hz), 6.27 (s, 1H), 6.81 (d, 2H, J= 8.4Hz), 7.20 (d, 2H, J= 8.4Hz) <sup>13</sup>C NMR (CDCl<sub>3</sub>, 75MHz): δ 36.8, 55.2, 56.5, 61.6, 62.0, 86.6, 90.5, 106.6, 113.8, 128.1, 130.4, 135.6, 150.6, 158.5, 162.7, 170.6, 196.5; MS (APCI): m/z 345.3 [M+1]<sup>+</sup>; HPLC analyses: t<sub>R</sub>= 3.30 min (96.14% pure at 330nm) on the C<sub>18</sub> analytical column; Mobile phase, solvent system A (MeOH and 0.1% HCOOH in H<sub>2</sub>O) with a gradient of MeOH 100% to 70% from 0 to 5 min, 70% to 50% from 5 to 7 min and then 50% MeOH from 7 to 10 min; t<sub>R</sub>= 3.54 min (96.30% pure at 330nm) on the C<sub>18</sub> analytical column, Mobile phase: solvent system B (CH<sub>3</sub>CN and 0.1% HCOOH in H<sub>2</sub>O) with a gradient of CH<sub>3</sub>CN 100% to 70% from 0 to 5 min, 70% to 50% from 5 to 7 min, 50% to 70% CH<sub>3</sub>CN from 7 to 9 min and then 70% CH<sub>3</sub>CN from 9 to 12 min.

### 2.5.3 General procedure for the synthesis of 4, 6-dimethoxy-indanones (Compounds **6-1** to **6-2**)

#### 2.5.3.1. 3, 5-Dimethoxypropanoic acid (I-1)

The method of Bauta et al<sup>103</sup> was followed. 3, 5-Dimethoxycinnamic acid (1.50 g, 7.20 mmol), 10% Pd/C (0.08 g, 0.072 mmol), and solid ammonium formate (0.5 g, 7.92

mmol) was dissolved in methanol (50ml). The mixture was shaken in a Parr hydrogenator in the presence of H<sub>2</sub> gas (50 psi) under room temperature conditions (30 °C) for 16 hours, after which the mixture was filtered through celite. The collected residue was rinsed with methanol and the combined filtrate and washing were removed under reduced pressure. Distilled water (15 ml) was added to the residue and the resulting suspension was cooled to 0 °C before it was acidified with 4 M HCl to pH <2. The suspension was filtered by suction filtration to give 3, 5-dimethoxypropanoic acid as a white solid at 95% yield; mp: 59-61°C (lit: 61-62 °C)<sup>124</sup>; <sup>1</sup>H NMR (CDCl<sub>3</sub>, 300MHz): δ 6.33 – 6.37 (m, 3H), 3.78 (s, 6H), 2.88 – 2.93 (m, 2H), 2.65– 2.70 (m, 2H); MS (ESI): m/z 233.1 [M+Na]<sup>+</sup>.

#### 2.5.3.2. 5, 7-Dimethoxy-2, 3-dihydro-1H-inden-1-one (I-2)

The method of Bauta et al<sup>103</sup> was followed. 3, 5-Dimethoxypropanoic acid (1.00 g, 4.76 mmol) and methanesulfonic acid (10 ml) were heated under reflux at 95°C for 6 hours. Cold distilled water (20 ml) was then added the mixture followed by 50% sodium hydroxide (10 ml) to neutralize methanesulfonic acid. The mixture was then extracted with ethyl acetate (4 x 50 ml) and the organic fraction was subsequently washed with 5% NaHCO<sub>3</sub> (4 x 20 ml), dried with anhydrous Na<sub>2</sub>SO<sub>4</sub> and evaporated in vacuo to give a light brown solid. This was purified by column chromatography with dichloromethane/methanol (99:1) as eluting solvent to give 5,7-dimethoxy-2,3-dihydro-1H-inden-1-one as a tan-colored solid at 42% yield; mp: 99-101°C (lit: 99-100°C)<sup>103</sup>; <sup>1</sup>H NMR (CDCl<sub>3</sub>, 300MHz): δ 2.63 – 2.67 (m, 2H), 3.01 – 3.05 (m, 2H), 3.88 (s, 3H), 3.92 (s, 3H), 6.31 (s, 1H), 6.49 (s, 1H); MS (APCI): m/z 193.3 [M+1]<sup>+</sup>.

### 2.5.3.3. Condensation of I-2 with substituted benzaldehydes

To a solution of I-2 in methanol (10 ml) was added the appropriately substituted benzaldehyde (1.1 to 1.5 equiv), followed by a solution of KOH (500 mg, 8.92 mmol) in distilled water (1 ml). The mixture was stirred at room temperature for 3 hours. The desired compound was obtained as a precipitate, removed by suction filtration and recrystallized in methanol or ethanol to yield the purified compound (**6-1** to **6-20**). In the case of **6-5**, **6-6**, **6-16** to **6-19**, the phenolic hydroxyl groups on the benzaldehydes were initially protected before the reaction and then removed to give the final product as described in Section 2.5.7.

### 2.5.4 General procedure for the synthesis of 4, 6-dimethoxy-aza-aurones (Compounds **7-1** to **7-8**)

#### 2.5.4.1. 2-Amino-4,6-dimethoxy- $\alpha$ -chloroacetophenone (AZ-1)

The method of Sugasawa et al<sup>106</sup> was followed. To a stirred solution of dry benzene (6ml), boron trichloride 1M in dichloromethane (5.5ml, 5.5mmol) was added. A solution of 3,5- dimethoxyaniline (0.77mg, 5mmol) in dry benzene (6ml) was added drop-wise under ice cooling. To the resulting mixture containing the 3,5- dimethoxyaniline boron trichloride complex was added chloroacetonitrile (0.38ml, 6mmol) and then aluminium trichloride (718, 5.4mmol). The mixture was refluxed for 6h under argon, during which time the mixture separated into two layers. HCl gas was evolved and absorbed by a drying tube containing calcium chloride. The reaction was then cooled to room temperature and 1M HCl (100ml) was added to give the ketimine as a yellow precipitate. The ketimine was hydrolyzed by heating the mixture to 80°C with stirring for 30 mins during which the precipitate would have dissolved. The cooled mixture was then extracted with dichloromethane (three times), and the

organic layer was washed with water, dried (sodium sulphate) and concentrated to give a yellow powder. This yellow powder was purified by column chromatography with a hexane/ethyl acetate (2:1) as eluant to give pure yellow solid, AZ-1, with a yield of 70%;  $^1\text{H}$  NMR ( $\text{CDCl}_3$ , 300MHz):  $\delta$  3.79 (s, 3H), 3.85 (s,3H), 4.75 (s, 2H), 5.74 (d, 2H, J= 4.5 Hz) 6.52 (br s,  $-\text{NH}_2$ );  $^{13}\text{C}$  NMR ( $\text{CDCl}_3$ , 75MHz):  $\delta$  52.3, 55.2, 55.4, 88.2, 92.0, 102.9, 154.6, 162.9, 164.7, 191.2 MS (APCI); m/z 230.1  $[\text{M}+1]^+$ .

#### 2.5.4.2. 1-Acetyl-4,6-dimethoxy-2,3-dihydro-1H-indole-3-one (AZ-2)

The method of Lawson et al<sup>105</sup> was followed with some modification. AZ-1 (307mg, 1.34mmol) was dissolved in acetic anhydride (10ml) and the solution was heated at 80-85°C for 1 hour, after which acetic anhydride was removed by vacuum distillation. An off-white solid was obtained as the residue and it was purified by column chromatography with hexane/ethyl acetate (3:1) as eluting solvents. 2-(Acetylamino)-4,6-dimethoxy-alpha-chloroacetophenone was obtained as a white solid in 82% yield.  $^1\text{H}$  NMR ( $\text{CDCl}_3$ , 300MHz):  $\delta$  2.23 (s, 3H), 3.89 (s,3H), 3.90 (s, 3H), 4.78 (s, 2H), 6.19 (d, 1H, J= 2.1 Hz), 8.09 (d, 1H, J= 2.1 Hz), 11.76 (br s,  $-\text{NH}$ ); MS (APCI): m/z 294.0  $[\text{M}+1]^+$ . 2-(Acetylamino)-4,6-dimethoxy-alpha-chloroacetophenone (87mg, 0.322mmol) was reacted with  $\text{K}_2\text{CO}_3$  (66mg), KI (70mg) in dry acetone (10ml), with heating (150°C, 12 min) in a microwave reactor (Biotage Initiator<sup>®</sup>) after which the reaction mixture was filtered to remove the solid residues and the filtrate was evaporated under reduced pressure to obtain a crude solid. The crude product was purified by column chromatography with a dichloromethane/methanol (99:1) as eluting solvents. AZ-2 was obtained as a pink-colored solid in 66% yield.  $^1\text{H}$  NMR ( $\text{CDCl}_3$ , 300MHz):  $\delta$  2.29 (s, 3H), 3.91 (s,3H), 3.92 (s, 3H), 4.24 (s, 2H), 6.15 (s, 1H), 7.71 (s, 1H).



#### 2.5.4.3. Condensation of AZ-2 with substituted benzaldehydes

The method of Gerby et al<sup>125</sup> was followed. To a solution of AZ-2 in methanol (10 ml) was added the appropriately substituted benzaldehyde (1.1 to 1.5 equiv), followed by a solution of KOH (500 mg, 8.92 mmol) in distilled water (1 ml). The solution was heated at 60 °C under reflux for 4 hours or by heating in the microwave reactor (110°C, 5 min), after which methanol was removed by evaporation in vacuo and the precipitate was taken into H<sub>2</sub>O (20 ml). The solution was neutralized by adding HCl (1M), then extracted with CH<sub>2</sub>Cl<sub>2</sub> (3 x 50 ml). The organic solution was dried over anhydrous Na<sub>2</sub>SO<sub>4</sub>, the solvent was removed under reduced pressure and the crude product was purified by column chromatography with dichloromethane/acetone (98:2) as eluting solvents to give the aza-aurones **7-1** - **7-8**. For aza-aurone **7-8**, protection and deprotection of the phenolic hydroxyl group on the benzaldehyde was carried out as described in section 2.5.7.

#### 2.5.5. General procedure for the synthesis of 2'-hydroxy-4', 6'-dimethoxychalcones (Compounds **11-1** to **11-5**)

The method of Dao et al<sup>108</sup> was followed. To a solution of 2'-hydroxy-4', 6'-dimethoxyacetophenone (Sigma-Aldrich Chemical Company Inc, Singapore) in methanol (10 ml) was added the appropriately substituted benzaldehyde (1.1 equiv), followed by a solution of KOH (500 mg, 8.92 mmol) in distilled water (1 ml). The mixture was stirred at room temperature (30°C) overnight after which the solvent was removed under reduced pressure and 4M HCl was added to acidify the mixture. A precipitate was formed, removed by suction filtration and recrystallized in methanol-ethanol (1:1) to give the desired product (**11-1** to **11-5**).

#### 2.5.6. General procedure for the synthesis of 5, 7-dimethoxy flavones (Compounds **12-1** to **12-5**)

The method of Dao et al<sup>108</sup> was followed. To a solution of the 2'-hydroxy-4', 6'-dimethoxychalcone in DMSO was added a catalytic amount of iodine (0.1equiv) and the reaction mixture was refluxed at 180°C for 1.5 - 2 hours. The reaction mixture was then cooled to room temperature and poured into saturated solution of sodium thiosulfate. It was extracted with ethyl acetate (3 x 50ml) and the combined organic layers were washed with brine (3 x 50ml) and dried over anhydrous Na<sub>2</sub>SO<sub>4</sub>. The residue obtained on removal of the solvent was purified by column chromatography using hexane/ethyl acetate (1:4) as eluting solvents to give the 5, 7-dimethoxy flavones **12-1 -12-5**.

#### 2.5.7. Protection and deprotection of phenolic hydroxyl groups on 3-hydroxybenzaldehyde, 4-hydroxybenzaldehyde, 3, 4-dihydroxybenzaldehyde, 3, 5-dihydroxybenzaldehyde, 3-hydroxy-4-methoxybenzaldehyde and 4-hydroxy-3-methoxybenzaldehyde

The hydroxylated benzaldehyde (3 mmol), pyridinium p-toluenesulphonate (0.2 mmol) and 3, 4-dihydro-2H-pyran (8 mmol) were dissolved in dichloromethane (10ml) and stirred for 4 hours at room temperature. The reaction mixture was then washed with 1M Na<sub>2</sub>CO<sub>3</sub> (20ml, 3 times). The organic layer was dried over anhydrous Na<sub>2</sub>SO<sub>4</sub> and concentrated in vacuo to give the tetrahydropyranyl ether as a yellow colored liquid which was used without further purification for the subsequent condensation reaction with benzofuranone, indanone or indolinone. At the end of the reaction, the tetrahydropyranyl ether was removed by acidifying the reaction mixture with 4M HCl and stirring for 3 to 4 hours at 30°C after which the hydroxylated (ring B) product would be obtained as a precipitate and removed by suction filtration to give the crude hydroxylated aurone, indanone

and aza-aurone respectively. If no precipitation occurred, the reaction mixture was extracted with  $\text{CH}_2\text{Cl}_2$  (3 x 50ml). The combined organic layers were washed with brine (2 x 50ml), dried over anhydrous  $\text{Na}_2\text{SO}_4$ , filtered and evaporated under reduced pressure to give crude residue.

#### 2.5.8. X-ray crystallography of compounds **1-2** and **6-20**

Compounds **1-2** and **6-20** were grown in methanol and mounted on glass fibres. X-ray data were collected with a Bruker AXS SMART APEX diffractometer, using Mo  $K_\alpha$  radiation at 223 K, with the SMART suite of Programs (SMART version 5.628 (200), Bruker AXS Inc., Madison, WI). Data was processed and corrected for Lorentz and polarization effects with SAINT (SAINT+ version 6.22a (2001) Bruker AXS Inc., Madison, WI), and for absorption effect with SADABS (SADABS, version 2.10 (2001), University of Göttingen). Structural solution and refinement were carried out with the SHELXTL, suite of programs (SHELXTL, Version 6.14 (2000), Bruker AXS Inc., Madison, WI). The structure of each compound was solved by direct methods to locate the heavy atoms, followed by difference maps for the light non-hydrogen atoms. All non-hydrogen atoms were generally given anisotropic displacement parameters in the final model whereas hydrogen atoms were placed at calculated positions.

#### 2.5.9 High pressure liquid chromatography (HPLC) analyses

The purity of compounds was verified by high pressure liquid chromatography (HPLC) on the Waters Delta 600-2487 system or the Agilent Technologies system. Briefly, the compounds were first dissolved in methanol and injected through a 20 $\mu\text{l}$  loop at a flow rate of 0.5ml/min, with UV detections from 300 to 400nm. An Agilent Technologies Zorbax

C<sub>18</sub> column (4.6 x 150mm, 5µm particle size) was used for analysis. Elution was carried out with two different mobile phases: methanol, 0.1% HCOOH in water and acetonitrile, 0.1% HCOOH in water and monitored at  $\lambda_{\text{max}}$  of 300 to 400nm. The retention times and percentage peaks were recorded for each compound. Compounds were considered to be sufficiently pure for biological evaluation if peak areas exceeded 95%.

## 2.6 Summary

The synthesis of 65 compounds comprising aurones, aza-aurones, indanones, chalcones and flavones were successfully achieved. Of the 65 compounds, 37 (57%) have not been reported based on a search with Scifinder Scholar database. All final compounds were of at least 95% pure based on elemental analyses and reversed phase HPLC with two different mobile phases. Assignment of *E/Z* configuration was made by NMR spectroscopy (2D-NOESY), x-ray analysis or by comparison with spectroscopic data reported in the literature.

### **Chapter 3: Effects of aurones and related compounds on the efflux of pheophorbide a (PhA) by ABCG2 over-expressing human breast cancer (MDA-MB-231/R) cells and calcein-AM (CAM) by ABCB1 over-expressing Mardin-Darby canine kidney (MDCK) cells**

#### 3.1. Introduction

This chapter describes the effects of the Series 1-12 compounds on the efflux of an ABCG2 substrate pheophorbide a (PhA) by a human breast cancer cell line that over-expressed ABCG2 (MDA-MB-231/R). The objective of these investigations was to provide insight into the structure-activity relationships that were critical in influencing the interaction of aurones with the ABCG2 transporter. To determine if the structural requirements were specific to ABCG2 or shared with ABCB1, the compounds were investigated for their effects on the efflux of calcein-AM (CAM) by ABCB1-overexpressing Mardin-Darby canine kidney cells (MDCK/MDR1).

#### 3.2. Experimental

##### 3.2.1. Cell lines and materials for biological assay

Fumitremorgin C (FTC), calcein acetoxymethyl ester (calcein-AM, CAM), verapamil, cyclosporin A were purchased from Sigma-Aldrich, St Louis, MO, USA. Pheophorbide a (PhA) was purchased from Frontier Scientific, Utah, USA. The breast cancer cells MDA-MB-231 were stably transfected with expression vectors for wild type 482R ABCG2 (R cells) or pcDNA3.1 (parental V cells). They were kindly provided by Dr. Douglas D. Ross (Greenebaum Cancer Center, University of Maryland, Baltimore, USA). Both MDA-MB-231/V and MDA-MB-231/R cells were cultured in 75cm<sup>3</sup> flasks with RPMI 1640 (Invitrogen Corporation, CA, USA) culture media supplemented with 10% fetal bovine

serum (Hyclone, UT, USA) at 37°C in a 5% CO<sub>2</sub> humidified atmosphere. The culture media contained 0.1mg/ml streptomycin sulfate and 0.1mg/ml penicillin G (Sigma Chemical Co, St Louis, MO, USA) and 1.0mg/ml geneticin (Invitrogen Corporation, CA, USA). Mardin-Darby canine kidney wild type (MDCKII/WT) cells and cells transfected with the expression vector for human *mdr1* cDNA (MDCKII/MDR1) were gifts from Dr. Anton Berns (Netherlands Cancer Institute, Antoni van Leeuwenhoek Hospital, Amsterdam, Netherlands). The cells were grown in DMEM medium containing 10% fetal bovine serum and 0.1mg/ml streptomycin sulfate and penicillin G.

### 3.2.2. Procedure for western blot analysis

Fifteen microgram of cell lysates from MDA-MB-231 R and V cells, and 40 microgram of cell lysates from MDCKII /WT (wild type) and MDCKII/MDR1 were subjected to electrophoresis on 7.5% sodium dodecyl sulphate-polyacrylamide gel (SDS-PAGE) and transferred to nitrocellulose membranes (Bio-Rad Laboratories Pte Ltd, Singapore) for overnight blocking at room temperature. The blots were probed with primary antibodies followed by horseradish peroxidase-conjugated anti-mouse secondary antibody (Pierce Chemicals, Rockford, IL). The primary antibodies used were anti-ABCG2 (BXP-21) and anti- ABCB1 (C219) (Signet Laboratories, Inc, Dedham, MA). The blots were washed and incubated with West Femto luminal/enhancer solution (Pierce Chemicals, Rockford, IL) and Stable Peroxide solution for 5 min. The membranes were analyzed with FluorChem<sup>TM</sup> 9900 (Alpha Innotech Corporation, San Leandro, CA).

### 3.2.3. Procedure for PhA accumulation assay

Pheophorbide a (PhA) accumulation assay was carried out on MDA-MB-231/R cells following a reported method<sup>126</sup> with some modifications. Briefly, the cells were grown in

75cm<sup>2</sup> flasks to 90% confluency and transferred to black-walled, clear-bottomed 96 well plates at a density of 20 000 cells/well. They were incubated at 37<sup>0</sup>C, 5% CO<sub>2</sub> atmosphere for 24 hours after which media was removed and 100µl of test compound (at different concentrations) was added to each well and incubated for a further 30 minutes. The final concentration of DMSO in the well was kept at not more than 0.1% v/v. PhA (100µl, final concentration in well = 1 µM) was added to each well and incubated for 18 hours. After this time, the media was removed and the cells were washed once with 200 µl of cold PBS, followed by addition of 100 µl of cold PBS. Fluorescence was read immediately at λ<sub>excitation</sub> 395 nm and λ<sub>emission</sub> 670 nm on a Tecan Infinite M200 fluorescence plate reader in top read mode. FTC (10 µM) was employed as the positive control and its effect on PhA fluorescence was concurrently monitored in each run.

EC<sub>50</sub> is the concentration of test compound required to increase accumulation of PhA to 50% of the maximum levels obtained with 10 µM PhA. It was determined by monitoring PhA fluorescence (expressed as a % of the fluorescence obtained with 10 µM FTC) at different concentrations of test compound and plotting these values against the concentration of test compounds. Equation 3-1 was used to calculate % PhA accumulation at a given concentration of test compound.

PhA accumulation (% of maximal accumulation) at a specific concentration of test compound

$$= \frac{[\text{Fluorescence}_{\text{R cells + test compound+ PhA}} - \text{Fluorescence}_{\text{R cells + 0.1\% DMSO}}]}{[\text{Fluorescence}_{\text{R cells + 10}\mu\text{M FTC + PhA}} - \text{Fluorescence}_{\text{R cells + 0.1\% DMSO}}]} \times 100\% \quad [3-1]$$

The % PhA accumulation values were plotted against the logarithmic concentrations of test compound using GraphPad Prism (Version 4.00, GraphPad Software, San Diego, CA). The equation used by the software to calculate EC<sub>50</sub> was based on a four-parameter logistic

equation with variable Hill slope and constrained top and bottom values of 100 and 0 respectively (Equation 3-2):

$$Y = \frac{\text{bottom} + (\text{top} - \text{bottom})}{[1 + 10^{(\log EC_{50} - X) \text{ HillSlope}}]} \quad [3-2]$$

where X is the logarithm of concentration of test compound and Y is the response (% PhA accumulation). The EC<sub>50</sub> of each compound was obtained from 3 independent determinations to give the mean value and standard error of the mean (SEM). Fluorescence of test compounds in the absence of PhA is considered negligible as washing step with PBS before the reading of PhA fluorescence would have removed most of the test compounds.

#### 3.2.4. Procedure for calcein-AM (CAM) accumulation assay

A previously described method was followed with some modifications<sup>127</sup>. Briefly, MDCKII/MDR1 and MDCKII/WT cells were grown to 80-90% confluency, trypsinized and seeded in 96-well plates at a cell density of  $2.5 \times 10^4$  cells/well. After incubation at 37°C for 24 h, a monolayer of cells was obtained at the bottom of the well. The medium was decanted and the monolayer carefully washed with PBS. Stock solutions (10 mM) of test compounds were prepared in DMSO and diluted with Hank's Buffered Saline Solution (HBSS) such that the addition of an aliquot (100 µl) gave a final concentration of 10 µM test compound in the well. The final concentration of DMSO in each well was kept at not more than 0.1% v/v. After incubation for 30 min (37°C, 5% CO<sub>2</sub> atmosphere), calcein-AM in HBSS-DMSO (100 µl) was added to each well to give a final concentration of 2 µM. Incubation was continued for another 10 min, after which measurement of fluorescence was started at 10 min intervals, for a further period of 50 minutes (total incubation time = 60 minutes) on a Tecan Infinite M200 fluorescence microplate reader with  $\lambda_{\text{excitation}}$  of 485 nm and  $\lambda_{\text{emission}}$  of 535 nm.



Concurrent determinations were made for the positive controls verapamil and cyclosporin A at 10  $\mu$ M. The % accumulation of calcein-AM was calculated at the 60<sup>th</sup> minute after the addition of calcein-AM with Equation 3-3:

$$\text{Calcein-AM accumulation (\%)} = \frac{[\text{Fluorescence}_{\text{MDCKII/MDR1 + test compound}}]}{[\text{Fluorescence}_{\text{MDCKII/MDR1}}]} \times 100 \quad [3-3]$$

The EC<sub>50</sub> of selected compounds were also determined following the approach reported by Pick et al<sup>40</sup>. EC<sub>50</sub> was defined as the concentration of test compound required to achieve 50% of the maximum response (Y<sub>max</sub>) in terms of % accumulation of calcein-AM obtained with 3 $\mu$ M cyclosporin A after a total incubation time of 60 minutes. The selection of 3 $\mu$ M cyclosporin A was explained in Section 3.3.1. The maximal response (Y<sub>max</sub>) of the test compound at a given concentration was obtained by applying the one phase exponential association as shown in Equation 3-4 (GraphPad Prism, Version 4.00, GraphPad Software, San Diego, CA):

$$Y = Y_{\text{max}} * [1 - \exp(-K * X)] \quad [3-4]$$

where X is time (minutes) of incubation, Y is fluorescence reading of calcein and K is rate constant.

The Y<sub>max</sub> reading of calcein in the presence of a specific concentration of the test compound was normalized to the Y<sub>max</sub> reading elicited by 3 $\mu$ M cyclosporin A using Equation 3-5:

Normalised  $Y_{\max}$  reading of calcein in the presence of test compound at a specific concentration

$$= \frac{Y_{\max\_Test\ compound} - Y_{\max\_MDR1\ cells}}{Y_{\max\ 3\mu M\ CSA} - Y_{\max\ MDR1\ cells}} \times 100\% \quad [3-5]$$

where  $Y_{\max}$  are fluorescence readings of calcein obtained using Equation 3-4

The normalized  $Y_{\max}$  values (dependent variable) were expressed as % of the maximum fluorescence obtained in the presence of 3  $\mu$ M cyclosporin A and plotted against the corresponding logarithmic concentrations of test compound (independent variable).  $EC_{50}$  values were determined by applying the four-parameter logistic equation (Equation 3-2) found in GraphPad Prism (Version 4.00, GraphPad Software, San Diego, CA).  $EC_{50}$  determinations were carried out on 3 separate occasions and reported as the mean  $\pm$  standard error of mean (SEM). Fluorescence of test compounds in the absence of calcein was not considered in Equation 3-3 as it was previously found that fluorescence readings ( $\lambda_{excitation(485\text{ nm})}$ ,  $\lambda_{emission(535\text{ nm})}$ ) of representative compounds (**1-25**, **3-1**, **6-10**, **7-2**, **11-5**, **12-4**) at 30 $\mu$ M accounted for not more than 3% of the  $Y_{\max}$  readings elicited by the compounds alone at 30 $\mu$ M.

### 3.2.5. Statistical Analysis

Data were analyzed for statistically significant differences using Student's t-test or one-way ANOVA followed by Dunnett post hoc test (SPSS 15.0 for Windows, Chicago, IL). p values < 0.05 were considered statistically significant.

### 3. 3. Results

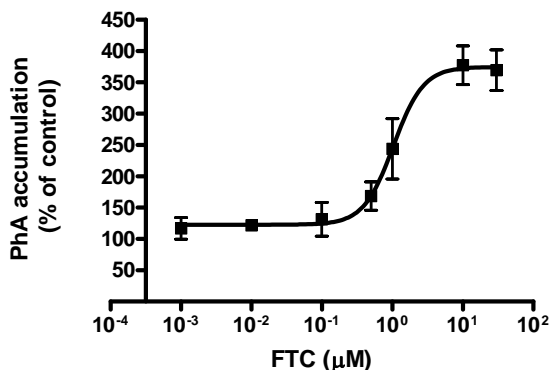
#### 3.3.1. Determination of EC<sub>50</sub> from PhA assay

PhA is one of the substances produced from the catabolism of chlorophyll. It is a specific substrate of ABCG2 as its transport is only observed in cell lines that overexpress ABCG2 and not ABCB1 or MRP1 (ABCC1)<sup>128</sup>. PhA is strongly fluorescent and its uptake into cells is accompanied by an increase in intracellular fluorescence. In cells that overexpress ABCG2, PhA is rapidly transported out of the cell and this is accompanied by a decrease in intracellular fluorescence. In the presence of substances that inhibit or compete with PhA transport from ABCG2 over-expressing cells, the efflux of PhA is reduced and an increase in intracellular fluorescence is observed. The assay has high throughput capabilities and has been used to screen compound libraries for ABCG2 inhibitory activity<sup>126</sup>. For the determination of EC<sub>50</sub> of the test compounds, the effect of FTC on PhA efflux by MDA-MB-231/R cells was first monitored at several concentrations (1 nM to 30 μM). Fluorescence readings obtained at each concentration of FTC was normalized to that obtained in the absence of FTC (control) using the expression:

PhA accumulation (% of control)

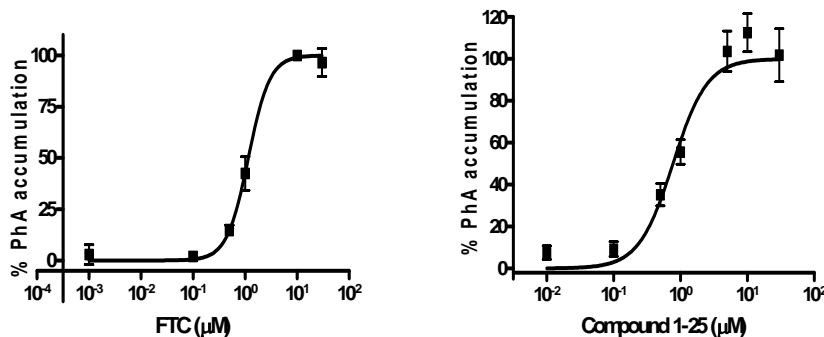
$$= \frac{[\text{Fluorescence}_{\text{R cells + FTC (at a given concentration) + PhA}} - \text{Fluorescence}_{\text{R cells only (blank)}}]}{[\text{Fluorescence}_{\text{R cells + 0.1\% DMSO + PhA}} - \text{Fluorescence}_{\text{R cells only (blank)}}]} \times 100\%$$

Figure 3-1: Dose response curve of PhA accumulation (% of control) against concentration of FTC ( $\mu\text{M}$ ). Control = MDA-MB-231/R cells exposed to PhA in the absence of FTC. Error bars represent SD from 3 independent experiments.



When plotted against concentration of FTC, a sigmoidal dose response curve was obtained (Figure 3-1). It was observed that at 10  $\mu\text{M}$  FTC, PhA fluorescence reached a maximum value and did not increase at higher concentrations of FTC. Hence, the reading obtained with 10  $\mu\text{M}$  FTC was taken as the maximum achievable fluorescence at the prevailing experimental conditions. Thus, readings obtained with other test compounds were expressed as a % of this maximum value (Equation 3-1) to quantify their effects on PhA accumulation. These values (% PhA accumulation) were then plotted against the concentration of test compound at which they were obtained to give a dose response curve for the determination of  $\text{EC}_{50}$ . Figures 3-2 show representative dose response curves of FTC and compound **1-25**.

Figures 3-2: Dose response curves of % PhA accumulation versus varying concentrations of FTC ( $\mu\text{M}$ ) and compound 1-25 ( $\mu\text{M}$ ).

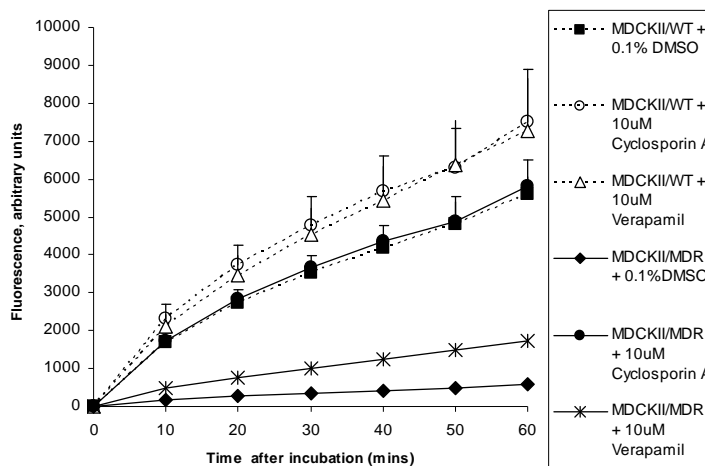


### 3.3.2. Determination of EC<sub>50</sub> from CAM assay

Calcein acetoxymethyl ester (calcein AM, CAM) is a substrate of ABCB1. It is a non-fluorescent, highly lipid soluble dye that readily permeates cells where it is then cleaved by endogenous esterases to the hydrophilic and intensely fluorescent calcein. Calcein is not a substrate of ABCB1 and is retained in the cytosol. Previous studies have shown that there was a good correlation between the level of ABCB1 expression and intracellular calcein fluorescence<sup>129</sup>.

When ABCB1 over-expressing MDCKII/MDR1 cells or the parental wild type cells (MDCKII/WT) were incubated with CAM, intracellular calcein fluorescence increased with time (Figure 3-3). The rate and magnitude of increase were significantly diminished in MDCKII/MDR1 cells due to the high levels of ABCB1 present. When examined in the presence of ABCB1 inhibitors verapamil and cyclosporin A, increases in calcein fluorescence were observed for both ABCB1 overexpressing and parental cells but with significantly greater increases in the MDCKII/MDR1 cells. Notably, there was a 10-fold (MDCKII/MDR1 + 0.1% DMSO versus MDCKII/MDR1 + 10  $\mu$ M Cyclosporin A) difference in accumulation of calcein fluorescence in MDCKII/MDR1 cells exposed to cyclosporin A (10  $\mu$ M) as compared to 1.34-fold (MDCKII/WT + 0.1% DMSO versus MDCKII/WT + 10  $\mu$ M Cyclosporin A) in parental cells exposed to the same concentration of cyclosporin A. Another inhibitor, verapamil (10  $\mu$ M) showed a similar trend but with smaller increases in both MDCKII/MDR1 (3-fold) and parental (1.3-fold) cells. This may be due to the weaker potency of verapamil as an ABCB1 inhibitor.

Figure 3-3: Fluorescence readings of accumulated calcein over time (up to 60 min of incubation time after addition of calcein-AM) in parental MDCKII/WT (dotted lines) and the Pgp over-expressing MDCKII/MDR1 cells (full lines). Data are expressed as mean  $\pm$  S.D, n = 3.



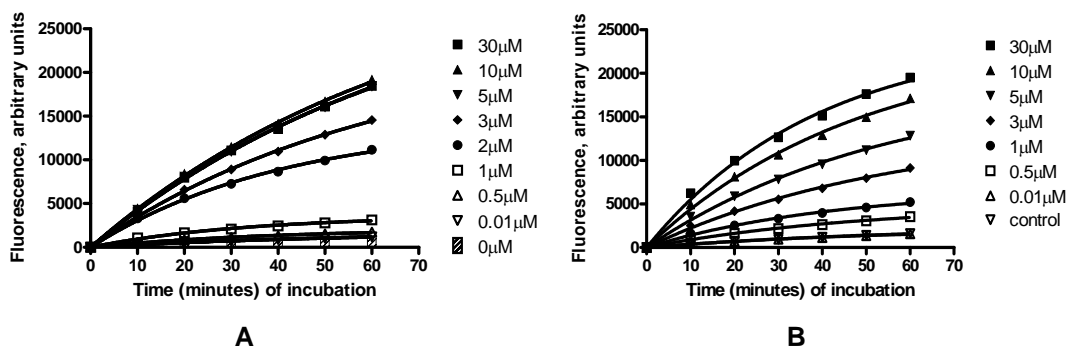
The Series 1-12 compounds were evaluated for their effects on the efflux of CAM from MDCKII/MDR1 cells at a concentration of 10, 5 or 1  $\mu$ M. Fluorescence readings obtained at these concentrations were expressed as a % of reading obtained in the presence of calcein alone (Equation 3-3) and quantified as % calcein-AM accumulation at the 50<sup>th</sup> minute. The choice of concentration (10, 5 or 1  $\mu$ M) was based on the EC<sub>50</sub> of the test compound on the PhA assay. For compounds with EC<sub>50</sub>  $\geq$  10  $\mu$ M, the concentration used for the CAM assay was 10  $\mu$ M while those with EC<sub>50</sub> < 5  $\mu$ M were evaluated at 1  $\mu$ M. For compounds with EC<sub>50</sub> that were between 5  $\mu$ M and 10  $\mu$ M, they were evaluated at 5  $\mu$ M. These cut-off values were set arbitrarily.

To obtain a more accurate assessment of the potency of the compounds as inhibitors of CAM efflux, EC<sub>50</sub> values were determined for selected compounds. As one of the objectives of this chapter was to draw comparative SAR for ABCG2 and ABCB1, it was of interest to determine the CAM accumulation of compounds that had low EC<sub>50</sub> for PhA accumulation. EC<sub>50</sub> values were also determined for those compounds that had high levels of

calcein-AM accumulation. Thus for each series,  $EC_{50}$  were determined for 2 compounds that were the most potent inhibitors of PhA efflux and another 2 compounds associated with the highest % calcein accumulation at the test concentration (presumably potent inhibitors of CAM efflux). As seen in the sections to follow, there were instances where no compound was selected from a particular series and cases where a single compound fulfilled both criteria set for the PhA and CAM assays.

As described in 3.3.1, the fluorescence of PhA in the presence of 10  $\mu$ M FTC was equated to the “maximum achievable response” and used as a standard for comparison to give % PhA accumulation for test compounds (Equation 3-1). In the CAM assay, the fluorescence of calcein in the presence of 3  $\mu$ M cyclosporin A was employed for the same purpose in Equation 3-5. This concentration of cyclosporin A was used because preliminary experiments with representative compounds showed that a fairly constant maximum fluorescence ( $Y_{max}$ ) was obtained at the highest concentrations tested and that these  $Y_{max}$  values coincided with the fluorescence reading of 3  $\mu$ M cyclosporin A. Figures 3-4 shows fluorescence-time curves obtained with cyclosporin A and a representative compound **1-26** when tested over a range of concentrations. For **1-26**, the maximum fluorescence ( $Y_{max}$ ) obtained at 30  $\mu$ M was equivalent to the  $Y_{max}$  reading obtained with 3  $\mu$ M cyclosporin A.

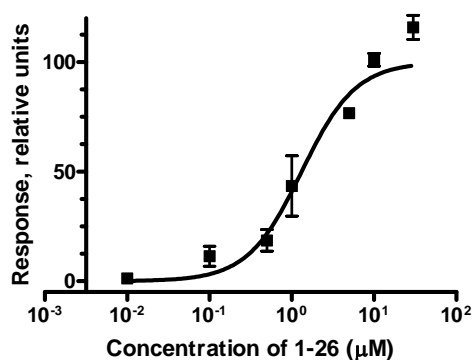
Figures 3-4: Fluorescence-time curves of (A) cyclosporin A and (B) compound 1-26 at various concentrations



To obtain the  $EC_{50}$  of **1-26**, the normalized  $Y_{max}$  values of different concentrations of **1-26** were expressed as a % of the maximum fluorescence obtained in the presence of 3  $\mu\text{M}$  cyclosporin A (Equation 3-5) and plotted against concentration to give a sigmoidal dose response curve (Figure 3-5).

Figure 3-5: Dose response curve for the % accumulation of calcein-AM versus concentration of compound 1-26 in MDCKII/MDR1 cells.

**Dose response curve for compound 1-26**

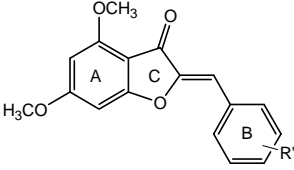


3.3.3. Effect of structural modifications on efflux of PhA by ABCG2 over-expressing human breast cancer (MDA-MB-231/R) cells

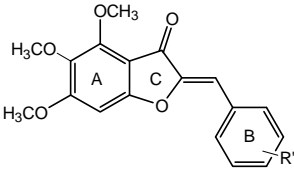
The  $EC_{50}$  of the Series 1-12 compounds for increasing PhA accumulation in ABCG2 over-expressing MDA-MD-231/R cells are given in Table 3-1. The  $EC_{50}$  for the established ABCG2 inhibitor FTC was concurrently determined. A one-way ANOVA with post-hoc showed that none of the compounds were more potent than FTC on this assay but several ( $n = 15$ , indicated with # in Table 3-1) were comparable in potency to FTC.

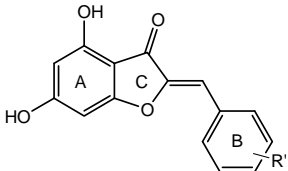


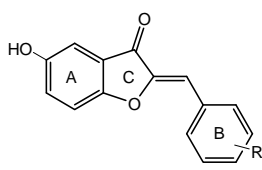
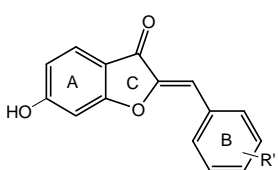
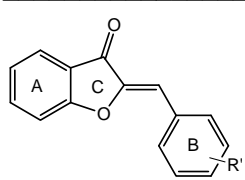
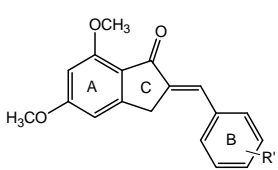
Table 3-1: EC<sub>50</sub> (μM) values of compounds obtained from Pheophorbide a (PhA)

	Compound	R'	PhA assay EC <sub>50</sub> (SEM) [μM]
 <p>4, 6-Dimethoxy aurones (Series 1)</p>	FTC	-	1.26 (0.19)
	1-1	H	6.72 (0.53)
	1-2	2'-OCH <sub>3</sub>	6.33 (0.51)
	1-3	3'-OCH <sub>3</sub>	10.65 (0.70)
	1-4	4'-OCH <sub>3</sub>	10.89 (0.78)
	1-5	2'-OH	3.31 (0.24) <sup>#</sup>
	1-6	3'-OH	1.82 (0.19) <sup>#</sup>
	1-7	4'-OH	6.88 (0.36)
	1-8	2'-Cl	11.14 (1.32)
	1-9	3'-Cl	6.01 (0.56)
	1-10	4'-Cl	>10
	1-11	2'-CH <sub>3</sub>	>10
	1-12	3'-CH <sub>3</sub>	11.68 (0.74)
	1-13	4'-CH <sub>3</sub>	9.56 (0.37)
	1-14	3'-CN	7.73 (0.88)
	1-15	4'-CN	>10
	1-16	2'-F	6.03 (0.40)
	1-17	3'-F	4.78 (0.41)
	1-18	4'-F	>30
	1-19	4'-CF <sub>3</sub>	11.73 (0.61)
	1-20	3'-OH, 4'-OCH <sub>3</sub>	2.21 (0.11) <sup>#</sup>
	1-21	3'-OCH <sub>3</sub> , 4'-OH	2.44 (0.16) <sup>#</sup>
	1-22	2', 3'-(OH) <sub>2</sub>	>30
	1-23	2', 4'-(OH) <sub>2</sub>	>30
	1-24	3', 4'-(OH) <sub>2</sub>	3.08 (0.16) <sup>#</sup>
	1-25	3', 4'-(OCH <sub>3</sub> ) <sub>2</sub>	1.07 (0.07) <sup>#</sup>
	1-26	3', 5'-(OCH <sub>3</sub> ) <sub>2</sub>	0.91 (0.06) <sup>#</sup>

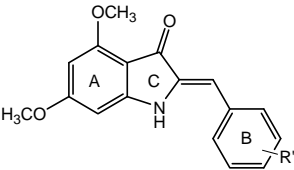
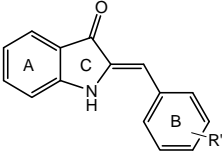
1-27	3', 4'-F <sub>2</sub>	8.07 (0.60)
1-28	3', 5'-F <sub>2</sub>	>10

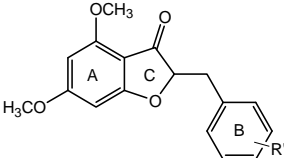
Compound	R'	PhA assay EC <sub>50</sub> (SEM) [μM]	
 4, 5, 6-Trimethoxy aurones (Series 2)	2-1	H	15.34 (1.20)
	2-2	2'-Cl	15.01 (1.08)
	2-3	3'-Cl	5.42 (0.24)
	2-4	4'-Cl	>10
	2-5	2'-OCH <sub>3</sub>	5.69 (0.11)
	2-6	3'-OCH <sub>3</sub>	9.27 (1.06)
	2-7	4'-OCH <sub>3</sub>	11.95 (1.02)
	2-8	3'-CN	>10
	2-9	3'-OH	4.53 (0.33)
	2-10	3'-CH <sub>3</sub>	8.85
	2-11 <sup>a</sup>	cyclohexane	>50

Compound	R'	PhA assay EC <sub>50</sub> (SEM) [μM]	
 4, 6-Dihydroxy aurones (Series 3)	3-1	H	>30
	3-2	2'-OCH <sub>3</sub>	>30
	3-3	3'-OCH <sub>3</sub>	>30
	3-4	4'-Cl	>30
	3-5	3'-OCH <sub>3</sub> , 4'-OH	>30

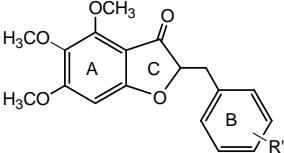
	Compound	R'	PhA assay EC <sub>50</sub> (SEM) [μM]
	4-1	H	>30
	4-2	2'-OCH <sub>3</sub>	>30
	4-3	4'-Cl	>30
5-Hydroxy aurones (Series 4)			
	4-4	H	>30
	4-5	2'-OCH <sub>3</sub>	>30
	4-6	4'-Cl	>30
6-Hydroxy aurones (Series 4)			
	Compound	R'	PhA assay EC <sub>50</sub> (SEM) [μM]
	5-1	H	>30
	5-2	2'-OH	>50
	5-3	3'-OH	>30
	5-4	2'-Cl	>50
	5-5	3'-Cl	>30
	5-6	3'-OCH <sub>3</sub>	>30
	5-7	3'-CN	>30
	5-8	3'-CH <sub>3</sub>	>50
Unsubstituted aurones (Series 5)			
	Compound	R'	PhA assay EC <sub>50</sub> (SEM) [μM]
	6-1	H	9.10 (0.55)
	6-2	2'-OCH <sub>3</sub>	8.48 (0.56)
	6-3	3'-OCH <sub>3</sub>	4.44 (0.53)
	6-4	4'-OCH <sub>3</sub>	>30
	6-5	3'-OH	1.76 (0.19) <sup>#</sup>
4, 6-Dimethoxy indanones (Series 6)			

6-6	4'-OH	8.10 (0.84)
6-7	2'-Cl	>5
6-8	3'-Cl	2.58 (0.04)
6-9	4'-Cl	>30
6-10	3'-CN	1.98 (0.09) <sup>#</sup>
6-11	4'-CN	>10
6-12	2'-CH <sub>3</sub>	>10
6-13	3'-CH <sub>3</sub>	2.62 (0.06) <sup>#</sup>
6-14	4'-CH <sub>3</sub>	>10
6-15	3', 5'-(OCH <sub>3</sub> ) <sub>2</sub>	2.06 (0.10) <sup>#</sup>
6-16	3', 5'-(OH) <sub>2</sub>	>30
6-17	3'-OCH <sub>3</sub> , 4'-OH	2.90 (0.31)
6-18	3'-OH, 4'-OCH <sub>3</sub>	2.51 (0.19) <sup>#</sup>
6-19	3', 4'-(OH) <sub>2</sub>	3.55 (0.17)
6-20	3', 4'-(OCH <sub>3</sub> ) <sub>2</sub>	1.17 (0.07) <sup>#</sup>

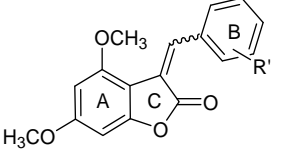
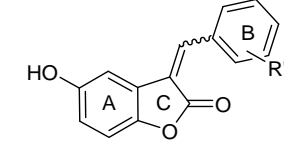
	Compound	R'	PhA assay EC <sub>50</sub> (SEM) [μM]	
 <p>4, 6-Dimethoxy azaaurones (Series 7)</p>	7-1	H	>30	
	7-2	3'-OCH <sub>3</sub>	8.62 (0.60)	
	7-3	4'-OCH <sub>3</sub>	>50	
	7-4	3'-Cl	4.61 (0.25)	
	7-5	4'-Cl	6.97 (0.56)	
	7-6	3'-CN	>30	
	7-7	3'-CH <sub>3</sub>	8.49 (0.7)	
	7-8	3'-OH	>30	
	 <p>Unsubstituted azaaurones (Series 7)</p>	7-9	3'-OCH <sub>3</sub>	>30
		7-10	3'-OH, 4'-OCH <sub>3</sub>	>30

	Compound	R'	PhA assay EC <sub>50</sub> (SEM) [μM]
	8-1	H	>50
	8-2	2'-OH	>50

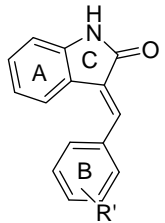
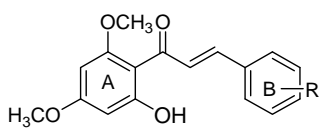
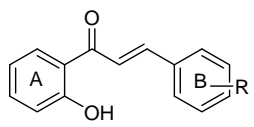
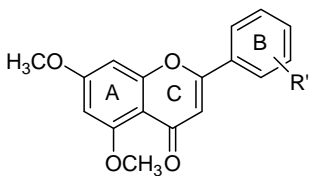
4, 6-Dimethoxy dehydro  
aurones (Series 8)

	8-3	4'-OCH <sub>3</sub>	>50
---	-----	---------------------	-----

4, 5, 6-Trimethoxy dehydro  
aurones (Series 8)

	Compound	R'	PhA assay EC <sub>50</sub> (SEM) [μM]
	9-1	H	>30
	9-2	4'-Cl	>30
	9-3	H	>30
	9-4	2'-OCH <sub>3</sub>	>30
	9-5	4'-Cl	>30

5-Hydroxy isoaurones  
(Series 9)

	Compound	R'	PhA assay EC <sub>50</sub> (SEM) [ $\mu$ M]
 <p>Unsubstituted indolinones (Series 10)</p>	10-1	H	>30
	10-2	3'-Cl	>30
	10-3	3', 5'-(OCH <sub>3</sub> ) <sub>2</sub>	>30
	Compound	R'	PhA assay EC <sub>50</sub> (SEM) [ $\mu$ M]
 <p>2'-Hydroxy,4',6'-dimethoxy chalcones (Series 11)</p>	11-1	H	>50
	11-2	3 -OCH <sub>3</sub>	>50
	11-3	4 -OCH <sub>3</sub>	>50
	11-4	3, 4 -(OCH <sub>3</sub> ) <sub>2</sub>	6.13 (0.58)
	11-5	3, 5 -(OCH <sub>3</sub> ) <sub>2</sub>	2.89 (0.19)
 <p>2'-Hydroxy chalcones (Series 11)</p>	11-6	4-Cl	>30
	11-7	4-CH <sub>3</sub>	>30
	11-8	4-OCH <sub>3</sub>	>30
	Compound	R'	PhA assay EC <sub>50</sub> (SEM) [ $\mu$ M]
 <p>5,7-Dimethoxy flavones (Series 12)</p>	12-1	H	13.45 (0.95)
	12-2	3' -OCH <sub>3</sub>	9.69 (1.51)
	12-3	4' -OCH <sub>3</sub>	21.10 (3.36)
	12-4	3', 4'-(OCH <sub>3</sub> ) <sub>2</sub>	2.45 (0.23) <sup>#</sup>
	12-5	3', 5'-(OCH <sub>3</sub> ) <sub>2</sub>	2.32 (0.38) <sup>#</sup>

#No significant difference ( $p > 0.05$  by one-way ANOVA followed by Dunnett post hoc test) between Fumitremorgin C (FTC) and test compound. Other compounds not indicated with # were significantly less active ( $p < 0.05$ ) than FTC.

<sup>a</sup> Phenyl ring B of **2-11** is replaced with a cyclohexyl ring.

#### 3.3.3.1. Series 1-5 compounds with mono-substituted ring B

Series 1-5 comprise aurones that were substituted on ring A with 4,6-dimethoxy (Series 1), 4,5,6-trimethoxy (Series 2), 4,6-dihydroxyl (Series 3) and 5 or 6- hydroxyl (Series 4) groups. Ring A of Series 5 was not substituted. Ring B was mostly mono-substituted except for a handful of compounds that were disubstituted on ring B.

A significant finding to emerge from the  $EC_{50}$  values of these compounds was the inactivity of the aurones with hydroxyl groups on ring A (mono and dihydroxyl) as well as those with an unsubstituted ring A. The inactivity of the hydroxylated aurones (Series 4,5) was in stark contrast to the strong ABCG2 inhibitory activity reported for dihydroxylated flavones like chrysin. It was evident that structural requirements for flavones and aurones in their interaction with ABCG2 shared few overlapping features.

This was in spite of fairly varied groups (electron donating or withdrawing, lipophilic or hydrophilic) on ring B. Clearly, the state of substitution on ring A was critical in determining activity and based on the compounds available for comparison, aurones with methoxylated ring A are superior to those without groups on ring A or with hydroxylated rings A.

Ring B of the 4,6-dimethoxyaurones (Series 1) was comprehensively substituted with groups that were representative of the four quadrants in the Craig Plot<sup>97</sup>. For instance,  $OCH_3$  and OH are  $-\sigma -\pi$  groups, Cl, F,  $CF_3$  are  $+\sigma +\pi$  groups,  $CH_3$  is  $-\sigma +\pi$  and CN is  $+\sigma -\pi$ . The location of the group on ring B (2', 3' or 4') was also varied for  $OCH_3$ , OH, Cl,  $CH_3$  and F. The activities of the Series 1 compounds showed that the aurone with an unsubstituted ring B

**(1-1)** was actually quite active with an  $EC_{50}$  of 6.72  $\mu\text{M}$ . Moreover, the fold-variation in the activity of Series 1 compounds (based on those with determinable  $EC_{50}$  values) was surprisingly narrow (6.5-fold) in spite of the varied substitutions on ring B. These observations suggested that the type of groups (electron donating or withdrawing, lipophilic or hydrophilic) on ring B had a lesser influence on activity, in so far as ring A was kept in its 4,6-dimethoxylated state. In fact, the position of the group and not the type of group present, may have a more critical role. If so, the 4' position on ring B would be the least favored. Notably, of the four compounds without  $EC_{50}$  values (cited as  $> 10 \mu\text{M}$  or  $> 30 \mu\text{M}$ ), three were 4' isomers. Conversely, better activity was associated with the 3' position. The most active analog in Series 1 was the compound with 3'-OH (**1-6**,  $EC_{50}$  1.82 $\mu\text{M}$ ) and in three other isomeric series (Cl, CN, F), the 3' isomer was consistently more active than the 2' or 4' isomer.

The  $EC_{50}$  values of the trimethoxyaurones of Series 2 also showed limited variation (3.4-fold), reinforcing the notion that substitution on ring B generally had little influence on activity. As to whether a trimethoxylated or dimethoxylated ring A was preferred, a side by side comparison of  $EC_{50}$  values suggested that the dimethoxylated ring A was comparable if not better than its trimethoxylated counterpart. For example, comparing the ring B unsubstituted analogs of both series (**1-1**  $EC_{50}$  6.72  $\mu\text{M}$ ; **2-1**  $EC_{50}$  15.34  $\mu\text{M}$ ), greater activity was found for the dimethoxylated analog **1-1**. The most active Series 2 analog was **2-9** (3'-OH,  $EC_{50}$  4.53  $\mu\text{M}$ ) but it was less active than the most active Series 1 compound **1-6** (3'-OH,  $EC_{50}$  1.82  $\mu\text{M}$ ). Coincidentally or otherwise, both **2-9** and **1-6** had 3'-OH on ring B. Another notable observation was the inactivity of **2-11** in which ring B was replaced by cyclohexyl. This substitution was only found in Series 2 and the significant loss in activity associated with this change suggested the need to retain an aromatic ring B.



### 3.3.3.2. Series 1-5 compounds with di-substituted ring B

With the exception of **3-5**, the other compounds with di-substituted ring B belonged to Series 1. Di-substitution on ring B was carried out with 4 “types” of groups: di-methoxy, di-fluoro, di-hydroxy and hydroxyl(OH)-methoxy(OCH<sub>3</sub>). The effects of di-substitution on activity were not readily predicted from the activities of the corresponding mono-substituted analogs. Thus, while the hydroxylated analogs (**1-5**, **1-6**, **1-7**) were exceptionally active (EC<sub>50</sub> 1.82 μM to 6.88 μM), the dihydroxylated analogs (**1-22**, **1-23**, **1-24**) prove otherwise, with only **1-24** (3',4'-(OH)<sub>2</sub>, EC<sub>50</sub> 3.08 μM) having a measurable EC<sub>50</sub> value. In the case of the methoxylated analogs, the dimethoxy compounds (**1-25**, **1-26**) showed outstanding activities (EC<sub>50</sub> 0.91 μM, 1.07 μM) unlike the weakly active mono-methoxy analogs. On the other hand, activities of di-fluoro and mono-fluoro analogs were generally well matched.

The most active compounds in Series 1 were the dimethoxy analogs **1-26** (3',5'-(OCH<sub>3</sub>)<sub>2</sub> EC<sub>50</sub> 0.91 μM) and **1-25** (3',4'-(OCH<sub>3</sub>)<sub>2</sub> EC<sub>50</sub> 1.07 μM). Starting from **1-25**, replacing both methoxy groups with hydroxyl groups gave **1-24** (3',4'-(OH)<sub>2</sub> EC<sub>50</sub> 3.08 μM) and replacing either methoxy group with OH resulted in **1-20** (3'-OH,4'-OCH<sub>3</sub>) and **1-21** (3'-OCH<sub>3</sub>, 4'-OH). As seen from their EC<sub>50</sub> values, only a slight decline in activity was evident. It is tempting to propose that 3' and 4' were “privileged” positions on ring B. The 3',5'-positions may also share this favored status but unfortunately there were not as many compounds available for comparison. It was noted however that of the two di-fluoro analogs, 3',4'-difluoro **1-27** was significantly more active than 3',5'-difluoro **1-28**. Besides Series 1, there was one other compound in Series 3 (3-5) that had a di-substituted ring B. This compound was inactive in spite of having a 3'-OCH<sub>3</sub> and 4'-OH ring B, further reinforcing the view that the substitution on ring A was more critical than the substitution on ring B.

### 3.3.3.3. Ring C modifications that result in no activity

Of the five modifications that were proposed for ring C (summarized in Figure 3-7), two changes resulted in a total loss of activity. These are the reduction of the exocyclic double bond to give dehydroaurones (Series 8) and the relocation of the carbonyl C=O and exocyclic double bond to give isoaurones (Series 9) and indolinones (Series 10). Clearly, an intact double bond and its location must be retained for activity.

### 3.3.3.4. Ring C modifications: Replacement of O with CH<sub>2</sub> or NH

The oxygen atom of the aurone ring C was replaced by a methylene (CH<sub>2</sub>) group to give the indanones of Series 6 or nitrogen (NH) to give azaaurones of Series 7. 4,6-Dimethoxy groups were retained on the ring A of both templates except for two azaaurones (**7-9**, **7-10**) which had unsubstituted ring A. The results revealed an interesting similarity between the SAR of Series 1 and Series 6. These were (i) the narrow variation in EC<sub>50</sub> for analogs with monosubstituted ring B (5-fold variation compared to 6-fold in Series 1), (ii) the association of the 3' position with better activity than the 2' and 4' analogs, (iii) the 3'-OH analog 6-5 (EC<sub>50</sub> 1.76 μM) was also the most active mono-substituted ring B analog and (iv) the exceptionally good activities (EC<sub>50</sub> < 5 μM) of the di-substituted ring B analogs. A notable difference was that moving from the mono-substituted to di-substituted state of ring B did not show as marked an improvement in activity as was observed in Series 1. One reason was that Series 6 comprised many potent compounds (50% with EC<sub>50</sub> < 5 μM), including mono-substituted ring B analogs. In comparison, most of the potent compounds in Series 1 (EC<sub>50</sub> < 5 μM) were the di-substituted ring B analogs.

The Series 7 azaaurones was a small series of 10 compounds, of which 8 were 4,6-dimethoxyazaaurones (**7-1** to **7-8**) and 2 were ring A unsubstituted azaaurones (**7-9**, **7-10**).

There were obvious differences in the SAR of Series 7 and Series 1. First, the ring B unsubstituted azaaurone (**7-1**) was inactive ( $EC_{50} > 30 \mu\text{M}$ ) but substitution of ring B (with  $\text{OCH}_3$ , Cl,  $\text{CH}_3$ ) resulted in significant improvements in activity. Second, it was not so evident that the 3' position on ring B was a favored position among the azaaurones. For example, the 3'OH (**7-8**) and 3'CN (**7-6**) analogs were essentially inactive in Series 7 whereas they were highly favored groups in Series 1 and 6. Again, the inactivity of **7-9** and **7-10** (unsubstituted ring A) confirmed the importance of retaining methoxy groups on ring A.

#### 3.3.3.5. Ring C modifications: Cleavage of ring C

The chalcones of Series 11 were structurally related to aurones as ring C cleaved analogs. Only 2 chalcones (**11-4**, **11-5**) were inhibitors of PhA efflux and both compounds had dimethoxy groups on ring B. It would seem that activity was influenced by the substitution on ring B to a greater degree than on ring A, in contrast to other series (1, 2, 6, 7) where the reverse was observed. On the other hand, the association of good activity with dimethoxy groups on ring B was common to many potent compounds in the various series. Evaluation with more chalcones would be required to establish a reliable SAR trend.

#### 3.3.3.6. Ring C modifications: Expansion of ring C

The flavones of Series 12 were structurally related to both the Series 11 chalcones (**11-1** to **11-5**) and Series 1 aurones. The chalcones were obtained by cleavage of the flavone ring C at O1-C2 position while the expansion of ring C in aurones (with the double bond in ring C) gave flavones. Unlike the chalcones, the ring B unsubstituted or monosubstituted flavones (**12-1** to **12-3**) were now active on the PhA assay but only comparable or less active than the aurones (**1-1**, **1-3** and **1-4**) in terms of  $EC_{50}$ . The most potent flavones were the 3'4'-

dimethoxy (**12-4**, EC<sub>50</sub> 2.45 μM) and 3'5'-dimethoxy (**12-5**, EC<sub>50</sub> 2.32 μM) analogs. As mentioned earlier, the same di-methoxylated ring B was present in the most potent analogs in the Series 1 aurones, Series 6 indanones and Series 11 chalcones. It may be that this moiety has unique structural features or physicochemical properties that enhance its ability to interfere with the ABCG2 mediated transport of PhA.

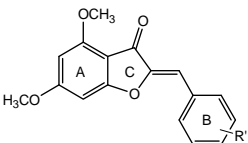
The variation in activity among the flavones, aurones and chalcones indicated that an intact ring C was preferred. Less critical for activity were the size of ring C (5- or 6-membered) and the endocyclic / exocyclic placement of the double bond. An intact double bond was essential for aurones (dehydroaurones were inactive) but less so for flavones where the reduction of the 2,3 double bond to give flavanones retained activity but at a lower level than flavones<sup>64</sup>.

#### 3.3.4. Effect of structural modifications on efflux of calcein-AM (CAM) by ABCB1 over-expressing MDCKII/MDR1 cells

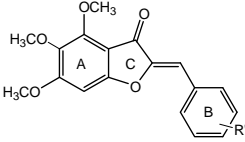
Series 1-12 compounds were evaluated at a fixed concentration on the CAM assay. The concentration used was related to the EC<sub>50</sub> of the compound for reducing PhA efflux from MBA-MV-231 /R cells as described earlier (Section 3.3.1). For convenience, only 3 concentrations (1, 5 and 10 μM) were used. Therefore if a compound had an EC<sub>50</sub> of 2.44 μM on the PhA assay, it would be tested at 1 μM on the CAM assay. In this way, a quick assessment of the ability of the test compound to reduce the efflux of CAM could be at or near the concentration of its EC<sub>50</sub> for PhA efflux (by 50%). However, as CAM efflux was evaluated at only one concentration, comparing % CAM accumulation with EC<sub>50</sub> for PhA efflux would not be a reliable means of deducing the selectivity of the compound for either transporter. Table 3-2 gives the % CAM accumulation of Series 1-12 compounds at the

specified concentration. The ABCB1 inhibitors verapamil and cyclosporin A were concurrently monitored at a fixed concentration of 10  $\mu$ M. Several compounds, notably the flavones, were more potent than verapamil at increasing the accumulation of CAM, even when tested at concentrations < 10  $\mu$ M.

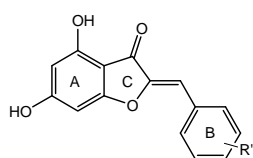
Table 3-2: Accumulation of calcein-AM in MDCKII/MDR1 cells in the presence of test compounds.

	Compound	R'	Conc used	Calcein-AM accumulation (% of control) <sup>a</sup>	
	MDCKII/MDR1 (control)			100	
	MDCKII/MDR1 (vera)		10	214.0 (7.7)	
	MDCKII/MDR1 (cyclo)		10	605.3 (29.2)	
	1-1	H	5	139.3 (5.8)	
	4, 6-Dimethoxy auronones (Series 1)	1-2	2'-OCH <sub>3</sub>	5	105.0 (5.9)
		1-3	3'-OCH <sub>3</sub>	10	173.9 (7.1)
		1-4	4'-OCH <sub>3</sub>	10	107.5 (7.0)
		1-5	2'-OH	1	81.1 (3.4)
		1-6	3'-OH	1	103.0 (4.5)
		1-7	4'-OH	5	156.4 (9.7)
		1-8	2'-Cl	10	110.9 (9.6)
		1-9	3'-Cl	5	128.6 (10.8)
		1-10	4'-Cl	10	131.0 (3.7)
		1-11	2'-CH <sub>3</sub>	10	92.1 (2.0)
		1-12	3'-CH <sub>3</sub>	10	153.5 (9.3)
		1-13	4'-CH <sub>3</sub>	5	111.6 (6.4)
		1-14	3'-CN	5	251.4(20.0) <sup>++</sup>
		1-15	4'-CN	10	166.8 (7.7)

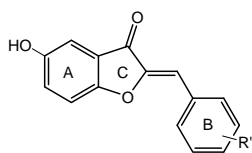
1-16	2'-F	5	151.0 (7.8)
1-17	3'-F	1	108.0 (7.0)
1-18	4'-F	10	150.7 (7.4)
1-19	4'-CF <sub>3</sub>	10	120.0 (5.3)
1-20	3'-OH, 4'-OCH <sub>3</sub>	1	94.0 (3.3)
1-21	3'-OCH <sub>3</sub> , 4'-OH	1	92.0 (5.3)
1-22	2', 3'-(OH) <sub>2</sub>	10	98.9 (1.7)
1-23	2', 4'-(OH) <sub>2</sub>	10	102.1 (8.8)
1-24	3', 4'-(OH) <sub>2</sub>	1	98.0 (4.2)
1-25	3', 4'-(OCH <sub>3</sub> ) <sub>2</sub>	1	146.2 (4.9)
1-26	3', 5'-(OCH <sub>3</sub> ) <sub>2</sub>	1	137.5 (6.4)
1-27	3', 4'-F <sub>2</sub>	5	114.5 (1.1)
1-28	3', 5'-F <sub>2</sub>	10	93.9 (5.8)

	Compound	R'	Conc used	Calcein-AM accumulation (% of control) <sup>a</sup>
 <p>4, 5, 6-Trimethoxy aurones (Series 2)</p>	2-1	H	10	158.2 (7.2)
	2-2	2'-Cl	10	122.2 (8.2)
	2-3	3'-Cl	5	169.5 (10.9)
	2-4	4'-Cl	10	98.9 (3.3)
	2-5	2'-OCH <sub>3</sub>	5	216.5 (12.1)
	2-6	3'-OCH <sub>3</sub>	5	204.9 (12.3)

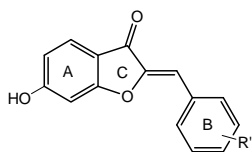
	2-7	4'-OCH <sub>3</sub>	10	365.8 (22.1) <sup>++</sup>
	2-8	3'-CN	10	102.1 (6.4)
	2-9	3'-OH	1	92.6 (3.1)
	2-10	3'-CH <sub>3</sub>	5	334.6 (10.6) <sup>++</sup>
	2-11 <sup>b</sup>	cyclohexane	10	197.9 (12.8)
	Compound	R'	Conc used	Calcein-AM accumulation (% of control) <sup>a</sup>



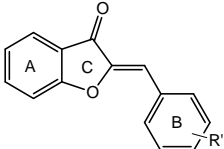
4, 6-Dihydroxy aurones (Series 3)	3-1	H	10	84.2 (3.4)
	3-2	2'-OCH <sub>3</sub>	10	82.5 (2.4)
	3-3	3'-OCH <sub>3</sub>	10	80.0 (4.4)
	3-4	4'-Cl	10	79.1 (6.2)
	3-5	3'-OCH <sub>3</sub> , 4'-OH	10	76.2 (7.0)
	Compound	R'	Conc used	Calcein-AM accumulation (% of control) <sup>a</sup>

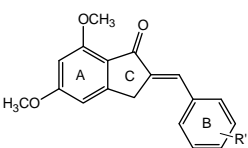


5-Hydroxy aurones (Series 4)	4-1	H	10	79.5 (2.9)
	4-2	2'-OCH <sub>3</sub>	10	94.1 (7.8)
	4-3	4'-Cl	10	92.7 (9.4)



6-Hydroxy aurones (Series 4)	4-4	H	10	86.9 (6.0)
	4-5	2'-OCH <sub>3</sub>	10	88.6 (6.6)
	4-6	4'-Cl	10	100.6 (8.8)

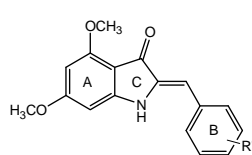
	Compound	R'	Conc used	Calcein-AM accumulation (% of control) <sup>a</sup>
 Unsubstituted auronones (Series 5)	5-1	H	10	87.7 (1.5)
	5-2	2'-OH	10	73.9 (2.9)
	5-3	3'-OH	10	82.6 (3.0)
	5-4	2'-Cl	10	85.7 (3.9)
	5-5	3'-Cl	10	93.4 (2.2)
	5-6	3'-OCH <sub>3</sub>	10	98.9 (4.4)
	5-7	3'-CN	10	161.3 (17.3)
	5-8	3'-CH <sub>3</sub>	10	83.6 (1.3)

	Compound	R'	Conc used	Calcein-AM accumulation (% of control) <sup>a</sup>
 4, 6-Dimethoxyindanones (Series 6)	6-1	H	5	151.2 (8.5)
	6-2	2'-OCH <sub>3</sub>	5	99.5 (3.7)
	6-3	3'-OCH <sub>3</sub>	1	381.3 (12.4) <sup>++</sup>
	6-4	4'-OCH <sub>3</sub>	10	161.4 (16.7)
	6-5	3'-OH	1	90.7 (5.6)
	6-6	4'-OH	5	96.3 (2.8)
	6-7	2'-Cl	5	102.6 (4.3)
	6-8	3'-Cl	1	147.6 (2.0)
	6-9	4'-Cl	10	193.1 (5.1)
	6-10	3'-CN	1	98.2 (4.8)



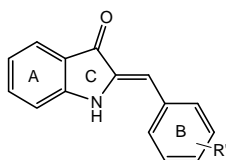
6-11	4'-CN	10	104.2 (4.4)
6-12	2'-CH <sub>3</sub>	10	293.5 (18.6) <sup>++</sup>
6-13	3'-CH <sub>3</sub>	1	90.5 (1.4)
6-14	4'-CH <sub>3</sub>	10	278.2 (13.1) <sup>++</sup>
6-15	3', 5'-(OCH <sub>3</sub> ) <sub>2</sub>	1	176.8 (13.2)
6-16	3', 5'-(OH) <sub>2</sub>	10	94.1 (7.3)
6-17	3'-OCH <sub>3</sub> , 4'-OH	1	98.5 (2.8)
6-18	3'-OH, 4'-OCH <sub>3</sub>	1	93.6 (4.7)
6-19	3', 4'-(OH) <sub>2</sub>	1	89.1 (2.8)
6-20	3', 4'-(OCH <sub>3</sub> ) <sub>2</sub>	1	147.8 (5.7)

Compound	R'	Conc used	Calcein-AM accumulation (% of control) <sup>a</sup>
----------	----	-----------	---



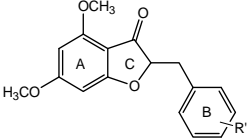
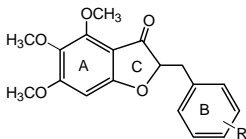
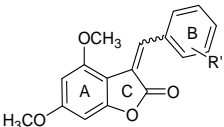
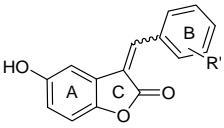
4, 6-Dimethoxy azaaurones (Series 7)

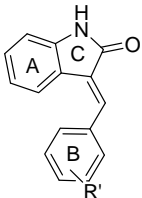
7-1	H	10	100.9 (3.5)
7-2	3'-OCH <sub>3</sub>	5	206.4 (5.0)
7-3	4'-OCH <sub>3</sub>	10	127.7 (6.6)
7-4	3'-Cl	1	102.7 (6.1)
7-5	4'-Cl	5	170.0 (6.6)
7-6	3'-CN	10	151.2 (5.7)
7-7	3'-CH <sub>3</sub>	5	118.1 (8.5)
7-8	3'-OH	10	103.1 (4.1)



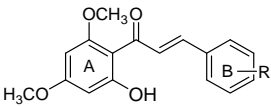
Unsubstituted azaaurones (Series 7)

7-9	3'-OCH <sub>3</sub>	10	85.1 (5.3)
7-10	3'-OH, 4'-OCH <sub>3</sub>	10	92.5 (7.8)

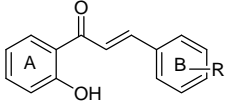
	Compound	R'	Conc used	Calcein-AM accumulation (% of control) <sup>a</sup>
 <p>6-Dimethoxy dehydro aurones (Series 8)</p>	8-1	H	10	85.3 (3.4)
	8-2	2'-OH	10	94.9 (1.1)
	8-3	4'-OCH <sub>3</sub>	10	111.1 (3.8)
 <p>4, 5, 6-Trimethoxy dehydro aurones (Series 8)</p>				
	Compound	R'	Conc used	Calcein-AM accumulation (% of control) <sup>a</sup>
	 <p>4,6-Dimethoxy isoaurones (Series 9)</p>	9-1	H	10
9-2		4'-Cl	10	76.8 (5.9)
 <p>5-Hydroxy isoaurones (Series 9)</p>		9-3	H	10
	9-4	2'-OCH <sub>3</sub>	10	127.3 (3.0)
	9-5	4'-Cl	10	90.2 (6.2)

	Compound	R'	Conc used	Calcein-AM accumulation (% of control) <sup>a</sup>
	10-1	H	10	77.0 (6.8)
	10-2	3' -Cl	10	94.8 (2.0)
	10-3	3', 5'-(OCH <sub>3</sub> ) <sub>2</sub>	10	114.1 (8.0)

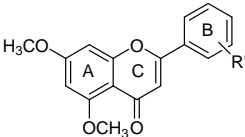
Unsubstituted indolinones (Series 10)

	Compound	R'	Conc used	Calcein-AM accumulation (% of control) <sup>a</sup>
	11-1	H	10	127.6 (7.0)
	11-2	3' -OCH <sub>3</sub>	10	98.6 (10.8)
	11-3	4' -OCH <sub>3</sub>	10	97.4 (6.2)
	11-4	3', 4'-(OCH <sub>3</sub> ) <sub>2</sub>	5	95.7 (11.5)
	11-5	3', 5'-(OCH <sub>3</sub> ) <sub>2</sub>	1	80.8 (7.5)

2'-Hydroxy,4',6'-dimethoxy chalcones (Series 11)

	11-6	4 -Cl	10	82.3 (7.0)
	11-7	4 -CH <sub>3</sub>	10	75.8 (3.8)
	11-8	4 -OCH <sub>3</sub>	10	84.4 (5.1)

2'-Hydroxy chalcones (Series 11)

	Compound	R'	Conc used	Calcein-AM accumulation (% of control) <sup>a</sup>
	12-1	H	10	208.2 (6.4)
	12-2	3' -OCH <sub>3</sub>	5	304.9 (16.7) <sup>++</sup>
	12-3	4' -OCH <sub>3</sub>	10	265.7 (17.4)

5,7-Dimethoxy flavones (Series 12)

12-4	3', 4'-(OCH <sub>3</sub> ) <sub>2</sub>	1	283.4 (20.7) <sup>++</sup>
12-5	3', 5'-(OCH <sub>3</sub> ) <sub>2</sub>	1	288.6 (13.0) <sup>++</sup>

<sup>a</sup> The accumulation of calcein-AM was calculated at the 60<sup>th</sup> minute after addition of CAM using the following equation: Calcein-AM accumulation =  $[F_{\text{MDCKII / MDR1 + test compound}}] / [F_{\text{MDCKII / MDR1 (Control)}}] \times 100 \%$ . Data from at least three independent experiments were expressed as mean  $\pm$  S.E.M (in brackets).

<sup>b</sup> Phenyl ring B of **2-11** is replaced with a cyclohexyl ring.

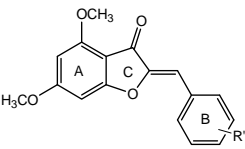
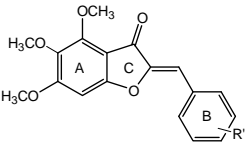
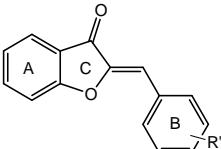
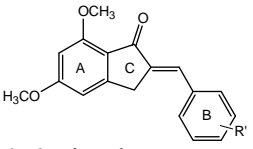
<sup>++</sup> Significant difference ( $p < 0.05$ ) between compounds at their respective concentrations and Verapamil (at 10 $\mu$ M) by Dunnett (2-sided) post doc test.

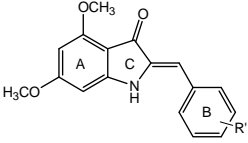
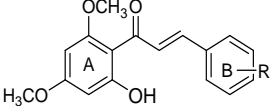
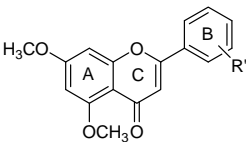
Assuming that “inactive” compounds were those that accumulated CAM to  $\leq 110\%$  at 10  $\mu$ M and “active” compounds were those that accumulated CAM to  $\geq 200\%$  at the test concentration, the structural profiles of these classes of compounds could be deduced. Inactive compounds were mostly found among hydroxylated aurones, isoaurones, dehydroaurones and aurones with unsubstituted ring A. Also included were azaaurones with unsubstituted ring A, indolinones and chalcones. Active compounds were found among di- and tri-methoxyaurones, indanones, azaaurones and flavones. In total, 14 active compounds were identified (**1-14**, **2-5 to 2-7**, **2-10**, **6-3**, **6-12**, **6-14**, **7-2**, **12-1 to 12-5**). Of these compounds, flavones were strongly represented (5 compounds) followed by the trimethoxyaurones (4 compounds). Another common feature of these active compounds was the presence of methoxy groups on ring B. Nine of the 14 active compounds had this feature and most of them had 3'-methoxy substitution (6 of 14 actives).

The EC<sub>50</sub> for accumulation of CAM was determined for selected compounds to provide a more accurate assessment of their effects on efflux activity of the ABCB1 transporter. As stated earlier (Section 3.3.2), where possible, 4 compounds were selected from each series: 2 compounds which had the lowest EC<sub>50</sub> from the PhA assay, and 2

compounds with the highest % CAM accumulation. In total, 20 compounds were evaluated and their EC<sub>50</sub> values on both PhA and CAM assays are given in Table 3-3.

Table 3-3: EC<sub>50</sub> (μM) for PhA accumulation and CAM accumulation of selected compounds

Compound	R'	PhA assay EC <sub>50</sub> (SEM) [μM]	CAM assay EC <sub>50</sub> (SEM) [μM]	
 Verapamil	-		>30	
	1-3	3'-OCH <sub>3</sub>	10.65 (0.70)	4.73 (0.27)
	1-14	3'-CN	7.73 (0.88)	3.59 (0.32)
	1-25	3', 4'-(OCH <sub>3</sub> ) <sub>2</sub>	1.07 (0.07)	1.10 (0.01)
4, 6-Dimethoxy aurones (Series 1)	1-26	3', 5'-(OCH <sub>3</sub> ) <sub>2</sub>	0.91 (0.06)	2.27 (0.14)
	 4, 5, 6-Trimethoxy aurones (Series 2)	2-3	3'-Cl	5.42 (0.24)
2-7		4'-OCH <sub>3</sub>	11.95 (1.02)	3.64 (0.08)
2-9		3'-OH	4.53 (0.33)	12.40 (1.36)
2-10		3'-CH <sub>3</sub>	8.85	4.88 (0.35)
 Unsubstituted aurones (Series 5)	5-7	3'-CN	>30	>30
	 4, 6-Dimethoxy indanones (Series 6)	6-3	3'-OCH <sub>3</sub>	4.44 (0.53)
6-5		3'-OH	1.76 (0.19)	>30
6-12		2'-CH <sub>3</sub>	>10	>10
6-20		3', 4'-(OCH <sub>3</sub> ) <sub>2</sub>	1.17 (0.07)	2.53 (0.34)

	Compound	R'	PhA assay	CAM assay
			EC <sub>50</sub> (SEM) [ $\mu$ M]	EC <sub>50</sub> (SEM) [ $\mu$ M]
 4, 6-Dimethoxy aza-aurones (Series 7)	7-2	3'-OCH <sub>3</sub>	8.62 (0.60)	5.12 (0.81)
	7-4	3'-Cl	4.61 (0.25)	>30
	7-5	4'-Cl	6.97 (0.56)	9.80 (1.05)
 2'-Hydroxy, 4',6'-dimethoxy chalcones (Series 11)	11-5	3, 5 -(OCH <sub>3</sub> ) <sub>2</sub>	2.89 (0.19)	>30
 5,7-Dimethoxy flavones (Series 12)	12-2	3' -OCH <sub>3</sub>	9.69 (1.51)	8.16 (0.75)
	12-4	3', 4'-(OCH <sub>3</sub> ) <sub>2</sub>	2.45 (0.23)	6.34 (1.45)
	12-5	3', 5'-(OCH <sub>3</sub> ) <sub>2</sub>	2.32 (0.38)	2.27 (0.33)

The results showed that the compounds could be broadly divided into those that inhibited PhA and CAM efflux to approximately the same extent and those that inhibited PhA efflux to a greater degree than CAM efflux. The 1<sup>st</sup> group of compounds would be considered non-selective inhibitors of either transporter while the 2<sup>nd</sup> group of compounds would be preferred inhibitors of ABCG2 than ABCB1. The dimethoxyaurones and flavones were well represented in the 1<sup>st</sup> group (non-selective for either transporter). On the other hand, preferred inhibitors of PhA efflux (2<sup>nd</sup> group) were found across the different series, with no specific concentration in any series. It was interesting that none of the investigated compounds inhibited CAM efflux to a greater degree than PhA efflux.

### 3.4. Discussion

The objective of this chapter was to understand the SAR of aurone-ABCG2 interactions and to identify, where possible, features that were specific for this interaction. To achieve this end, a means of quantifying the aurone-ABCG2 interaction was required and this was provided by the EC<sub>50</sub> for the accumulation of the substrate PhA in ABCG2 over-expressing cells (MDA-MB-231/R). To investigate the selectivity of the interaction, comparison was made to the aurone-ABCB1 interaction which was quantified by the EC<sub>50</sub> for the accumulation of CAM in ABCB1 over expressing cells (MDCKII/MDR1). The validity of these approaches was confirmed by observations that parental MDA-MB-231/V cells accumulated less PhA (ca 5 x lower) than MDA-MB-231/R cells. Similarly, parental MDCKII/WT cells accumulated less CAM (ca 6 x lower) than MDCKII/MDR1 cells. In addition, Western blot analyses demonstrated that MDA-MB-231/R cells over-expressed ABCG2 and had no detectable ABCB1, while MDCKII/MDR1 cells over-expressed ABCB1 with little or no detectable ABCG2 (Appendix 3-1).

The findings of this chapter showed that aurones were capable of increasing the accumulation of PhA in ABCG2 over-expressing cells. Notably, the most potent aurones identified (**1-25** EC<sub>50</sub> 0.91 μM; **1-26** EC<sub>50</sub> 1.17 μM) were equipotent to the established ABCG2 inhibitor FTC (EC<sub>50</sub> 1.26 μM). An analysis of structure-activity relationships showed that the state of substitution on ring A was a critical feature for activity and in this regard, methoxy groups on ring A were favored over hydroxyl groups or an unsubstituted ring A. Thus, the dimethoxyaurones (Series 1) and trimethoxyaurones (Series 2) yielded several active analogs, whereas the hydroxylated aurones (Series 3 and 4) and ring A unsubstituted aurones (Series 5) were essentially inactive. Interestingly, the inactivity of the latter series was observed even when the ring B of these compounds was substituted with

groups that were associated with the lowest EC<sub>50</sub> values among the active dimethoxy and trimethoxyaurones. In the case of these active series, introducing a wide variety of groups on ring B resulted in compounds that showed narrow variations in their EC<sub>50</sub> values (12.9 and 3.4-fold respectively, based on 21 dimethoxyaurones and 8 trimethoxyaurones with determinable values).

Mono- and di-substitution were explored on ring B of the dimethoxyaurones (Series 1). In the case of mono-substitution, the position and nature of the substituents were found to be important in influencing activity. In this regard, position 3' on ring B appeared to be the preferred position and its favored status was observed not only among the dimethoxyaurones but also in other active series like the Series 6 indanones, Series 7 azaaurones and Series 12 flavones. Di-substitution of ring B was particularly interesting because the most potent analogs identified from several series (Series 1, 6, 12) were di-substituted analogs. The preferred substituents were dimethoxy, hydroxyl-methoxy and to a lesser degree, dihydroxy groups.

The structural modifications on ring C provided further insight into structure-activity requirements. Notably, the importance of maintaining an intact exocyclic double bond and the relative positions of the carbonyl and exocyclic double bond were highlighted from the inactivity of the dehydroaurones and the isoaurones. An intact exocyclic double bond may be required to maintain planarity and reduce the flexibility of the aurone template. In this regard, a planar aurone may be more critical than a planar flavone for ABCG2 interaction. This was deduced from the flavanones which were only less active (ca 6-fold) than flavones when assessed for their effects on mitoxantrone accumulation in ABCG2 overexpressing MCF-7 cells<sup>64</sup>.

The inactivity of the isoaurones showed that positioning of the carbonyl group vis-à-vis the exocyclic double bond was critical. Steric factors may be in play because the

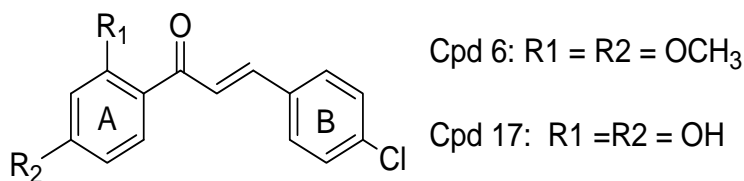


isoaurones exist predominately as *E* isomers<sup>130</sup> and in this configuration, rings A and B are in close proximity. Electronic factors may also play a part as the carbonyl function in isoaurones is now part of a lactone in ring C. This would weaken the electron withdrawing effect of the carbonyl group as shown by the Swain and Lupton F (inductive) and R (resonance) values of an ester (-COOC<sub>2</sub>H<sub>5</sub>; F = 0.47; R = 0.67) and ketone (-COCH<sub>3</sub>; F = 0.50; R = 0.90), where numerically larger values indicated a stronger electron withdrawing effect<sup>107</sup>. A weaker electron withdrawing effect of the carbonyl in isoaurones would enhance the electron density on the exocyclic double bond and this may somehow adversely affect activity.

In contrast to the aforementioned changes to ring C which had significant effects on activity, replacing the aurone O with methylene CH<sub>2</sub> or amino NH did not result in marked changes. In particular, the replacement of O with CH<sub>2</sub> to give the indanones of Series 6 retained many of the SAR features observed for dimethoxyaurones, such as the importance of the 3' position on ring B and the outstanding activities of ring B di-methoxylated analogs. The Series 6 indanones were in fact a more potent series than the Series 1 dimethoxyaurones. In contrast, the azaaurones of Series 7 bore little resemblance in terms of SAR to the dimethoxyaurones. There was however one common feature, namely the switch in the carbonyl and exocyclic double bonds in ring C of the azaaurone to give indolinones (Series 10) also abolished activity. Thus, it was concluded that the ring C oxygen of aurones can be replaced by CH<sub>2</sub> (a non-H bond acceptor and donor) as well as NH (a H bond donor) but with some loss in activity for the latter.

Chalcones have been reported to increase the accumulation of mitoxantrone in MDA-MB-231/R cells<sup>91</sup>. Active analogs were chalcones with 2,4-dimethoxy (compound 6) and 2,4-dihydroxy (compound 17) groups on ring A and 4'-chloro on ring B (Figure 3-6).

Figure 3-6: Chalcones reported to increase mitoxantrone accumulation in MDA-MB-231 /R cells<sup>91</sup>.



In that report, the active chalcones 6 and 17 (both at 0.5  $\mu$ M) re-sensitized MDA-MB-231/R cells to mitoxantrone as seen from the lower EC<sub>50</sub> values of mitoxantrone (2.72  $\mu$ M and 2.22  $\mu$ M in the presence of 6 and 17 respectively). In Section 5-3, it was shown that chalcone 11-5 at the same concentration of 0.5  $\mu$ M reduced the EC<sub>50</sub> of mitoxantrone on MDA-MB-231 /R cells to 0.07  $\mu$ M. Although these experiments were done by different investigators, the results could be compared because the EC<sub>50</sub> of mitoxantrone on MDA-MB-231 /R cells were found to be similar (3.40  $\mu$ M<sup>91</sup> versus 3.45  $\mu$ M). Clearly, 2-hydroxyl-4,6-dimethoxy substitution (**11-5**) was superior to either 2,4-dimethoxy (Compound 6) or 2,4-dihydroxy (Compound 17) substitution on ring A of the chalcone, although the presence of methoxy groups on ring B of **11-5** may have also contributed to its good activity.

Structurally, the chalcones (**11-1** to **11-5**) were ring C-open analogs of the dimethoxyaurones (**1-1**, **1-3**, **1-4**, **1-25**, **1-26**). The result of ring opening was a general loss in activity that was more evident for some chalcones (11-1 to 11-3) than others (11-4, 11-5). The greater flexibility of the template arising from the absence of ring C may have contributed to the diminished activity.

Like the chalcones, the flavones had been reported to be ABCG2 inhibitors<sup>65</sup>. Zhang et al<sup>64</sup> noted the preference for 5,7-dihydroxy groups on ring A of the flavone and proposed that 5-OH fulfilled the role of a H bond donor while 7-OH was required as a H bond acceptor. Thus, they reported that replacing the 5,7-dihydroxy groups of flavones with 5,7-dimethoxy

groups resulted in an approximate 4-fold decrease in activity. An  $EC_{50}$  of 1.4  $\mu\text{M}$  was assigned to 5,7-dimethoxyflavone based on the accumulation of mitoxantrone in ABCG2 overexpressing MCF-7 MX100 cells. In this chapter, the  $EC_{50}$  of 5,7-dimethoxyflavone (**12-1**) was found to be ten times higher (13.4  $\mu\text{M}$ ). The difference was likely due to the different assay protocols (PhA assay versus mitoxantrone accumulation). Assuming that this 10-fold difference in  $EC_{50}$  values could be extrapolated to the other Series 12 compounds, then the activities of the potent analogs **12-4** and **12-5** would be comparable to chrysin (5,7-dihydroxyflavone:  $EC_{50}$  0.39  $\mu\text{M}$ <sup>64</sup>, Chrysin ranked 3<sup>rd</sup> among the 25 flavonoids evaluated in that study and if the extrapolation holds true, that would mean that methoxylation of the flavone ring need not necessarily be adverse to activity, provided methoxy groups were present on both rings A and B.

Compared to the dimethoxyaurones, the flavones were weaker inhibitors of PhA efflux when ring B was monosubstituted or left unsubstituted, but were comparable to the aurones when ring B was dimethoxylated. Thus, the 5-membered ring C of aurones could be replaced with the 6-membered ring C of flavones without significant loss of activity.

Flavones have also been investigated for their inhibitory activities on ABCB1 and comparisons of the structural features required for interaction with ABCG2 and ABCB1 had been reported. These were discussed in Chapter 1 and summarized in Figure 1-4. Based on these findings, the flavones of Series 12 were expected to interact with both ABCB1 and ABCG2. They had features like the intact 2,3 double bond and ring B attached to C2 which were essential for both interactions. The 5,7-dimethoxy groups on ring A (particularly 5-methoxy) was not favoured but could have been offset by the methoxy group(s) on ring B which was a neutral feature for ABCB1 interaction but favored for ABCG2 interaction. As

anticipated, the flavones of Series 12 were found to target both ABCB1 and ABCG2, as seen from their closely matched EC<sub>50</sub> values on the PhA and CAM assays.

Compounds that were inactive on both PhA and CAM assays were readily identified and these were the ring A hydroxylated aurones, ring A unsubstituted aurones, dehydroaurones, isoaurones, ring A unsubstituted azaaurones, 2-OH chalcones and indolinones. Thus, structural features that were critical for interaction with ABCG2 (double bond, position of carbonyl bond on ring C, substituted ring A) were also required for interaction with ABCB1. The inactivity of hydroxylated aurones was not anticipated, given that hydroxylated flavones interacted strongly with both ABCB1 and ABCG2<sup>64, 73</sup>.

It was noted that there were no compound that inhibited CAM efflux at a lower EC<sub>50</sub> than PhA efflux. It may be that only a handful of compounds were evaluated for their EC<sub>50</sub> values on the CAM efflux assay and some active compounds could have been missed. On the other hand, compounds that had the highest %CAM accumulation (Table 3-2) were shortlisted for EC<sub>50</sub> determination and none of them had lower EC<sub>50</sub> values than those found from the PhA assay. At most, several compounds had comparable EC<sub>50</sub> values and until more investigations are carried out, it may be inferred that the templates investigated here are not ABCB1-specific.

In view of this observation, the question may be asked if the present templates favored interaction with ABCG2 or with both ABCB1 and ABCG2. Going by the EC<sub>50</sub> values listed in Table 3-3, the flavones and dimethoxyaurones had features that promoted interaction with both ABCG2 and ABCB1. The chalcones (**11-5**) may have a preference for ABCG2, which would agree with an earlier report<sup>91</sup>. As for the other series (trimethoxyaurones, indanones, azaaurones), a mixed profile was observed.

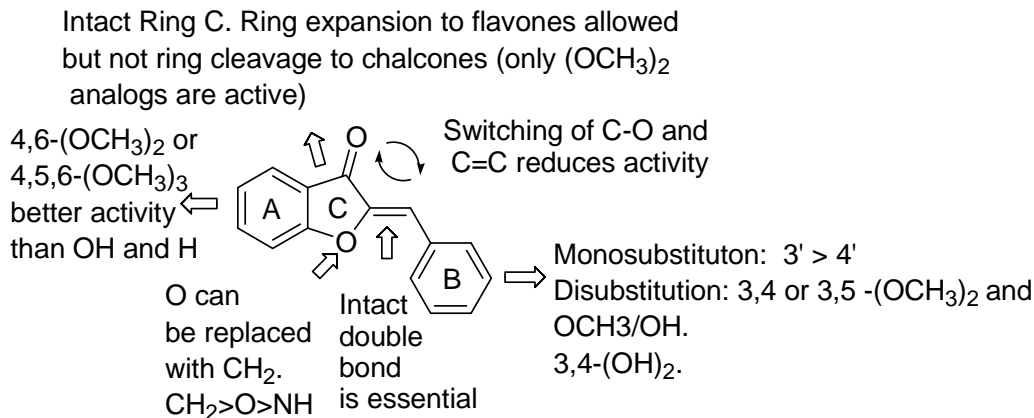
One of the objectives of the present investigation was to determine how variation in lipophilicity across the series affected interactions with ABCG2 and ABCB1. Going by the

SlogP values of the unsubstituted ring B of each series, lipophilicity varied from 2.714 (dihydroxyaurone **3-1**) to 3.526 (indanone **6-1**) which was less than a fold difference. A wider SlogP range was observed when individual compounds were considered (highest SlogP 4.65 for **1-19** to lowest SlogP 2.428 for **3-5**). The inactive dehydroaurones and hydroxylated aurones were generally associated with lower lipophilicities and this was indicative of a lipophilicity threshold below which activity was lost. But there was no convincing evidence to suggest that an increase in lipophilicity predisposed towards better activities. Even among the inactive dehydroaurones and hydroxylated aurones, there were members with SlogP values (**3-4** SlogP 3.367, **8-3** Slog 2.907) that fall within the range of active analogs. The most active compounds **1-24**, **1-25** had lipophilicity values that were not exceptionally high. More likely, there was an optimum lipophilicity required for activity.

### 3.5. Conclusions

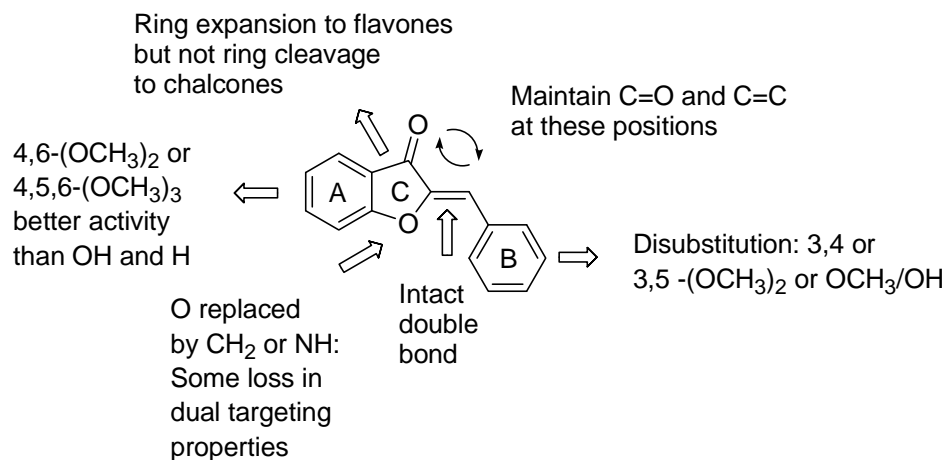
The findings in this chapter are summarized as follows: (i) The aurone template was associated with the ability to inhibit PhA efflux from ABCG2 over-expressing cells. Key SAR requirements are shown in Figure 3-7: The most potent analogs identified in this chapter were equivalent to FTC in terms of their EC<sub>50</sub> values.

Figure 3-7: Summary of SAR requirements for aurone-ABCG2 interaction.



(ii) The dimethoxyaurones were associated with the ability to inhibit CAM efflux from ABCB1 overexpressing cells. Thus, they targeted both transporters and were similar to flavones in this respect. Features common to both interactions are summarized in Figure 3-8.

Figure 3-8: Summary of common SAR requirements for aurone-ABCG2 and aurone-ABCB1 interactions.



## **Chapter 4: Efflux of pheophorbide a (PhA) by ABCG2 over-expressing human breast cancer (MDA-MB-231/R) cells and calcein-AM (CAM) by ABCB1 over-expressing Mardin-Darby canine kidney (MDCK) cells by aurones and related compounds: Quantitative Structure-Activity Relationships (QSAR) and Derivation of Pharmacophore**

### 4.1. Introduction

In Chapter 3, a qualitative assessment of the structural requirements of aurones and related compounds for the inhibition of the efflux of PhA from ABCG2 over-expressing MDA-MB-231/R cells was presented. In this chapter, the results were evaluated quantitatively to provide a more detailed understanding of the key features that direct the interaction with ABCG2. Two quantitative structure-activity relationship (QSAR) approaches were used - a modified Free-Wilson approach using sub-structural features in the test compounds and a conventional QSAR based on physicochemical properties of the test compounds. An attempt was also made to derive the pharmacophore for the inhibition of PhA efflux from MDA-MB-231/R cells.

### 4.2. Experimental

#### 4.2.1. Modified Free Wilson Analysis

The EC<sub>50</sub> values (expressed as -log EC<sub>50</sub>) of 112 compounds (Table 3-1) were used in this analysis. Compounds **1-19** and **2-11** were excluded because the features on their ring B were found only in these compounds. Thus they were singular variables and had to be omitted otherwise the results of the analysis would be dependent on the experimental error of this one activity value<sup>131</sup>. Nineteen substructure features were identified (Table 4-1) and a value of “1” or “0” was assigned to the stated feature for each compound. A value of “1”

indicated the presence of the feature in the compound and “0” implied the absence of the feature. A reference compound which had “0” values for the 19 substructural features was arbitrarily selected (**5-1** was chosen for this role). Details on the assignment of these features to the test compounds are given in Appendix 4-1. A linear regression analysis was carried out with PASW Statistics 18 (Chicago IL) using the stepwise and backward modes, with pEC<sub>50</sub> as the dependent variable and the 19 substructural features as independent variables. The regression coefficient of the substructure in the equation indicated its relative contribution to the model (numerically larger value implies a greater contribution) and its relationship to the dependent variable. A positive coefficient denoted a direct correlation and a negative coefficient denoted an inverse correlation.

Table 4-1: Independent variables (substructure features) used in the modified Free-Wilson analysis for inhibition of PhA efflux for 110 compounds.

Ring A	Ring C	Ring B
Dimethoxy groups	CH <sub>2</sub> in place of O	Substitution at 2'
Trimethoxy groups	NH in place of O	Substitution at 3'
Hydroxy groups (1 or more)	Ring A – double bond – C=O motif (to identify isoaurones and indolinones).	Substitution at 4'
		Substitution at 5'
	Absence of exocyclic double bond (to identify dehydroaurones)	Presence of CH <sub>3</sub> O
		Presence of OH
	Absence of Ring C (to identify chalcones)	Presence of CH <sub>3</sub> Presence of F
	Absence of 5 membered ring C (to identify chalcones and flavones)	Presence of Cl Presence of CN

The modified Free-Wilson analysis was also applied to compounds that had EC<sub>50</sub> values for inhibition of efflux of PhA and CAM from ABCG2 and ABCB1 over-expressing



cells respectively. These compounds were listed in Table 3-3. Two compounds had singular sub-structural features and were removed. They were **6-12** which was the only compound with 2' substituent on ring B and **2-10** which had to be omitted because without **6-12**, it was the only compound with a methyl group on ring B. Two compounds were included in the analysis, namely the reference compound **5-1** and the chalcone **11-4**. If the latter was not included, the chalcone **11-5** would have to be removed because its substructure would be recognized as a singular variable. This was deemed to be undesirable because the chalcones introduced structural diversity to the list of compounds and was proposed to be selective for ABCG2. Compounds **5-1** and **11-4** were assigned  $EC_{50\text{ CAM}}$  of  $> 30\mu\text{M}$ , which was not unreasonable as both were weakly active when screened at a fixed concentration.

The independent variables used for the analysis are given in Table 4-2. Details on their assignment to the test compounds are given in Appendix 4-2. Linear regression was carried out with PASW Statistics 18 (Chicago IL) using the stepwise and backward modes.

Table 4-2: Independent variables (substructure features) used in the modified Free-Wilson analysis for inhibition of PhA and CAM for 20 compounds.

Ring A	Ring C	Ring B
Dimethoxy groups	CH <sub>2</sub> in place of O	Substitution at 3'
Trimethoxy groups	NH in place of O	Substitution at 4'
	Absence of Ring C (to identify chalcones)	Substitution at 5'
	Absence of 5 membered ring C (to identify chalcones and flavones)	Presence of -OCH <sub>3</sub>
		Presence of OH
		Presence of Cl
		Presence of CN

#### 4.2.2. Auto-QSAR by MOE

Analysis was carried out on selected Series 1, 2, 6, 7 (**7-1 to 7-8**), 11 (**11-1 to 11-5**) and 12 (n =77). The other series were excluded because they had estimated EC<sub>50</sub> values for the inhibition of PhA efflux. There were however compounds (n = 24) within the selected series that also had estimated EC<sub>50</sub> values but these were not omitted as they were members of “active” series.

The 77 compounds were drawn in their non-protonated states and imported into a molecular database in MOE (Molecular Operating Environment Version 2008.1001, Chemical Computing Group, Montreal, Canada). The "wash" routine in MOE was followed to refine the structures by adding explicit hydrogen atoms (for example, if there are ionizable groups in the molecule). Next, they were minimized using the MMFF94x force field with a gradient setting of 0.05 kcal mol<sup>-1</sup> Å<sup>-1</sup>. A set of 28 descriptors (2D and 3D, Table 4-3) were collected for the 77 compounds (Appendix 4-3). The 77 compounds were divided into a training set of 63 compounds and a test set of 14 randomly selected compounds (**1-3, 1-8, 1-13, 1-18, 1-23, 1-28, 2-5, 2-10, 6-4, 6-9, 6-19, 7-4, 11-1, 12-1**). QSAR was generated with the training set using the AutoQuaSAR module in MOE. AutoQuaSAR used Principal Component Regression (PCR) and Partial Least Squares Projection to Latent Structures (PLS) to generate linear models and assigned the contribution made by each descriptor to the model. The process was iterative and repeated by deleting unnecessary descriptors until a predictive model was obtained. After each run, outliers were identified and these were removed from the training set and re-evaluated. Two outliers were identified (**1-22** and **6-16**) in the course of the runs and the final model comprised 61 compounds.

Table 4-3: Descriptors used to generate QSAR model by AutoQuaSAR by MOE

2D Descriptors		3D descriptors	
Molar refractivity (mr)	No. of bonds (b_counts)	No. of Hydrogen Bond Acceptors (HBA) (a_acc)	HOMO Energy (PM3_HOMO)
Log P (o/w)	No. of rotatable bonds (b_rotN)	No. of Hydrogen Bond Donors (HBD) (a_don)	LUMO energy (PM3_LUMO)
SlogP	No. of rotatable single bonds (b_1rotN)	No. of hydrophobic atoms (a_hyd)	Potential Energy (E)
VDW area	Fraction of rotatable single bonds (b_1rotR)	No. of basic atoms (a_base)	Water accessible surface area (ASA)
VDW volume	Fraction of rotatable bonds (b_rotR)	VDW surface area of HBD (vsa_don)	VDW volume (Volume)
Polar surface area (TPSA)		VDW surface area of HBA (vsa_acc)	VDW surface area (VSA)
log S (solubility)		VDW surface area of hydrophobic atoms (vsa_hyd)	Water accessible surface area of hydrophobic atoms (ASA_H)
Molecular weight (Weight)		VDW polar surface area (vsa_pol)	

#### Pharmacophore model

A database of 112 compounds from Series 1-12 was prepared as described in Section 4.2.2. A test set of 22 compounds (**1-5, 1-10, 1-15, 1-20, 1-25, 2-2, 2-7, 3-5, 4-2, 5-1, 5-6, 6-1, 6-6, 6-11, 6-16, 7-1, 7-6, 8-3, 9-4, 10-1, 11-1, 12-1**) was randomly selected from the original panel of 112 compounds. The remaining 90 compounds were assigned as the “training” set. The Conformation Import module of MOE was used to generate a conformer library for the training set. The conformers were constructed by dissecting the molecules into overlapping fragments, each of which was subjected to a stochastic conformational search<sup>132</sup>. The results

of this search were stored in a fragment conformer library. The final conformers were derived by re-assembling the fragment conformations by superposing the overlapping atoms. The number of conformations was limited to 250 per compound. The default molecular mechanics parameters of the software were used.

The Pharmacophore Elucidator module in MOE was used to generate the pharmacophore models. The models were assessed by their % overlap scores (goodness of alignment) and its “classification accuracy” which was ability to separate actives from inactives. Compounds with  $EC_{50}$  values  $<15\mu\text{M}$  were considered as “actives” while compounds with  $EC_{50}$  values  $\geq 15\mu\text{M}$  were considered as “inactives”. Approximately half of the training set was active compounds by this definition. Manual inspection of the top ranking models was carried out to determine the reasonableness of the pharmacophore. Pharmacophoric features were treated as solid spheres with a radius of 1.4 Å. The final pharmacophore was validated by applying it to the test set compounds as well as to an “external” database comprising 27 compounds of which 13 compounds were reported to be inhibitors of ABCG2 (Appendix 4-4). The 13 compounds were FTC, elacridar, gefitinib, genistein, imatinib, novobiocin, tectochrysin, dimethoxylated chalcone, methoxylated acridone, tariquidar, reserpine, estrone and quercetin<sup>91, 133, 134</sup>. The 14 inactive compounds were either not reported to be ABCG2 inhibitors and were compiled from the ZINC database or were reported as noninhibitors of ABCG2 (verapamil and etoposide) from the literature<sup>133, 135, 136</sup>.

## 4.3. Results

### 4.3.1. Modified Free Wilson Analysis

#### 4.3.1.1. Analysis of compounds with $EC_{50}$ values for inhibition of PhA efflux

In total, 110 compounds were analyzed by this approach, after removing two compounds that had singular variables. Indicator variables were generated for structural features (Table 4-1) that were absent from a reference compound (**5-1**). Regression of the data gave an equation of the form  $pEC_{50} = \text{Constant} + k_1X_1 + k_2X_2 + k_3X_3 + \dots + k_nX_n$  where  $X_n$  was the indicator variable and  $k_n$  was the contribution of the substituent. The constant represented the activity of the structures studied<sup>137</sup>.

The linear regression equations were generated by the stepwise and backward methods. In the stepwise method, the variable with the largest  $p$  value was removed if its value exceeded the default value of  $p = 0.10$ . The equation was recomputed without the variable and the process was repeated until no more variables could be removed. Then the variable not in the equation with the smallest  $p$  value was entered if its value was smaller than  $p = 0.05$ . All variables in the equation were again examined for removal and the process was continued until no variables could be removed and no variables not in the equation were eligible for entry. The backward method considered only those variables with  $p$  values that were greater than  $p = 0.10$ . These were removed in a stepwise manner until the final equation was obtained. Because only an upper limit of  $p$  was considered for removal of variables ( $p > 0.10$ ), the backward method was more likely to generate equations that had more variables and better statistics.

It was found that the two approaches were comparable, both in terms of statistics and variables identified (Table 4-4), although one additional feature (CH<sub>2</sub> in place of O in ring C) was identified as a significant variable by the backward but not stepwise method. The square of the correlation coefficient ( $R^2$ ) gives the degree of variation in activity ( $pEC_{50}$ ) that is explained by the equation. The adjusted  $R^2$  is a modification of  $R^2$  adjusted for the number of variables in the equation. Unlike  $R^2$ , the adjusted  $R^2$  increases only if the new term improves the model more than would be adjusted by chance. The F statistic serves to evaluate the

overall significance of the regression equation, which for both regression equations was  $p < 0.001$ .

Table 4-4: Modified Free Wilson Analysis of  $pEC_{50 \text{ PhA}}$  of 110 compounds by Linear Regression (Stepwise and Backward).

Independent variables	Stepwise: <i>F</i> 20.986; <i>R</i> <sup>2</sup> 0.552; <i>Adjusted R</i> <sup>2</sup> 0.526; <i>SE of estimate</i> 0.315. <i>Standardized coefficients (p)</i>	Backward <i>F</i> 18.739; <i>R</i> <sup>2</sup> 0.565; <i>Adjusted R</i> <sup>2</sup> 0.535; <i>SE of estimate</i> 0.312. <i>Standardized coefficients (p)</i>
Dimethoxy on ring A	0.561 (0.000)	0.519 (0.000)
Trimethoxy on ring A	0.289 (0.000)	0.294 (0.000)
3' on ring B	0.359 (0.000)	0.354 (0.000)
No exocyclic double bond	-0.235 (0.001)	-0.223 (0.001)
NH in ring C	-0.219 (0.002)	-0.194 (0.006)
CH <sub>2</sub> in ring C	NIL	0.125 (0.091)
No ring C	-0.147 (0.031)	-0.127 (0.063)

Equation 4-1: Stepwise

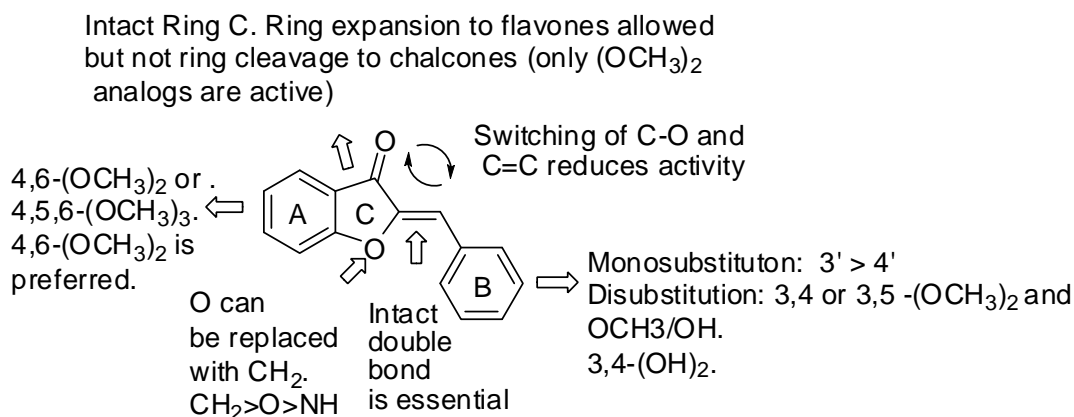
$$pEC_{50 \text{ PhA}} = 4.455 (0.066) + 0.531 (0.071) \text{ Dimethoxy} + 0.437 (0.115) \text{ Trimethoxy} + 0.328 (0.063) \text{ B3}' - 0.654 (0.190) [\text{No double bond}] - 0.308 (0.096) \text{ NH} - 0.257 (0.117) [\text{No ring C}]$$

Equation 4-2: Backward

$$pEC_{50 \text{ PhA}} = 4.447 (0.066) + 0.491 (0.074) \text{ Dimethoxy} + 0.444 (0.114) \text{ Trimethoxy} + 0.323 (0.062) B3' + 0.147 (0.086) CH_2 - 0.622 (0.189) [\text{No double bond}] - 0.272 (0.098) NH - 0.223 (0.118) [\text{No ring C}]$$

The results of the analysis were largely in agreement with the qualitative results deduced in Chapter 3. Figure 4-1 summarized the QSAR for the inhibition of PhA efflux by aurones.

Figure 4-1: Summary of QSAR requirements for aurone-ABCG2 interaction.



Both dimethoxy and trimethoxy groups on Ring A were identified in the equations 4-1 and 4-2. Going by the magnitude of the standardized coefficients of these variables (Table 4-4), the dimethoxy fragment made a more significant contribution to activity than the trimethoxy fragment. On ring B, only the position on the ring was identified as a significant contributor to activity. No ring B substituent (methoxy, halogen, methyl, hydroxyl, cyano) was identified in either equation, reinforcing the notion that the substitution on ring A was more critical than substitution on ring B. Of the ring B positions, the 3' position emerged as the most favored. The standardized coefficient associated with the 3' position showed that its contribution to activity was 2<sup>nd</sup> only to the ring A dimethoxy groups, and exceeded that of the trimethoxy fragment. As mentioned in Chapter 3, the most active compounds in each series

had groups at 3' position if ring B was mono- or di-substituted. Di-substitution of ring B resulted in some of the most active compounds and in each case, the 3' position was invariably occupied. However, di-substitution on ring B was not identified as a significant contributor to activity in the equations.

The importance of maintaining an intact double bond was emphasized in the analysis by the negative coefficient associated with the “no double bond” variable. In the same way, the loss of ring C had a negative effect on activity. However, the expansion of ring C (favorable for activity) and the “switch” in the positions of the carbonyl and exocyclic double bonds (unfavorable for activity) were not captured by the equations. This was attributed to the limited variation in activity for compounds that had these features, namely the flavones, isoaurones and indolinones.

Replacing the aurone O with an NH (azaaurones) had an adverse effect on activity. In contrast, replacing the aurone O with a methylene CH<sub>2</sub> had a positive effect on activity, but it was identified only by the backward method.

#### 4.3.1.2. Analysis on selected compounds with EC<sub>50</sub> values for inhibition of PhA efflux and CAM efflux.

In total, 20 compounds were analyzed by the modified Free-Wilson approach by stepwise and backward methods. The results of the analysis are presented in Tables 4-5 and 4-6. The regression equations (4-5, 4-6) generated by the backward approach had more favorable statistical parameters (R<sup>2</sup>, adjusted R<sup>2</sup>, F, standard error) but there were also more variables in the equations. The equations (4-3, 4-4) generated by the more rigorous stepwise approach had fewer variables and poorer statistics, in particular Equation (4-3) generated for PhA efflux activity had adjusted R<sup>2</sup> < 0.5.



Table 4-5: Modified Free Wilson Analysis of pEC<sub>50</sub> PhA and pEC<sub>50</sub> CAM of 20 compounds  
Linear Regression (Stepwise)

Dependent variable	pEC <sub>50</sub> PhA	pEC <sub>50</sub> CAM
Independent variables	<i>F</i> 6.823; <i>R</i> <sup>2</sup> 0.445; <i>Adjusted R</i> <sup>2</sup> 0.380; <i>SE of estimate</i> 0.339. <i>Standardized coefficients (p)</i>	<i>F</i> 16.337; <i>R</i> <sup>2</sup> 0.658; <i>Adjusted R</i> <sup>2</sup> 0.617; <i>SE of estimate</i> 0.288. <i>Standardized coefficients (p)</i>
Dimethoxy on ring A	0.952 (0.002)	-
Trimethoxy on ring A	0.556 (0.050)	-
Methoxy on ring B	-	0.714 (0.000)
No ring C	-	-0.625 (0.001)

As seen from Table 4-5, the regression equation (4-3) for PhA efflux activity evaluated by the stepwise approach had only two variables – dimethoxy and trimethoxy groups on ring A. These features were also captured in the 1<sup>st</sup> analysis (Equation 4-1) involving 110 compounds and accorded high levels of contribution to activity. Thus, their appearance in Equation 4-3 reinforced the significance of these features for the inhibition of PhA efflux.

Equation 4-3: Stepwise

$$pEC_{50 \text{ PhA}} = 4.523 (0.240) + 0.924 (0.256) \textit{Dimethoxy} + 0.655 (0.310) \textit{Trimethoxy}$$

The regression equation (4-4) for CAM efflux obtained by stepwise approach was also sparse in terms of variables. Interestingly, the equation emphasized the importance of methoxy groups on ring B and an intact ring C. No reference was made to ring A features.

Equation 4-4: Stepwise

$$pEC_{50\text{ CAM}} = 4.806 (0.102) + 0.662 (0.137) B\text{-methoxy} - 0.945 (0.223) [No\ ring\ C]$$

Taken together, a template that was associated with inhibition of both PhA and CAM efflux would have methoxy groups on both rings A and B, coupled with an intact ring C (Figure 4-2). Reference is made to Figure 3-8 in which the features for both activities were proposed based on the qualitative assessment of SAR. As can be seen, there is generally good agreement between the earlier qualitative deductions and the more quantitative results obtained by the modified Free Wilson approach. There were however some features that were not captured by the present analysis, such as the replacement of the aurone O by NH or CH<sub>2</sub>, the role of the exocyclic double bond and the switch in carbonyl/double bond positions. The absence of the latter two features was anticipated as they were not included as substructural features in the analysis (Table 4-2).

Figure 4-2: Summary of common QSAR requirements for aurone-ABCG2 and aurone-ABCB1 interactions.

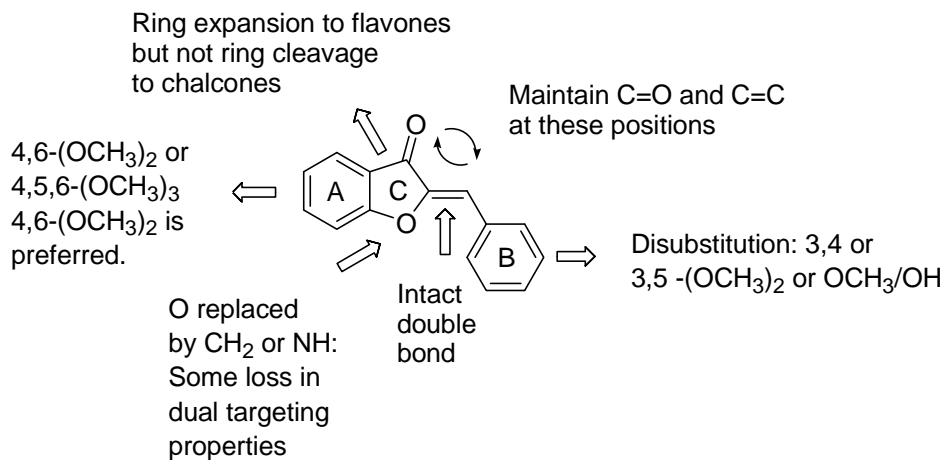


Table 4-6 summarizes the statistics and standardized coefficients of the variables generated in the regression equations for pEC<sub>50 PhA</sub> and pEC<sub>50 CAM</sub> by the backward approach.

Table 4-6: Modified Free Wilson Analysis of pEC<sub>50 PhA</sub> and pEC<sub>50 CAM</sub> of 20 compounds Linear Regression (Backward)

Dependent variable	pEC <sub>50 PhA</sub>	pEC <sub>50 CAM</sub>
Independent variables	<i>F</i> 17.76; <i>R</i> <sup>2</sup> 0.968; <i>Adjusted R</i> <sup>2</sup> 0.914; <i>SE of estimate</i> 0.127. <i>Standardized coefficients (p)</i>	<i>F</i> 12.575; <i>R</i> <sup>2</sup> 0.901; <i>Adjusted R</i> <sup>2</sup> 0.830; <i>SE of estimate</i> 0.192. <i>Standardized coefficients (p)</i>
Dimethoxy on ring A	0.607 (0.013)	0.813 (0.000)
Trimethoxy on ring A	0.428 (0.045)	0.763 (0.001)
3' on ring B	0.714 (0.000)	-
4' on ring B	0.767 (0.000)	0.242 (0.055)
5' on ring B	0.743 (0.000)	0.292 (0.031)
CH <sub>2</sub> in ring C	0.177 (0.080)	-

Methoxy on ring B	-0.980 (0.017)	-
Cyano on ring B	-0.600 (0.007)	-
Chloro on ring B	-0.531 (0.048)	-0.510 (0.001)
Hydroxyl on ring B	-0.331 (0.151)	-0.474 (0.001)
No ring C	-0.219 (0.037)	-0.588 (0.000)
No 5-membered ring C	-0.224 (0.059)	-0.255 (0.072)

The equation (4-5) for inhibition of PhA efflux had 12 variables compared to only 2 variables (Equation 4-3) by the stepwise approach.

Equation 4-5: Backward

$$\text{pEC}_{50 \text{ PhA}} = 4.523 (0.127) + 0.589 (0.179) \text{ Dimethoxy} + 0.503 (0.206) \text{ Trimethoxy} + 0.208 (0.102) \text{ CH}_2 + 0.840 (0.132) \text{ B3}' + 0.703 (0.093) \text{ B4}' + 0.874 (0.105) \text{ B5}' - 0.840 (0.271) \text{ B-methoxy} - 0.840 (0.222) \text{ B-cyano} - 0.625 (0.261) \text{ B-chloro} - 0.464 (0.288) \text{ B-hydroxyl} - 0.307 (0.119) [\text{No ring C}] - 0.218 (0.097) [\text{No 5-membered ring C}]$$

Notably, the dimethoxy and trimethoxy groups were still included in this equation and ranked highly as significant contributors to activity. Also captured by Equation 4-5 were the methylene CH<sub>2</sub> and an intact ring C, both of which were positive contributors to activity. An important difference from Equation (4-3) (pEC<sub>50</sub> PhA, stepwise) was the inclusion of variables pertaining to the substitution on ring B. The 3', 4' and 5' positions were identified, possibly a reference to the positive contribution made by di-substitution on this ring. On the other hand, the equation accorded a negative role to all the substituents on ring B (including the methoxy group) which was difficult to comprehend. Another notable feature is the

occurrence of both “No 5-membered ring C” and “No ring C” fragment with negative coefficients in Equation 4-5. This is a “signature” for chalcones because only chalcones would be assigned indicator variables of “1” for these two features. Thus, the appearance of these 2 variables in Equation 4-5 may be a reference to the poor inhibition of PhA efflux activity associated with chalcones.

Equation 4-6: Backward

$$\text{pEC}_{50 \text{ CAM}} = 4.521 (0.136) + 0.852 (0.161) \text{ Dimethoxy} + 0.969 (0.202) \text{ Trimethoxy} + 0.240 (0.111) B4' + 0.371 (0.150) B5' - 0.649 (0.135) B\text{-chloro} - 0.717 (0.170) B\text{-hydroxyl} - 0.889 (0.179) [\text{No ring C}] - 0.267 (0.134) [\text{No 5-membered ring C}]$$

Equation 4-6 was derived by the backward approach. Compared to Equation 4-4 (stepwise approach), more variables (8) were identified and of these, only one variable (no ring C) from the stepwise approach (Equation 4-4) was retained. The methoxy groups on ring A (dimethoxy, trimethoxy) were new, as well as the positions /groups on ring B. It was of interest to note that the other variable found in Equation 4-4 – methoxy on ring B – was not captured by Equation 4-6. However, other ring B groups (OH, Cl) were identified in this equation as negative contributors to activity.

Mention should be made of the favored locations on ring B (4' and 5') identified by Equation 4-6. These positions (notably 5') would be given indicator variables of “1” in compounds with di-substituted ring B. Therefore, they may be an indirectly reference to the positive contribution by a di-substituted ring B. Occurrence of both “No 5-membered ring C” and “No ring C” fragment with negative coefficients in Equation 4-6 may be a reference to poor inhibition of CAM efflux activity associated with chalcones.

Taken together, the backward approach provided a more detailed profile of a template that inhibited both PhA and CAM efflux. It would have a ring A with di- or tri-methoxy groups, an intact 5-membered ring C with O as heteroatom, a ring B that was di-substituted at 3'4' or 3'5'-positions, and preferably not with chloro or hydroxyl groups. A notable omission was the methoxy group on ring B which was a key feature in the template deduced by the stepwise approach.

#### 4.3.2. QSAR for inhibition of PhA efflux by ABCG2-overexpressing cell lines using AutoQuaSAR from MOE

The analysis was carried out on compounds from Series 1,2,6,7 (7-1 to 7-8), 11 (11-1 to 11-5) and 12. From the 77 compounds in these series, a training set of 63 compounds was randomly selected. In the course of deriving the model, two outliers were removed to give 61 compounds in the final training set. Because of the large number of descriptors (28) used to derive the model, a limit of 6 was imposed on the number of descriptors to be identified by the model. The final model had the following characteristics:

Number of compounds = 61, number of variables/descriptors = 28 (to select top 6)

$R^2 = 0.619$ ; Cross-validated  $R^2 = 0.508$

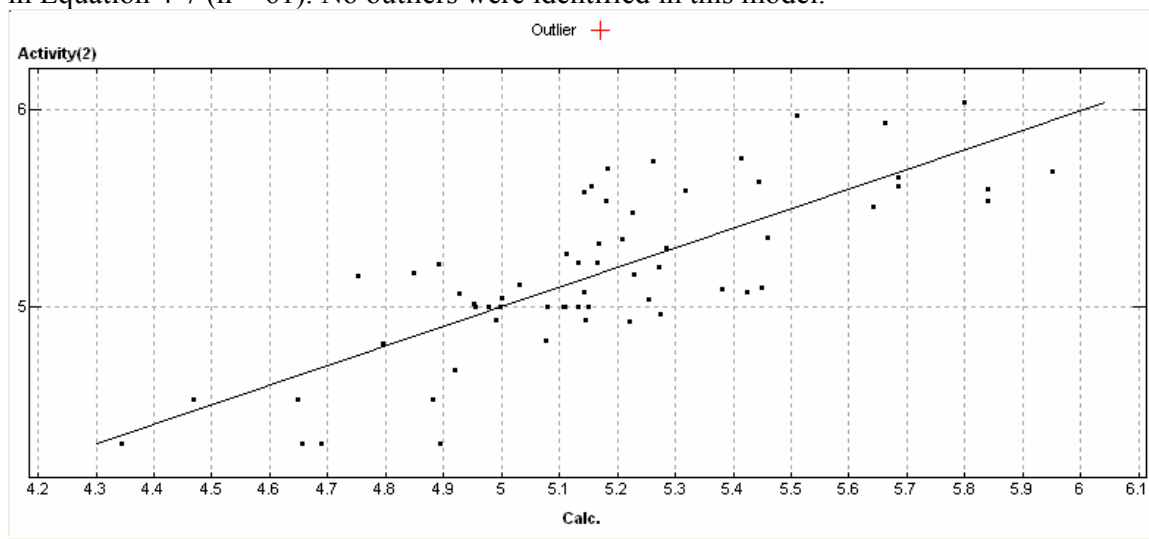
Root mean square error (RMSE) = 0.256; Cross validated RMSE = 0.293.

Estimated linear model (Equation 4-7):

$$\text{pEC}_{50 \text{ PhA}} = 1.671 - 1.365 \text{ SlogP} - 0.041 [\text{Polar surface area}] + 0.019 [\text{Molecular Weight}] + 0.779 [\text{No of HBA}] - 0.490 [\text{No of rotatable bonds}] + 0.892 [\log P \text{ o/w}]$$

A plot of the predicted versus actual  $\text{pEC}_{50}$  values is given in Figure 4-3.

Figure 4-3: Plot of actual versus predicted/calculated  $pEC_{50}$  values based on the model given in Equation 4-7 ( $n = 61$ ). No outliers were identified in this model.



Equation 4-7 showed that activity was positively influenced by an increase in molecular weight, log P and number of H bond acceptor groups. It was adversely affected by an increase in SlogP, polar surface area and number of rotatable bonds. The software ranked these descriptors in order of their relative contributions to the model. The rank order was Number of HBA (Most important, 1.0) > Polar surface area (0.76), number of rotatable bonds (0.75), SlogP (0.73) > molecular weight (0.54), log P (0.54).

An important question to be addressed with respect to Equation 4-7 was the relationship of these descriptors to structural features in the test compounds. The emphasis on the number of H bond acceptors was a likely reference to the methoxy groups on rings A and B, in keeping to the key roles accorded to them in the modified Free Wilson approach (Section 4.3.1) and the qualitative deductions described in Chapter 3. The increase in molecular weight may also be attributed to the presence of methoxy groups on rings A/B. Two lipophilicity descriptors were present in Equation 4-7. SlogP is the estimated lipophilicity of the compound in its protonated state while LogP provides a measure of the lipophilicity of the compound in its neutral state. Since most of the test compounds do not

have acidic or basic groups, SlogP and LogP provided estimated measures of the lipophilicity of the neutral compound. As mentioned in Chapter 2 (Section 2.2.2), the azaaurones of Series 7 were exceptions but in spite of their ionized states, their Slog P values were found to be in the same range as their LogP values.

It was interesting to note that in Equation 4-7, activity ( $pEC_{50}$ ) was inversely related to SlogP but directly related to Log P. This meant that low SlogP values (greater polarity) but high LogP values (less polarity) favored good activity. The conflicting trends may be traced to the fact that LogP discriminated between the ring B isomers and consistently assigned a higher LogP value to the 3' isomer. On the other hand, the SlogP values of 2', 3' and 4' isomers were the same. As the 3' position was identified as a key structural feature for inhibition of PhA efflux (Section 4.3.1), potent compounds with 3' groups had higher log P values but lower SlogP values than their 2' or 4' isomers with the same groups. While this may provide a plausible explanation for the conflicting observation, the question remains as to how lipophilicity affected activity. The inverse relationship between activity and SlogP may be more reliable for the following reasons. First, SlogP was ranked ahead of LogP in terms of significance to the model. Second, compounds with the highest SlogP or LogP values in the dataset were those that had halogens or methyl groups on ring B, and they were not particularly active inhibitors of PhA efflux.

The equation 4-7 also identified the number of rotatable bonds as an important determinant of activity. Compounds with greater flexibility (more rotatable bonds) were deemed to be less active. This relationship may have been influenced by the chalcones and the trimethoxyaurones. The chalcones were more flexible due to the loss of ring C while the methoxy groups on ring A of the trimethoxyaurones contributed to the increase in number of rotatable bonds. Most of these compounds have weak to moderate activity.



The inverse relationship between polar surface area and activity was again puzzling. Polar surface area was inversely related to both lipophilicity terms and directly related to number of H bond acceptors when assessed by their Spearman rho values. For this reason, one would expect activity to be directly, and not inversely, affected by polar surface area. As in the case of the rotatable bonds, the relationship between polar surface area and activity may be influenced by specific series of compounds. In this case, the indanones of Series 6, azaaurones (Series 7) and the chalcones (Series 11) may have a role. The indanones were moderately active and had small polar surface areas, while the poorly active chalcones and azaaurones had larger polar surface areas.

To validate the model, it was used to predict the activity of the 14 test compounds. The correlation between the predicted and actual pEC<sub>50</sub> values of the test set was found to be poor ( $R^2 < 0.1$ ). Thus while the model described by Equation 4-7 may be statistically acceptable, it had poor predictability. The limited range of activities in the test compounds could have contributed to this outcome. There is only a 50-fold range in the activities of the test compounds, which may not be adequate for a robust QSAR analysis.

#### 4.3.3. Establishing a pharmacophore model for inhibition of PhA efflux

The final pharmacophore model derived from the database of 90 compounds is given in Figure 4-4. It comprised 4 pharmacophoric features, namely two aromatic features (orange spheres) at rings A and B, one hydrophobic feature (green sphere) centred at the methyl of the methoxy group at C4 and a H bond acceptor projection point (blue sphere) in close proximity to the oxygen atom of the methoxy group at C6. The distances between the pharmacophoric features are illustrated in Figure 4-5.

Figure 4-4: Pharmacophore model of ABCG2 modulators

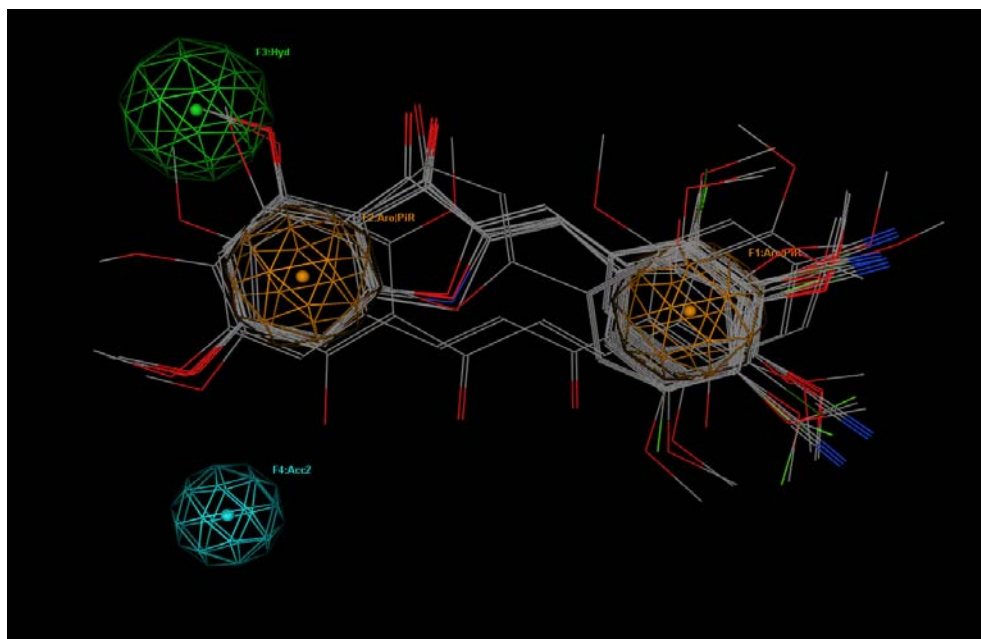
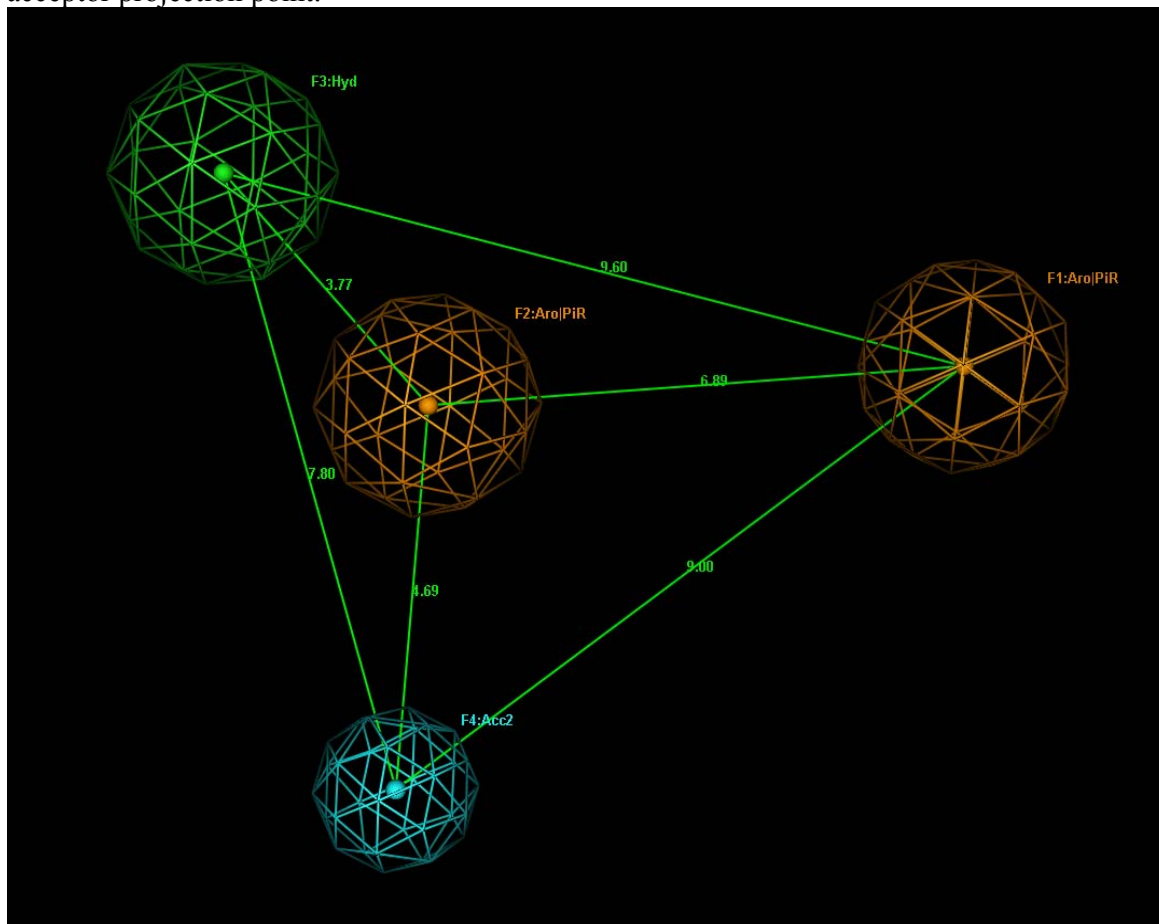


Figure 4-5: Distances ( $\text{\AA}$ ) between pharmacophoric features in the model. Pharmacophoric features are depicted as spheres: Green: hydrophobic; Orange: aromatic; Blue: H bond acceptor projection point.



In the next step, the pharmacophore model was evaluated for its ability to distinguish between active and inactive compounds in the test set of compounds and the external database. A table called the confusion matrix<sup>138</sup> was drawn up for this purpose. The confusion matrix contained information on the number of active compounds that were correctly predicted by the model to be actives. It also presented the number of inactive compounds that were correctly predicted by the model to be inactives.

Table 4-7: Confusion matrix for test set of 22 compounds

	True Actives	True Inactives	Total
Predicted Actives	9	7	16
Predicted Inactives	1	5	6
Total	10	12	22

Table 4-7 is the confusion matrix for the internal test set of 22 compounds. Of the 10 “True Actives” (2<sup>nd</sup> column), 9 were correctly predicted by the model to be actives (“Predicted Actives”, 2<sup>nd</sup> row) while 1 compound was incorrectly predicted to be active (“Predicted Inactives”, 3<sup>rd</sup> row). The 3<sup>rd</sup> column in Table 4-7 refers to the 12 “True Inactives”. Here, 7 compounds were incorrectly predicted by the model to be actives (“Predicted Actives”) while 5 were correctly predicted by the model to be inactive (“Predicted Inactives”). Thus, when applied to the internal test set, the pharmacophore was “over-optimistic” as it over-predicted the number of active compounds. While there were only 10 active compounds, the model identified 16 to be active, thus giving a ratio of 1.6 for Predicted Actives / True Actives. The accuracy of the model in evaluating the test set is given by Equation 4-8:

Equation 4-8:

$$\% \text{ Accuracy} = [\text{TP} + \text{TN}] / [\text{TP} + \text{TN} + \text{FP} + \text{FN}] \times 100$$

where TP is the number of true positives, TN is the number of true negatives, FP is the number of false positives and FN the number of false negatives. In this case, the % accuracy is  $[9 + 5] / 22 = 63.6$ .

The confusion matrix for the external database is given in Table 4-8. Of the 13 active compounds, only 6 were predicted to be active by the pharmacophore model. On the other hand, all 14 inactive compounds were correctly predicted to be inactive. Thus the % accuracy of the pharmacophore model when applied to the external database was 74.1%. It would seem that the model was less well suited at predicting actives than inactives with respect to the external data base (ratio of 0.46 for Predicted Actives / True Actives). There are many reasons for this outcome. First, as the training database was derived largely from auronones and structurally related compounds, it should perform better at identifying actives from the internal database than the external database which comprise structurally diverse compounds. Second, a critical assumption in pharmacophore elucidation was that the test compounds share a common mechanism of action and/or bind to a common site on the protein. This was more likely to hold true for a set of structurally similar analogs than for a library of structurally diverse compounds<sup>139</sup>. Another confounding factor is the presence of multiple substrate binding sites in ABCG2. In addition, the use of different substrates (PhA was used in this investigation) and methods (like flow cytometry to monitor accumulation of substrate) to assess inhibitory activity greatly influence the results. Thus, it was noted that the proposed pharmacophore model did not recognize FTC as an inhibitor (Figure 4-6) but correctly predicted gefitinib and novobiocin as inhibitors (Figures 4-7 and 4-8). It is tempting to propose that gefitinib and novobiocin, but not FTC, binds at the same site as the compounds in the training set. Overall, the pharmacophore model performed well with an accuracy of 64-74% when validated against two databases.

Table 4-8: Confusion matrix for external database of 27 compounds

	True Actives	True Inactives	Total
Predicted Actives	6	0	6
Predicted Inactives	7	14	21
Total	13	14	27

Figure 4-6: Alignment of structure of FTC to the pharmacophore model represented by two orange spheres (aromatic features), one cyano sphere (projected hydrogen bond acceptor) and one green sphere (hydrophobic feature).

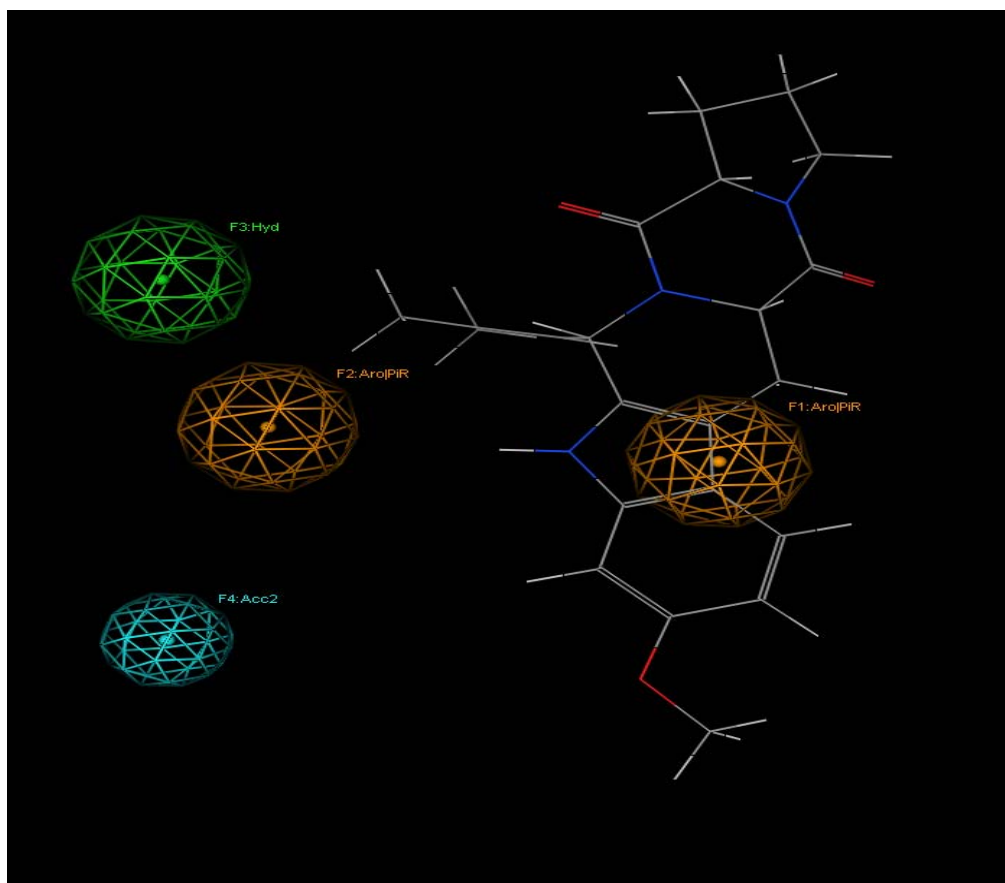


Figure 4-7: Alignment of gefitinib to the pharmacophore model represented by two orange spheres (aromatic features), one cyano sphere (projected hydrogen bond acceptor) and one green sphere (hydrophobic feature).

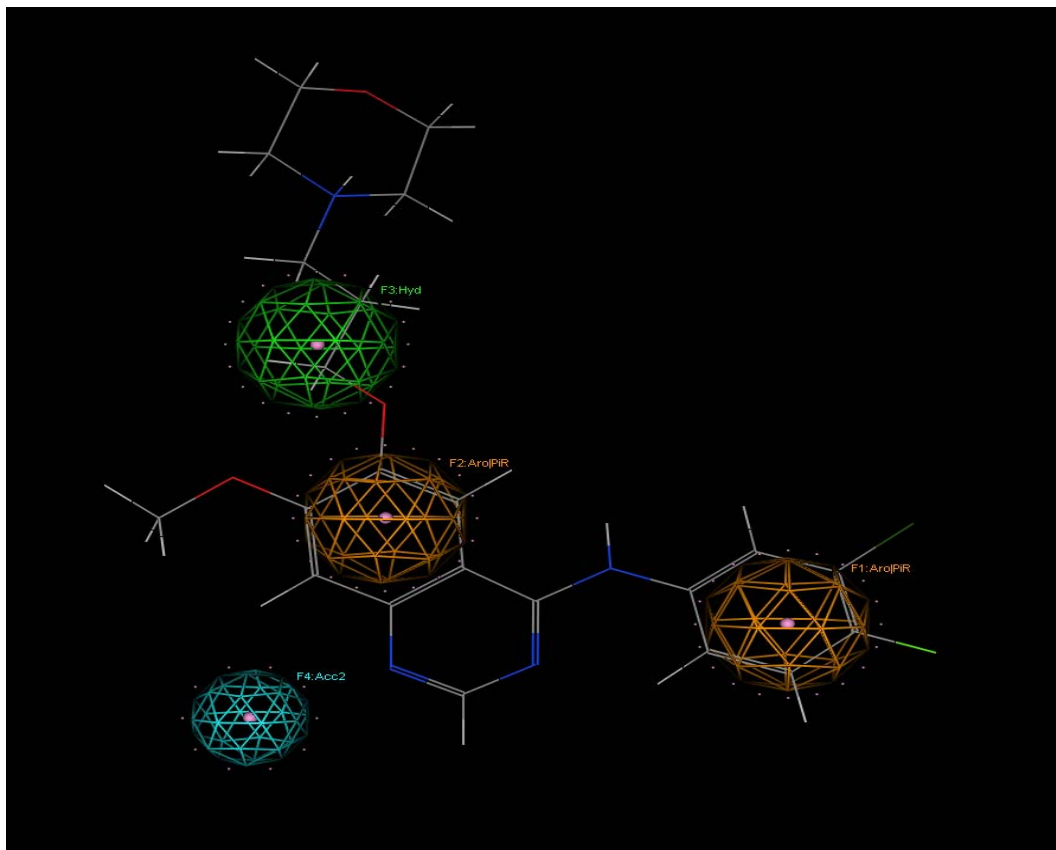
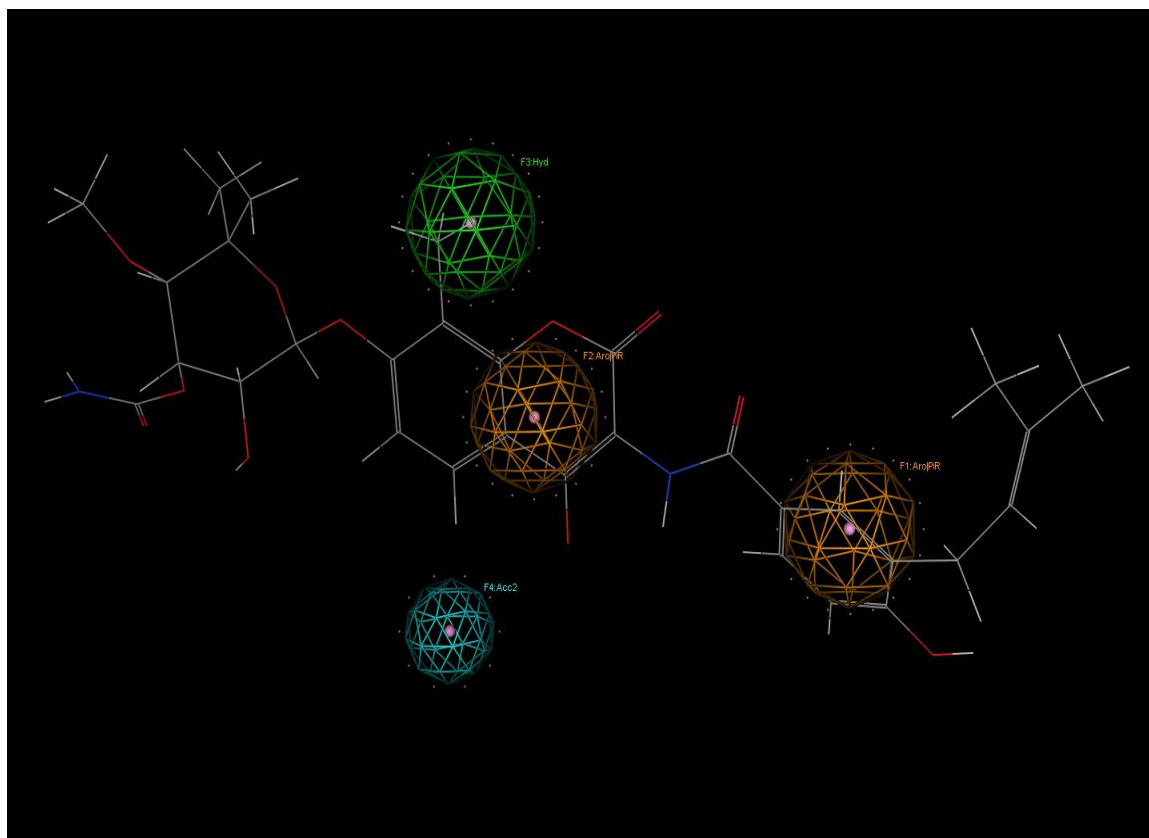


Figure 4-8: Alignment of structure of Novobiocin to the pharmacophore model represented by two orange spheres (aromatic features), one cyano sphere (projected hydrogen bond acceptor) and one green sphere (hydrophobic feature).





#### 4.4. Discussion

As the x-ray crystal structure of the human ABCG2 has yet to be resolved, direct molecular modeling using the structure of the transport protein cannot be used to probe the structural requirements involved in protein-ligand interactions. Homology modeling based on the crystal structures of bacterial ABC transporters is an option but are generally not precise enough for virtual screening of substrates and inhibitors<sup>41</sup>. Hence, indirect ligand-based molecular modeling is widely used to analyze the transport or inhibitory activities of ABCG2 ligands in an effort to identify pharmacophoric features and to generate QSAR for the interaction with ABCG2.

Not many QSAR studies have been carried out to investigate ABCG2 inhibitors and substrates. The most comprehensive study to date is possibly the report by Matsson et al<sup>70</sup> who investigated structurally diverse compounds for inhibition of mitoxantrone efflux from an ABCG2 overexpressing cell line. They developed a robust and validated QSAR model to distinguish between ABCG2 inhibitors and non-inhibitors. In spite of the large number of compounds (123) and descriptors (152) used in the analysis, the model identified only two descriptors as key features, namely logD7.4 (D: distribution coefficient at pH 7.4) and molecular polarizability. Based on this model, ABCG2 inhibitors were characterized by a logD7.4 of at least 0.5 to permit passive diffusion across membranes, and features that promoted  $\pi$ - $\pi$  interactions and H bonding with the protein (encoded in the descriptor molecular polarizability). A pharmacophore model consisting of a H bond acceptor and two hydrophobic features was also generated.

Another noteworthy study was that by Zhang et al<sup>64</sup> on the ABCG2 inhibitory activity of flavonoids. Besides providing a detailed qualitative SAR, a QSAR was carried out on 25 flavonoids using genetic algorithm coupled with multiple linear regression. The model

identified three descriptors - log P, overall number of carbon-carbon double bonds in the molecule and the moment of displacement between the centre of mass and the centre of dipole along the inertial Y-axis. The lipophilicity parameter and number of double bonds were directly correlated to activity while the moment of displacement was inversely correlated to activity.

Other QSAR studies have focused on congeneric series of compounds as ABCG2 inhibitors. Cramer et al<sup>58</sup> investigated the inhibitor selectivity of propafenones for ABCG2 and ABCB1. They found that minor modifications in structure resulted in marked shifts in inhibitory preferences. QSAR models were derived for both the inhibition of ABCB1 and ABCG2 but only the model for ABCG2 was statistically robust. The descriptors in this model were number of rotatable bonds, H bond acceptors and the van der Waals hydrophobic surface area. Pick and co-workers<sup>40</sup> carried out 2D-and 3D-QSAR analyses on derivatives of tariquidar, a known inhibitor of ABCB1. A modified Free-Wilson analysis was used to develop the 2D QSAR for inhibition of ABCG2 and ABCB1 while the 3D QSAR was investigated by CoMFA/CoMSIA. Interestingly, the 3D models showed a significant contribution by a H bond donor field to ABCG2 inhibition but not ABCB1 inhibition. On the other hand, a H bond acceptor field was found to benefit ABCB1 inhibition.

In this chapter, QSAR for the inhibition of PhA efflux by the series 1-12 compounds were investigated by a modified Free-Wilson using sub-structural fragments and a conventional QSAR using physicochemical properties. The models generated by these approaches were statistically significant but the model from the modified Free Wilson approach was not validated while the conventional QSAR equation generated by AutoQuaSAR did not adequately predict the activity of the test set compounds. The latter may be due to the limited variation (ca 50-fold) in inhibitory activities of the test compounds.

These limitations notwithstanding, the SAR findings from these methods were broadly in accord and also agreed with the qualitative SAR deductions described in Chapter 3.

The modified Free Wilson approach identified dimethoxy (and to a lesser degree, trimethoxy) groups on ring A, an intact ring C (preferably retaining the aurone O but could be replaced by CH<sub>2</sub> but not NH), an intact exocyclic double bond and substitution at 3' position of ring B as key features for inhibition of PhA efflux /ABCG2 activity. The key physicochemical descriptors in the QSAR equation found ready references to structural features identified in the modified Free Wilson approach. The high-weightage parameter “number of H bond acceptors” in the QSAR equation was attributed to the methoxy groups with their electron rich oxygen atoms. The negative influence of increasing the number of rotatable bonds was linked to the requirement for an intact ring C (notably, to avoid ring opening to give chalcones) and an intact exocyclic double bond.

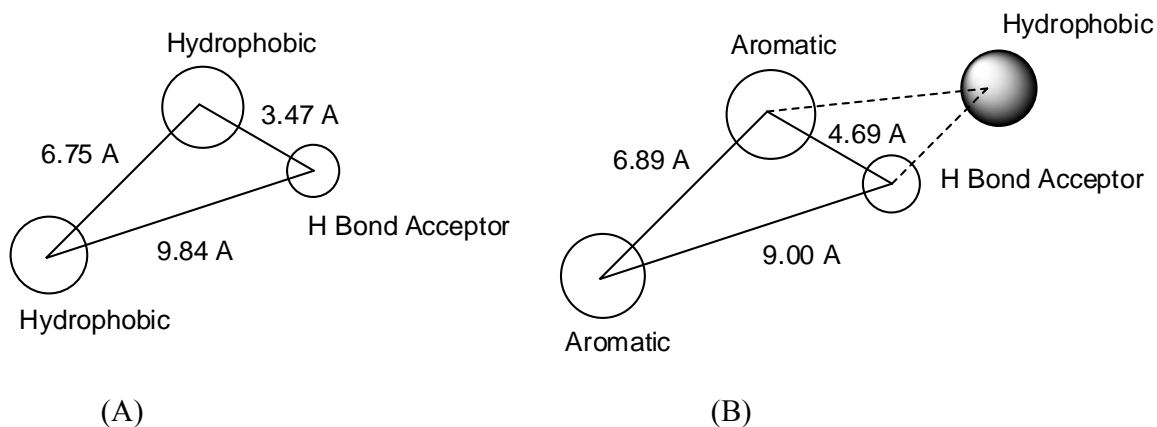
The lipophilicity requirements were more difficult to reconcile, in part due to the contrasting effects of lipophilicity and polar surface area cited in the equation. This may reflect the limited robustness of the QSAR equation which failed to adequately validate the test set of compounds. On the other hand, literature reports also indicated a lack of agreement on the effect of lipophilicity on ABCG2 inhibitory activity. Mattson et al<sup>70</sup> proposed that high lipophilicity was not necessary for the binding of ligands to ABCG2 but was a prerequisite for reaching the binding site in sufficient amounts to elicit an inhibitory effect. In contrast, other investigators<sup>40, 64</sup> found inhibitory activity to be associated with more lipophilic compounds. Lipophilicity was cited as one of the most highly predictive descriptor for ABCG2 inhibitory potency within a series of propafenone analogues<sup>140</sup>. In this present series of compounds, it was noted that the lipophilic compounds with groups like halogens or methyl groups on ring B were not the most potent while the hydrophilic compounds like those with hydroxyl or cyano groups on ring B were not necessarily the least active. The

lipophilicity and polar surface area requirements may reflect interplay between these features that are specific to the present series of compounds. Extrapolation to the global lipophilicity requirements for activity should thus be done with caution, if at all.

Doyle et al<sup>10</sup> reported that the amino acids in the intracellular loops and the transmembrane domains of ABCG2 were rich in aromatic and H bond donor side chains. The pharmacophore model developed in this chapter had aromatic features and a H bond acceptor projection point that were complementary to the nature of the protein/binding site. The aromatic features coincided with rings A and B while the remaining two features in the pharmacophore – H bond acceptor projection point and hydrophobic feature - were associated with the two methoxy groups on ring A. It was reassuring to note that the methoxy groups were consistently identified as positive features across the different models, reinforcing their role in activity. A H bond acceptor role for the methoxy groups was also deduced from the QSAR equation but a contribution to hydrophobicity by one (and not both) of the groups was not apparent from the other models.

A comparison between the pharmacophore model derived in this chapter and that proposed by Mattson et al<sup>70</sup> which was obtained from 29 ABCG2 inhibitors showed several similarities. In terms of pharmacophoric features, both models identified a H bond acceptor projection point and aromatic/hydrophobic features. A comparison of the distances between these features (Figure 4-9) showed that if the aromatic features in the present model were reassigned as hydrophobic features, the distances between the hydrophobic and H bond acceptor features were surprising close to that reported by Mattson (Figure 4-9). These observations, together with the satisfactory accuracy (64-74%) of the present model when assessed against two databases, suggested that it could be potentially useful in predicting compounds with ABCG2 inhibitory activity.

Figure 4-9: Distances between features found in the pharmacophore models reported by (A) Mattson et al and (B) in this chapter.



The modified Free-Wilson approach was also applied to a small number of compounds ( $n = 20$ ) that had been evaluated for inhibition of both PhA and CAM efflux by ABCG2 and ABCB1 overexpressing cells. The more rigorous stepwise method of analysis showed that inhibitor selectivity for ABCG2 and ABCB1 was determined by different parts of the molecule. A methoxylated ring A was required for ABCG2 inhibitor while a methoxylated ring B and an intact ring C were essential for ABCB1 inhibition. Accordingly, a compound that have combined these required features would function as a dual inhibitor of the 2 proteins, which was indeed the case for several methoxylated analogs of Series 1,6, 7, 11 and 12. When evaluated by the less stringent backward approach, the unique structural requirements identified by the stepwise mode were not apparent. Now, a methoxyated ring A and intact ring C were common requirements for inhibition of both ABCG2 and ABCB1, However, substitution at 3' on ring B and a C ring with CH<sub>2</sub> in place of O (equivalent to Series 6) were uniquely identified for inhibition of ABCG2. By this approach, a dual inhibitor would be an aurone (not an indanone) that was dimethoxylated on ring A and had a disubstituted ring B. As there were shortcomings in both the stepwise and backward modes, as elaborated in Section 4.3.1, further validation with a larger data set of compounds would be necessary before a conclusion is reached.

#### 4.5. Conclusion

Three ligand-based indirect molecular modeling approaches were investigated to elucidate the structural requirements for the inhibition of PhA efflux by the Series 1-12 compounds. In general, there was broad agreement across the different methods on the critical features for activity. Notably, the methoxy groups on ring A were highlighted by all approaches. Their possible contributions to the interaction with the protein were elucidated by the pharmacophore model to be that of a H bond acceptor and a hydrophobic interaction point. The positive influence of maintaining an intact ring C and exocyclic double bond for activity were emphasized by the two QSAR approaches. The pharmacophore model for ABCG2 inhibition showed good agreement with a previously reported model in the literature, both in terms of the types of features identified and their spatial orientation.

## **Chapter 5: Investigations into the effects of aurones and related compounds on the efflux activity of ABCG2 over-expressing MDA-MB-231 cells.**

### 5.1. Introduction

In Chapter 3, the aurones and related compounds of Series 1-12 were screened for their effects on the accumulation of the ABCG2 substrate PhA in MDA-MB-231/R cells which over-expressed ABCG2. Six of the 12 series of compounds were found to increase the accumulation of PhA in the ABCG2 over-expressing cells, with several compounds displaying activities that were comparable to the established ABCG2 inhibitor FTC. There were however, several questions relating to the mode of interaction of these compounds with ABCG2, that could not be satisfactorily addressed by the PhA assay. Foremost was the inability of the assay to determine if the test compound reduced the efflux of PhA from the ABCG2 overexpressing cells by inhibiting the transport activity of the protein, or by competing with PhA for occupancy of the substrate binding site(s) on the protein. Second, it was necessary to confirm that the compounds were capable of inhibiting the efflux of other substrates besides PhA. The ABCG2 protein has multiple sites for binding substrates<sup>141, 142</sup> and unless the test compounds could interfere with the efflux of diverse substrates from ABCG2 overexpressing cells, their modulatory properties would remain questionable. Hence the investigations in this chapter were undertaken to address these issues. The experiments carried out are summarized as follows:

- (i) To confirm the functional relevance of the reduced PhA efflux from MDA-MB-231/R cells observed for several compounds in Chapter 3, selected members were tested for their ability to re-sensitize MDA-MB-231/R cells to mitoxantrone.
- (ii) To address whether the re-sensitization of MDA-MB-231/R cells to mitoxantrone might be associated with the inhibition of ABCG2-mediated drug efflux, the cellular accumulation of mitoxantrone was evaluated in the presence of test compounds by flow cytometric analysis.

(iii) To demonstrate a direct interaction between test compound and ABCG2, two biochemical assays were carried out. These were the ATPase assay and the photoaffinity labeling of ABCG2 with [<sup>125</sup>I] iodoarylazidoprazosin.

(iv) To determine if the test compounds interacted with ABCG2 as substrates of ABCG2, differential growth inhibitory IC<sub>50</sub> of selected test compounds were determined on ABCG2 over-expressing and parental (wild-type) MDA-MB-231 cells.

(iv) To exclude the down-regulation of ABCG2 protein expression as a contributory mechanism for the reduced transport activity of ABCG2, protein levels were monitored by Western blot analysis in the presence of a test compound, and the test compound combined with mitoxantrone.

In view of the complexity and low throughput nature of some of these assays and the large number of compounds available, not all the compounds were investigated in the above experiments. However, effort was made to include as many potent compounds identified from the PhA assay in the above mentioned assays.

## 5.2. Experimental

### 5.2.1. Cell lines and materials for biological assay

The descriptions in section 3.2.1 apply. Mitoxantrone (MX) was purchased from Sigma-Aldrich, St Louis, Mo (USA). Human colon carcinoma HCT116 and normal human diploid embryonic lung fibroblasts IMR-90 were purchased from American Type Culture Collection (Rockville, MD). HCT116 cells were cultured in McCoy's 5A modified medium supplemented with 10% FBS, 0.1% penicillin G and 0.1% streptomycin. IMR-90 cells were grown in Eagle's Minimal Essential Medium (EMEM) supplemented with 10% FBS, 0.3% L-glutamine, 0.1% penicillin G and 0.1% streptomycin. Cells were sub-cultured when they reached 80-90% confluency and used within 10 passages for the assays. Cell lines and



materials for ATPase assay and photoaffinity labeling assay of ABCG2 with [<sup>125</sup>I] IAAP were kindly provided by Dr Suresh V. Ambudkar, Laboratory of Cell Biology, Centre for Cancer Research, National Cancer Institute, NIH, Bethesda, Maryland. Both assays were carried out by in his laboratory by Dr Chung-Pu Wu.

### 5.2.2. Mitoxantrone Sensitization

The ability of aurones to re-sensitize MDA-MB-231/R cells to mitoxantrone (MX) was assessed by determining the growth inhibitory IC<sub>50</sub> of MX in the presence of various concentrations of the test compound. Stock solutions of MX, FTC and test compounds were prepared in DMSO and diluted with media so that final concentration in the well did not exceed 1% v/v DMSO. Cells (10<sup>4</sup>) were seeded in 96-well plates and incubated for 24 h, after which the culture medium in each well was replaced with fresh medium containing various concentrations of MX and test compound (0.05 μM, 0.5 μM or 1 μM). FTC (10 μM), a specific inhibitor of ABCG2, was tested as positive control. After 72 hours of incubation, the drug-containing medium was removed and cells were washed once with PBS. 100 μl of 0.5 mg/ml MTT was added to each well, incubated for 3 h at 37°C, after which the MTT solution was decanted and DMSO (100 μl) was added to dissolve the purple formazan crystals. Absorbance was read at 590 nm on a Tecan Infinite M200 microplate reader with at least three separate determinations made for each concentration of test compound. The absorbance values obtained at a known concentration of MX were averaged and adjusted by subtracting the absorbance of empty wells (“blank”). This value was expressed as a percentage of the average absorbance obtained from control wells (wells with cells and media containing 1% DMSO) which had been similarly adjusted with readings of blank wells, to give % surviving cells at a given concentration of MX. The IC<sub>50</sub> value of MX was the

concentration required to reduce cell viability to 50% of control cells treated under similar experimental conditions. It was determined from the sigmoidal curve obtained by plotting % surviving cells versus concentration of MX using GraphPad Prism (Version 4.00, GraphPad Software, San Diego, CA). The software used the four-parameter logistic Equation 5-1 (variable Hill slope and constrained top and bottom values of 100 and 0 respectively) given by the expression:

$$Y = \frac{\text{bottom} + (\text{top} - \text{bottom})}{[1 + 10^{(\log \text{EC}_{50} - X) \times \text{HillSlope}}]}, \quad [5-1]$$

where  $X$  is the logarithm of concentration and  $Y$  is the response (% surviving cells). The  $\text{IC}_{50}$  of MX was obtained from the mean of two or more independent determinations with SD given in parentheses for  $n \geq 3$  determinations.

### 5.2.3. Mitoxantrone accumulation studies

The accumulation of mitoxantrone (MX) by MDA-MB-231/R and MDA-MB-231/V cells was determined by flow cytometry<sup>143</sup>. Stock solutions of test compounds, MX and FTC were prepared in DMSO and diluted with media to give the desired concentrations. The final concentration of DMSO was kept at no more than 0.1% v/v. Briefly, cells were grown in 75 cm<sup>3</sup> flasks to ca 90% confluency, trypsinized, washed with ice-cold PBS and re-suspended in serum-free RPMI medium at a cell density of 10<sup>6</sup> cells/ml. MDA-MB-231/R cells were incubated with various concentrations of test compound (0.05  $\mu\text{M}$ , 0.5  $\mu\text{M}$ , 5  $\mu\text{M}$ ) or vehicle (0.1% DMSO in RPMI) at 37°C for 15 min, followed by the addition of MX (3  $\mu\text{M}$ ) for 30 min. FTC (10  $\mu\text{M}$ ) was tested as positive control. After the incubation period, ice-cold PBS (10 ml) was added to stop the process and the cells were removed by centrifugation (2000 rpm, 5 minutes, 4°C). The cell pellet was washed with ice-cold PBS (3x) and re-suspended

in cold PBS for the determination of the intracellular concentration of MX on a flow cytometer (Cyan ® Research Flow Cytometer, Dako, Glostrup, Denmark). Cells were excited at the wavelength of 488 nm and the emission wavelength of 680 nm was recorded by a long-pass filter for the detection of MX fluorescence. The data was analyzed with the software Summit version 4.3 (Dako, Glostrup, Denmark). MX levels in the cells were normalized to the vehicle control (0.1% DMSO) which was taken to be 100%. At least 3 independent determinations were made for each test compound. MX accumulation in the MDA-MB-231/R cells was expressed by the following equation:

$$\% \text{ MX Accumulation in R cells} = \frac{[\text{Area}_{(\text{R cells} + \text{test compound} + \text{MX})} - \text{Area}_{(\text{R cells})}]}{[\text{Area}_{(\text{R cells} + \text{MX})} - \text{Area}_{(\text{R cells})}] \times 100 \%} \quad [5-2]$$

#### 5.2.4. ATPase assay

The ATPase assay was carried out by Dr Chung-Pu Wu (Laboratory of Cell Biology, Centre for Cancer Research, National Cancer Institute, NIH, Bethesda, Maryland) following a reported method<sup>144</sup>. Briefly, crude membrane protein (10 µg of crude membrane) from High Five insect cells expressing ABCG2 were incubated with test compound at various concentrations in the presence and absence of BeFx (0.2 mmol/L beryllium sulfate and 2.5mmol/L sodium fluoride) in ATPase assay buffer (50 mM MES-Tris (pH6.8), 50 mM KCl, 5 mM NaN<sub>3</sub>, 1 mM EGTA, 1 mM ouabain, 2 mM DTT, 10 mM MgCl<sub>2</sub>) for 10 min at 37°C. The reaction was initiated by the addition of 5 mM ATP, incubated for 20 min, 37°C, and terminated by addition of SDS solution (final concentration of 2.5%). Release of inorganic phosphate was quantified by a colorimetric reaction. The specific activity was recorded as BeFx-sensitive ATPase activity<sup>145, 146</sup>.

#### 5.2.5. Photoaffinity labeling of ABCG2 with [<sup>125</sup>I]Iodoarylazidoprazosin (IAAP)

The effect of test compounds on the photoaffinity labeling of ABCG2 by [<sup>125</sup>I] IAAP was carried out by Dr Chung-Pu Wu (Laboratory of Cell Biology, Centre for Cancer Research, National Cancer Institute, NIH, Bethesda, Maryland) following a reported method<sup>144</sup>. ABCG2 in MCF-7 FLV1000 cells (ABCG2-overexpressing human breast cancer cells) was photo-labeled with [<sup>125</sup>I] IAAP as described<sup>147</sup>. Briefly, crude membranes (50µg/ml) from MCF-7 FLV1000 cells were incubated with 5µM of test compound or 5µM of FTC for 10 minutes at room temperature in 50 mM Tris-HCl (pH 7.5), after which was added 3-6 nM [<sup>125</sup>I] IAAP (2,200 Ci/mmol, Perkin Elmer Life Sciences, Wellesley, MA). The samples were incubated for 5 min under subdued light and then exposed to ultraviolet (365nm) light for 10 min. The labeled ABCG2 was immunoprecipitated using the BXP-21 antibody and processed as described by Shukla and co-workers<sup>147</sup>. The radioactivity in the ABCG2 band was quantified using the STORM 860 PhosphorImager system (Molecular Dynamics, Sunnyvale, CA) and ImageQuaNT software (Molecular Dynamics).

#### 5.2.6. Western blot analysis

Compound **1-26** [2-(3, 5-dimethoxybenzylidene)-4,6-dimethoxybenzofuran-3(2H)-one] was incubated at 0.5µM or 1µM with MDA-MB-231/R and V cells for 72 hours following the protocol described in Section 3.2.2. MDA-MB-231/R cells were also separately exposed to a combination of **1-26** (0.5 µM or 1 µM) and MX (0.1µM), while MDA-MB-231/V cells were exposed to **1-26** (0.5 µM or 1 µM) and MX (0.01µM). After 72 hours, the samples were subjected to western blot analysis as described in Section 3.2.2.

### 5.2.7. Cytotoxicity Studies

The cytotoxicity profiles of the test compounds were determined by the MTT assay as described in Section 5.2.2. The cell lines tested were the human breast cancer cell lines MDA-MB-231 (V and R), human colon carcinoma cell line HCT 116 and the normal human fibroblasts IMR-90. Stock solutions of test compounds were prepared in DMSO and diluted with media to give concentrations of 5  $\mu\text{M}$  and 10  $\mu\text{M}$  for investigations on MDA-MB-231 (V and R) cells, and 5  $\mu\text{M}$  only on the other two cell lines. The final concentration of DMSO in the well was kept at  $\leq 1\%$  v/v. Cell survival was determined as a % of control cells and at least two determinations were made for each concentration of test compound.

### 5.2.8. Statistical analysis

Data were analyzed by paired-samples t test and one-way ANOVA followed by a Bonferroni or Dunnett's post hoc test (SPSS 15.0 for Windows, Chicago, IL) for statistical significance.  $p < 0.05$  was considered significant. Non-parametric Spearman correlation analysis was also carried out on SPSS 15.0 for Windows.

## 5.3. Results

### 5.3.1. Mitoxantrone Sensitization

In order to confirm the functional relevance of the reduction in PhA efflux from ABCG2-overexpressing MDA-MB-231/R cells ("R cells") by test compounds (Chapter 3), selected members were assessed for their ability to re-sensitize these cells to killing by the cytotoxic ABCG2 substrate mitoxantrone (MX). The  $\text{IC}_{50}$  of MX on the MDA-MB-231/V cells ("V cells") which had normal levels of ABCG2 was 0.09  $\mu\text{M}$  ( $\pm 0.07$ ). This was increased to 3.45  $\mu\text{M}$  ( $\pm 1.34$ ) in ABCG2-overexpressing R cells. The 38-fold difference in

the IC<sub>50</sub> values of MX on these two cell types was ascribed to the higher levels of ABCG2 in the R cells which led to the extrusion of MX and hence, a higher concentration to effect cell death. When the IC<sub>50</sub> of MX on R cells was assessed in the presence of 0.5 μM FTC, it was reduced to 0.67 μM, giving a resistance index of 7.4. This value indicated that MX was now 7.4 times less sensitive on the ABCG2 over-expressing R cells compared to the parental V cells. However, a higher concentration of FTC (10 μM) achieved a resistance index of only 3.7 and could not fully restore the MX sensitivity of R cells to the same level as that observed in V cells. A higher concentration of FTC could not be tested as this would lead to cell death.

Eleven compounds were examined for their ability to re-sensitize R cells to MX. They were **1-3**, **1-6**, **1-9**, **1-14**, **1-25**, **1-26**, **3-1**, **6-15**, **7-1**, **11-5** and **12-5**. A large number of dimethoxyaurones (Series 1) were selected in line with the focus of the thesis. Of these compounds, **1-3**, **1-6**, **1-9** and **1-14** were monosubstituted at the 3' position on ring B, which was proposed to be a favored position for activity. Compounds **1-25** and **1-26** were selected for their outstanding potencies on the PhA assay and for comparison, the indanone (**6-15**), chalcone (**11-5**) and flavone (**12-5**) counterparts of **1-26**, all of which had 3' 5' dimethoxy groups on ring B, were included. These compounds were also among the most potent inhibitors of PhA efflux in their respective groups. The dihydroxyaurone **3-1** and azaaurone **7-1** which were inactive on the PhA assay were selected as negative controls. The IC<sub>50</sub> of MX on the R cells was evaluated in the presence of 0.5 μM or 0.05 μM test compound, with **1-26** and **6-15** tested at an additional concentration of 1 μM. At these concentrations, the test compounds did not affect the viability of the R cells (Section 5.3.6). The results are given in Table 5-1. Representative curves for the IC<sub>50</sub> determination of MX in the presence of compounds **1-26** and **6-15** (1 μM) are given in Figures 5-1.

Table 5-1: Effects of selected test compounds on IC<sub>50</sub> of mitoxantrone in MDA-MD-231 /R cells

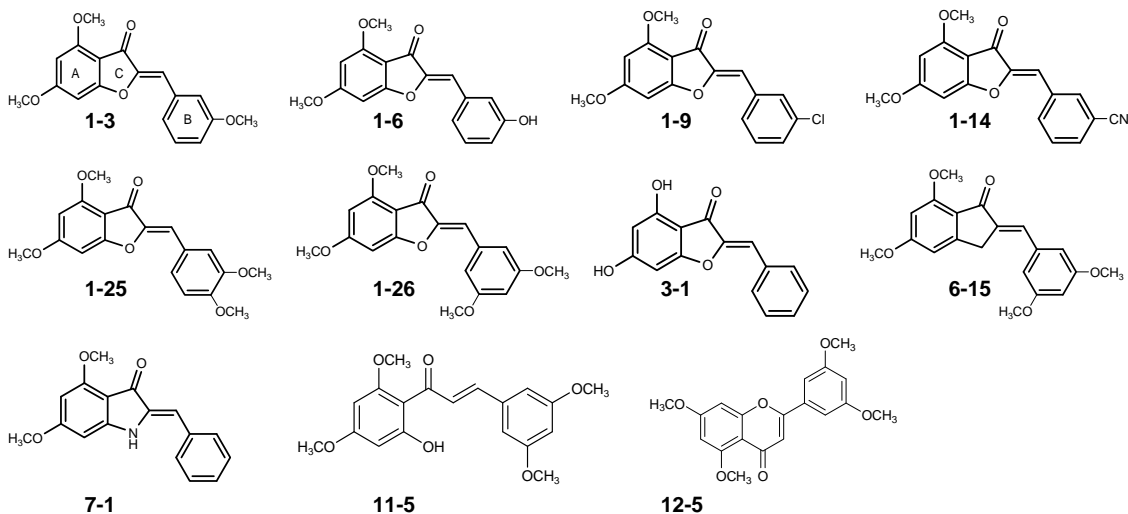
IC <sub>50</sub> of mitoxantrone (μM) <sup>b</sup>		
Compound <sup>a</sup>	MDA-MB-231/R	Fold resistance index <sup>c</sup>
Mitoxantrone <sup>d</sup>	3.45 (1.34)	3.45/0.09 = 38.3
<b>0.05 μM</b>		
<b>1-3</b>	1.11 (0.19) <sup>e ****</sup>	12.3
<b>1-6</b>	1.77 (0.67)*	19.7
<b>1-9</b>	1.67 (0.52)**	18.6
<b>1-14</b>	0.95 (0.27)***	10.6
<b>1-25</b>	0.52 (0.09)***	5.8
<b>1-26</b>	0.37 (0.14)***	4.1
<b>3-1</b>	1.37 (0.42)**	15.2
<b>6-15</b>	0.21 (0.07)***	2.3
<b>7-1</b>	0.56 (0.19)***	6.2
<b>11-5</b>	0.21 (0.04)***	2.3
<b>12-5</b>	0.10 (0.02)***	1.1
FTC	0.87 (0.22)***	9.7
<b>0.5 μM</b>		
<b>1-3</b>	0.15 (0.04)***	1.7
<b>1-6</b>	0.26 (0.10)***	2.9
<b>1-9</b>	0.14 (0.07)***	1.6
<b>1-14</b>	0.30 (0.17)***	3.3
<b>1-25</b>	0.09 (0.03)***	1.0
<b>1-26</b>	0.06 (0.02)***	0.7
<b>3-1</b>	0.36 (0.1)***	4.0
<b>6-15</b>	0.02 (0.01)***	0.2
<b>7-1</b>	0.16 (0.07)***	1.8

<b>11-5</b>	0.07 (0.01)***	0.8
<b>12-5</b>	0.07 (0.03)***	0.8
FTC <sup>e</sup>	0.67	7.4

**1 $\mu$ M**

<b>1-26</b>	0.05 (0.03)***	0.6
<b>6-15</b>	0.03 (0.02)***	0.3

<sup>a</sup> Structures of 11 compounds are as follow:



<sup>b</sup> Mean of two or more independent determinations. SD is given in parentheses for  $n \geq 3$  determinations.

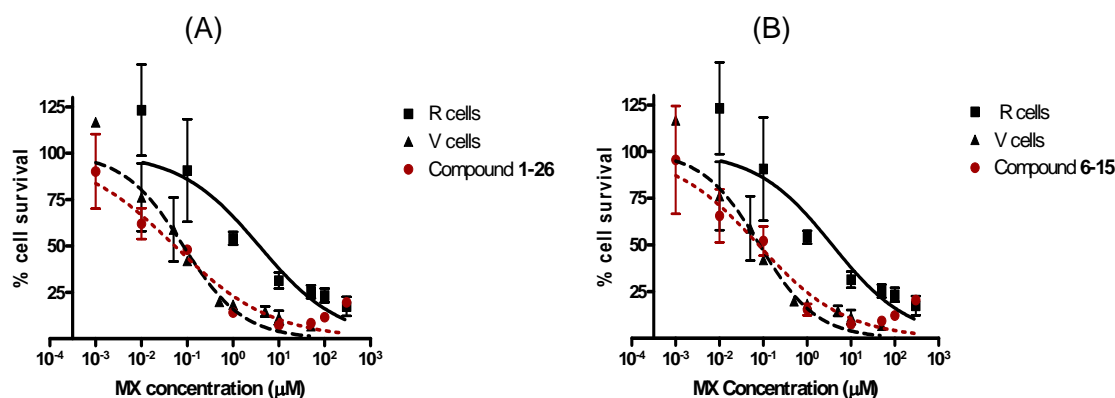
<sup>c</sup> Fold resistance index =  $IC_{50}$  of MX<sub>R cells + test compound</sub> /  $IC_{50}$  of MX<sub>V cells</sub>. A compound that totally re-sensitized R cells to MX would have a resistance index of 1.

<sup>d</sup>  $IC_{50}$  value of MX in MDA-MB-231/V cells in the absence of test compound = 0.09 (0.07)  $\mu$ M

<sup>e</sup> Significant difference ( $*p < 0.05$ ,  $**p < 0.01$ ,  $***p < 0.001$ ) between  $IC_{50}$  of MX in the presence of test compound and  $IC_{50}$  of MX (control) in MDA-MB-231/R cells. (One-way ANOVA followed by Bonferroni post-hoc test)

Figures 5-1: Dose response curves of MX determined in the presence of (A) **1-26** and (B) **6-15** on MDA-MB-231/R cells. Also depicted are the dose response curves of MX on MDA-MB-231/V cells and MDA-MB-231/R cells, without test compound **1-26** or **6-15**.





The results in Table 5-1 showed that the  $IC_{50}$  values of MX on R cells were reduced in the presence of all the test compounds. The effect was concentration dependent and a greater reduction in the  $IC_{50}$  of MX was observed at a higher concentration of test compound ( $0.5 \mu\text{M} > 0.05 \mu\text{M}$ ). When compared to FTC which was also tested at  $0.05 \mu\text{M}$  and  $0.5 \mu\text{M}$ , many of the compounds were comparable or exceeded FTC in their ability to re-sensitize R cells to MX. Compounds **1-25**, **1-26**, **6-15**, **7-1**, **11-5**, **12-5** at  $0.05 \mu\text{M}$  had resistance indices that were smaller than FTC at the same concentration. Of these compounds, the strong reversal property of **7-1** was surprising as it was inactive on the PhA assay. Similarly, **3-1** which was inactive on the PhA assay showed reasonable activity on this assay. Thus results from the PhA assay could not be reliably extrapolated to the MX re-sensitization assay.

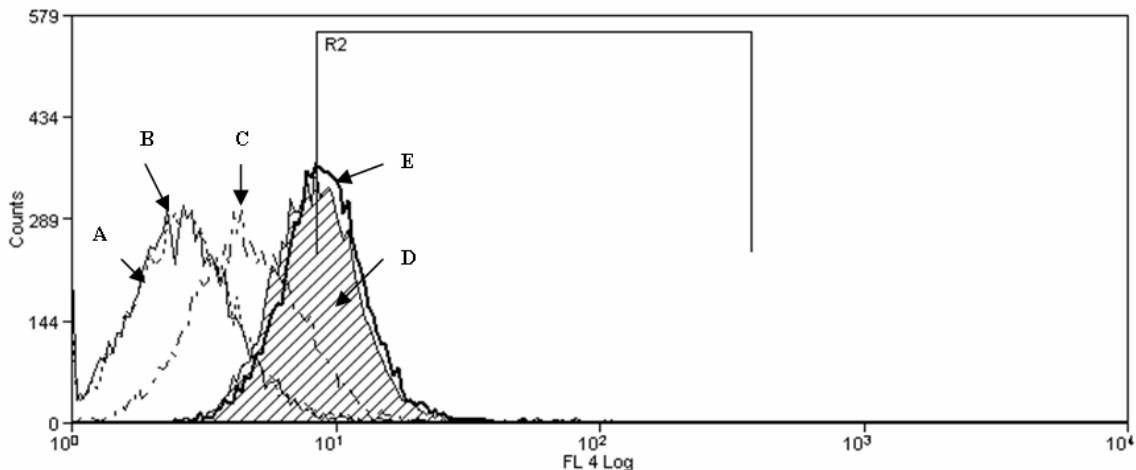
When evaluated at a higher concentration of  $0.5 \mu\text{M}$ , the compounds demonstrated improved re-sensitization properties. All had resistance indices that exceeded FTC and some compounds, notably **1-26**, **6-15**, **11-5** and **12-5**, completely restored the MX sensitivity of R cells to the same level of the V cells (resistance index  $\leq 1.0$ ). The two most active compounds **1-26** and **6-15** were further tested at  $1 \mu\text{M}$  and as anticipated, R cells treated with these compounds were completely responsive to the cytotoxic effects of MX.

### 5.3.2. Cellular accumulation of mitoxantrone in MDA-MB-231/R cells

To address whether the reversal of MX resistance by test compounds described in the preceding section was associated with the inhibition of ABCG2-mediated efflux, the cellular accumulation of MX was evaluated in the presence of selected compounds. Only the Series 1 dimethoxyaurones (**1-1** to **1-15**) were monitored here because these experiments were done early in the candidature when only these compounds were available for testing. The compounds were examined at concentrations of 5.0  $\mu\text{M}$ , 0.5  $\mu\text{M}$  and 0.05  $\mu\text{M}$ . Briefly, the method involved incubating the test compound with R or V cells, followed by addition of MX, after which the cells were processed for the detection of fluorescent MX by flow cytometry.

Figure 5-2 is the output of a typical accumulation experiment. The x axis measures the fluorescence intensity (on a log scale) of the cells and the y axis gives the number of cells. Each curve shows the distribution of cells according to their fluorescence levels.

Figure 5-2. Representative FACS histograms of MX Accumulation in (A) MDA-MB-231/V cells; (B) MDA-MB-231/R cells; (C) MDA-MB-231/R cells + MX; (D) test compound **1-3** (5  $\mu\text{M}$ ) + MX in MDA-MB-231/R cells; (E) MDA-MB-231/V cells + MX.



The autofluorescence curves (A and B) of R and V cells were found on the extreme left of the Figure, in keeping with the intrinsically low levels of fluorescence of these cells. Curve C equivalent to R cells + MX was displaced to the left of curve E (V cells + MX) because R cells accumulated less MX than V cells. Compound **1-3** at 5  $\mu\text{M}$  shifted the MX fluorescence curve in the presence of R cells (curve D) to the right, such that it overlapped with curve E. This was an indication that **1-3** inhibited the efflux of MX from R cells by ABCG2.

In order to quantify the extent of these effects, a vertical marker R2 was arbitrarily set on curve B (autofluorescence curve of R cells) such that the area to the right of it was  $\leq 5\%$  of the total area. This was referred to as the “area of defined region” and it was monitored for each test compound to give the % MX accumulation using equation (5-2). This area would be enlarged in the presence of a compound that inhibited MX efflux from R cells and correspondingly reduced if the test compound was a weaker inhibitor of MX efflux.

The results are shown in Table 5-2. The test compounds increased MX accumulation in a concentration dependent manner. At the lowest concentration tested (0.05  $\mu\text{M}$ ), none of the compounds increased MX accumulation to any significant extent. At higher concentrations (0.5  $\mu\text{M}$ , 5  $\mu\text{M}$ ), significant levels of MX accumulation were observed. Notably, the levels of accumulation approached or exceeded that observed for FTC even though the latter was tested at a higher concentration of 10  $\mu\text{M}$ .

Again, extrapolation of the results from this assay to the PhA and MX re-sensitization assays have to be done cautiously. For example, the compounds did not increase MX accumulation at the lowest concentration of 0.05  $\mu\text{M}$  but in the MX re-sensitization assay, several members (**1-3**, **1-6**, **1-9**, **1-14**) were effective at this concentration. Ranking of **1-3**, **1-6**, **1-9** and **1-14** by the 3 different assays also did not give consistent trends. While **1-6** was

ranked most potent in the PhA assay, it was not highly ranked in the MX re-sensitization assay (at 0.5  $\mu$ M, Table 5-1) and on the MX accumulation assay (0.5  $\mu$ M, Table 5-2), it was equipotent to **1-9**.

Table 5-2: Accumulation of MX in MDA-MB-231/R cells in presence of test compounds (**1-1** to **1-15**)

		MDA-MB-231/R MX accumulation (% of control) <sup>a</sup>		
		Aurone concentration (μM)		
Compound	R	5μM	0.5μM	0.05μM
Control (0.1% DMSO)		100		
FTC (10μM)		237 (60.9)* <sup>b</sup>		
<b>1-1</b>	H	283 (86.6)*	209 (32.7)*	150 (5.1)
<b>1-2</b>	2' -OCH <sub>3</sub>	251 (46.8)	217 (25.1)*	148 (18.2)
<b>1-3</b>	3' -OCH <sub>3</sub>	294 (70.9)**	222 (31.9)*	169 (18.0)
<b>1-4</b>	4' -OCH <sub>3</sub>	278 (57.1)*	215 (30.1)*	146 (21.8)
<b>1-5</b>	2' -OH	235 (50.5)	214 (29.9)*	131 (16.3)
<b>1-6</b>	3' -OH	273 (65.5)*	235 (29.1)**	139 (11.1)
<b>1-7</b>	4' -OH	263 (54.3)*	219 (26.7)*	138 (23.5)
<b>1-8</b>	2' -Cl	275 (62.9)*	226 (22.6)**	148 (30.3)
<b>1-9</b>	3' -Cl	275 (55.3)*	231 (30.9)**	160 (20.9)
<b>1-10</b>	4' -Cl	233 (23.8)	195 (44.0)	125 (8.7)
<b>1-11</b>	2' -CH <sub>3</sub>	321 (146)**	163 (53.6)	72.6 (24.0)
<b>1-12</b>	3' -CH <sub>3</sub>	291 (46.2)**	203 (60.2)*	117 (14.1)
<b>1-13</b>	4' -CH <sub>3</sub>	268 (48.7)*	130 (27.1)	88.8 (13.8)
<b>1-14</b>	3' -CN	358 (64.7)***	172 (40.5)	117 (29.4)
<b>1-15</b>	4' -CN	187 (39.6)	161 (50.9)	81.0 (31.4)

<sup>a</sup> MX Accumulation (% of control) in MDA-MB-231/R cells calculated as:

$$\text{MX Accumulation (\% of control)} = [\text{Area}_{(\text{cells} + \text{test compound} + \text{MX})} - \text{Area}_{(\text{cells})} / \text{Area}_{(\text{cells} + \text{MX})} - \text{Area}_{(\text{cells})}] \times 100 \%$$

Values are expressed as mean of two or more independent determinations. S.D. in brackets for  $n = 3$  determinations.

<sup>b</sup> Significant difference ( $*p < 0.05$ ,  $**p < 0.01$ ,  $***p < 0.001$ ) between MX accumulation in the presence of test aurone and control (0.1% DMSO), (One-way ANOVA followed by Dunnett post-hoc test)

The accumulation of MX in the presence of test compounds was also investigated on the sensitive MDA-MB-231/V cells. It was found that at 5 $\mu$ M, the aurones did not significantly alter the level of MX accumulation in the MDA-MB-231/V cells (Table 5-3). The inability of the test compounds to increase MX accumulation in V cells was in sharp contrast to the significant levels of accumulation in R cells observed earlier (Table 5-2). This finding clearly implicated a role for the inhibition of ABCG2-mediated efflux of MX for these compounds.

Table 5-3: Accumulation of MX in MDA-MB-231/V cells in the presence of test compounds (**1-1** to **1-15**) at 5  $\mu$ M

Compound	R	MX Accumulation (% of control) <sup>a</sup>
	Control (0.1% DMSO)	100 <sup>b</sup>
	FTC (10 $\mu$ M)	104.2
<b>1-1</b>	H	99.9
<b>1-2</b>	2'-OCH <sub>3</sub>	100.8
<b>1-3</b>	3'-OCH <sub>3</sub>	103.3
<b>1-4</b>	4'-OCH <sub>3</sub>	103.8
<b>1-5</b>	2'-OH	108.8
<b>1-6</b>	3'-OH	106.3
<b>1-7</b>	4'-OH	101.4
<b>1-8</b>	2'-Cl	90.0
<b>1-9</b>	3'-Cl	109.7
<b>1-10</b>	4'-Cl	107.5
<b>1-13</b>	4'-CH <sub>3</sub>	106.9
<b>1-14</b>	3'-CN	97.2
<b>1-15</b>	4'-CN	97.7

<sup>a</sup> % MX Accumulation (% of control) in MDA-MB-231/V cells =

$$\frac{[Area (V\ cells + test\ compound + MX) - Area (V\ cells)]}{Area (V\ cells + MX) - Area (V\ cells)} \times 100 \%$$

### 5.3.3. ABCG2 ATPase activity

The effects of selected test compounds on ABCG2-mediated ATP hydrolysis were examined using High Five insect cells over-expressing ABCG2. The compounds stimulated beryllium fluoride-sensitive basal ABCG2-ATPase activity in a concentration dependent manner with maximum stimulation of approximately 3-fold achieved for most compounds (Figures 5-3, Appendix 5-1). Table 5-4 gives the  $K_m$  values of the test compounds, where  $K_m$  is the concentration required to stimulate ABCG2 ATPase activity by 50%.

Figures 5-3: Effect of increasing concentration of representative compounds **1-26** and **8-1** on BeFx-sensitive ABCG2 ATPase activity.

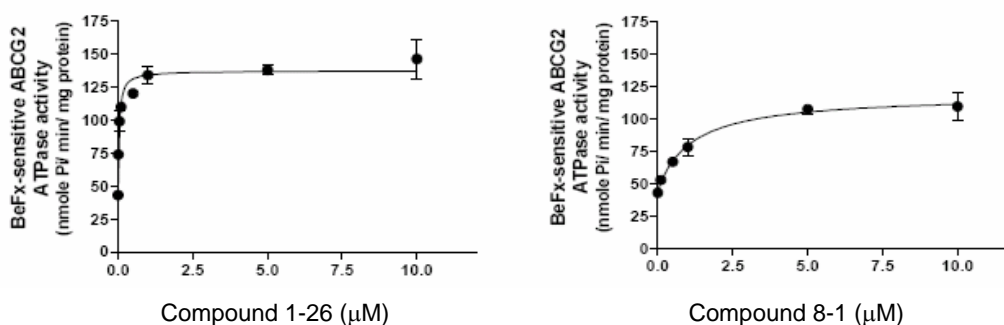


Table 5-4:  $K_m$  (μM) of selected compounds for ABCG2 ATPase activity in High Five insect cell crude membranes and  $EC_{50}$  (μM) values for increasing PhA accumulation in MDA-MB-231/R cells

Compound	$K_m$ (μM) (ABCG2 ATPase assay) <sup>a</sup>	$EC_{50}$ (μM) (PhA assay) <sup>b</sup>
<b>1-1</b>	0.14(0.055)	6.72 (0.53)
<b>1-25</b>	0.048 (0.021)	1.07 (0.07)
<b>1-26</b>	0.037 (0.013)	0.91 (0.06)
<b>3-1</b>	0.37 (0.084)	>30
<b>5-1</b>	0.19 (0.076) <sup>c</sup>	>30
<b>6-1</b>	0.31 (0.13)	9.10 (0.55)
<b>7-1</b>	0.37 (0.083) <sup>c</sup>	>30
<b>8-1</b>	1.1 (0.19) <sup>c</sup>	>50
<b>9-1</b>	0.20 (0.062)	>30
<b>6-15</b>	0.22 (0.11) <sup>c</sup>	2.06 (0.10)
<b>6-20</b>	0.043 (0.014)	1.17 (0.07)



<b>11-1</b>	0.66 (0.11) <sup>c</sup>	>50
<b>11-4</b>	0.19 (0.054) <sup>c</sup>	6.13 (0.58)
<b>11-5</b>	0.21 (0.071) <sup>c</sup>	2.89 (0.19)
<b>12-1</b>	0.16 (0.025) <sup>c</sup>	13.45 (0.95)
<b>12-4</b>	4.5 (1.5) <sup>c</sup>	2.45 (0.23)
<b>12-5</b>	0.065 (0.025)	2.32 (0.38)

<sup>a</sup> K<sub>m</sub> (μM): concentration required to stimulate ABCG2 ATPase activity by 50%. (Values in parentheses are SD of three or more determinations)

<sup>b</sup> EC<sub>50</sub> values from Table 3-1 in Chapter 3

<sup>c</sup> Less than 3 fold magnitude increase in ATPase activity at highest concentration tested. Solubility problems were encountered with **12-4**.

It is seen from Table 5-4 that all the compounds stimulated ATPase activity to varying degrees. Potent stimulators had lower K<sub>m</sub> values and these were found for the dimethoxyaurones **1-25**, **1-26**, indanone **6-20** and flavone **12-5** which had nanomolar K<sub>m</sub> values. The ability of these compounds to stimulate ATPase activity stood at odds with the earlier finding that they were potent inhibitors of PhA efflux from the R cells. Compound **1-1** which stimulated ATPase activity with a K<sub>m</sub> of 0.14 μM also increased MX accumulation in R cells (Table 5-2). This anomaly had been noted by others<sup>148</sup> and the consensus was that the ATPase assay was not always suitable for distinguishing between potential substrates, inhibitors or other types of transport modulators. The assay does however provide an indication of the propensity of the test compound to interact with the ABCG2 protein to bring about an increase in ATP hydrolysis.

The K<sub>m</sub> and EC<sub>50</sub> values of the compounds in Table 5-4 were found to be statistically correlated when analyzed by bivariate correlation with a Spearman's rho value of 0.623 (*p*=0.008). Thus compounds that interacted with great affinity with ABCG2 (low K<sub>m</sub> values) were also those that strongly inhibited PhA efflux from R cells. Outliers would be **6-15**, **11-5** and **12-4** which were among the potent inhibitors of PhA efflux but had unexpectedly high

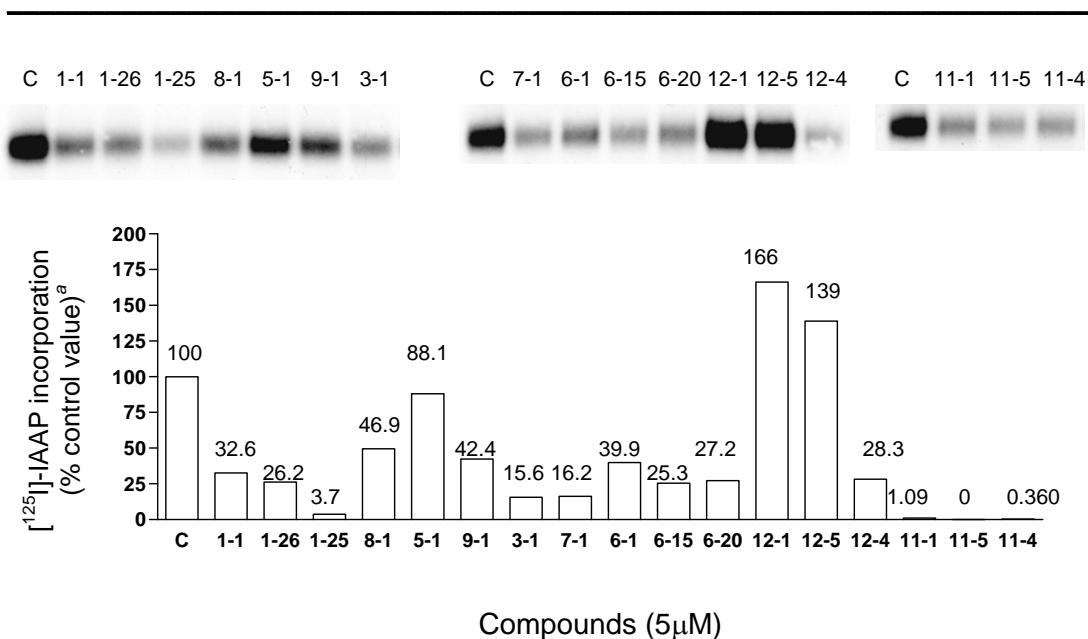
K<sub>m</sub> values. In the case of **12-4**, this discrepancy was attributed to solubility problems encountered in the ATPase assay which may have led to an inaccurate determination of K<sub>m</sub>. However there was no suitable explanation for the anomalous behavior of **6-15** and **11-5**.

### 5.3.3. Photoaffinity labeling of ABCG2/BCRP with [<sup>125</sup>I]Iodoarylazidoprazosin ([<sup>125</sup>I]-IAAP)

Test compounds listed in Table 5-4 were tested for their ability to inhibit the photolabelling of ABCG2 with [<sup>125</sup>I]-IAAP in membranes isolated from ABCG2 overexpressing MCF-7 FLV 1000. Briefly, the membranes were incubated with [<sup>125</sup>I]-IAAP and then irradiated to promote covalent linkage of the labeled compound to the protein. The radioactively labeled ABCG2 protein was then solubilized, separated by gel electrophoresis and protein labeling was visualized and quantified by autoradiography. In the absence of test compound, the labeled ABCG2 protein was detected as an opaque band on the autoradiogram (Lane C in Figure 5-5). If the compound had a greater affinity for the binding site than IAAP, then photoaffinity labelling of the site would be greatly diminished and the intensity of the photo-labeled ABCG2 band would be correspondingly reduced.

As seen in Figure 5-4 and Appendix 5-2, the test compounds at 5 μM had varied effects on the photo-affinity labelling of ABCG2. The ABCG2 band intensity was retained unchanged in the presence of flavones **12-1**, **12-5** and the ring A unsubstituted aurone **5-1**, indicating that they did not compete with [<sup>125</sup>I]-IAAP for occupancy for the binding site. In contrast, the other compounds reduced [<sup>125</sup>I]-IAAP incorporation by 50% or more, indicating a strong competition with IAAP for the same binding site. Notably, the chalcones **11-1**, **11-4**, **11-5** and dimethoxyaurone **1-25** almost completely inhibited photolabelling of ABCG2 at 5 μM.

Figure 5-4: Photoaffinity labelling of ABCG2 with [<sup>125</sup>I]-IAAP in the absence (C, control) or presence of test compounds evaluated at 5 μM.



<sup>a</sup> % [<sup>125</sup>I]-IAAP incorporation = [<sup>125</sup>I]-IAAP signals obtained in the presence of test compound (5 μM) – [<sup>125</sup>I]-IAAP signals obtained in the presence of FTC (5 μM). Values were average from 2 independent experiments. The subtraction for [<sup>125</sup>I]-IAAP signals due to FTC was required to correct for signals arising from non-specific binding of [<sup>125</sup>I]-IAAP to the substrate binding site.

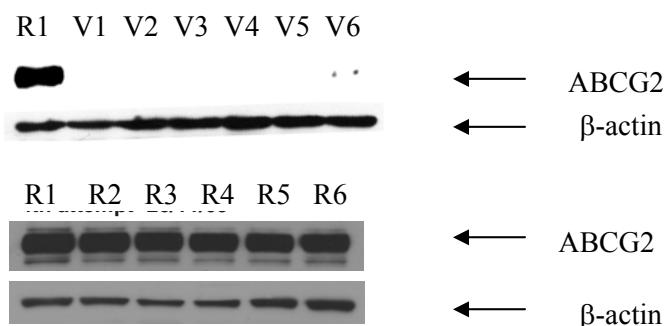
#### 5.3.4. Western blot analysis

Thus far, the investigations had focused on the effects of the test compounds on the efflux activity of ABCG2. It is possible that the compounds interfered with transcription and translation processes involved in the production of ABCG2. If these processes were inhibited, ABCG2 expression would be reduced and this would translate to a reduction in its functional activity. To investigate this possibility, the ABCG2 over-expressing R cells were incubated with a representative test compound (**1-26**) at two concentrations 1 μM and 0.5 μM. As reported earlier (**5.3.1**), **1-26** successfully re-sensitized R cells to MX at these concentrations. The R cell lysates were prepared and analyzed by western blotting to determine if ABCG2 levels were reduced on incubation with **1-26**. In addition, the combination of **1-26** and MX was similarly investigated on R cells. To avoid cellular toxicity, MX was investigated at 0.1

$\mu\text{M}$  on R cells, which was more than 10 fold lower than its  $\text{IC}_{50}$  of  $3.45 \mu\text{M}$  ( $\pm 1.34$ ). The same experiments were repeated on V cells but this time, MX was investigated at  $0.01 \mu\text{M}$  in keeping with its more potent effects on V cells ( $\text{IC}_{50} 0.09 \pm 0.07 \mu\text{M}$ ).

The results are given in Figure 5-6. In this figure, lanes with R and V refer to lysates derived from R and V cells respectively. It is seen that **1-26** did not decrease ABCG2 expression in R cells at  $1 \mu\text{M}$  (R3) or  $0.5 \mu\text{M}$  (R2) as visual inspection showed band intensities to be similar to that of the control band (R1). Similarly, no change in band intensity was observed in the presence of MX ( $0.1 \mu\text{M}$ , R4). When R cells were treated with a combination of MX and **1-26** ( $0.5 \mu\text{M}$  or  $1 \mu\text{M}$ ), the intensities of the ABCG2 band was not diminished compared to the control (R5, R6). ABCG2 could not be detected in lysates prepared in the V cells, and this situation was unchanged on treatment with MX, **1-26** or both (V1 – V6). Therefore, the results showed that **1-26** did not reduce ABCG2 levels in R cells at the test concentrations or when combined with MX. Thus, its ability to re-sensitize R cells to MX (Section 5.3.1.) was likely due to effects on the functional activity of ABCG2 rather than a reduction in protein levels.

Figure 5-5: Western blot analyses showing the effects of compound **1-26** (alone or in combination with MX) on ABCG2 expression in MDA-MB-231/R and V cells<sup>a</sup>



<sup>a</sup> Blots presented are representative blots from three independent determinations

Lanes R1, V1: DMSO (1%) (negative control)

Lanes R2, V2: **1-26** (0.5 $\mu$ M) ;

Lanes R3, V3: **1-26** (1  $\mu$ M) ;

Lane R4: MX (0.1 $\mu$ M);

Lane V4: MX (0.01 $\mu$ M);

Lane R5: **1-26** (0.5 $\mu$ M) + MX (0.1 $\mu$ M);

Lane V5: **1-26** (0.5 $\mu$ M) + MX (0.01 $\mu$ M);

Lane R6: **1-26** (1 $\mu$ M) + MX (0.1 $\mu$ M);

Lane V6: **1-26** (1  $\mu$ M) + MX (0.01 $\mu$ M).

### 5.3.5. Growth inhibitory effects on MDA-MB-231/R and MDA-MB-231/V cells

The preceding section has shown that selected compounds (including potent analogs **1-25**, **1-26**, **6-15**, **6-20**) interacted with ABCG2 to stimulate ATPase activity and compete with IAAP for binding to its site on the protein. The question was then asked if the test compounds were substrates of ABCG2 and were themselves transported out of cells by the protein. If they were substrates, they would be able to compete with other substrates (MX, PhA, IAAP) for efflux by ABCG2, especially if their structural features permit occupancy of these binding sites. It would also be in keeping with the strong stimulation of ATPase activity which pointed to the presence of an actively transported substrate, although exceptions have been noted.

An indirect means of determining the status of the test compounds as substrates was employed in this section. It involved the determination of the growth inhibitory effects of the compounds on the R and V cells at a fixed concentration. The rationale was that if the compound was a substrate of ABCG2, it would exhibit diminished anti-proliferative effects (higher % cell survival) on R cells as compared to V cells, as it would be actively transported out of the cells by the high levels of ABCG2. On the other hand, if it was not a substrate of ABCG2, it would affect viability of R and V cells to the same degree.

Selected compounds from Series 1, 3, 6, 7, 9, 8, 11 and 12 were examined at 5  $\mu$ M and/or 10  $\mu$ M. The results are presented as % cell survival at a stated concentration in Table 5-5.

Table 5-5: Effects of selected compounds on percentage cell survival in MDA-MB-231/R and MDA-MB-231/V cells<sup>a</sup>

Compound	% Cell Survival			
	MDA-MB-231/R		MDA-MB-231/V	
	10μM	5μM	10μM	5μM
<b>1-1</b>	122 (9)	ND <sup>b</sup>	101	ND <sup>b</sup>
<b>1-2</b>	126 (31)	ND	86	ND
<b>1-3</b>	112(12)	ND	133	ND
<b>1-4</b>	136 (16)	ND	122	ND
<b>1-5</b>	115 (16)	ND	101	ND
<b>1-6</b>	105 (11)	ND	83	ND
<b>1-7</b>	114 (8)	ND	156	ND
<b>1-8</b>	115	ND	37	62
<b>1-9</b>	103 (16)	ND	102	ND
<b>1-10</b>	126 (21)	ND	87	ND
<b>1-11</b>	116 (32)	ND	134	ND
<b>1-12</b>	83 (32)	ND	90	ND
<b>1-13</b>	116 (40)	ND	120	ND
<b>1-14</b>	113 (8)	ND	158	ND
<b>1-15</b>	108 (7)	ND	179	ND
<b>1-25</b>	65 (4) <sup>d*</sup>	82 (7)	86 (4)*	90 (2)
<b>1-26<sup>c</sup></b>	32 (4)*	35 (7)	37 (3)*	65 (19)
<b>3-1</b>	77 (21)	88 (24)	108 (4)	112 (7)
<b>5-1</b>	60 (8)*	68 (10) <sup>e*</sup>	103 (7)*	98 (9)*
<b>6-1</b>	94 (10)	92 (10)	108 (5)	109 (14)
<b>6-15</b>	61 (10)*	65 (14)	93 (4)*	100 (9)
<b>6-20</b>	73 (13)	83 (10)	101 (5)	109 (13)
<b>7-1</b>	93 (9)	101 (15)	110 (3)	111 (7)
<b>8-1</b>	56 (7)*	59 (6)*	108 (10)*	108 (8)*
<b>9-1</b>	68 (6)*	91 (10)*	97 (8)*	102 (6)*
<b>11-1</b>	75 (4)*	112 (23)	92 (3)*	103 (4)
<b>11-4</b>	71 (12)	84 (4)	89 (1)	92 (6)
<b>11-5</b>	75 (14)	71 (2)*	84 (3)	90 (2)*

<b>12-1</b>	70 (3)*	94 (16)	97 (3)*	105 (6)
<b>12-4</b>	63 (16)	76 (13)	91 (4)	103 (6)
<b>12-5</b>	68 (4)*	88 (6)	88 (1)*	101 (3)

---

<sup>a</sup> Percentage cell survival = (Average absorbance of wells with test compounds at 590nm/ Average absorbance of wells with medium and 1% DMSO) x 100%. Values are mean of two or more independent determinations. S.D. in brackets for  $n = 3$  determinations.

<sup>b</sup> ND, not determined

<sup>c</sup> % cell survival for compound **1-26** at 1 $\mu$ M in MDA-MB-231/R cells is  $88 \pm 10\%$ .

<sup>d</sup> Significant difference ( $*p < 0.05$ ) between % cell survival in MDA-MB-231/R cells and V cells at 10 $\mu$ M

<sup>e</sup> Significant difference ( $*p < 0.05$ ) between % cell survival in MDA-MB-231/R cells and V cells at 5 $\mu$ M

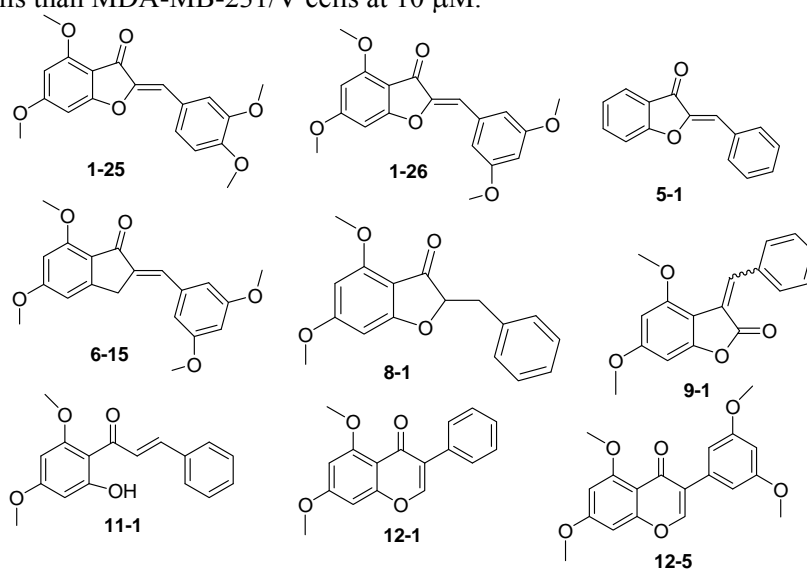


Based on the growth inhibitory levels on the R and V cells, three “categories” of compounds were evident. The first category comprised compounds that showed a substrate-like profile, namely lesser growth inhibitory effects on R cells compared to V cells at the same concentration. These compounds were exclusively 4,6-dimethoxyaurones of Series 1, namely **1-2** ( $R' = 2'OCH_3$ ), **1-6** ( $R' = 3'OH$ ), **1-8** ( $R' = 2'Cl$ ) and **1-10** ( $R' = 4'Cl$ ). No less than a 20% margin was observed in the cell survival values on R versus V cells. Notably, **1-8** (10  $\mu$ M) showed a large difference in cell survival values, with 115% viability on R cells and only 37% viability on V cells. However, as only two determinations were made on V cells for these compounds, statistical differences between the cell survival values in R and V cells could not be established. Thus, there is preliminary evidence to support a substrate role for a small number of 4, 6-dimethoxyaurones. Of these compounds, only **1-6** was recognized as a potent inhibitor of PhA efflux and was able to re-sensitize R cells to MX at a low concentration of 0.5  $\mu$ M.

The 2<sup>nd</sup> category of compounds were those that had a non-substrate profile in that they had similar growth inhibitory effects on both R and V cells ( $p > 0.05$ ). They included potent inhibitors of PhA efflux (and other assays), namely the indanone **6-20**, chalcones **11-4** and flavone **12-4**.

The last category comprised compounds that had greater growth inhibitory effects on R cells than V cells ( $p < 0.05$ ). Thus, they defied classification as substrates or non-substrates. Nine compounds from diverse series were associated with this category (Figure 5-6). Except for **1-25**, **1-26**, **6-15** and **12-5** which were potent inhibitors of PhA efflux, the other compounds were inactive on the PhA assay. The implication of this class of compounds should await further investigations ( $IC_{50}$  determinations) to confirm their selectivity on R cells.

Figure 5-6: Structures of test compounds associated with lower % cell survival values on MDA-MB-231/R cells than MDA-MB-231/V cells at 10  $\mu$ M.



The dimethoxyaurones **1-1** to **1-10**, **1-13** and **1-15** were also evaluated for antiproliferative activity on the human colon cancer HCT116 and the normal embryonic lung fibroblast IMR 90 cells (Table 5-6). Except for **1-8**, the other compounds did not affect the viability of HCT116 cells. Compound **1-8** was one of the 4 compounds that had a substrate-like profile (greater growth inhibitory effects on V cells than R cells). It had a pronounced growth inhibitory effect on HCT116 cells (27% cell survival at 5  $\mu$ M) but did not affect the viability of the normal fibroblast cells. The other test compounds had essentially no effect on the viability of the normal fibroblast cells which is a desirable property. Again,  $IC_{50}$  determinations would be required for confirmation.

Table 5-6: Effects of selected compounds on percentage cell survival in HCT 116 and IMR 90 cells<sup>a</sup>

Compound	% Cell Survival	
	HCT116	IMR 90
	5 $\mu$ M	5 $\mu$ M
<b>1-1</b>	76	>100
<b>1-2</b>	67	88
<b>1-3</b>	74	>100

<b>1-4</b>	80	92
<b>1-5</b>	56	>100
<b>1-6</b>	93	97
<b>1-7</b>	94	>100
<b>1-8</b>	27	93
<b>1-9</b>	50	>100
<b>1-10</b>	60	>100
<b>1-11</b>	ND <sup>b</sup>	ND
<b>1-12</b>	ND	ND
<b>1-13</b>	81	>100
<b>1-14</b>	ND	ND
<b>1-15</b>	94	>100

---

<sup>a</sup> Percentage cell survival = (Average absorbance of wells with test compounds at 590nm/ Average absorbance of wells with medium and 1% DMSO) x 100%. Values are mean of two independent determinations.

<sup>b</sup> ND, not determined

#### 5.4. Discussion

The objective of this chapter was to provide a better understanding of the effects of the Series 1-12 compounds on the transport activity of ABCG2. A number of different experiments were carried out to provide insight into this problem. Based on the results obtained from the PhA efflux assay (Chapter 3), selected compounds were examined for their ability to re-sensitize ABCG2 over-expressing MDA-MB-231/R cells to mitoxantrone (MX), a cytotoxic drug that is also an ABCG2 substrate. Also included were compounds that were potent inhibitors of PhA efflux in their respective groups, namely **1-25**, **1-26**, **6-15**, **11-5** and **12-5**. These compounds effectively increased the sensitivity of ABCG2 over-expressing MDA-MB-231/ R cells to MX at 0.05  $\mu$ M and were more potent than the FTC tested at the same concentration. At a higher concentration of 0.5  $\mu$ M, they completely reversed the resistance of R cells to MX. While the effectiveness of these potent compounds may be anticipated, a surprising observation was that compounds that were inactive on the PhA assay

were also effective in re-sensitizing R cells to MX and even exceeded FTC in restoring MX sensitivity to R cells at 0.5  $\mu$ M. Hence extrapolation of results from different assays should be done with caution. The lack of concurrence among assays may reflect differences in the sensitivities of the methods employed.

To demonstrate that the re-sensitization of R cells to MX was related to an increase in the intracellular MX concentration, several dimethoxyaurones from Series 1 were examined for their effects on MX accumulation in R cells by cell cytometry analysis. Of these compounds, three members (**1-3**, **1-6**, **1-9**) had been evaluated on the MX re-sensitization experiments. They were found to significantly increase intracellular MX in R cells at the same concentration (0.5  $\mu$ M) at which they re-sensitized R cells to MX. Moreover, they did not increase MX accumulation in the parental V cells which had normal levels of ABCG2. Taken together, these results supported the view that the dimethoxyaurones enhanced the potency of MX on R cells by reducing its ABCG2-mediated efflux from the cells. Aside from these 3 dimethoxyaurones, most of the remaining compounds also increased MX accumulation. As expected, it was difficult to draw parallels between their potencies on the PhA efflux assay and the MX accumulation results. There were potent compounds on the PhA assay that did not increase MX accumulation even at the highest concentration tested (**1-2**: R' = 2'-OCH<sub>3</sub>; **1-5**: R' = 2'-OH), inactive compounds on the PhA assay that significantly increased MX accumulation (**1-11**: R' = 2'-CH<sub>3</sub>) as well as compounds where there was apparent agreement between the two activities.

The MX accumulation assay also served the useful purpose of adding breadth to the type of ABCG2 substrates investigated in this chapter. This is important because ABCG2 is known to have multiple substrate binding sites<sup>140, 141</sup> and a compound that is able to modulate the efflux of different substrates is potentially more useful than one whose activity is limited

to a single substrate. MX is a synthetic anthracenedione while PhA is a naturally occurring chlorophyll metabolite. The ability of the dimethoxyaurones (**1-3**, **1-6**, **1-9**) to inhibit the efflux of these chemically diverse ABCG2 substrates is a good indicator of their potential usefulness as modulators of ABCG2 activity.

Typically, ABC transport modulators can either bind and compete with substrate binding at the substrate-binding site(s) or interfere with ATP binding or hydrolysis by binding to the ATP binding site. Both mechanisms result in the inhibition of transport activity. Thus far, several test compounds had demonstrated potent modulatory effects on the efflux activity of ABCG2. To confirm that these effects were the result of a direct interaction with the protein, it was necessary to exclude the likelihood that the test compounds interfered with the upstream processes of gene transcription and translation which would result in a reduction in ABCG2 content and functional activity. Western blot analysis confirmed that a representative potent dimethoxyaurone (**1-26**) did not reduce the ABCG2 content in R cells. Similar findings were obtained from R cell lysates incubated with **1-26** and MX, providing further support that the re-sensitization of R cells to MX in the presence of **1-26** was not related to changes in the level of ABCG2 but to an interaction with the protein. Evidence of a direct interaction with ABCG2 were adduced from the results of the ABCG2 ATPase assay and photo-affinity labeling of ABCG2 by [<sup>125</sup>I]-IAAP.

The transport of substrates and the hydrolysis of ATP are closely linked events in ABC transporters. Theoretically, the effect of a compound on the ATPase activity of the transporter should give valuable clues on the nature of its interaction with the protein. Activation of ATP turnover suggested the presence of an actively transported compound (substrate) while inhibition (if examined in a fully activated transporter) indicated direct interference with the transporter function or the presence of a substrate with a very low transport rate<sup>127</sup>. However, there were many exceptions to this relationship. For example, the

ABCG2 inhibitor curcumin stimulated ATPase activity<sup>149</sup> and PhA (ABCG2 substrate) had a biphasic effect on ATPase activity, stimulating ATP hydrolysis at low concentrations and inhibiting it at higher concentrations<sup>143</sup>. Verapamil, a well known inhibitor of ABCB1, was a strong stimulator of ABCB1-associated ATPase activity<sup>79</sup>. This was attributed to its lipophilic nature which allowed verapamil to function as a “fast diffusing substrate”, partitioning rapidly into the cell membrane and transported out of the cell as rapidly as it got in. Thus, a futile cycle of ATP hydrolysis was activated with no net transport of the substrate<sup>150</sup>. In view of these contradictory observations, the general consensus was that modulation of transporter-specific ATP hydrolysis by a given compound was not a reliable means of determining if a compound was a substrate or inhibitor of the transporter, but it does confirm the ability of the substance to interact with the transporter<sup>127</sup>. Seventeen test compounds were examined on the ABCG2-ATPase assay and all stimulated ATPase activity by 2-3 times that of the basal level activity. A significant correlation was observed between the ATPase stimulatory properties of the compounds ( $K_m$ ) and their inhibition of PhA efflux ( $EC_{50}$ ) by R cells. Thus the more potent stimulators of ATPase (**1-25**, **1-26**, **6-20**, **12-5**) were also potent inhibitors of PhA efflux. Although not determined here, the  $K_m$  of MX was reported by the same lab who carried out these assays to be 2  $\mu\text{M}$ <sup>143</sup>. Tentatively, the most potent analog identified here may be at least 50 times more potent than MX in stimulating ATPase.

[<sup>125</sup> I]-IAAP is a photoaffinity analog of prazosin that has been widely used to characterize the substrate binding sites of ABCG2<sup>146</sup>. A compound that reduces the photo-labeling of ABCG2 is deduced to interact with the substrate (IAAP) binding site of the protein although the reduction in IAAP binding could be due to conformational changes induced by the substance under investigation. The same compounds investigated on the

ATPase assay were examined for their effects on IAAP binding. Except for 3 compounds (flavones **12-1**, **12-5** and the unsubstituted aurone **5-1**), the remaining compounds reduced the photo-affinity labeling of ABCG2 at 5  $\mu$ M. Barring the induction of conformational changes in the protein, the present findings supported an interaction by the compounds with the IAAP binding site of ABCG2, with particularly strong affinities associated with chalcones.

Having shown that several compounds modulated ABCG2 activity by reducing the efflux of known ABCG2 substrates (PhA, MX) and competing with others (IAAP) for occupancy of binding sites, it was of interest to determine if they were themselves recognized as substrates of ABCG2. An indirect approach based on the differential growth inhibitory activities of the test compounds on R and V cells was employed for this purpose. The rationale was that a non- substrate of ABCG2 should have nearly equivalent growth inhibitory effects on R and V cells while a substrate should have weaker effects on R cells than V cells. The recommended method for identifying substrates and non-substrates is to carry out bi-directional transporter assays using polarized epithelial cells lines like Caco-2 (for ABCB1) or an equivalent cell line that over-expressed ABCG2<sup>151</sup> but this was not carried out here due to a lack of resources.

Of the 31 compounds examined for their differential growth inhibitory effects, the majority were deduced to be non-substrates of ABCG2 as no difference was observed in the cell survival levels of the R and V cells. Included within this number were potent compounds from the PhA assay, namely **6-20** and **12-5**. These compounds also effectively re-sensitized R cells to MX. A small number of compounds had a substrate-like profile (greater % cell survival of R cells than V cells) while 9 compounds from diverse groups defied classification based on the present criteria. It is worth noting that the Series 1 dimethoxyaurones was the only series that yielded “non-substrates” (majority) and “substrates”. Moreover, compounds

with a substrate-like profile were characterized by having mono-substituted ring B, with groups mostly at 2' or 4' positions, and a strong representation (2 out of 4) of chloro on ring B.

The growth inhibitory assays also showed that the dimethoxyaurones were remarkably non-toxic on normal /non-cancer cells although IC<sub>50</sub> determinations would be necessary for confirmation.

### 5.5. Conclusion

A number of different experimental protocols were carried out to examine the interactions of dimethoxyaurones and related analogs on ABCG2. In view of the large number of compounds available coupled with the complexity and low throughput nature of some of these methods, not all the compounds could be investigated on all assays. Nonetheless, an attempt was made to investigate compounds that were potent inhibitors of PhA efflux (dimethoxyaurones **1-25**, **1-26**; indanones **6-15**, **6-20**; chalcone **11-5**; flavones **12-4**, **12-5**) on most of these assays.

The findings of this chapter provided convincing evidence that these potent analogs interacted directly with ABCG2 to inhibit transport activity. These compounds bind at the IAAP substrate site to prevent photo-affinity labeling of ABCG2 by [<sup>125</sup>I]-IAAP. They also competed with PhA and possibly MX for occupancy of their respective binding sites, leading to a reduction in the efflux of these substrates by ABCG2. They stimulated ABCG2 ATPase activity with nanomolar K<sub>m</sub> values but were not substrates of ABCG2 themselves. Most of them re-sensitized R cells to MX and were more effective than FTC in this respect. There were instances where some compounds did not retain the expected levels of potency across the various assays but these were anticipated given the multiple binding sites found in ABCG2 and the different sensitivities of the assays involved.



Earlier investigations on the interaction of aurones with a related transporter ABCB1 led to a proposed dual interaction with the ATP binding site and an adjacent substrate binding site. An interaction with the ATP binding site would require evidence from photo-affinity labeling experiments with [ $\alpha$ - $^{32}$ P] 8-azidoATP which binds specifically with the nucleotide binding domains of numerous ATP transporters. As this was not carried out here, it is not known if the compounds interacted with the ATP binding site of ABCG2. There was more certainty that the compounds interacted with one or more substrate binding sites on ABCG2, notably those for PhA, MX and/or IAAP. Most likely, they competed for occupancy of these sites, thus inhibiting the efflux of the bona fide substrate by ABCG2. In the absence of an ABCG2 substrate, the present evidence suggested that they were not transported by ABCG2, implying that these compounds did not bind with sufficient affinity to their putative sites to stimulate the hydrolysis of ATP necessary for transport.

## Chapter 6: *In vivo* evaluation of a 4, 6-dimethoxyaurone analog (1-26) in mice bearing human breast cancer cells (MDA-MB-231) xenografts

### 6.1. Introduction

A review of the literature revealed several reports on the reversal effects of compounds on ABCB1-overexpressing tumor xenografts. Dai and co-workers<sup>152</sup> reported that the co-administration of FG020326 (a tri-aryl substituted imidazole derivative) with paclitaxel or vincristine significantly enhanced the antitumor activity in mice bearing KBc200 (vincristine selected ABCB2-overexpressing human oral epidermoid carcinoma cells) xenografts. The same laboratory also reported the successful reversal of KBc200 resistance to epirubicin (an anthracycline anticancer agent) in mice by the agent bromotetrandrine<sup>153</sup>. On the other hand, there are fewer reports demonstrating the *in vivo* capabilities of agents reversing multi-drug resistance linked to ABCG2. A recent report by Shukla and co-workers showed that oral administration of curcumin (inhibitor of ABCG2) enhanced the intestinal absorption of sulfasalazine in mice, thereby increasing the bioavailability of this ABCG2-specific substrate<sup>154</sup>.

In view of the evidence presented in Chapters 3 and 5 on the potential of dimethoxyaurones and related analogs as modulators of ABCG2 activity, it was of interest to determine if their *in vitro* efficacies could be translated to an *in vivo* setting. These findings would be a useful addition to the limited investigations available in this area. Hence in this chapter, a representative test compound was examined for its ability to increase the survival of mice bearing an ABCG2 over-expressing human breast cancer xenograft when used in combination with mitoxantrone (MX). The compound chosen for investigation was the dimethoxyaurone **1-26** [2-(3, 5-dimethoxybenzylidene)-4,6-dimethoxybenzofuran-3(2H)-one] which was identified on several assays (Chapters 3 and 5) to be a potent inhibitor of

ABCG2-mediated efflux. To reiterate, **1-26** was the most potent inhibitor of PhA efflux in MDA-MB-231 /R cells ( $EC_{50}$  0.91  $\mu$ M), it completely restored MX sensitivity to R cells at 0.5  $\mu$ M and interacted with high affinity to ABCG2 as shown from the ABCG2-ATPase and [ $^{125}$ I]-IAAP photoaffinity labeling assays. The objective of this chapter was to determine if the ability of **1-26** to re-sensitize R cells to MX *in vitro* would be observed in mice bearing an ABCG2-overexpressing tumor xenograft.

## 6.2 Experimental

### 6.2.1 Materials

Mitoxantrone (MX) and dimethyl sulfoxide (Pharmaceutical grade) were purchased from Sigma Chemical Co., St Louis, MO, USA. The synthesis and characterization of **1-26** [2-(3, 5-dimethoxybenzylidene)-4, 6-dimethoxybenzofuran-3(2H)-one] was described in Chapter 2 (Section 2.3.1, Appendix 2-1). Ketamine was obtained from Parnell Laboratories Pte Ltd (Australia). Medetomidine and atipamezole were purchased from Pfizer New Zealand Ltd (Auckland, NZ).

### 6.2.2. Cell Lines

The breast cancer cell line MDA-MB-231, stably transfected with expression vectors for wild type 482R ABCG2 (R cells) and pcDNA3.1 (parental V cells) were kindly provided by Dr. Douglas D. Ross (Greenebaum Cancer Center, University of Maryland, Baltimore, USA). Both cell lines were assessed to be pathogen-free by Laboratory Animal Centre of the National University of Singapore.

### 6.2.3 *In vivo* studies

Experimental protocols for the *in vivo* study were approved by the National University of Singapore Institutional Animal Care and Use Committee [IACUC 106/09(A) 09] and were in accordance to National Advisory Committee for Laboratory Animal Research guidelines for the care and use of animals for scientific purposes. Balb/c female athymic nude mice (of 18 to 20g body weight, 8 weeks old) were obtained from the Biological Resource Centre (Singapore). Animals were kept under controlled environmental conditions (19-26 °C, relative humidity < 70%, 12 h dark-light cycle) with free access to water and standard feed.

To establish the tumor xenograft, the mice were first sedated by an intraperitoneal injection of an anaesthetic cocktail (0.1 ml/10 g) comprising ketamine (0.75 ml of 100 mg/ml stock solution) and medetomidine (1 ml of 1 mg/ml stock solution) diluted to 10 ml with 0.9% saline. Once sedated, MDA-MB-231/V or MDA-MB-231/R cells (15 million cells per ml of RPMI-1640 media supplemented with 10% fetal bovine serum, 0.1mg/ml streptomycin sulfate and penicillin G, and 1.0mg/ml geneticin) at a density of 15 million cells/ml were injected orthotopically into one of the mammary fat pads of the animal. To reverse the sedation, the animal was injected (intraperitoneal) with the reversal agent atipamezole (0.1 ml of 5 mg/ml stock solution in 9.9ml of 0.9% saline) in a volume equivalent to the amount of anaesthetic used.

Drug treatment was started 13 to 18 days post injection of tumor cells when the animal developed palpable mammary tumors of 5 to 9 mm diameter at the injection site. The mice were randomized into those with R or V xenografts, with at least 4 mice in each treatment group. For animals in the R group, the treatment groups were animals receiving (i) vehicle control (1% v/v DMSO in saline); (ii) Test compound **1-26** (0.2 mg/kg, equivalent

to 10 $\mu$ M); (iii) MX (4mg/kg); and (iv) a combination of **1-26** (10 $\mu$ M) and MX (4 mg/kg). Similar treatment groups were extended to animals bearing the V xenografts. All drug solutions were freshly prepared prior to injection and sterilized by filtration using a 0.20 micron size DMSO-safe Acrodisc syringe filter. The final concentration of DMSO in these solutions was  $\leq 1\%$  (v/v). The solutions were administered intratumorally in a volume of 0.1ml. Only one administration was made throughout the entire study period.

Mice were closely monitored, weighed and tumor size was measured at least 3 times weekly. For tumor size measurement, length (L= the longer diameter) and width (W= the shorter diameter) of the tumor were measured with electronic vernier calipers and reported up to 2 decimal places. Tumor volume (V) was calculated as  $V = L \times (W^2/2)$ . Survival (in days) of mice in the different treatment groups were monitored throughout the period of study. Mice were euthanized according to the criteria of the IACUC-approved treatment protocol. Euthanasia was administered when the animals were observed to have (i) tumor size  $> 1.5$ cm in diameter; (ii) ulcerated, infected or inflamed tumor; (iii) ruffled fur, hunched back appearance or inappetent state; (iv) 10% or more loss of body weight over 24 hours, or 20% or more loss of body weight compared to control group and (v) be in a moribund or pre-moribund state. Mice that did not meet the criteria for euthanasia were sacrificed 60 days post tumor inoculation.

The survival analysis took into consideration the occurrence of censored events. These were identified as events in which (i) the animal was still alive after 60 days post tumor inoculation; (ii) the animal died due to unrelated causes such as sudden death after tumor inoculation, (iii) there was deviation from an ellipsoidal tumor shape such as secondary growth next to the original tumor, and (iv) the animal was put down due to other conditions cited for euthanasia that were not related to tumor size  $> 1.5$  cm in diameter.

#### 6.2.4. Statistical analysis

Data were analyzed by Kaplan-Meier (with log rank test) and Cox proportional hazards model on SPSS version 15 (Chicago, IL) following the method described by Chan et al<sup>155</sup>. *p* values < 0.05 were considered significant.

#### 6.3. Results

Median survival times (in days) were monitored for mice with R and V xenografts and on the different treatment schedules. The results are presented in Table 6-1 and as survival curves in Figures 6-1.

Table 6-1: Kaplan-Meier analysis<sup>a</sup> for comparison between treatment schemes in mice with MDA-MB-231/V induced xenografts and MDA-MB-231/R induced xenografts.

Human cell line xenograft	Treatment groups			
	Control (1% DMSO)	<b>1-26</b> only	MX only	<b>1-26 + MX</b>
<b>MDA-MB-231/V</b>				
Median survival time (days)	12	15	29	25
Number treated	5	5	5	4
Number of censored events	0	2	1	2
ILS (%) <sup>b</sup>	-	25	142	108
Log-rank test ( <i>p</i> ) <sup>c</sup>		<i>0.356</i>	<i>0.013*</i>	<i>0.008**</i>
<b>MDA-MB-231/R</b>				
Median survival time (days)	12	15	17	25
Number treated	4	4	5	5
Number of censored events	0	1	1	1
ILS (%) <sup>b</sup>	-	25	42	108
Log-rank test ( <i>p</i> ) <sup>c</sup>		<i>0.169</i>	<i>0.055</i>	<i>0.007**</i>

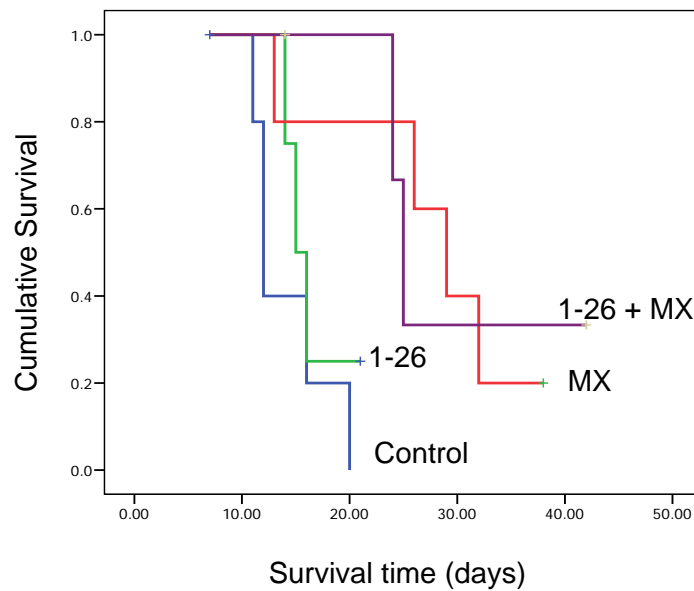
<sup>a</sup> Kaplan-Meier analysis was carried out on SPSS Ver 15.0 (Chicago, IL)

<sup>b</sup> ILS= % increase in median life span = [(median survival time for treated group - median survival time for control) / median survival time for control] x 100%

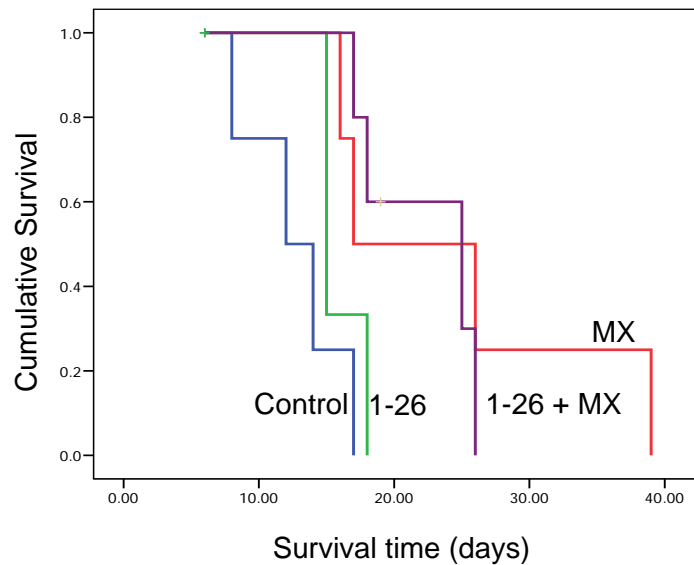
<sup>c</sup> Statistical significance between treatment group and control group \* $p < 0.05$  ; \*\* $p < 0.01$ .

Figures 6-1(a) and 6-1(b): Survival plots of Balb/c nude mice inoculated with (A) parental MDA-MB-231/V and (B) ABCG2-overexpressing MDA-MB-231/R cells and subjected to different treatment schedules (i) Control (DMSO + saline); (ii) **1-26** (0.2 mg/kg); (iii) MX (4 mg/kg) (iv) **1-26** (0.2 mg/kg) + MX (4 mg/kg)

(A)



(B)



As shown in Table 6-1, for mice bearing the V xenografts, the median survival time for untreated (control) animals was 12 days. This was increased to 15 days in mice treated with test compound **1-26**, which was equivalent to a 25% increase in median life span (ILS) compared to the control untreated animals. The log-rank test did not identify this increase in life span to be a significant event. While **1-26** did not increase the life span of the animal, it also did not hasten its demise, implying that the compound was non-toxic to the animal. In the case of treatment with MX, median survival time was increased to 29 days or 142% of the control survival time. The log rank test recognized this to be a significant lengthening of life span ( $p < 0.05$ ). When animals were treated with test compound and MX, there was a fall in the % ILS to 108% but this relatively small increase (compared to the 142% ILS observed for MX) was still deemed to be statistically significant ( $p < 0.01$ ) by the log-rank test. These results were largely anticipated. Since the xenograft was established with parental V cells which had normal ABCG2 levels, MX would retain its effectiveness against the tumor and prolonged survival time. The significant outcome following treatment with **1-26** and MX in combination probably reflected a dominant contribution by MX.

In the case of animals bearing the R xenograft, mean survival times for untreated animals were similar to that obtained for animals bearing the V xenograft. Treatment with **1-26** also prolonged survival by an insignificant 25% which reinforced the view that **1-26** was essentially non-toxic to the animal. Notably, treatment with MX caused only a modest increase in median life span to 42% which was not deemed to be significantly different from untreated animals. Thus, it was clear that the xenograft induced by ABCG2-overexpressing R cells was resistant to MX to some degree and thus MX was not effective in prolonging survival of the tumor bearing animal. On the other hand, combined treatment with MX and **1-26** raised the life span to 108%, which was a significant increase ( $p < 0.01$ ) based on the



log-rank test. These results indicated that the presence of **1-26** enhanced the efficacy of MX on the R cell-induced xenograft.

Eight censored events were encountered in this study (Table 6-1). A censored event is one in which death was attributed to causes that were unrelated to disease progression. Since tumor size was taken as an indicator of disease progression, unexpected death of the animal or an event that necessitated euthanasia (other than the increase of tumor diameter > 1.5 cm) was considered censored. Of the 8 censored events, 1 was due to the survival of the animal (treated with MX on V xenograft) beyond the study period of 60 days while the rest were related to events described in Section 6.2.3.

The median survival times of animals with R or V xenografts and treated with the different protocols were further analyzed to determine how these variables influenced the outcome of the experiments. The variables (or confounders) were the type of xenograft (R or V –xenografts induced with R cells may be more aggressive than those induced with V cells), tumor size (treatment was started when tumor volume was estimated to be greater than 100 mm<sup>3</sup> and this may be too large to influence the treatment outcome) and the treatment protocols (animals treated with vehicle, MX, **1-26** or a combination of **1-26** and MX). To determine the effect of these confounders, the data was analyzed by the Cox proportional hazards model<sup>155</sup>. This model (also called Cox regression model) is multivariate in nature unlike the Kaplan Meier analysis which is univariate. The results are presented in Table 6-2.

Table 6-2: Estimates of variables in experimental model by Cox regression.

	Significance <sup>a</sup>	Hazard Ratio (HR)	95.0% Confidence Intervals for Hazard Ratio	
			Lower	Upper
Tumour type	.056	2.400	.977	5.895
Tumour size	.098	2.217	.862	5.698
Treatment group	.001*			
Treatment group (aurone only)	.288	.564	.196	1.621
Treatment group (MX only)	.000*	.069	.017	.269
Treatment group (aurone + MX)	.000*	.107	.031	.368

<sup>a</sup> Significant difference (\* $p < 0.05$ )

The important parameters to consider in Table 6-2 are the hazard ratio and the level of significance ( $p$  values) associated with each variable. A hazard ratio of  $> 1$  was interpreted to mean that the variable compared to its reference was likely to have a shorter time to the event (death of animal) while a ratio  $< 1$  had the opposite meaning (less likely to have a shorter time to event). From the table, it was seen that the tumor type (R xenograft compared to the reference V xenograft) and tumor size (initial volume size  $> 100 \text{ mm}^3$  compared to reference volume size  $< 100 \text{ mm}^3$ ) had  $p$  values  $> 0.05$  and hazard ratios  $> 1$ . Thus these variables did not contribute significantly to the experimental outcome. On the other hand, the type of treatment received by the animals was identified to be a significant confounder ( $p = 0.001$ ) and of the different types of treatment, two of them – animals treated with MX alone and a combination of MX and **1-26** – had hazard ratios  $< 1$  and were also significantly different ( $p < 0.01$ ) from the reference group (animals receiving vehicle). These results implied that animals on these treatment schedules were more likely to have significantly longer life spans than untreated animals. As noted earlier, Kaplan Meier analyses also

identified the combined MX and **1-26** treatment and MX treatment (on V xenografts) to significantly increase the life-span of mice. Only the treatment with the test compound **1-26** was not a significant confounder, reinforcing the notion that **1-26** was essentially non-toxic on the test animal.

The weights of the mice were monitored on a regular basis to determine if they suffered weight loss (indicative of toxicity) under the different treatment schedules. As seen from Figures 6-2 and 6-3, the weight of the mice bearing V or R xenografts remained relatively constant on the various treatment arms, implying that the animals did not encounter serious toxicity issues.

Although the volumes of the tumors were monitored throughout the period of study, analysis of data based on changes in tumor volumes proved to be unsatisfactory. This was because the time to death for mice bearing R or V xenografts under the different treatment schedules varied considerably. The last remaining mouse with R xenograft treated with MX survived for 39 days while the first mouse with R xenograft treated with vehicle control met the criteria for euthanasia (tumor size > 1.5cm in diameter) after only 8 days. For this reason, an alternative measure, survival time, was used as the dependent variable in this study.

Figures 6-2(a-d): Weight changes of mice bearing MDA-MB-231/V xenografts over time.

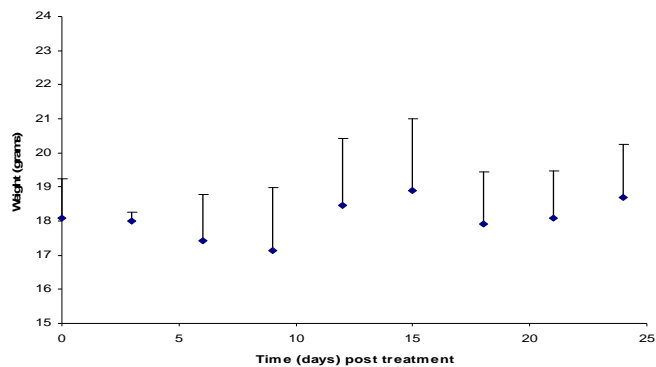


Figure 6-2a: Weight changes (in grams) of mice bearing MDA-MB-231/V tumor over time (days) post treatment with MX (4mg/kg) and compound **1-26** (10 $\mu$ M)

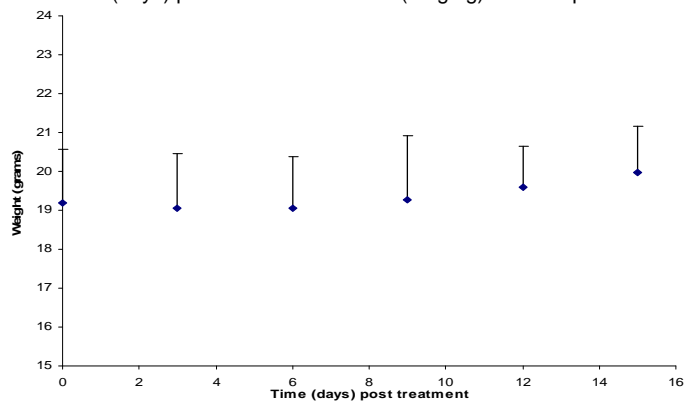


Figure 6-2c: Weight changes (in grams) of mice bearing MDA-MB-231/V tumor over time (days) post treatment with compound **1-26** (10 $\mu$ M)

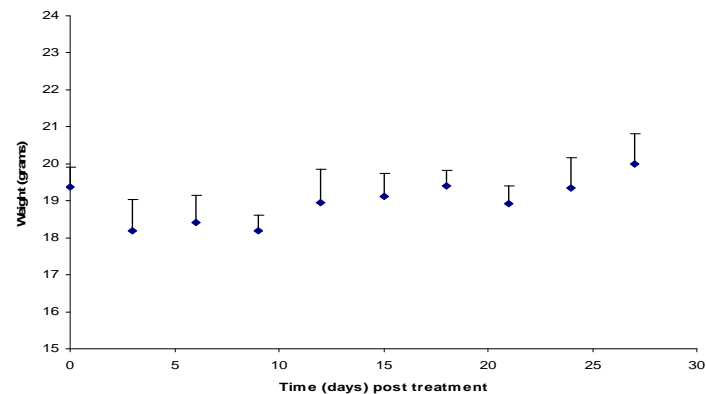


Figure 6-2b: Weight changes (in grams) of mice bearing MDA-MB-231/V tumor over time (days) post treatment with MX (4mg/kg)

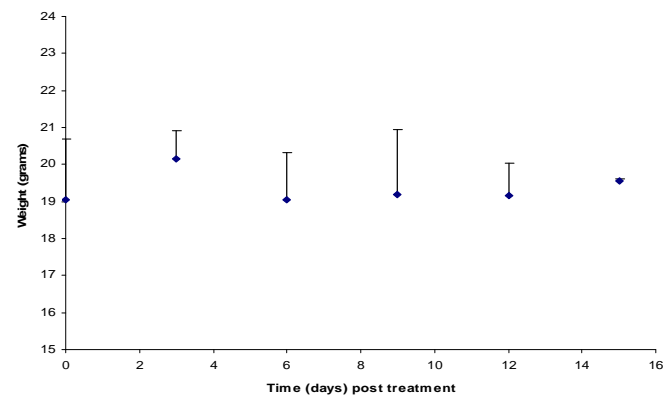


Figure 6-2d: Weight changes (in grams) of mice bearing MDA-MB-231/V tumor over time (days) post treatment with DMSO control

Figures 6-3(a-d): Weight changes (grams) of mice bearing MDA-MB-231/R xenografts over time.

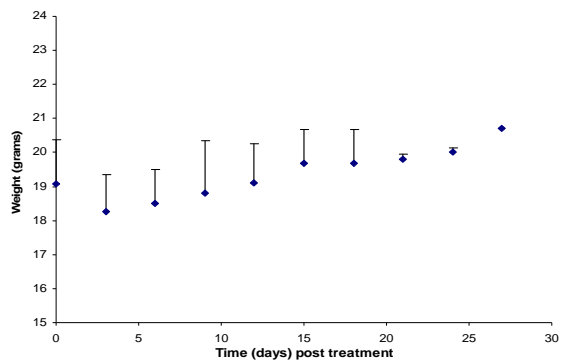


Figure 6-3a: Weight changes (in grams) of mice bearing MDA-MB-231/R tumor over time (days) post treatment with MX (4mg/kg) and compound **1-26** (10 $\mu$ M)

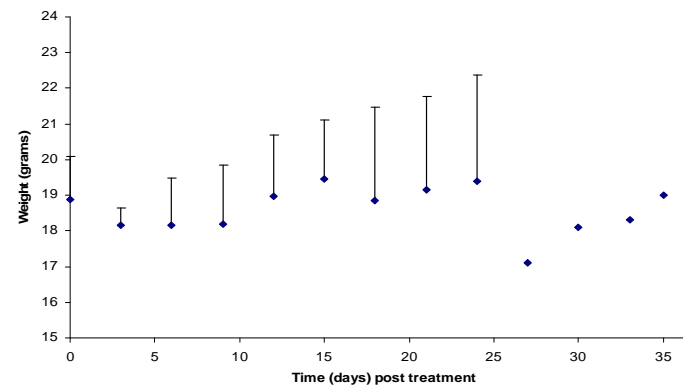


Figure 6-3b: Weight changes (in grams) of mice bearing MDA-MB-231/R tumor over time (days) post treatment with MX (4mg/kg)

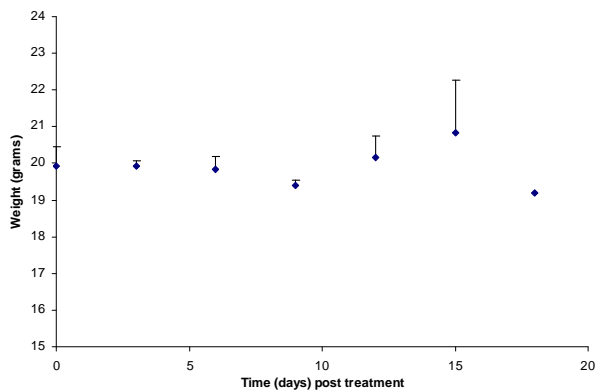


Figure 6-3c: Weight changes (in grams) of mice bearing MDA-MB-231/R tumor over time (days) post treatment with compound **1-26** (10 $\mu$ M)

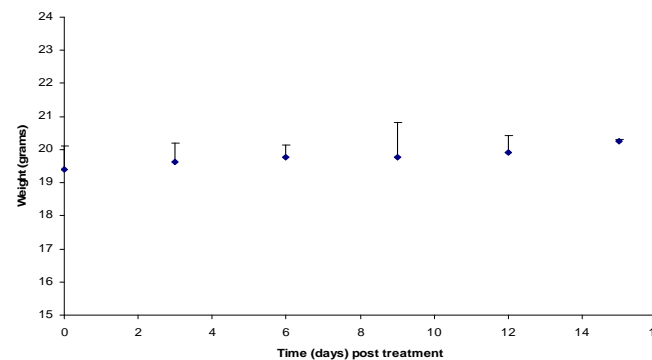


Figure 6-3d: Weight changes (in grams) of mice bearing MDA-MB-231/R tumor over time (days) post treatment with DMSO control

#### 6.4. Discussion

Animal studies with Balb/c athymic nude mice were carried out with the objective of evaluating the *in vivo* efficacy of a representative dimethoxyaurone **1-26** in sensitizing an ABCG2-overexpressing human breast cancer (MDA-MB-231/R) xenograft to the cytotoxic effects of mitoxantrone (MX). These experiments would determine if the *in vitro* potency of **1-26** as a potent modulator of ABCG2 and sensitizer of MX activity in a cell-based assay could bring about an increase in survival of mice bearing an MX-unresponsive xenograft induced by ABCG2-overexpressing R cells.

The xenograft was induced by inoculating R cells or parental V cells into the mammary fat pad of the animal. It was chosen as the site for tumor implantation because tumor induction in nude mice was reported to be higher (100%) in the mammary pad as compared to subcutaneous inoculation into the flank of the animal where the “take up” rate was estimated to be 40%<sup>156</sup>. Furthermore, Clarke and co-workers had reported mammary fat pads to be the preferred site for inducing mammary tumor xenografts<sup>157</sup>.

The test compound **1-26** was administered in a single dose of 0.2 mg /kg (equivalent to 10  $\mu$ M) which was higher than the concentration (1  $\mu$ M) of **1-26** required to re-sensitize R cells to MX in the *in vitro* study (Section 5.3.1). Compound **1-26** was not evaluated for MX accumulation in R cells by flow cytometry analysis but related compounds that were examined were effective at 5  $\mu$ M (Section 5.3.2). As the pharmacokinetic profile of **1-26** has not been investigated, it seemed reasonable to use a higher concentration (10  $\mu$ M) for the *in vivo* study to compensate for losses that might be incurred due to distribution and metabolic processes. Although there were initial fears that this dose of **1-26** might be toxic to the animals, it was not found to be so as discussed later.

The other consideration was the dose of MX to be used and here, the report of Almond et al<sup>158</sup> showed that the maximum tolerable dose of MX was 8-16mg/kg in mice

injected subcutaneously with murine mammary adenocarcinoma cells. Thus a dose of 4mg/kg MX was used in this study. The method and frequency of administration were based on the above mentioned report (above) which investigated the efficacy of free MX versus MX-loaded albumin microspheres injected intratumorally on one occasion into tumor-bearing mice. Thus a single intratumoral injection was carried out. An advantage of intratumoral administration was that the drug(s) would be largely localized within the tumor mass, thereby minimizing systemic toxicity.

Kaplan-Meier analysis showed that treatment of mice bearing V or R xenografts with **1-26** did not significantly increased survival times. Treatment with **1-26** was also not identified in the Cox regression as a confounding factor in the experiments. Therefore, the consensus was that **1-26** had no effect on the progression of the tumor and had limited *in vivo* toxicity at the dose used. On the other hand, treatment with MX was identified as a confounding factor by the Cox regression. It significantly increased survival time of mice with xenografts induced by V cells but not R cells, which was in keeping with the status of MX as a substrate of ABCG2.

Another confounding factor in the experiments was treatment with the combination of MX and **1-26**. Kaplan-Meier analysis showed that median survival times of mice with V and R xenografts were increased on treatment with this combination. That the life span of mice with R xenografts were increased when treated with the combination but not when treated with MX alone, implied a role for the ABCG2 modulatory property of **1-26** in increasing the sensitivity of the tumor to the cytotoxic effects of MX. On the other hand, the efficacy of the combination in mice bearing the V xenografts was likely to be due to the presence of MX and not **1-26**, since MX alone significantly increased the lifespan of the treated animals.

## 6.5. Conclusion

The findings in this chapter showed that the concurrent administration of the dimethoxyaurone **1-26** and MX was effective in prolonging the survival of mice bearing ABCG2 over-expressing tumor cells. When given separately, neither **1-26** nor MX significantly prolonged the life span of the tumor bearing animals. These findings were ascribed to the ABCG2 modulatory properties of **1-26** which had been demonstrated *in vitro*. It would be of interest to determine if the administration of the drugs by a non-intratumoral route would give rise to the same results. To do this, the pharmacokinetic profiles of **1-26** alone and in combination with MX would be required. With this information, the doses of **1-26** and MX could be adjusted to optimize its *in vivo* effects.



## Chapter 7: Conclusions and Future Work

The aim of the thesis was to test the hypothesis that aurones interacted with the ABC protein ABCG2 to modulate its activity. ABCG2 is a clinically relevant transport protein linked with multi-drug resistance to cancer chemotherapy and the ability of aurones to interfere with its efflux activity would underscore the potential of this template for the design of agents with multi-drug reversal properties. The hypothesis was driven by several factors. First, aurones are a lesser known group of flavonoids, a class of compounds widely known to modulate the efflux activity of several ABC efflux proteins including ABCG2. Flavonoids like chrysin, techtochrysin, apigenin, quercetin and kaempferol had demonstrated potent ABCG2 and ABCB1 modulatory properties and there was a possibility that aurones would do likewise. Second, several 4, 6-dimethoxyaurones were already known to increase the uptake of ABCB1 substrates (rhodamine 123, paclitaxel) into human cancer cell lines that over-express ABCB1. Third, the benzofuranone ring of aurones is structurally related to the adenine ring of ATP and the mimicry of these templates could predispose aurones to an interaction with the nucleotide binding domain of the transport protein. In fact, this has been demonstrated for aurones in their interaction with the C-terminal cytosolic domain of murine ABCB1.

The hypothesis was investigated by approaches described in Chapters 2-6. Twelve series of compounds comprising 112 functionalized aurones and related analogs were synthesized to provide the structural diversity necessary for the derivation of structure-activity relationships. They were screened for inhibition of the efflux of PhA by ABCG2 overexpressing human breast cancer cells (R cells) as described in Chapter 3. Several dimethoxyaurones (Series 1), benzylideneindanones (Series 6), dimethoxyflavones (Series 12) were found to inhibit PhA efflux at potencies that were comparable to the established ABCG2 inhibitor FTC.

A qualitative assessment of the structural features required for this activity highlighted important roles for (i) a methoxylated ring A but not a hydroxylated or unsubstituted ring A; (ii) an intact exocyclic double bond attached to a 5-membered ring C, which could be expanded to a 6-membered ring with the double bond enclosed within the ring, as in the Series 12 flavones; and (iii) the location of the double bond on ring C which should be one carbon removed from ring A as deduced from the inactivity of isoaurones and benzylidene indolinones. Inhibitory activity was diminished when the aurone O was replaced by NH but generally increased when replaced with a methylene CH<sub>2</sub>. Also noted was the lesser role accorded to ring B compared to ring A. Thus, in the presence of an appropriately substituted ring A, ring B appeared to play a subsidiary role. This was corroborated by the limited changes in activity when a wide range of groups were introduced to ring B. On the other hand, di-substitution of ring B, particularly with methoxy groups at 3',4' or 3',5' positions, yielded the most potent inhibitors of PhA efflux among the dimethoxyaurones (**1-25**, **1-26**), benzylideneindanones (**6-15**, **6-20**) and dimethoxyflavones (**12-4**, **12-5**).

It was gratifying to note that many of these qualitative deductions were reinforced in a QSAR approach based on the modified Free-Wilson method. The equation generated by the modified Free Wilson approach ranked the methoxy groups on ring A as significant contributors to activity. These groups were also identified as H bond acceptors and hydrophobic features in a pharmacophore model. The equation also identified the positive contribution made by an intact ring C and exocyclic double bond to activity. The only reference to ring B in the equation was a term pertaining to occupancy of the 3' position on the ring but not the group that should be present.

The issue of how lipophilicity affected activity was more complicated. In spite of several reports indicating a direct relationship between ABCG2 inhibition and lipophilicity, this trend was not evident from the present findings. Qualitative deductions

pointed to a reduction in activity when lipophilicity was increased but there was a threshold below which activity also decreased. QSAR failed to provide consensus, with conflicting trends observed with SlogP, logP and polar surface area. Perhaps the relationship was parabolic rather than linear, with an optimal lipophilicity associated with methoxylated compounds while those with hydroxylated or halogenated groups were too hydrophilic or too lipophilic respectively.

Noting that aurones were first reported for their interaction with ABCB1, the question was asked if the present series of aurones and related compounds interacted with ABCG2 exclusively or with both ABCG2 and ABCB1. The results supported the view that interactions of aurones with ABCB1 and ABCG2 involved broadly similar structural features. Thus, hydroxylated aurones, isoaurones, dehydroaurones with no activity on the PhA efflux assay were similarly inactive on the CAM assay. In addition, a small number of potent inhibitors of the PhA efflux were also potent inhibitors of CAM efflux. Between these extremes of activity, there was considerable variability among compounds from different series. Analysis by the modified Free Wilson approach proposed a dual acting compound to be one with methoxy groups on both rings A and B, and an intact ring C.

The functional relevance of the reduced PhA efflux from ABCG2 over-expressing cells was confirmed in subsequent experiments that showed the ability of selected compounds to re-sensitize these cells to the cytotoxic effects of mitoxantrone. Re-sensitization was observed at concentrations as low as 0.5  $\mu$ M, with the more potent analogs (**1-26**, **1-25**, **6-14**, **12-4**, **12-5**) restoring complete sensitivity to the ABCG2 over-expressing cells. For a few compounds, the re-sensitization to mitoxantrone was linked to an increase in the accumulation of intracellular mitoxantrone.

Evidence was adduced to support a direct interaction between ABCG2 and selected analogs. The ABCG2 ATPase assay showed stimulation of ATPase activity by 2-3 times the basal activity, with the most potent inhibitors (**1-25**, **1-26**, **6-20**, **12-5**)

stimulating ATPase activity at nanomolar  $K_m$  values. The photoaffinity-labeling of ABCG2 by [ $^{125}$  I]-IAAP was reduced in the presence of several potent analogs, pointing to competition for the substrate (IAAP) binding site on ABCG2. The likelihood of the compounds interfering with upstream cellular processes involved in the synthesis of the ABCG2 protein was also excluded.

In view of this finding, the question was asked if the test compounds interacted with ABCG2 at substrate binding site(s) or at the ATP binding site. The present findings supported the view that most of the compounds, including the most potent members, competed with specific substrates (PhA, mitoxantrone, IAAP) for binding on the protein, but on occupancy of these sites, were not themselves transported out of the cells. Thus, they were not substrates of ABCG2. As to whether they blocked the efflux of ABCG2 substrates by interfering with the binding and hydrolysis of ATP, this was not investigated in the thesis.

In the final chapter of the thesis, the *in vivo* efficacy of a representative aurone **1-26** in sensitizing an ABCG2-overexpressing human breast cancer (MDA-MB-231/R) xenograft induced in Balb/c mice to the cytotoxic effects of mitoxantrone was demonstrated. The combination of **1-26** and mitoxantrone significantly increased the life span of the treated animals in contrast to animals that were treated with mitoxantrone alone. Thus, the potent ABCG2 modulatory properties of **1-26** observed *in vitro* could be translated to xenograft-bearing animals.

In conclusion, the findings of this thesis supported the hypothesis that aurones were a promising template with modulatory properties on the ABCG2 (and to a lesser extent ABCB1) transport protein. There were well defined structural requirements for interaction with ABCG2 and analogs with potent modulatory properties that were equivalent or exceeded that of FTC were identified. At least one candidate (**1-26**) had the

potential for further advancement to preclinical evaluation as a non-toxic and potent dual modulator of ABCG2 and ABCB1 transport activity.

The present work has raised questions and issues that could be pursued in future investigations. First, more test compounds should be quantified with  $EC_{50}$  values to determine their inhibitory effects on the CAM efflux by ABCB1 over-expressing cell lines. In this way, a clearer picture on the structural requirements for interaction with ABCB1 versus ABCG2 would be available to guide future drug-design efforts, including the derivation of more reliable QSAR models. Second, investigations on ABCG2 modulatory properties as described in Chapter 5 were not carried out on all compounds on all assays because of the large number of compounds involved and the complexity of some of the assays. A focus on potent inhibitors of PhA efflux would be appropriate, and in this context, these compounds should be comprehensively investigated on all the assays. Notably, the mitoxantrone accumulation assay was omitted for most of the potent compounds and this should be rectified. Third, there was indirect evidence that the compounds were not substrates of ABCG2. Confirmation of their non-substrate status would require bi-directional transporter assays using Caco-2 or ABCG2 overexpressing polarized epithelial cell lines. Furthermore, it was not conclusively established if the compounds interacted with substrate or ATP binding sites (or both) on ABCG2. To show that these compounds specifically occupied the ATP binding site photoaffinity labeling experiments with [ $\alpha$ - $^{32}$ P] 8-azidoATP would be required. The 4<sup>th</sup> point pertains to the *in vivo* experiments carried out with **1-26**. Another route of administration (not intra-tumoral) should be explored although this would necessitate a more detailed understanding of the pharmacokinetic profiles of **1-26** alone and in combination with mitoxantrone. Lastly, to support the advancement of any of the promising compounds to preclinical studies, some understanding of the metabolic profiles of the potent compounds should be available. These studies could be carried out with human microsomes to

determine if there is activation or inhibition of the key metabolizing cytochrome P450 enzymes. In particular, there is limited information on the pathways involved in the metabolism of aurones.

## Bibliography

1. Pérez-Tomás, R., Multidrug resistance: retrospect and prospects in anti-cancer drug treatment. *Curr Med Chem* **2006**, *13* (16), 1859-1876.
2. Szakács, G.; Paterson, J.; Ludwig, J.; Booth-Genthe, C.; Gottesman, M., Targeting multidrug resistance in cancer. *Nat Rev Drug Discov* **2006**, *5* (3), 219-234.
3. Hyde, S.; Emsley, P.; Hartshorn, M.; Mimmack, M.; Gileadi, U.; Pearce, S.; Gallagher, M.; Gill, D.; Hubbard, R.; Higgins, C., Structural model of ATP-binding proteins associated with cystic fibrosis, multidrug resistance and bacterial transport. *Nature* **1990**, *346* (6282), 362-365.
4. Hegedus, C.; Szakacs, G.; Homolya, L.; Orban, T. I.; Telbisz, A.; Jani, M.; Sarkadi, B., Ins and outs of the ABCG2 multidrug transporter: an update on in vitro functional assays. *Adv Drug Deliv Rev* **2009**, *61* (1), 47-56.
5. Gottesman, M.; Fojo, T.; Bates, S., Multidrug resistance in cancer: role of ATP-dependent transporters. *Nat Rev Cancer* **2002**, *2* (1), 48-58.
6. Lee, C., Reversing agents for ATP-binding cassette drug transporters. *Methods Mol Biol* **2010**, *596*, 325-340.
7. Juliano, R.; Ling, V., A surface glycoprotein modulating drug permeability in Chinese hamster ovary cell mutants. *Biochim Biophys Acta* **1976**, *455* (1), 152-162.
8. Doyle, L.; Ross, D., Multidrug resistance mediated by the breast cancer resistance protein BCRP (ABCG2). *Oncogene* **2003**, *22* (47), 7340-7358.
9. Allikmets, R.; Schriml, L.; Hutchinson, A.; Romano-Spica, V.; Dean, M., A human placenta-specific ATP-binding cassette gene (ABCP) on chromosome 4q22 that is involved in multidrug resistance. *Cancer Res* **1998**, *58* (23), 5337-5339.
10. Doyle, L.; Yang, W.; Abruzzo, L.; Krogmann, T.; Gao, Y.; Rishi, A.; Ross, D., A multidrug resistance transporter from human MCF-7 breast cancer cells. *Proc Natl Acad Sci U S A* **1998**, *95* (26), 15665-15670.
11. Lee, J.; Scala, S.; Matsumoto, Y.; Dickstein, B.; Robey, R.; Zhan, Z.; Altenberg, G.; Bates, S., Reduced drug accumulation and multidrug resistance in human breast cancer cells without associated P-glycoprotein or MRP overexpression. *J Cell Biochem* **1997**, *65* (4), 513-526.
12. Calcagno, A.; Kim, I.; Wu, C.; Shukla, S.; Ambudkar, S., ABC drug transporters as molecular targets for the prevention of multidrug resistance and drug-drug interactions. *Curr Drug Deliv* **2007**, *4* (4), 324-333.
13. Krishnamurthy, P.; Schuetz, J., Role of ABCG2/BCRP in biology and medicine. *Annu Rev Pharmacol Toxicol* **2006**, *46*, 381-410.

14. Rosenberg, M.; Bikadi, Z.; Chan, J.; Liu, X.; Ni, Z.; Cai, X.; Ford, R.; Mao, Q., The human breast cancer resistance protein (BCRP/ABCG2) shows conformational changes with mitoxantrone. *Structure* **2010**, *18* (4), 482-493.
15. McDevitt, C.; Collins, R.; Conway, M.; Modok, S.; Storm, J.; Kerr, I.; Ford, R.; Callaghan, R., Purification and 3D structural analysis of oligomeric human multidrug transporter ABCG2. *Structure* **2006**, *14* (11), 1623-1632.
16. Xu, J.; Liu, Y.; Yang, Y.; Bates, S.; Zhang, J., Characterization of oligomeric human half-ABC transporter ATP-binding cassette G2. *J Biol Chem* **2004**, *279* (19), 19781-19789.
17. Aller, S.; Yu, J.; Ward, A.; Weng, Y.; Chittaboina, S.; Zhuo, R.; Harrell, P.; Trinh, Y.; Zhang, Q.; Urbatsch, I.; Chang, G., Structure of P-glycoprotein reveals a molecular basis for poly-specific drug binding. *Science* **2009**, *323* (5922), 1718-1722.
18. Eckford, P.; Sharom, F., ABC efflux pump-based resistance to chemotherapy drugs. *Chem Rev* **2009**, *109* (7), 2989-3011.
19. Kerns, E. H.; Di, L., *Drug-like properties : concepts, structure design and methods : from ADME to toxicity optimization*. Academic Press: Amsterdam; Boston, 2008; p 103-121.
20. Trock, B.; Leonessa, F.; Clarke, R., Multidrug resistance in breast cancer: a meta-analysis of MDR1/gp170 expression and its possible functional significance. *J Natl Cancer Inst* **1997**, *89* (13), 917-931.
21. Abolhoda, A.; Wilson, A.; Ross, H.; Danenberg, P.; Burt, M.; Scotto, K., Rapid activation of MDR1 gene expression in human metastatic sarcoma after in vivo exposure to doxorubicin. *Clin Cancer Res* **1999**, *5* (11), 3352-3356.
22. Szakács, G.; Jakab, K.; Antal, F.; Sarkadi, B., Diagnostics of multidrug resistance in cancer. *Pathol Oncol Res* **1998**, *4* (4), 251-257.
23. Pallis, M.; Das-Gupta, E., Flow cytometric measurement of functional and phenotypic P-glycoprotein. *Methods Mol Med* **2005**, *111*, 167-181.
24. Karászi, E.; Jakab, K.; Homolya, L.; Szakács, G.; Holló, Z.; Telek, B.; Kiss, A.; Rejtő, L.; Nahajevszky, S.; Sarkadi, B.; Kappelmayer, J., Calcein assay for multidrug resistance reliably predicts therapy response and survival rate in acute myeloid leukaemia. *Br J Haematol* **2001**, *112* (2), 308-314.
25. Robey, R. W.; Polgar, O.; Deeken, J.; To, K. W.; Bates, S. E., ABCG2: determining its relevance in clinical drug resistance. *Cancer Metastasis Rev* **2007**, *26* (1), 39-57.
26. Diestra, J.; Scheffer, G.; Català, I.; Maliapaard, M.; Schellens, J.; Scheper, R.; Germà-Lluch, J.; Izquierdo, M., Frequent expression of the multi-drug resistance-associated protein BCRP/MXR/ABCP/ABCG2 in human tumours detected by the



BXP-21 monoclonal antibody in paraffin-embedded material. *J Pathol* **2002**, *198* (2), 213-219.

27. Jonker, J.; Freeman, J.; Bolscher, E.; Musters, S.; Alvi, A.; Titley, I.; Schinkel, A.; Dale, T., Contribution of the ABC transporters Bcrp1 and Mdr1a/1b to the side population phenotype in mammary gland and bone marrow of mice. *Stem Cells* **2005**, *23* (8), 1059-1065.

28. Sung, J.; Cho, H.; Yi, H.; Lee, C.; Kim, H.; Kim, D.; Abd El-Aty, A.; Kim, J.; Landowski, C.; Hediger, M.; Shin, H., Characterization of a stem cell population in lung cancer A549 cells. *Biochem Biophys Res Commun* **2008**, *371* (1), 163-167.

29. Hirschmann-Jax, C.; Foster, A.; Wulf, G.; Nuchtern, J.; Jax, T.; Gobel, U.; Goodell, M.; Brenner, M., A distinct "side population" of cells with high drug efflux capacity in human tumor cells. *Proc Natl Acad Sci U S A* **2004**, *101* (39), 14228-14233.

30. Haraguchi, N.; Utsunomiya, T.; Inoue, H.; Tanaka, F.; Mimori, K.; Barnard, G.; Mori, M., Characterization of a side population of cancer cells from human gastrointestinal system. *Stem Cells* **2006**, *24* (3), 506-513.

31. Yin, J.; Beuscher, A. t.; Andryski, S.; Stevens, R.; Schultz, P., Structural plasticity and the evolution of antibody affinity and specificity. *J Mol Biol* **2003**, *330* (4), 651-656.

32. Arkin, M.; Randal, M.; DeLano, W.; Hyde, J.; Luong, T.; Oslob, J.; Raphael, D.; Taylor, L.; Wang, J.; McDowell, R.; Wells, J.; Braisted, A., Binding of small molecules to an adaptive protein-protein interface. *Proc Natl Acad Sci U S A* **2003**, *100* (4), 1603-1608.

33. Sethi, D.; Agarwal, A.; Manivel, V.; Rao, K.; Salunke, D., Differential epitope positioning within the germline antibody paratope enhances promiscuity in the primary immune response. *Immunity* **2006**, *24* (4), 429-438.

34. Pedersen, J.; Matsson, P.; Bergström, C.; Norinder, U.; Hoogstraate, J.; Artursson, P., Prediction and identification of drug interactions with the human ATP-binding cassette transporter multidrug-resistance associated protein 2 (MRP2; ABCC2). *J Med Chem* **2008**, *51* (11), 3275-3287.

35. Seelig, A., A general pattern for substrate recognition by P-glycoprotein. *Eur J Biochem* **1998**, *251* (1-2), 252-261.

36. Didziapetris, R.; Japertas, P.; Avdeef, A.; Petrauskas, A., Classification analysis of P-glycoprotein substrate specificity. *J Drug Target* **2003**, *11* (7), 391-406.

37. Cianchetta, G.; Singleton, R.; Zhang, M.; Wildgoose, M.; Giesing, D.; Fravolini, A.; Cruciani, G.; Vaz, R., A pharmacophore hypothesis for P-glycoprotein substrate recognition using GRIND-based 3D-QSAR. *J Med Chem* **2005**, *48* (8), 2927-2935.

38. Raub, T., P-glycoprotein recognition of substrates and circumvention through rational drug design. *Mol Pharm* **2006**, *3* (1), 3-25.
39. Demel, M. A., Comparison of Contemporary Feature Selection Algorithms: Application to the Classification of ABC-Transporter Substrates. *QSAR Comb. Sci.* **2009**, *28* (10), 1087-1091.
40. Pick, A.; Müller, H.; Wiese, M., Structure-activity relationships of new inhibitors of breast cancer resistance protein (ABCG2). *Bioorg Med Chem* **2008**, *16* (17), 8224-8236.
41. Nicolle, E.; Boumendjel, A.; Macalou, S.; Genoux, E.; Ahmed-Belkacem, A.; Carrupt, P. A.; Di Pietro, A., QSAR analysis and molecular modeling of ABCG2-specific inhibitors. *Adv Drug Deliv Rev* **2009**, *61* (1), 34-46.
42. Di, L.; Kerns, E.; Carter, G., Drug-like property concepts in pharmaceutical design. *Curr Pharm Des* **2009**, *15* (19), 2184-2194.
43. Robey, R.; To, K.; Polgar, O.; Dohse, M.; Fetsch, P.; Dean, M.; Bates, S., ABCG2: a perspective. *Adv Drug Deliv Rev* **2009**, *61* (1), 3-13.
44. Lemos, C.; Jansen, G.; Peters, G., Drug transporters: recent advances concerning BCRP and tyrosine kinase inhibitors. *Br J Cancer* **2008**, *98* (5), 857-862.
45. Türk, D.; Szakács, G., Relevance of multidrug resistance in the age of targeted therapy. *Curr Opin Drug Discov Devel* **2009**, *12* (2), 246-252.
46. Shukla, S.; Robey, R. W.; Bates, S. E.; Ambudkar, S. V., Sunitinib (Sutent, SU11248), a small-molecule receptor tyrosine kinase inhibitor, blocks function of the ATP-binding cassette (ABC) transporters P-glycoprotein (ABCB1) and ABCG2. *Drug Metab Dispos* **2009**, *37* (2), 359-365.
47. Elkind, N.; Szentpétery, Z.; Apáti, A.; Ozvegy-Laczka, C.; Várady, G.; Ujhelly, O.; Szabó, K.; Homolya, L.; Váradi, A.; Buday, L.; Kéri, G.; Német, K.; Sarkadi, B., Multidrug transporter ABCG2 prevents tumor cell death induced by the epidermal growth factor receptor inhibitor Iressa (ZD1839, Gefitinib). *Cancer Res* **2005**, *65* (5), 1770-1777.
48. Honjo, Y.; Hrycyna, C.; Yan, Q.; Medina-Pérez, W.; Robey, R.; van de Laar, A.; Litman, T.; Dean, M.; Bates, S., Acquired mutations in the MXR/BCRP/ABCP gene alter substrate specificity in MXR/BCRP/ABCP-overexpressing cells. *Cancer Res* **2001**, *61* (18), 6635-6639.
49. Ozvegy, C.; Váradi, A.; Sarkadi, B., Characterization of drug transport, ATP hydrolysis, and nucleotide trapping by the human ABCG2 multidrug transporter. Modulation of substrate specificity by a point mutation. *J Biol Chem* **2002**, *277* (50), 47980-47990.

50. Ozvegy-Laczka, C.; Köblös, G.; Sarkadi, B.; Váradi, A., Single amino acid (482) variants of the ABCG2 multidrug transporter: major differences in transport capacity and substrate recognition. *Biochim Biophys Acta* **2005**, *1668* (1), 53-63.
51. Takada, T.; Suzuki, H.; Sugiyama, Y., Characterization of polarized expression of point- or deletion-mutated human BCRP/ABCG2 in LLC-PK1 cells. *Pharm Res* **2005**, *22* (3), 458-464.
52. Ejendal, K.; Diop, N.; Schweiger, L.; Hrycyna, C., The nature of amino acid 482 of human ABCG2 affects substrate transport and ATP hydrolysis but not substrate binding. *Protein Sci* **2006**, *15* (7), 1597-1607.
53. Pozza, A.; Perez-Victoria, J.; Sardo, A.; Ahmed-Belkacem, A.; Di Pietro, A., Purification of breast cancer resistance protein ABCG2 and role of arginine-482. *Cell Mol Life Sci* **2006**, *63* (16), 1912-1922.
54. Hadjeri, M.; Barbier, M.; Ronot, X.; Mariotte, A.; Boumendjel, A.; Boutonnat, J., Modulation of P-glycoprotein-mediated multidrug resistance by flavonoid derivatives and analogues. *J Med Chem* **2003**, *46* (11), 2125-2131.
55. Shukla, S.; Wu, C.; Ambudkar, S., Development of inhibitors of ATP-binding cassette drug transporters: present status and challenges. *Expert Opin Drug Metab Toxicol* **2008**, *4* (2), 205-223.
56. Ruff, P.; Vorobiof, D.; Jordaan, J.; Demetriou, G.; Moodley, S.; Nosworthy, A.; Werner, I.; Raats, J.; Burgess, L., A randomized, placebo-controlled, double-blind phase 2 study of docetaxel compared to docetaxel plus zosuquidar (LY335979) in women with metastatic or locally recurrent breast cancer who have received one prior chemotherapy regimen. *Cancer Chemother Pharmacol* **2009**, *64* (4), 763-768.
57. Kühnle, M.; Egger, M.; Müller, C.; Mahringer, A.; Bernhardt, G.; Fricker, G.; König, B.; Buschauer, A., Potent and selective inhibitors of breast cancer resistance protein (ABCG2) derived from the p-glycoprotein (ABCB1) modulator tariquidar. *J Med Chem* **2009**, *52* (4), 1190-1197.
58. Cramer, J.; Kopp, S.; Bates, S.; Chiba, P.; Ecker, G., Multispecificity of Drug Transporters: Probing Inhibitor Selectivity for the Human Drug Efflux Transporters ABCB1 and ABCG2. *ChemMedChem* **2007**, *2* (12), 1783-1788.
59. Jekerle, V.; Klinkhammer, W.; Scollard, D.; Breitbach, K.; Reilly, R.; Piquette-Miller, M.; Wiese, M., In vitro and in vivo evaluation of WK-X-34, a novel inhibitor of P-glycoprotein and BCRP, using radio imaging techniques. *Int J Cancer* **2006**, *119* (2), 414-422.
60. Wang, R.; Kuo, C.; Lien, L.; Lien, E., Structure-activity relationship: analyses of p-glycoprotein substrates and inhibitors. *J Clin Pharm Ther* **2003**, *28* (3), 203-228.
61. van Loevezijn, A.; Allen, J.; Schinkel, A.; Koomen, G., Inhibition of BCRP-mediated drug efflux by fumitremorgin-type indolyl diketopiperazines. *Bioorg Med Chem Lett* **2001**, *11* (1), 29-32.

62. Brooks, T.; Kennedy, D.; Gruol, D.; Ojima, I.; Baer, M.; Bernacki, R., Structure-activity analysis of taxane-based broad-spectrum multidrug resistance modulators. *Anticancer Res* **2004**, *24* (2A), 409-415.
63. Sugimoto, Y.; Tsukahara, S.; Imai, Y.; Ueda, K.; Tsuruo, T., Reversal of breast cancer resistance protein-mediated drug resistance by estrogen antagonists and agonists. *Mol Cancer Ther* **2003**, *2* (1), 105-112.
64. Zhang, S.; Yang, X.; Coburn, R.; Morris, M., Structure activity relationships and quantitative structure activity relationships for the flavonoid-mediated inhibition of breast cancer resistance protein. *Biochem Pharmacol* **2005**, *70* (4), 627-639.
65. Ahmed-Belkacem, A.; Pozza, A.; Muñoz-Martínez, F.; Bates, S.; Castanys, S.; Gamarro, F.; Di Pietro, A.; Pérez-Victoria, J., Flavonoid structure-activity studies identify 6-prenylchrysin and tectochrysin as potent and specific inhibitors of breast cancer resistance protein ABCG2. *Cancer Res* **2005**, *65* (11), 4852-4860.
66. Katayama, K.; Masuyama, K.; Yoshioka, S.; Hasegawa, H.; Mitsuhashi, J.; Sugimoto, Y., Flavonoids inhibit breast cancer resistance protein-mediated drug resistance: transporter specificity and structure-activity relationship. *Cancer Chemother Pharmacol* **2007**, *60* (6), 789-797.
67. Imai, Y.; Tsukahara, S.; Asada, S.; Sugimoto, Y., Phytoestrogens/flavonoids reverse breast cancer resistance protein/ABCG2-mediated multidrug resistance. *Cancer Res* **2004**, *64* (12), 4346-4352.
68. Ahmed-Belkacem, A.; Macalou, S.; Borrelli, F.; Capasso, R.; Fattorusso, E.; Tagliatalata-Scafati, O.; Di Pietro, A., Nonprenylated rotenoids, a new class of potent breast cancer resistance protein inhibitors. *J Med Chem* **2007**, *50* (8), 1933-1938.
69. Gandhi, Y.; Morris, M., Structure-activity relationships and quantitative structure-activity relationships for breast cancer resistance protein (ABCG2). *AAPS J* **2009**, *11* (3), 541-552.
70. Matsson, P.; Englund, G.; Ahlin, G.; Bergström, C.; Norinder, U.; Artursson, P., A global drug inhibition pattern for the human ATP-binding cassette transporter breast cancer resistance protein (ABCG2). *J Pharmacol Exp Ther* **2007**, *323* (1), 19-30.
71. Lee, C.; Chew, E.; Go, M., Functionalized auroenes as inducers of NAD(P)H:quinone oxidoreductase 1 that activate AhR/XRE and Nrf2/ARE signaling pathways: synthesis, evaluation and SAR. *Eur J Med Chem* **2010**, *45* (7), 2957-2971.
72. Li, N.; Liu, J.; Zhang, J.; Yu, B., Comparative evaluation of cytotoxicity and antioxidative activity of 20 flavonoids. *J Agric Food Chem* **2008**, *56* (10), 3876-3883.
73. Conseil, G.; Baubichon-Cortay, H.; Dayan, G.; Jault, J.; Barron, D.; Di Pietro, A., Flavonoids: a class of modulators with bifunctional interactions at vicinal ATP- and steroid-binding sites on mouse P-glycoprotein. *Proc Natl Acad Sci U S A* **1998**, *95* (17), 9831-9836.

74. Di Pietro, A.; Godinot, C.; Bouillant, M.; Gautheron, D., Pig heart mitochondrial ATPase: properties of purified and membrane-bound enzyme. Effects of flavonoids. *Biochimie* **1975**, *57* (8), 959-967.
75. Hirano, T.; Oka, K.; Akiba, M., Effects of synthetic and naturally occurring flavonoids on Na<sup>+</sup>,K<sup>+</sup>-ATPase: aspects of the structure-activity relationship and action mechanism. *Life Sci* **1989**, *45* (12), 1111-1117.
76. Thiagarajah, P.; Kuttan, S.; Lim, S.; Teo, T.; Das, N., Effect of myricetin and other flavonoids on the liver plasma membrane Ca<sup>2+</sup> pump. Kinetics and structure-function relationships. *Biochem Pharmacol* **1991**, *41* (5), 669-675.
77. Hagiwara, M.; Inoue, S.; Tanaka, T.; Nunoki, K.; Ito, M.; Hidaka, H., Differential effects of flavonoids as inhibitors of tyrosine protein kinases and serine/threonine protein kinases. *Biochem Pharmacol* **1988**, *37* (15), 2987-2992.
78. Akiyama, T.; Ishida, J.; Nakagawa, S.; Ogawara, H.; Watanabe, S.; Itoh, N.; Shibuya, M.; Fukami, Y., Genistein, a specific inhibitor of tyrosine-specific protein kinases. *J Biol Chem* **1987**, *262* (12), 5592-5595.
79. Litman, T.; Druley, T.; Stein, W.; Bates, S., From MDR to MXR: new understanding of multidrug resistance systems, their properties and clinical significance. *Cell Mol Life Sci* **2001**, *58* (7), 931-959.
80. Shapiro, A.; Ling, V., Positively cooperative sites for drug transport by P-glycoprotein with distinct drug specificities. *Eur J Biochem* **1997**, *250* (1), 130-137.
81. Mitsunaga, Y.; Takanaga, H.; Matsuo, H.; Naito, M.; Tsuruo, T.; Ohtani, H.; Sawada, Y., Effect of bioflavonoids on vincristine transport across blood-brain barrier. *Eur J Pharmacol* **2000**, *395* (3), 193-201.
82. Boumendjel, A.; Di Pietro, A.; Dumontet, C.; Barron, D., Recent advances in the discovery of flavonoids and analogs with high-affinity binding to P-glycoprotein responsible for cancer cell multidrug resistance. *Med Res Rev* **2002**, *22* (5), 512-529.
83. Alvarez, A.; Real, R.; Pérez, M.; Mendoza, G.; Prieto, J.; Merino, G., Modulation of the activity of ABC transporters (P-glycoprotein, MRP2, BCRP) by flavonoids and drug response. *J Pharm Sci* **2010**, *99* (2), 598-617.
84. Boumendjel, A.; Bois, F.; Beney, C.; Mariotte, A.; Conseil, G.; Di Pietro, A., B-ring substituted 5,7-dihydroxyflavonols with high-affinity binding to P-glycoprotein responsible for cell multidrug resistance. *Bioorg Med Chem Lett* **2001**, *11* (1), 75-77.
85. Chan, K.; Zhao, Y.; Chow, T.; Yan, C.; Ma, D.; Burkett, B.; Wong, I.; Chow, L.; Chan, T., Flavonoid dimers as bivalent modulators for p-glycoprotein-based multidrug resistance: structure-activity relationships. *ChemMedChem* **2009**, *4* (4), 594-614.

86. Zhang, S.; Yang, X.; Morris, M., Combined effects of multiple flavonoids on breast cancer resistance protein (ABCG2)-mediated transport. *Pharm Res* **2004**, *21* (7), 1263-1273.
87. Boumendjel, A., Aurones: a subclass of flavones with promising biological potential. *Curr Med Chem* **2003**, *10* (23), 2621-2630.
88. Lawrence, N. J.; Rennison, D.; McGown, A. T.; Hadfield, J. A., The Total Synthesis of an Aurone Isolated from *Uvaria hamiltonii*: Aurones and Flavones as Anticancer Agents. *Bioorg Med Chem Lett* **2003**, *13*, 3759-3763.
89. Boumendjel, A.; Beney, C.; Deka, N.; Mariotte, A.; Lawson, M.; Trompier, D.; Baubichon-Cortay, H.; Di Pietro, A., 4-Hydroxy-6-methoxyaurones with high-affinity binding to cytosolic domain of P-glycoprotein. *Chem Pharm Bull (Tokyo)* **2002**, *50* (6), 854-856.
90. Václavíková, R.; Boumendjel, A.; Ehrlichová, M.; Kovár, J.; Gut, I., Modulation of paclitaxel transport by flavonoid derivatives in human breast cancer cells. Is there a correlation between binding affinity to NBD of P-gp and modulation of transport? *Bioorg Med Chem* **2006**, *14* (13), 4519-4525.
91. Han, Y.; Riwanto, M.; Go, M.; Ee, P., Modulation of breast cancer resistance protein (BCRP/ABCG2) by non-basic chalcone analogues. *Eur J Pharm Sci* **2008**, *35* (1-2), 30-41.
92. Schoepfer, J.; Fretz, H.; Chaudhuri, B.; Muller, L.; Seeber, E.; Meijer, L.; Lozach, O.; Vangrevelinghe, E.; Furet, P., Structure-based design and synthesis of 2-benzylidene-benzofuran-3-ones as flavopiridol mimics. *J Med Chem* **2002**, *45* (9), 1741-1747.
93. Polgar, O.; Bates, S., ABC transporters in the balance: is there a role in multidrug resistance? *Biochem Soc Trans* **2005**, *33* (1), 241-245.
94. Zhang, W.; Go, M., Functionalized 3-benzylidene-indolin-2-ones: inducers of NAD(P)H-quinone oxidoreductase 1 (NQO1) with antiproliferative activity. *Bioorg Med Chem* **2009**, *17* (5), 2077-2090.
95. Liu, M.; Wilairat, P.; Croft, S.; Tan, A.; Go, M., Structure-activity relationships of antileishmanial and antimalarial chalcones. *Bioorg Med Chem* **2003**, *11* (13), 2729-2738.
96. Wildman, S. A.; Crippen, G. M., Prediction of Physicochemical Parameters by Atomic Contributions. *J. Chem. Inf. Comput. Sci* **1999**, *39*, 868-873.
97. Craig, N. P., Interdependence between Physical Parameters and Selection of Substituent Groups for Correlation Studies. *J Med Chem* **1971**, *14* (8), 680-684.
98. Lawrence, N.; McGown, A., The chemistry and biology of antimetabolic chalcones and related enone systems. *Curr Pharm Des* **2005**, *11* (13), 1679-1693.

99. Ducki, S.; Forrest, R.; Hadfield, J.; Kendall, A.; Lawrence, N.; McGown, A.; Rennison, D., Potent antimitotic and cell growth inhibitory properties of substituted chalcones. *Bioorg Med Chem Lett* **1998**, *8* (9), 1051-1056.
100. Zhang, S.; Yang, X.; Morris, M., Flavonoids are inhibitors of breast cancer resistance protein (ABCG2)-mediated transport. *Mol Pharmacol* **2004**, *65* (5), 1208-1216.
101. Beney, C.; Mariotte, A.-M.; Boumendjel, A., An Efficient Synthesis of 4,6-Dimethoxyaurones. *Heterocycles* **2001**, *55* (5), 967-972.
102. Varma, R. S.; Varma, M., Alumina-Mediated Condensation - a Simple Synthesis of Aurones. *Tetrahedron Letters* **1992**, *33* (40), 5937-5940.
103. Bauta, W.; Lovett, D.; Cantrell, W. J.; Burke, B., Formal synthesis of angiogenesis inhibitor NM-3. *J Org Chem* **2003**, *68*(15), 5967-5973.
104. Gupta, G. P.; Perk, J.; Acharyya, S.; de Candia, P.; Mittal, V.; Todorova-Manova, K.; Gerald, W. L.; Brogi, E.; Benezra, R.; Massague, J., ID genes mediate tumor reinitiation during breast cancer lung metastasis. *Proc Natl Acad Sci U S A* **2007**, *104* (49), 19506-19511.
105. Lawson, M. A.; Mariotte, A.-M.; Boumendjel, A., A short method for the synthesis of 4, 6-dimethoxy-1-azaurones. *Heterocyclic Communications* **2003**, *9* (2), 149-152.
106. Tsutomu, S.; Makoto, A.; Kazuyuki, S.; Akiko, K., Aminohaloborane in Organic Synthesis. 2. Simple Synthesis of Indoles and 1-Acyl-3-indolinones Using Specific Ortho alpha-chloroacetylation of anilines. *J. Org. Chem* **1979**, *44* (4), 578-586.
107. Smith, M. B.; March, J., *March's Advanced Organic Chemistry: Reactions, Mechanisms, and Structure*. Sixth Edition ed.; John Wiley & Sons, Inc: New Jersey, 2007; p 409-410.
108. Dao, T.; Chi, Y.; Kim, J.; Kim, H.; Kim, S.; Park, H., Synthesis and PGE2 inhibitory activity of 5,7-dihydroxyflavones and their O-methylated flavone analogs. *Arch Pharm Res* **2003**, *26* (5), 345-350.
109. Clayden, J.; Greeves, N.; Warren, S.; Wothers, P., *Organic Chemistry*. Oxford University Press: 2006; p 806-808.
110. Mphahlele, M., Molecular iodine-mediated cyclization of tethered heteroatom-containing alkenyl or alkynyl systems. *Molecules* **2009**, *14* (12), 4814-4837.
111. Miyake, H.; Takizawa, E.; Sasaki, M., Syntheses of Flavones via the Iodine-Mediated Oxidative Cyclization of 1,3-Diphenylprop-2-en-1-ones. *Bull. Chem. Soc. Jpn* **2003**, *76*, 835-836.

112. Ur-Rahman, A.; Choudhary, M. I.; Hayat, S.; Kahn, A. M.; Ahmed, A., Two New Aurones from Marine Brown Alga *Spatoglossum variabile*. *Chem Pharm Bull* **2001**, *49*.
113. Thakkar, K.; Cushman, M., A Novel Oxidative Cyclization of 2'-Hydroxychalcones to 4,5-Dialkoxyaurones by Thallium(III) Nitrate. *J Org Chem* **1995**, *60*, 6499-6510.
114. Brady, B. A.; Kennedy, J. A.; O'Sullivan, W. I., The Configuration of Aurones. *Tetrahedron* **1973**, *29*, 359-362.
115. Kemp, W., *Organic Spectroscopy*. Third Edition ed.; Macmillan: Basingstoke, 1991; p 99-101.
116. Pelter, A.; Ward, R. S.; Heller, H. G., Carbon-13 nuclear magnetic resonance spectra of (Z)- and (E)-aurones. *J. Chem. Soc., Perkin Trans. I* **1979**, *2*, 328-329.
117. Kevill, D. N., cis-trans Isomerism of Exocyclic alpha, beta-Unsaturated Indanones and Tetralones. *J Org Chem* **1964**, *29*, 1276-1278.
118. Perjési, P.; Nusser, T.; Tarczay, G.; Sohár, P., E-2-Benzylidenebenzocycloalkanones. Stereostructure and NMR spectroscopic investigation. *J Mol Struct*, **1999**, *479*, 13-19.
119. Ernest, I.; ilek, J. O.; Vejdelek, Z. J.; Protiva, M., Synthetic experiments in the group of hypotensive alkaloids. XXVI. Some new (-)-methyl reserpate esters. *Collect. Czech. Chem. Commun.* **1963**, *28*, 1022-1030.
120. Bolek, D.; Gütschow, M., Preparation of 4,6,3',4'-Tetrasubstituted Aurones via Aluminium Oxide-Catalyzed Condensation. *J. Heterocyclic Chem* **2005**, *42*, 1399-1403.
121. Morimoto, M.; Fukumoto, H.; Nozoe, T.; Hagiwara, A.; Komai, K., Synthesis and insect antifeedant activity of aurones against *Spodoptera litura* larvae. *J Agric Food Chem* **2007**, *55* (3), 700-705.
122. Shrinere, R. L.; Matson, E. J.; Damschroder, R. E., Derivatives of Coumaran. IV. The Structure of Tectorigenin. *J Am Chem Soc* **1939**, *61*, 2322-2327.
123. Wallez, V.; Durieux-Poissonnier, S.; Chavatte, P.; Boutin, J.; Audinot, V.; Nicolas, J.; Bennejean, C.; Delagrangé, P.; Renard, P.; Lesieur, D., Synthesis and structure-affinity-activity relationships of novel benzofuran derivatives as MT(2) melatonin receptor selective ligands. *J Med Chem* **2002**, *45* (13), 2788-2800.
124. Salway, A. H., Action of Sodium Amalgam on Methylene Ethers. *J Chem Soc* **1910**, *97*, 2413-2418.
125. Gerby, B.; Boumendjel, A.; Blanc, M.; Bringuier, P. P.; Champelovier, P.; Fortune, A.; Ronot, X.; Boutonnat, J., 2-Arylidenedihydroindole-3-ones: design,



synthesis, and biological activity on bladder carcinoma cell lines. *Bioorg Med Chem Lett* **2007**, *17* (1), 208-213.

126. Henrich, C.; Robey, R.; Bokesch, H.; Bates, S.; Shukla, S.; Ambudkar, S.; Dean, M.; McMahon, J., New inhibitors of ABCG2 identified by high-throughput screening. *Mol Cancer Ther* **2007**, *6* (121), 3271-3278.

127. Liu, X.; Tee, H.; Go, M., Functionalized chalcones as selective inhibitors of P-glycoprotein and breast cancer resistance protein. *Bioorg Med Chem* **2008**, *16* (1), 171-180.

128. Hegedus, C.; Szakács, G.; Homolya, L.; Orbán, T.; Telbisz, A.; Jani, M.; Sarkadi, B., Ins and outs of the ABCG2 multidrug transporter: an update on in vitro functional assays. *Adv Drug Deliv Rev* **2009**, *61* (1), 47-56.

129. Liminga, G.; Nygren, P.; Larsson, R., Microfluorometric evaluation of calcein acetoxymethyl ester as a probe for P-glycoprotein-mediated resistance: effects of cyclosporin A and its nonimmunosuppressive analogue SDZ PSC 833. *Exp Cell Res* **1994**, *212* (2), 291-296.

130. Lee, C. Y. Investigations on aurones as chemopreventive agents. National University of Singapore, Singapore, 2009.

131. Burger, A., *Burger's medicinal chemistry and drug discovery*. Sixth Edition ed.; Wiley: Hoboken, N.J., 2003; Vol. 1, p 521.

132. Wermuth, C. G.; Ganellin, C. R.; Lindberg, P.; Mitscher, L. A., IUPAC Recommendations on Nomenclature and Symbols and Technical reports from Commissions - Chemistry and Human Health Glossary of terms used in medicinal Division, Medicinal Chemistry chemistry (IUPAC Recommendations 1998) Section. *Pure & Appl. Chem.* **1998**, *70*, 1129-1143.

133. Henrich, C.; Bokesch, H.; Dean, M.; Bates, S.; Robey, R.; Goncharova, E.; Wilson, J.; McMahon, J., A high-throughput cell-based assay for inhibitors of ABCG2 activity. *J Biomol Screen* **2006**, *11* (2), 176-183.

134. Boumendjel, A.; Macalou, S.; Ahmed-Belkacem, A.; Blanc, M.; Di Pietro, A., Acridone derivatives: design, synthesis, and inhibition of breast cancer resistance protein ABCG2. *Bioorg Med Chem* **2007**, *15* (8), 2892-2897.

135. Robey, R.; Steadman, K.; Polgar, O.; Morisaki, K.; Blayney, M.; Mistry, P.; Bates, S., Pheophorbide a is a specific probe for ABCG2 function and inhibition. *Cancer Res* **2004**, *64* (4), 1242-1226.

136. Ozvegy, C.; Litman, T.; Szakács, G.; Nagy, Z.; Bates, S.; Váradi, A.; Sarkadi, B., Functional characterization of the human multidrug transporter, ABCG2, expressed in insect cells. *Biochem Biophys Res Commun* **2001**, *285* (1), 111-117.

137. Patrick, G. L. *An introduction to medicinal chemistry*, Fourth Edition; Oxford University Press: Oxford; New York, 2009; p 390-391.

138. Provost, F.; Fawcett, T.; Kohavi, R. In *The Case Against Accuracy Estimation for Comparing Induction Algorithms.*, Proceedings of the 15th International Conference on Machine Learning . Morgan Kaufmann Publishers Inc: 1998; pp 445-553.
139. Kubinyi, H.; Folkers, G.; Martin, Y. C., *3D QSAR in drug design*. Kluwer Academic: Boston, Mass, 1998; p 117-136.
140. Ecker, G.; Stockner, T.; Chiba, P., Computational models for prediction of interactions with ABC-transporters. *Drug Discov Today* **2008**, *13* (7-8), 311-317.
141. Ejendal, K.; Hrycyna, C., Differential sensitivities of the human ATP-binding cassette transporters ABCG2 and P-glycoprotein to cyclosporin A. *Mol Pharmacol* **2005**, *67* (3), 902-911.
142. Giri, N.; Agarwal, S.; Shaik, N.; Pan, G.; Chen, Y.; Elmquist, W., Substrate-dependent breast cancer resistance protein (Bcrp1/Abcg2)-mediated interactions: consideration of multiple binding sites in in vitro assay design. *Drug Metab Dispos* **2009**, *37* (3), 560-570.
143. Minderman, H.; Suvannasankha, A.; O'Loughlin, K.; Scheffer, G.; Scheper, R.; Robey, R.; Baer, M., Flow cytometric analysis of breast cancer resistance protein expression and function. *Cytometry* **2002**, *48* (2), 59-65.
144. Wu, C.; Shukla, S.; Calcagno, A.; Hall, M.; Gottesman, M.; Ambudkar, S., Evidence for dual mode of action of a thiosemicarbazone, NSC73306: a potent substrate of the multidrug resistance linked ABCG2 transporter. *Mol Cancer Ther* **2007**, *6* (12 Pt 1), 3287-3296.
145. Shukla, S.; Robey, R.; Bates, S.; Ambudkar, S., Sunitinib (Sutent, SU11248), a small-molecule receptor tyrosine kinase inhibitor, blocks function of the ATP-binding cassette (ABC) transporters P-glycoprotein (ABCB1) and ABCG2. *Drug Metab Dispos* **2009**, *37* (2), 359-365.
146. Henrich, C.; Robey, R.; Takada, K.; Bokesch, H.; Bates, S.; Shukla, S.; Ambudkar, S.; McMahon, J.; Gustafson, K., Botryllamides: natural product inhibitors of ABCG2. *ACS Chem Biol* **2009**, *4* (8), 637-647.
147. Shukla, S.; Robey, R.; Bates, S.; Ambudkar, S., The calcium channel blockers, 1,4-dihydropyridines, are substrates of the multidrug resistance-linked ABC drug transporter, ABCG2. *Biochemistry* **2006**, *45* (29), 8940-8951.
148. Glavinas, H.; Krajcsi, P.; Cserepes, J.; Sarkadi, B., The role of ABC transporters in drug resistance, metabolism and toxicity. *Curr Drug Deliv* **2004**, *1* (1), 27-42.
149. Chearwae, W.; Shukla, S.; Limtrakul, P.; Ambudkar, S., Modulation of the function of the multidrug resistance-linked ATP-binding cassette transporter ABCG2 by the cancer chemopreventive agent curcumin. *Mol Cancer Ther* **2006**, *5* (8), 1995-2006.

150. Cooray, H.; Janvilisri, T.; van Veen, H.; Hladky, S.; Barrand, M., Interaction of the breast cancer resistance protein with plant polyphenols. *Biochem Biophys Res Commun* **2004**, *317* (1), 269-275.
151. Giacomini, K.; Huang, S.; Tweedie, D.; Benet, L.; Brouwer, K.; Chu, X.; Dahlin, A.; Evers, R.; Fischer, V.; Hillgren, K.; Hoffmaster, K.; Ishikawa, T.; Keppler, D.; Kim, R.; Lee, C.; Niemi, M.; Polli, J.; Sugiyama, Y.; Swaan, P.; Ware, J.; Wright, S.; Yee, S.; Zamek-Gliszczynski, M.; Zhang, L.; Consortium, I. T., Membrane transporters in drug development. *Nat Rev Drug Discov* **2010**, *9* (3), 215-236.
152. Dai, C.; Liang, Y.; Chen, L.; Zhang, X.; Deng, W.; Su, X.; Shi, Z.; Wu, C.; Ashby, C. J.; Akiyama, S.; Ambudkar, S.; Chen, Z.; Fu, L., Sensitization of ABCB1 overexpressing cells to chemotherapeutic agents by FG020326 via binding to ABCB1 and inhibiting its function. *Biochem Pharmacol* **2009**, *78* (4), 355-364.
153. Chen, L.; Liang, Y.; Zhang, X.; Su, X.; Dai, C.; Wang, F.; Yan, Y.; Tao, L.; Fu, L., Reversal of P-gp-mediated multidrug resistance by Bromotetrandrine in vivo is associated with enhanced accumulation of chemotherapeutic drug in tumor tissue. *Anticancer Res* **2009**, *29* (11), 4597-4604.
154. Shukla, S.; Zaher, H.; Hartz, A.; Bauer, B.; Ware, J. A.; Ambudkar, S. V., Curcumin inhibits the activity of ABCG2/BCRP1, a multidrug resistance-linked ABC drug transporter in mice. *Pharm Res* **2009**, *26* (2), 480-487.
155. Chan, Y., Biostatistics 203. Survival analysis. *Singapore Med J* **2004**, *45* (6), 249-256.
156. Price, J.; Polyzos, A.; Zhang, R.; Daniels, L., Tumorigenicity and metastasis of human breast carcinoma cell lines in nude mice. *Cancer Res* **1990**, *50* (3), 717-721.
157. Clarke, R., Issues in experimental design and endpoint analysis in the study of experimental cytotoxic agents in vivo in breast cancer and other models. *Breast Cancer Res Treat* **1997**, *46* (2-3), 255-278.
158. Almond, B.; Hadba, A.; Freeman, S.; Cuevas, B.; York, A.; Detrisac, C.; Goldberg, E., Efficacy of mitoxantrone-loaded albumin microspheres for intratumoral chemotherapy of breast cancer. *J Control Release* **2003**, *91* (1-2), 147-155.
159. Ballio, A.; Marini-Bettolo, G. B., The constitution of cernuoside, the yellow pigment of the flowers of *Oxalis cernua*. *Gazzetta Chimica Italiana* **1955**, *85*, 1319-1328.
160. Di Vittorio, V., Synthesis and properties of some 4,6-dimethoxyaurones. *Rendiconti Istituto Superiore di Sanita (Italian Edition)* **1958**, *21*, 418-432.
161. Perkin, W. H.; Jr.; Ray, J. N.; Robinson, R., Synthesis of brazilin and hematoxylin and their derivatives. I. Veratrylidene-7-methoxychromanone and an account of a new synthesis of some benzopyrylium salts. *J Chem Soc* **1926**, 941-953.

162. Narasimhachari, N.; Seshadri, T. R., Synthetic experiments in the benzopyrone series. XI. Conversion of carthamidin and isocarthamidin into herbacetin and tangeretin. *Proc. Indian Acad. Sci.* **1949**, *30A*, 216-222.
163. Wagner, G.; Eppner, B., Synthesis of amidinobenzylidene derivatives of coumaran-3-one, 5,6-benzocoumaran-3-one and 1-thiocoumaran-3-one. *Pharmazie* **1979**, *34* (9), 527-530.
164. Kuck, D.; Paisdor, B.; Gruetzmacher, H. F., Benzannelated centropolyquinanes. 3. Synthesis of multiply substituted triptindans (9H,10H-4b,9a-([1,2]benzenomethano)indeno[1,2-a]indenes) with substituents in their molecular cavity. *Chemische Berichte* **1987**, *120* (4), 589-595.
165. Ganguly, A.; Bhattacharyya, P.; Bhattacharyya, A.; Adityachaudhury, N., Synthesis of candidone - a new flavanone isolated from *Tephrosia candida*. *Indian J. Chem. Sect. B: Org. Chem. Incl. Med. Chem.* **1988**, *27B*, 462-463.
166. Sekizaki, H., Synthesis of 2-benzylidene-3(2H)-benzofuran-3-ones (aurones) by oxidation of 2'-hydroxychalcones with mercury(II) acetate. *Bull. Chem. Soc. Jpn.* **1988**, *61* (4), 1407-1409.
167. Detsi, A.; Majdalani, M.; Kontogiorgis, C.; Hadjipavlou-Litina, D.; Kefalas, P., Natural and synthetic 2'-hydroxy-chalcones and aurones: synthesis, characterization and evaluation of the antioxidant and soybean lipoxygenase inhibitory activity. *Bioorg Med Chem* **2009**, *17* (23), 8073-8085.
168. Singh, O. V.; Muthukrishnan, M.; Sunderavadivelu, M., Synthesis of isoflavones containing naturally occurring substitution pattern by oxidative rearrangement of respective flavanones using thallium(III) p-tosylate. *Indian J. Chem. Sect. B: Org. Chem. Incl. Med. Chem.* **2005**, *44B* (12), 2575-2581.
169. Banerji, A.; Goomer, N. C., A new synthesis of flavones. *Synthesis* **1980**, *11*, 874-875.
170. Smith, J. A.; Maloney, D. J.; Hecht, S. M.; Lannigan, D. A., Structural basis for the activity of the RSK-specific inhibitor, SL0101. *Bioorg Med Chem* **2007**, *15* (14), 5018-5034.
171. Doporto, M. L.; Gallagher, K. M.; Gowan, J. E.; Hughes, A. C.; Philbin, E. M.; Swain, T.; Wheeler, T. S., Rearrangement in the demethylation of 2'-methoxyflavones. II. Further experiments and the determination of the composition of lotoflavin. *J Chem Soc* **1955**, 4249-4256.

## Appendix 2-1: Characterization of synthesized analogues

### (Z)-4, 6-Dimethoxy-2-(3'-methylbenzylidene)-benzofuran-3(2H)-one (**1-12**)

This compound was obtained from 4,6-dimethoxybenzofuran-3(2H)-one A-3 (0.10g, 0.51mmol), 3'-methylbenzaldehyde (0.77 mmol) and 50% KOH (1ml) as a pale yellow solid product (yield 66%) according to Scheme 2-2; mp 147-149 °C; <sup>1</sup>H NMR (DMSO-d<sub>6</sub>, 300MHz): δ 2.36 (s, 3H), 3.89 (s, 3H), 3.92 (s, 3H), 6.36 (s, 1H), 6.67 (s, 1H), 6.73 (s, 1H), 7.25 (d, 1H, J = 7.5 Hz), 7.37 (t, 1H, J = 7.5 Hz), 7.74 (d, 2H, J = 6.0 Hz); <sup>13</sup>C NMR (CDCl<sub>3</sub>, 75 MHz): δ 21.7, 56.3, 56.4, 89.4, 94.2, 105.5, 111.2, 128.5, 128.8, 130.5, 131.9, 132.7, 138.6, 148, 159.6, 169.1, 169.3, 181; MS (APCI) m/z [M+1]<sup>+</sup> 297.5; Anal. Calcd for C<sub>18</sub>H<sub>16</sub>O<sub>4</sub>: C, 72.96; H, 5.44; Found: C, 73.44; H, 6.65.

### (Z)-2-(3'-Cyanobenzylidene)-4, 6-dimethoxybenzofuran-3(2H)-one (**1-14**)

This compound was obtained from 4,6-dimethoxybenzofuran-3(2H)-one A-3 (0.10g, 0.51mmol), 3'-cyanobenzaldehyde (0.54 mmol) and 50% KOH (1ml) as a pale yellow solid product (yield 61%) according to Scheme 2-2; mp 226 °C; <sup>1</sup>H NMR (CDCl<sub>3</sub>, 300 MHz): CDCl<sub>3</sub> δ 3.93 (s, 3H), 3.95 (s, 3H), 6.15 (d, 1H, J = 1.9 Hz), 6.44 (d, 1H, J = 1.5 Hz), 6.68 (d, 1H, J = 7.5 Hz), 7.62-7.48 (m, 2H), 7.91 (d, 1H, J = 7.9 Hz), 8.27 (s, 1H); <sup>13</sup>C NMR (CDCl<sub>3</sub>, 75 MHz) δ 56, 56, 89.6, 94.7, 105.0, 107.8, 113.3, 118.8, 129.8, 132.2, 134.1, 134.1, 135.2, 149.2, 159.8, 169.4, 169.7, 180.4; IR (KBr, cm<sup>-1</sup>) 2230 (ν C≡N), 1698 (ν C=O); MS (APCI) m/z [M+H]<sup>+</sup> 308.5; High resolution MS: Calcd for C<sub>18</sub>H<sub>13</sub>NO<sub>4</sub>: 307.0845; Found: 307.0839; Anal Calcd for C<sub>18</sub>H<sub>13</sub>NO<sub>4</sub>: C, 70.35; H, 4.26; Found: C, 71.34; H, 5.51; HPLC retention times and peak areas (i) MeOH (60%)- water (40%): 1.45 min, 99.79% (ii) acetonitrile (50%)-water (50%): 1.63 min, 99.73%.

(Z)-2-(3-Hydroxy-4-methoxybenzylidene)-4,6-dimethoxybenzofuran-3(2H)-one (**1-20**)

This compound was obtained from 4,6-dimethoxybenzofuran-3(2H)-one A-3 (0.10g, 0.51mmol), 4-methoxy-3-(tetrahydro-pyran-2-yloxy)benzaldehyde (0.12g, 0.77 mmol) and 50% KOH (1ml) as a yellow solid (60% yield) according to Scheme 2-2: mp: 203-204°C (lit: 198-199°C)<sup>159</sup>; <sup>1</sup>H NMR (DMSO-d<sub>6</sub>, 300 MHz): δ 3.83 (s, 3H), 3.88 (s, 3H), 3.92 (s, 3H), 6.34 (d, 1H, J = 1.5 Hz), 6.59 (s, 1H), 6.64 (d, 1H, J = 1.5 Hz), 7.01 (d, 1H, J = 8.4 Hz), 7.33 (dd, 1H, J<sub>1</sub> = 1.8 Hz, J<sub>2</sub> = 1.8 Hz), 7.45 (d, 1H, J = 1.8 Hz), 9.24 (s, 1H); <sup>13</sup>C NMR (CDCl<sub>3</sub>, 75MHz): δ 55.93, 56.06, 56.16, 89.15, 93.94, 105.38, 110.55, 111.09, 116.48, 124.73, 126.13, 145.63, 146.96, 147.80, 159.30, 168.77, 168.86, 180.65; MS (APCI): m/z 329.5 [M+1]<sup>+</sup>; Anal. calcd for C<sub>18</sub>H<sub>16</sub>O<sub>6</sub>: C, 65.85; H, 4.91; Found: C, 65.82; H, 4.72.

(Z)-2-(3-Methoxy-4-hydroxybenzylidene)-4,6-dimethoxybenzofuran-3(2H)-one (**1-21**)

This compound was obtained from 4,6-dimethoxybenzofuran-3(2H)-one A-3 (0.10g, 0.51mmol), 3-methoxy-4-(tetrahydro-pyran-2-yloxy)benzaldehyde (0.12g, 0.77 mmol) and 50% KOH (1ml) as a yellow solid (52% yield) according to Scheme 2-2: mp: 247-248 °C (lit: 238 °C)<sup>160</sup>; <sup>1</sup>H NMR (DMSO-d<sub>6</sub>, 300 MHz): δ 3.84 (s, 3H), 3.88 (s, 3H), 3.91 (s, 3H), 6.32 (d, 1H, J = 1.5 Hz), 6.65 (s, 1H), 6.69 (d, 1H, J = 1.5 Hz), 6.88 (d, 1H, J = 8.4 Hz), 7.44 (dd, 1H, J<sub>1</sub> = 1.5 Hz, J<sub>2</sub> = 1.8 Hz), 7.52 (d, 1H, J = 1.5 Hz), 9.72 (s, OH); <sup>13</sup>C NMR (DMSO-d<sub>6</sub>, 75 MHz): δ 56.75, 57.12, 57.52, 90.86, 95.35, 105.33, 111.82, 115.97, 117.02, 124.52, 126.28, 146.74, 148.79, 149.74, 159.79, 168.96, 169.63, 179.89; MS (APCI): m/z 329.5 [M+1]<sup>+</sup>; Anal. calcd for C<sub>18</sub>H<sub>16</sub>O<sub>6</sub>: C, 65.85; H, 4.91; Found: C, 65.60; H, 4.91.

(Z)-2-(3, 4-Dihydroxybenzylidene)-4,6-dimethoxybenzofuran-3(2H)-one (**1-24**).

This compound was obtained from 4,6-dimethoxybenzofuran-3(2H)-one A-3 (0.10g, 0.51mmol), 3,4-bis(tetrahydro-2H-pyran-2-yloxy)benzaldehyde (0.11g, 0.77 mmol) and 50% KOH (1ml) as a yellow solid (58 % yield) according to Scheme 2-2: mp: 279-281°C; <sup>1</sup>H NMR (DMSO-d<sub>6</sub>, 300 MHz): δ 3.88 (s, 3H), 3.891 (s, 3H), 6.33 (d, 1H, J = 1.5 Hz), 6.54 (s, 1H), 6.62 (d, 1H, J = 1.2 Hz), 6.82 (d, 1H, J = 8.4 Hz), 7.23 (dd, 1H, J<sub>1</sub> = 1.5 Hz, J<sub>2</sub> = 1.8 Hz), 7.40 (d, 1H, J = 1.8 Hz); <sup>13</sup>C NMR (CDCl<sub>3</sub>, 75 MHz): δ 56.11, 56.44, 89.63, 94.23, 104.35, 111.01, 115.98, 117.93, 123.44, 124.26, 145.51, 145.58, 147.83, 158.83, 167.87, 168.58, 178.91; MS (APCI): m/z 315.8 [M+1]<sup>+</sup>; Anal. calcd for C<sub>17</sub>H<sub>14</sub>O<sub>6</sub> : C, 64.97; H, 4.49 ; Found: C, 64.62; H, 4.59; HPLC analyses: t<sub>R</sub> = 3.85 min (98.60% pure at 400nm) on the C<sub>18</sub> analytical column; Mobile phase: solvent system A (MeOH and 0.1% HCOOH in H<sub>2</sub>O) with a gradient of MeOH 100% to 70% from 0 to 5 min, 70% to 50% from 5 to 7 min and then 50% MeOH from 7 to 10 min; t<sub>R</sub> = 4.58 min (96.11% pure at 330nm) on the C<sub>18</sub> analytical column; Mobile phase: solvent system B (CH<sub>3</sub>CN and 0.1% HCOOH in H<sub>2</sub>O) with a gradient of CH<sub>3</sub>CN 100% to 70% from 0 to 5 min, 70% to 50% from 5 to 7 min, 50% to 70% CH<sub>3</sub>CN from 7 to 9 min and then 70% CH<sub>3</sub>CN from 9 to 12 min.

(Z)-2-(3, 4-Dimethoxybenzylidene)-4,6-dimethoxybenzofuran-3(2H)-one (**1-25**)

This compound was obtained from 4,6-dimethoxybenzofuran-3(2H)-one A-3 (0.10g, 0.51mmol), 3, 4-dimethoxybenzaldehyde (0.13g, 0.77 mmol) and 50% KOH (1ml) as a light yellow solid (79% yield) according to Scheme 2-2: mp: 180-181°C (lit: 175 °C)<sup>161</sup>; <sup>1</sup>H NMR (CDCl<sub>3</sub>, 300 MHz): δ 3.91, 3.92, 3.94 (s, 12H, OCH<sub>3</sub> x 4), 6.12 (s, 1H), 6.34 (s, 1H), 6.72 (s, 1H), 6.91 (d, 1H, J = 8.1 Hz), 7.42-7.45 (m, 2H); <sup>13</sup>C NMR (CDCl<sub>3</sub>, 75 MHz) δ 55.90, 55.90, 56.07, 56.16, 89.13, 93.91, 105.39, 111.15, 111.18, 113.54, 125.25,

125.52, 146.80, 148.94, 150.33, 159.33, 168.70, 168.70, 180.50; MS (APCI):  $m/z$  343.5  $[M+1]^+$ ; Anal. calcd for  $C_{19}H_{18}O_6$ : C, 66.66 ; H, 5.30; Found: C, 66.51; H, 5.12.

**(Z)-2-(3, 5-Dimethoxybenzylidene)-4,6-dimethoxybenzofuran-3(2H)-one (1-26)**

This compound was obtained from 4,6-dimethoxybenzofuran-3(2H)-one A-3 (0.10g, 0.51mmol), 3, 5-dimethoxybenzaldehyde (0.13g, 0.77 mmol) and 50% KOH (1ml) as a light yellow solid (58% yield) according to Scheme 2-2: mp: 181-182°C;  $^1H$  NMR ( $CDCl_3$ , 300 MHz):  $\delta$  3.85 (s, 6H,  $OCH_3 \times 2$ ), 3.91 (s, 3H,  $OCH_3$ ), 3.95 (s, 3H,  $OCH_3$ ), 6.13 (s, 1H), 6.36 (s, 1H), 6.50 (s, 1H), 6.69 (s, 1H), 7.031 (s, 2H);  $^{13}C$  NMR ( $CDCl_3$ , 75 MHz):  $\delta$  55.40, 55.40, 56.07, 56.16, 89.24, 94.08, 101.72, 105.10, 109.05, 109.05, 110.65, 134.13, 148.00, 159.40, 160.77, 160.77, 169.02, 169.02, 180.59; MS (APCI):  $m/z$  343.7  $[M+1]^+$ ; Anal. calcd for  $C_{19}H_{18}O_6$ : C, 66.66 ; H, 5.30; Found: C, 66.69; H, 5.11.

**(Z)-2-(3, 4-Difluorobenzylidene)-4,6-dimethoxybenzofuran-3(2H)-one (1-27)**

This compound was obtained from 4,6-dimethoxybenzofuran-3(2H)-one A-3 (0.10g, 0.51mmol), 3, 4-difluorobenzaldehyde (0.08g, 0.57 mmol) and 50% KOH (1ml) as a off-white solid (57% yield) according to Scheme 2-2: mp: 203-204°C;  $^1H$  NMR ( $CDCl_3$ , 300MHz):  $\delta$  3.93 (s, 3H), 3.97 (s, 3H), 6.16 (d, 1H,  $J= 1.5Hz$ ), 6.41 (d, 1H,  $J= 1.8Hz$ ), 6.66 (s, 1H), 7.16 – 7.25 (m, 1H), 7.47 – 7.51 (m, 1H), 7.78 – 7.85 (m, 1H);  $^{13}C$  NMR ( $CDCl_3$ , 75MHz):  $\delta$  56.2, 56.3, 89.3, 89.3, 94.3, 105.0, 108.3, 117.5, 117.7, 119.2, 119.4, 127.7 (2C), 127.8 (2C), 129.7, 129.8 (2C), 129.9, 148.0 (2C), 148.7, 148.8, 148.9, 149.0, 149.1, 152.0, 152.1, 152.3, 152.5, 159.5, 169.0, 169.3, 180.3 (more peaks than expected due to splitting); MS (APCI):  $m/z$  319.7  $[M+1]^+$ ; HPLC analyses:  $t_R= 4.99$  min (99.62% pure at 360nm) on the  $C_{18}$  analytical column; Mobile phase: solvent system A (MeOH and 0.1%  $HCOOH$  in  $H_2O$ ) with a gradient of MeOH 100% to 70% from 0 to 5 min, 70% to 50% from 5 to 7 min and then 50% MeOH from 7 to 10 min;  $t_R= 4.07$  min



(98.10% pure at 330nm) on the C<sub>18</sub> analytical column; Mobile phase: solvent system B (CH<sub>3</sub>CN and 0.1% HCOOH in H<sub>2</sub>O) with a gradient of CH<sub>3</sub>CN 100% to 70% from 0 to 5 min, 70% to 50% from 5 to 7 min, 50% to 70% CH<sub>3</sub>CN from 7 to 9 min and then 70% CH<sub>3</sub>CN from 9 to 12 min.

**(Z)-2-(3, 5-Difluorobenzylidene)-4,6-dimethoxybenzofuran-3(2H)-one (1-28)**

This compound was obtained from 4,6-dimethoxybenzofuran-3(2H)-one A-3 (0.10g, 0.51mmol), 3, 5-difluorobenzaldehyde (0.08g, 0.57 mmol) and 50% KOH (1ml) as a yellow solid (52% yield) according to Scheme 2-2: mp: 241-242°C; <sup>1</sup>H NMR (CDCl<sub>3</sub>, 300MHz): δ 3.94 (s, 3H), 3.97 (s, 3H), 6.16 (d, 1H, J= 1.5Hz), 6.42 (d, 1H, J= 1.8Hz), 6.64 (s, 1H), 6.78 – 6.85 (m, 1H), 7.35 – 7.42 (m, 2H); <sup>13</sup>C NMR (CDCl<sub>3</sub>, 75MHz): δ 56.3 (2C), 89.4, 94.4, 104.2, 104.53, 104.9, 107.9, 113.2, 113.4, 113.5, 113.6, 135.4, 135.6, 135.7, 148.9, 159.6, 161.3, 161.5, 164.6, 164.8, 169.1, 169.5, 180.3 (more peaks than expected due to splitting); MS (APCI): m/z 319.7 [M+1]<sup>+</sup>; HPLC analyses: t<sub>R</sub>= 5.20 min (100% pure at 360nm) on the C<sub>18</sub> analytical column; Mobile phase: solvent system A (MeOH and 0.1% HCOOH in H<sub>2</sub>O) with a gradient of MeOH 100% to 70% from 0 to 5 min, 70% to 50% from 5 to 7 min and then 50% MeOH from 7 to 10 min; t<sub>R</sub>= 3.92min (100% pure at 360nm) on the C<sub>18</sub> analytical column; Mobile phase: solvent system B (CH<sub>3</sub>CN and 0.1% HCOOH in H<sub>2</sub>O) with a gradient of CH<sub>3</sub>CN 100% to 70% from 0 to 5 min, 70% to 50% from 5 to 7 min, 50% to 70% CH<sub>3</sub>CN from 7 to 9 min and then 70% CH<sub>3</sub>CN from 9 to 12 min.

**(Z)-2-Benzylidene-4, 5, 6-trimethoxybenzofuran-3(2H)-one (2-1)**

This compound was obtained from 4,5,6-trimethoxybenzofuran-3(2H)-one A-4 (0.10g, 0.45mmol), benzaldehyde (0.06g, 0.54 mmol) and 50% KOH (1ml) as a yellow solid (35% yield) according to Scheme 2-2: mp: 135-137°C (lit: 142-143 °C)<sup>162</sup>; <sup>1</sup>H NMR

(CDCl<sub>3</sub>, 300MHz):  $\delta$  3.83 (s, 3H), 3.99 (s, 3H), 4.26 (s, 3H), 6.56 (s, 1H), 6.78 (s, 1H), 7.35 – 7.46 (m, 3H), 7.87 (d, 1H, J= 7.2Hz); <sup>13</sup>C NMR (CDCl<sub>3</sub>, 75MHz):  $\delta$  56.6, 61.6, 62.4, 90.5, 107.0, 111.2, 128.8, 129.4, 131.1, 132.5, 136.6, 147.7, 151.7, 161.7, 164.1, 180.9; MS (APCI): m/z 313.4 [M+1]<sup>+</sup>; Anal. calcd for C<sub>18</sub>H<sub>16</sub>O<sub>5</sub>: C, 69.22; H, 5.16; Found: C, 68.94; H, 5.01.

**(Z)-2-(2-Chlorobenzylidene)-4, 5, 6-trimethoxybenzofuran-3(2H)-one (2-2)**

This compound was obtained from 4,5,6-trimethoxybenzofuran-3(2H)-one A-4 (0.10g, 0.45mmol), 2-chlorobenzaldehyde (0.08g, 0.54 mmol) and 50% KOH (1ml) as a yellow solid (57% yield) according to Scheme 2-2: mp: 164-166°C; <sup>1</sup>H NMR (DMSO-d<sub>6</sub>, 300MHz):  $\delta$  3.69 (s, 3H), 3.96 (s, 3H), 4.12 (s, 3H), 6.96 (s, 1H), 7.01 (s, 1H), 7.43 – 7.54 (m, 2H), 7.62 (dd, 1H, J= 1.2, 1.2 Hz), 8.26 (dd, 1H, J= 1.5, 1.8 Hz); <sup>13</sup>C NMR (CDCl<sub>3</sub>, 75MHz):  $\delta$  56.7, 61.6, 62.5, 90.6, 106.3, 106.8, 126.9, 130.0, 130.2, 130.6, 131.9, 135.6, 136.7, 148.5, 151.9, 161.8, 164.1, 180.5; MS (APCI): m/z 347.4 [M+1]<sup>+</sup>; Anal. calcd for C<sub>18</sub>H<sub>15</sub>ClO<sub>5</sub>: C, 62.35; H, 4.36; Found: C, 62.23; H, 4.31.

**(Z)-2-(3-Chlorobenzylidene)-4, 5, 6-trimethoxybenzofuran-3(2H)-one (2-3)**

This compound was obtained from 4,5,6-trimethoxybenzofuran-3(2H)-one A-4 (0.10g, 0.45mmol), 3-chlorobenzaldehyde (0.08g, 0.54 mmol) and 50% KOH (1ml) as a yellow solid (69% yield) according to Scheme 2-2: mp: 141-143°C; <sup>1</sup>H NMR (CDCl<sub>3</sub>, 300MHz):  $\delta$  3.83 (s, 3H), 4.00 (s, 3H), 4.26 (s, 3H), 6.58 (s, 1H), 6.67 (s, 1H), 7.34 – 7.39 (m, 2H), 7.65 - 7.67 (m, 2H), 7.91 (s, 1H); <sup>13</sup>C NMR (CDCl<sub>3</sub>, 75MHz):  $\delta$  56.7, 61.6, 62.4, 90.7, 106.8, 109.3, 129.3 (2C), 130.0, 130.5, 134.3, 134.7, 136.8, 148.2, 151.8, 161.9, 164.1, 180.6; MS (APCI): m/z 347.5 [M+1]<sup>+</sup>; Anal. calcd for C<sub>18</sub>H<sub>15</sub>ClO<sub>5</sub>: C, 62.35; H, 4.36; Found: C, 62.30; H, 4.25.

**(Z)-2-(4-Chlorobenzylidene)-4, 5, 6-trimethoxybenzofuran-3(2H)-one (2-4)**

This compound was obtained from 4,5,6-trimethoxybenzofuran-3(2H)-one A-4 (0.10g, 0.45mmol), 4-chlorobenzaldehyde (0.08g, 0.54 mmol) and 50% KOH (1ml) as a yellow solid (53% yield) according to Scheme 2-2: mp: 187-188°C; <sup>1</sup>H NMR (CDCl<sub>3</sub>, 300MHz): δ 3.83 (s, 3H), 3.99 (s, 3H), 4.26 (s, 3H), 6.55 (s, 1H), 6.71 (s, 1H), 7.40 (d, 2H, J= 8.7 Hz), 7.80 (d, 2H, 8.4 Hz); <sup>13</sup>C NMR (CDCl<sub>3</sub>, 75MHz): δ 56.7, 61.6, 62.4, 90.6, 106.9, 109.7, 129.1, 131.0, 132.2, 135.3, 136.7, 147.8, 151.8, 161.8, 164.0, 180.7; MS (APCI): m/z 347.4 [M+1]<sup>+</sup>; Anal. calcd for C<sub>18</sub>H<sub>15</sub>ClO<sub>5</sub>: C, 62.35; H, 4.36; Found: C, 62.47; H, 4.42.

**(Z)-4,5,6-Trimethoxy-2-(2-methoxybenzylidene)benzofuran-3(2H)-one (2-5)**

This compound was obtained from 4,5,6-trimethoxybenzofuran-3(2H)-one A-4 (0.05g, 0.22mmol), 2-methoxybenzaldehyde (0.04g, 0.27 mmol) and 50% KOH (1ml) as a yellow solid (97% yield) according to Scheme 2-2: mp: 147-149°C; <sup>1</sup>H NMR (CDCl<sub>3</sub>, 300MHz): δ 3.82 (s, 3H), 3.89 (s, 3H), 3.97 (s, 3H), 4.26 (s, 3H), 6.54 (s, 1H), 6.92 (d, 1H, J= 8.4Hz), 7.03 (t, 1H, J= 7.7Hz), 7.32-7.37 (m, 2H), 8.21 (d, 1H, J= 7.5Hz); <sup>13</sup>C NMR (CDCl<sub>3</sub>, 75MHz): δ 55.6, 56.6, 61.6, 62.4, 90.5, 105.4, 107.2, 110.7, 120.7, 121.5, 131.0, 131.6, 136.5, 147.6, 151.7, 158.5, 161.4, 163.9, 180.8; MS (APCI): m/z 343.6 [M+1]<sup>+</sup>; Anal. calcd for C<sub>19</sub>H<sub>18</sub>O<sub>6</sub>: C, 66.66; H, 5.30; Found: C, 66.49; H, 5.10.

**(Z)-4,5,6-Trimethoxy-2-(3-methoxybenzylidene)benzofuran-3(2H)-one (2-6)**

This compound was obtained from 4,5,6-trimethoxybenzofuran-3(2H)-one A-4 (0.08g, 0.34mmol), 3-methoxybenzaldehyde (0.05g, 0.39 mmol) and 50% KOH (1ml) as a yellow solid (30% yield) according to Scheme 2-2: mp: 115-117°C; <sup>1</sup>H NMR(Acetone-d<sub>6</sub>, 300MHz): δ 3.75 (s, 3H), 3.87 (s, 3H), 4.01 (s, 3H), 4.18 (s, 3H), 6.65 (s, 1H), 6.83 (s, 1H), 6.99 (dd, 1H, J= 1.5, 2.1 Hz), 7.38 (t, 1H, J= 8.0 Hz), 7.50 (d, 2H, J= 6.9 Hz); <sup>13</sup>C

NMR (Acetone- $d_6$ , 75MHz): 55.6, 57.2, 61.5, 62.5, 92.1, 107.4, 110.7, 116.0, 117.0, 124.4, 130.7, 134.7, 137.9, 148.6, 152.3, 160.9, 163.0, 164.8, 180.7; MS (APCI):  $m/z$  343.4  $[M+1]^+$ ; Anal. calcd for  $C_{19}H_{18}O_6$ : C, 66.66; H, 5.30; Found: C, 66.65; H, 5.23.

**(Z)-4,5,6-Trimethoxy-2-(4-methoxybenzylidene)benzofuran-3(2H)-one (2-7)**

This compound was obtained from 4,5,6-trimethoxybenzofuran-3(2H)-one A-4 (0.10g, 0.45mmol), 4-methoxybenzaldehyde (0.07g, 0.54 mmol) and 50% KOH (1ml) as a yellow solid (48% yield) according to Scheme 2-2: mp: 145-147°C;  $^1H$  NMR ( $CDCl_3$ , 300MHz):  $\delta$  3.83 (s, 3H), 3.87 (s, 3H), 3.98 (s, 3H), 4.26 (s, 3H), 6.55 (s, 1H), 6.76 (s, 1H), 6.97 (d, 2H,  $J=8.7$ Hz), 7.84 (d, 2H,  $J=8.7$ Hz);  $^{13}C$  NMR ( $CDCl_3$ , 75MHz):  $\delta$  55.4, 56.6, 61.6, 62.4, 90.5, 107.3, 111.5, 114.4, 125.3, 132.9, 136.6, 146.6, 151.6, 160.7, 161.4, 163.8, 180.8; MS (APCI):  $m/z$  343.4  $[M+1]^+$ ; Anal. calcd for  $C_{19}H_{18}O_6$ : C, 66.66; H, 5.30; Found: C, 66.48; H, 4.92.

**(Z)-4,5,6-Trimethoxy-2-(3-cyanobenzylidene)benzofuran-3(2H)-one (2-8)**

This compound was obtained from 4,5,6-trimethoxybenzofuran-3(2H)-one A-4 (0.10g, 0.45mmol), 3-cyanobenzaldehyde (0.07g, 0.54 mmol) and 50% KOH (1ml) as a yellow solid (58% yield) according to Scheme 2-2: mp: 207-208°C;  $^1H$  NMR ( $CDCl_3$ , 300MHz):  $\delta$  3.83 (s, 3H), 4.02 (s, 3H), 4.26 (s, 3H), 6.62 (s, 1H), 6.69 (s, 1H), 7.54 (t, 1H,  $J=7.8$  Hz), 7.64 (d, 1H,  $J=7.8$  Hz), 7.92 (d, 1H,  $J=7.8$  Hz), 8.30 (s, 1H);  $^{13}C$  NMR ( $CDCl_3$ , 75MHz):  $\delta$  56.8, 61.6, 62.4, 90.8, 106.6, 107.9, 113.2, 118.6, 129.6, 132.1, 133.9, 133.9, 135.0, 136.9, 148.8, 151.9, 162.2, 164.1, 180.4; MS (APCI):  $m/z$  338.4  $[M+1]^+$ ; Anal. calcd for  $C_{19}H_{15}NO_5$ : C, 67.65; H, 4.48; Found: C, 67.58; H, 4.36.

**(Z)-2-(3-Hydroxybenzylidene)-4, 5, 6-trimethoxybenzofuran-3(2H)-one (2-9)**

This compound was obtained from 4,5,6-trimethoxybenzofuran-3(2H)-one A-4 (0.20g, 0.88mmol), 3-(tetrahydro-2H-pyran-2-yloxy)benzaldehyde (0.27g, 1.32mmol) and 50% KOH (1ml) as a yellow solid (26% yield) according to Scheme 2-2: mp: 173-174°C; <sup>1</sup>H NMR (DMSO-d<sub>6</sub>, 300MHz): δ 3.69 (s, 3H), 3.96 (s, 3H), 4.10 (s, 3H), 6.67 (s, 1H), 6.85 (d, 1H, J= 8.1Hz), 6.96 (s, 1H), 7.28 (t, 1H, J= 8.1Hz), 7.35-7.37 (m, 2H), 9.68 (s, -OH); <sup>13</sup>C NMR (CDCl<sub>3</sub>, 75MHz): δ 56.7, 61.7, 62.3, 90.6, 107.0, 111.5, 117.0, 117.6, 123.8, 129.9, 133.7, 136.6, 147.8, 151.7, 156.2, 162.0, 164.1, 181.1; MS (APCI): m/z 329.4 [M+1]<sup>+</sup>; Anal. calcd for C<sub>18</sub>H<sub>16</sub>O<sub>6</sub>: C, 65.85; H, 4.91; Found: C, 65.65; H, 5.22.

**(Z)-4,5,6-Trimethoxy-2-(3-methylbenzylidene)benzofuran-3(2H)-one (2-10)**

This compound was obtained from 4,5,6-trimethoxybenzofuran-3(2H)-one A-4 (0.10g, 0.45mmol), benzaldehyde (0.06g, 0.54 mmol) and 50% KOH (1ml) as a yellow solid (50% yield) according to Scheme 2-2: mp: 133-135°C; <sup>1</sup>H NMR (DMSO-d<sub>6</sub>, 300MHz): δ 2.38 (s, 3H), 3.69 (s, 3H), 3.97 (s, 3H), 4.10 (s, 3H), 6.73 (s, 1H), 7.01 (s, 1H), 7.26 (d, 1H J= 7.5 Hz), 7.39 (t, 1H, J= 7.8 Hz), 7.75 – 7.77 (m, 2H); <sup>13</sup>C NMR (CDCl<sub>3</sub>, 75MHz): δ 21.3, 56.5, 61.5, 62.3, 90.5, 106.9, 111.3, 128.2, 128.6, 130.3, 131.6, 132.3, 136.5, 138.3, 147.5, 151.6, 161.5, 163.9, 180.7; MS (APCI): m/z 327.5 [M+1]<sup>+</sup>; Anal. calcd for C<sub>19</sub>H<sub>18</sub>O<sub>5</sub>: C, 69.93; H, 5.56; Found: C, 69.88; H, 5.30.

**(Z)-2-(Cyclohexylmethylene)-4,5,6-trimethoxybenzofuran-3(2H)-one (2-11)**

The method of Wallez et al. (2002) was followed. Cyclohexaldehyde (0.36g, 0.321mmol) and activated basic aluminium oxide (0.98g) were added to a vigorously stirred solution of A-4 in 10ml of methylene chloride and allowed to stir overnight. After overnight stirring, aluminium oxide was filtered and washed abundantly with methylene chloride. The filtrate was then concentrated to give crude 2-11, which was purified by column

chromatography (hexane/ethyl acetate (4:1)) to give pure 2-11; yellow solid, 78% yield; mp: 86-88°C; <sup>1</sup>H NMR (CDCl<sub>3</sub>, 300MHz): δ 1.20 -1.43 (m, 5H), 1.65 -1.80 (m, 5H), 2.61- 2.71 (m, 1H), 3.80 (s, 3H), 3.94 (s, 3H), 4.21(s, 3H), 5.92 (d, 1H, J= 9.6Hz), 6.42 (s, 1H); <sup>13</sup>C NMR (CDCl<sub>3</sub>, 75MHz): δ 25.4, 25.7, 32.1, 35.1, 56.4, 61.5, 62.2, 90.2, 107.6, 120.1, 136.2, 148.0, 151.5, 161.6, 164.0, 180.8; MS (APCI): m/z 319.4 [M+1]<sup>+</sup>; Anal. calcd for C<sub>18</sub>H<sub>22</sub>O<sub>5</sub>: C, 67.91; H, 6.97; Found: C, 67.68; H, 6.46.

**(Z)-2-Benzylidenebenzofuran-3(2H)-one (5-1)**

This compound was obtained from benzofuran-3(2H)-one (0.10g, 0.75mmol), benzaldehyde (0.08g, 0.83mmol) and activated basic aluminium oxide (2.75g) as a yellow solid (84% yield) according to Scheme 2-3: mp: 102-104°C (lit: 98-99 °C)<sup>121</sup>; <sup>1</sup>H NMR (Acetone-d<sub>6</sub>, 300MHz): δ 6.86 (s, 1H), 7.32 (t, 1H, J= 7.4 Hz), 7.42 – 7.53 (m, 4H), 7.77 – 7.82 (m, 2H), 8.01 (d, 2H, J= 6.9 Hz); <sup>13</sup>C NMR (Acetone-d<sub>6</sub>, 75MHz): δ 113.7, 114.9, 123.2, 125.7, 126.0, 130.8, 131.7, 133.3, 134.2, 139.2, 148.6, 167.9, 185.6; MS (APCI): m/z 223.5 [M+1]<sup>+</sup>; Anal. calcd for C<sub>15</sub>H<sub>10</sub>O<sub>2</sub>: C, 81.07; H, 4.54; Found: C, 81.38; H, 4.32.

**(Z)-2-(3-Hydroxybenzylidene)benzofuran-3(2H)-one (5-3)**

This compound was obtained from benzofuran-3(2H)-one (0.15g, 1.13mmol), 3-(tetrahydro-2H-pyran-2-yloxy)benzaldehyde (0.35g, 1.69 mmol) and activated basic aluminium oxide (4.13g) as a yellow solid (10% yield) according to Scheme 2-3: mp: 193-194°C; <sup>1</sup>H NMR (Acetone-d<sub>6</sub>, 300MHz): δ 6.79 (s, 1H), 6.95 (dd, 1H, J= 1.8, 1.8 Hz), 7.31 – 7.36 (m, 2H), 7.47 – 7.55 (m, 3H), 7.77 – 7.82 (m, 2H), 8.70 (s, -OH); <sup>13</sup>C NMR (Acetone-d<sub>6</sub>, 75MHz): δ 113.9, 114.9, 119.2, 119.6, 123.3, 125.0, 125.7, 126.0, 131.8, 135.4, 139.1, 148.6, 159.6, 167.9, 185.6; MS (APCI): m/z 239.0 [M+1]<sup>+</sup>; Anal. calcd for C<sub>15</sub>H<sub>10</sub>O<sub>3</sub>: C, 75.62; H, 4.23; Found: C, 75.70; H, 3.92.

**(Z)-2-(3-Chlorobenzylidene)benzofuran-3(2H)-one (5-5)**

This compound was obtained from benzofuran-3(2H)-one (0.15g, 1.13mmol), 3-chlorobenzaldehyde (0.17g, 1.24mmol) and activated basic aluminium oxide (4.13g) as a yellow solid (14% yield) according to Scheme 2-3: mp: 102-104°C (lit: 98-99 °C)<sup>121</sup>; <sup>1</sup>H NMR (Acetone<sub>d-6</sub>, 300MHz): δ 6.84 (s, 1H), 7.35 (t, 1H, J= 7.5 Hz), 7.46 – 7.56 (m, 3H), 7.79 – 7.85 (m, 2H), 7.95 (d, 1H, J= 7.5 Hz), 8.06 (s, 1H); <sup>13</sup>C NMR (Acetone<sub>d-6</sub>, 75MHz): δ 111.9, 115.0, 123.0, 126.0, 126.1, 131.4, 131.6, 132.4, 132.5, 136.2, 136.3, 139.5, 149.2, 168.0, 185.6; MS (APCI): m/z 257.4 [M+1]<sup>+</sup>; Anal. calcd for C<sub>15</sub>H<sub>9</sub>ClO<sub>2</sub>: C, 70.19; H, 3.53; Found: C, 70.58; H, 3.36; HPLC analyses: t<sub>R</sub>= 4.31 min (96.05% pure at 330nm) on the C<sub>18</sub> analytical column; Mobile phase: solvent system A (MeOH and 0.1% HCOOH in H<sub>2</sub>O) with a gradient of MeOH 100% to 70% from 0 to 5 min, 70% to 50% from 5 to 7 min and then 50% MeOH from 7 to 10 min; t<sub>R</sub>= 4.84 min (95.27% pure at 330nm) on the C<sub>18</sub> analytical column; Mobile phase: solvent system B (CH<sub>3</sub>CN and 0.1% HCOOH in H<sub>2</sub>O) with a gradient of CH<sub>3</sub>CN 100% to 70% from 0 to 5 min, 70% to 50% from 5 to 7 min, 50% to 70% CH<sub>3</sub>CN from 7 to 9 min and then 70% CH<sub>3</sub>CN from 9 to 12 min.

**(Z)-2-(3-Methoxybenzylidene)benzofuran-3(2H)-one (5-6)**

This compound was obtained from benzofuran-3(2H)-one (0.10g, 0.75mmol), 3-methoxybenzaldehyde (0.12g, 0.90mmol) and activated basic aluminium oxide (2.75g) as a yellow solid (10% yield) according to Scheme 2-3: mp: 119-122°C (lit: 119-121 °C)<sup>123</sup>; <sup>1</sup>H NMR (Acetone<sub>d-6</sub>, 300MHz): δ 3.89 (s, 3H), 6.85 (s, 1H), 7.03- 7.06 (m, 1H), 7.34 (t, 1H, J= 7.4 Hz), 7.43 (t, 1H, J= 8.1 Hz), 7.53 (d, 1H, J= 8.4 Hz), 7.60 (d, 2H, J= 6.3 Hz), 7.78 – 7.84 (m, 2H); <sup>13</sup>C NMR (CDCl<sub>3</sub>, 75MHz): δ 55.4, 113.0 (2C), 115.8, 116.5, 121.6, 123.5, 124.3, 124.7, 129.9, 133.5, 137.0, 147.0, 159.8, 166.2, 184.8; MS (APCI): m/z 253.3 [M+1]<sup>+</sup>; Anal. calcd for C<sub>16</sub>H<sub>12</sub>O<sub>3</sub>: C, 76.18; H, 4.79; Found: C, 76.56; H, 4.55.

**(Z)-2-(3-Cyanobenzylidene)benzofuran-3(2H)-one (5-7)**

This compound was obtained from benzofuran-3(2H)-one (0.20g, 1.50mmol), 3-cyanobenzaldehyde (0.22g, 1.65mmol) and activated basic aluminium oxide (5.51g) as a yellow solid (77% yield) according to Scheme 2-3: mp: 172-173°C (lit: 172-174 °C)<sup>163</sup>; <sup>1</sup>H NMR(Acetone-d<sub>6</sub>, 300MHz): δ 6.90 (s, 1H), 7.36 (t, 1H, J= 7.5 Hz), 7.56 (d, 1H, J= 8.1 Hz), 7.71 – 7.86 (m, 4H), 8.31 (d, 1H, J=7.8 Hz), 8.40 (s, 1H); <sup>13</sup>C NMR(CDCl<sub>3</sub>, 75MHz): δ 109.7, 113.1, 113.3, 118.4, 121.2, 124.0, 124.9, 129.7, 132.5, 133.6, 134.3, 135.3, 137.5, 147.8, 166.3, 184.5; MS (APCI): m/z 248.4 [M+1]<sup>+</sup>; Anal. calcd for C<sub>16</sub>H<sub>9</sub>NO<sub>2</sub>: C, 77.72; H, 3.67; Found: C, 77.80; H, 3.53.

**(Z)-2-(3-Methylbenzylidene)benzofuran-3(2H)-one (5-8)**

This compound was obtained from benzofuran-3(2H)-one (0.10g, 0.75mmol), 3-methylbenzaldehyde (0.15g, 1.24mmol) and activated basic aluminium oxide (4.13g) as a yellow solid (32% yield) according to Scheme 2-3: mp: 71-74°C; <sup>1</sup>H NMR(Acetone-d<sub>6</sub>, 300MHz): δ 2.36 (s, 3H), 6.77 (s, 1H), 7.22 – 7.38 (m, 3H), 7.44 (d, 1H, J= 8.7 Hz), 7.73 – 7.80 (m, 4H); <sup>13</sup>C NMR (Acetone-d<sub>6</sub>, 75MHz): δ 22.4, 113.9, 114.9, 123.2, 125.6, 125.9, 130.4, 130.6, 132.5, 133.8, 134.1, 139.0, 140.3, 148.5, 167.8, 185.5; MS (APCI): m/z 237.4 [M+1]<sup>+</sup>; Anal. calcd for C<sub>16</sub>H<sub>12</sub>O<sub>2</sub>: C, 81.34; H, 5.12; Found: C, 81.59; H, 4.78.

**(E)-2-Benzylidene-5, 7-dimethoxy-2, 3-dihydro-1H-inden-1-one (6-1)**

This compound was obtained from 5, 7-dimethoxy-2,3-dihydro-1H-inden-1-one I-2 (0.10g, 0.52mmol), benzaldehyde (0.06g, 0.57 mmol) and 50% KOH (1ml) as a yellow solid (33% yield) according to Scheme 2-5: mp: 158 – 159°C; <sup>1</sup>H NMR (CDCl<sub>3</sub>, 300MHz): δ 3.90 (s, 3H), 3.94 (s, 2H), 3.95 (s, 3H), 6.35 (s, 1H), 6.57 (s, 1H), 7.33- 7.45 (m, 3H), 7.53 (s, 1H), 7.62 (d, 2H, J= 7.2 Hz); <sup>13</sup>C NMR (CDCl<sub>3</sub>, 75MHz): δ 32.6, 55.8, 55.9, 97.6, 101.6, 120.6, 128.8, 129.0, 130.4, 131.4, 135.6, 135.8, 154.5, 160.2, 166.9,



190.7; MS (APCI):  $m/z$  281.3  $[M+1]^+$ ; Anal. calcd for  $C_{18}H_{16}O_3$ : C, 77.12; H, 5.75; Found: C, 77.18; H, 5.84.

*(E)*-5, 7-Dimethoxy-2-(2-methoxybenzylidene)-2, 3-dihydro-1H-inden-1-one (**6-2**)

This compound was obtained from 5, 7-dimethoxy-2,3-dihydro-1H-inden-1-one I-2 (0.10g, 0.52 mmol), 2-methoxybenzaldehyde (0.08g, 0.57 mmol) and 50% KOH (1ml) as a off-white solid (50% yield) according to Scheme 2-5: mp: 202 – 203°C;  $^1H$  NMR (DMSO- $d_6$ , 300MHz):  $\delta$  3.86 (s, 3H), 3.87 (s, 3H), 3.88 (s, 3H), 3.95 (s, 2H), 6.51 (s, 1H), 6.72 (s, 1H), 7.03 – 7.12 (m, 2H), 7.41 (t, 1H,  $J=7.8$ Hz), 7.68 – 7.72 (m, 2H);  $^{13}C$  NMR (CDCl $_3$ , 75MHz):  $\delta$  32.6, 55.6, 55.7, 55.9, 97.6, 101.5, 111.0, 120.3, 120.9, 124.9, 126.2, 129.5, 130.4, 135.6, 154.6, 158.8, 160.2, 166.7, 190.8; MS (APCI):  $m/z$  311.3  $[M+1]^+$ ; Anal. calcd for  $C_{19}H_{18}O_4$ : C, 73.53; H, 5.85; Found: C, 73.41; H, 5.79.

*(E)*-5, 7-Dimethoxy-2-(3-methoxybenzylidene)-2, 3-dihydro-1H-inden-1-one (**6-3**)

This compound was obtained from 5, 7-dimethoxy-2,3-dihydro-1H-inden-1-one I-2 (0.10g, 0.52 mmol), 3-methoxybenzaldehyde (0.08g, 0.57 mmol) and 50% KOH (1ml) as a off-white solid (58% yield) according to Scheme 2-5: mp: 182 – 183°C;  $^1H$  NMR (DMSO- $d_6$ , 300MHz):  $\delta$  3.82 (s, 3H), 3.87 (s, 3H), 3.89 (s, 3H), 4.01 (s, 2H), 6.51 (s, 1H), 6.75 (s, 1H), 6.98 – 7.01 (m, 1H), 7.26 – 7.31 (m, 3H), 7.39 (t, 1H,  $J= 7.8$  Hz);  $^{13}C$  NMR (CDCl $_3$ , 75MHz):  $\delta$  32.6, 55.3, 55.8, 55.9, 97.6, 101.5, 114.7, 115.8, 120.6, 122.9, 129.7, 131.3, 135.8, 137.1, 154.4, 159.7, 160.2, 166.9, 190.7; MS (APCI):  $m/z$  311.0  $[M+1]^+$ ; Anal. calcd for  $C_{19}H_{18}O_4$ : C, 73.53; H, 5.85; Found: C, 73.53; H, 5.92.

*(E)*-5, 7-Dimethoxy-2-(4-methoxybenzylidene)-2, 3-dihydro-1H-inden-1-one (**6-4**)

This compound was obtained from 5, 7-dimethoxy-2,3-dihydro-1H-inden-1-one I-2 (0.10g, 0.52 mmol), 4-methoxybenzaldehyde (0.08g, 0.57 mmol) and 50% KOH (1ml) as

a orange solid (59% yield) according to Scheme 2-5: mp: 163 – 164°C; <sup>1</sup>H NMR (DMSO-d<sub>6</sub>, 300MHz): δ 3.82 (s, 3H), 3.86 (s, 3H), 3.88 (s, 3H), 3.95 (s, 2H), 6.50 (s, 1H), 6.73 (s, 1H), 7.04 (d, 2H, J= 8.7 Hz), 7.28 (s, 1H), 7.67 (d, 2H, J = 8.7 Hz); <sup>13</sup>C NMR (CDCl<sub>3</sub>, 75MHz): δ 32.5, 55.2, 55.6, 55.7, 97.4, 101.4, 114.2, 120.6, 128.4, 131.0, 132.0, 133.1, 154.2, 159.9, 160.2, 166.5, 190.7 MS (APCI): m/z 311.3 [M+1]<sup>+</sup>; Anal. calcd for C<sub>19</sub>H<sub>18</sub>O<sub>4</sub>: C, 73.53; H, 5.85; Found: C, 73.50; H, 5.80.

*(E)*-5, 7-Dimethoxy-2-(3-hydroxybenzylidene)-2, 3-dihydro-1H-inden-1-one (**6-5**)

This compound was obtained from 5, 7-dimethoxy-2,3-dihydro-1H-inden-1-one I-2 (0.14g, 0.72 mmol), 3-(tetrahydro-2H-pyran-2-yloxy)benzaldehyde (0.10g, 0.80 mmol) and 50% KOH (1ml) as a yellow solid (15% yield) according to Scheme 2-5: <sup>1</sup>H NMR (DMSO-d<sub>6</sub>, 300MHz): δ 3.82 (s, 3H), 3.85 (s, 3H), 3.91 (s, 2H), 6.47 (s, 1H), 6.69 (s, 1H), 6.78 (d, 1H, J= 7.8Hz), 7.05 – 7.11 (m, 2H), 7.16 (s, 1H), 7.23 (t, 1H, J= 7.8Hz); <sup>13</sup>C NMR (DMSO-d<sub>6</sub>, 75 MHz): δ 32.1, 55.7, 56.0, 97.6, 102.4, 116.5, 116.7, 119.4, 121.6, 130.0, 130.1, 135.9, 136.4, 154.5, 157.6, 159.7, 166.7, 189.2; MS (APCI): m/z 297.3 [M+1]<sup>+</sup>; HRMS (ESI) calcd for C<sub>18</sub>H<sub>17</sub>O<sub>4</sub> [M+1]<sup>+</sup> 297.1127, found 297.1100; Anal. calcd for C<sub>18</sub>H<sub>16</sub>O<sub>4</sub>: C, 72.96; H, 5.44; Found: C, 72.52; H, 5.51; HPLC analyses: t<sub>R</sub>= 3.25 min (96.1% pure at 360nm) on the C<sub>18</sub> analytical column; Mobile phase: solvent system A (MeOH and 0.1% HCOOH in H<sub>2</sub>O) with a gradient of MeOH 100% to 70% from 0 to 5 min, 70% to 50% from 5 to 7 min, 50% to 70% from 7 to 10 min and then 70% to 100% MeOH from 10 min to 15 min; t<sub>R</sub>= 3.27 min (99.5% pure at 330nm) on the C<sub>18</sub> analytical column; Mobile phase, solvent system B (CH<sub>3</sub>CN and 0.1% HCOOH in H<sub>2</sub>O) with a gradient of CH<sub>3</sub>CN 100% to 70% from 0 to 5 min, 70% to 50% from 5 to 7min, 50% to 70% from 7 to 9 min and then 70% to 100% CH<sub>3</sub>CN from 9 min to 12 min.

*(E)*-5, 7-Dimethoxy-2-(4-hydroxybenzylidene)-2, 3-dihydro-1H-inden-1-one (**6-6**)

This compound was obtained from 5, 7-dimethoxy-2,3-dihydro-1H-inden-1-one I-2 (0.10g, 0.54 mmol), 4-(tetrahydro-2H-pyran-2-yloxy)benzaldehyde (0.15g, 0.71 mmol) and 50% KOH (1ml) as a yellow solid (43% yield) according to Scheme 2-5: mp: 285 – 286°C; <sup>1</sup>H NMR (DMSO-d<sub>6</sub>, 300MHz): δ 3.84 (s, 3H), 3.86 (s, 3H), 3.89 (s, 2H), 6.47 (s, 1H), 6.70 (s,1H), 6.87 (d, 2H, J= 8.4 Hz), 7.23 (s, 1H), 7.55 (d, 2H, J= 8.7 Hz), 10. 02 (broad s, 1H); <sup>13</sup>C NMR (DMSO-d<sub>6</sub>, 75 MHz): δ 32.0, 55.5, 55.8, 97.4, 102.2, 115.9, 119.6, 126.3, 130.2, 132.3, 132.5, 154.2, 158.7, 159.4, 166.2, 189.3; MS (APCI): m/z 297.3 [M+1]<sup>+</sup>; Anal. calcd for C<sub>18</sub>H<sub>16</sub>O<sub>4</sub>: C, 72.96; H, 5.44; Found: C, 72.87; H, 5.64.

*(E)*-5, 7-Dimethoxy-2-(2-chlorobenzylidene)-2, 3-dihydro-1H-inden-1-one (**6-7**)

This compound was obtained from 5, 7-dimethoxy-2,3-dihydro-1H-inden-1-one I-2 (0.10g, 0.52 mmol), 2-chlorobenzaldehyde (0.08g, 0.57 mmol) and 50% KOH (1ml) as off-white solid (77% yield) according to Scheme 2-5: mp: 246 – 247°C; <sup>1</sup>H NMR (CDCl<sub>3</sub>, 300MHz): δ 3.86 (s, 2H), 3.89 (s, 3H), 3.96 (s, 3H), 6.39 (s, 1H), 6.53 (s, 1H), 7.28 - 7.34 (m, 2H), 7.45 (dd, 1H, J= 1.8, 2.1Hz), 7.61 – 7.64 (m, 1H), 7.89 (s, 1H); <sup>13</sup>C NMR (CDCl<sub>3</sub>, 75MHz): δ 32.0, 55.8, 55.9, 97.6, 101.6, 120.6, 126.6, 127.6, 129.7, 129.8, 130.2, 134.0, 135.8, 138.0, 154.5, 160.4, 167.0, 190.1; MS (APCI): m/z 315.3 [M+1]<sup>+</sup>; Anal. calcd for C<sub>18</sub>H<sub>15</sub>ClO<sub>3</sub>: C, 68.68; H, 4.80; Found: C, 68.46; H, 4.92.

*(E)*-5, 7-Dimethoxy-2-(3-chlorobenzylidene)-2, 3-dihydro-1H-inden-1-one (**6-8**)

This compound was obtained from 5, 7-dimethoxy-2,3-dihydro-1H-inden-1-one I-2 (0.10g, 0.52 mmol), 3-chlorobenzaldehyde (0.08g, 0.57 mmol) and 50% KOH (1ml) as a white solid (63% yield) according to Scheme 2-5: <sup>1</sup>H NMR (CDCl<sub>3</sub>, 300MHz): δ 3.91 (s, 3H), 3.94 (s, 2H), 3.96 (s, 3H), 6.36 (s, 1H), 6.59 (s, 1H), 7.32- 7.39 (m, 2H), 7.46- 7.50 (m, 2H), 7.60 (s, 1H); <sup>13</sup>C NMR (CDCl<sub>3</sub>, 75MHz): δ 32.5, 55.8, 55.9, 97.8, 101.6, 120.5,

128.7, 128.9, 129.7, 129.8, 130.0, 134.7, 136.9, 137.6, 154.3, 160.3, 167.1, 190.3; MS (APCI):  $m/z$  315.4  $[M+1]^+$ ; Anal. calcd for  $C_{18}H_{15}ClO_3$ : C, 68.68; H, 4.80; Found: C, 68.23; H, 4.67; HPLC analyses:  $t_R$  = 3.95 min (97.5% pure at 360nm) on the  $C_{18}$  analytical column; Mobile phase: solvent system A (MeOH and 0.1% HCOOH in  $H_2O$ ) with a gradient of MeOH 100% to 70% from 0 to 5 min, 70% to 50% from 5 to 7min, 50% to 70% from 7 to 10min and then 70% to 100% MeOH from 10min to 15min;  $t_R$  = 3.96 min (99.6% pure at 300nm) on the  $C_{18}$  analytical column; Mobile phase, solvent system B ( $CH_3CN$  and 0.1% HCOOH in  $H_2O$ ) with a gradient of  $CH_3CN$  100% to 70% from 0 to 5 min, 70% to 50% from 5 to 7min, 50% to 70% from 7 to 9 min and then 70% to 100%  $CH_3CN$  from 9 min to 12 min.

*(E)*-5, 7-Dimethoxy-2-(4-chlorobenzylidene)-2, 3-dihydro-1H-inden-1-one (**6-9**)

This compound was obtained from 5, 7-dimethoxy-2,3-dihydro-1H-inden-1-one I-2 (0.10g, 0.52 mmol), 4-chlorobenzaldehyde (0.08g, 0.57 mmol) and 50% KOH (1ml) as a white solid (50% yield) according to Scheme 2-5: mp: 173 – 175°C;  $^1H$  NMR ( $CDCl_3$ , 300MHz):  $\delta$  3.91 (s, 5H), 3.96 (s, 3H), 6.36 (s, 1H), 6.57 (s, 1H), 7.40 (d, 2H,  $J$  = 8.4 Hz) 7.48 (s, 1H), 7.55 (d, 2H,  $J$  = 8.4 Hz);  $^{13}C$  NMR ( $CDCl_3$ , 75MHz):  $\delta$  32.5, 55.8, 55.8, 97.6, 101.5, 120.5, 129.0, 129.9, 131.4, 134.2, 134.9, 136.0, 154.2, 160.2, 167.0, 190.4; MS (APCI):  $m/z$  315.3  $[M+1]^+$ ; Anal. calcd for  $C_{18}H_{15}ClO_3$ : C, 68.68; H, 4.80; Found: C, 68.81; H, 4.79.

*(E)*-5, 7-Dimethoxy-2-(3-cyanobenzylidene)-2, 3-dihydro-1H-inden-1-one (**6-10**)

This compound was obtained from 5, 7-dimethoxy-2,3-dihydro-1H-inden-1-one I-2 (0.10g, 0.52 mmol), 3-cyanobenzaldehyde (0.07g, 0.57 mmol) and 50% KOH (1ml) as an-off white solid (38% yield) according to Scheme 2-5: mp: 240 – 243°C;  $^1H$  NMR ( $DMSO-d_6$ , 300 MHz):  $\delta$  3.87 (s, 3H), 3.89 (s, 3H), 4.05 (s, 2H), 6.51 (s, 1H), 6.75 (s,

1H), 7.32 (s, 1H), 7.67 (t, 1H, J= 7.8 Hz), 7.85 (d, 1H, J= 7.5 Hz), 8.03 (d, 1H, J=7.8 Hz), 8.15 (s, 1H); <sup>13</sup>C NMR (DMSO-d<sub>6</sub>, 75 MHz): δ 32.0, 55.9, 56.2, 97.8, 102.7, 112.3, 118.9, 119.4, 128.0, 130.4, 132.6, 133.5, 135.0, 136.6, 138.7, 154.9, 160.1, 167.3, 189.3; MS (APCI): m/z 306.3 [M+1]<sup>+</sup>; Anal. calcd for C<sub>19</sub>H<sub>15</sub>NO<sub>3</sub>: C, 74.74; H, 4.95; Found: C, 74.7; H, 5.05.

*(E)*-5, 7-Dimethoxy-2-(4-cyanobenzylidene)-2, 3-dihydro-1H-inden-1-one (**6-11**)

This compound was obtained from 5, 7-dimethoxy-2,3-dihydro-1H-inden-1-one I-2 (0.10g, 0.52 mmol), 4-cyanobenzaldehyde (0.08g, 0.57 mmol) and 50% KOH (1ml) as a white solid (31% yield) according to Scheme 2-5: mp: 238 – 239°C; <sup>1</sup>H NMR (DMSO-d<sub>6</sub>, 300 MHz): δ 3.87 (s, 3H), 3.89 (s, 3H), 4.02 (s, 2H), 6.51 (s,1H), 6.71 (s, 1H), 7.34 (s, 1H), 7.87-7.93 (m, 4H); <sup>13</sup>C NMR (CDCl<sub>3</sub>, 75MHz): δ 32.5, 55.9, 56.0, 97.8, 101.7, 112.0, 118.6, 120.4, 128.9, 130.5, 132.5, 138.9, 140.2, 154.1, 160.5, 167.4, 189.9; MS (APCI): m/z 306.3 [M+1]<sup>+</sup>; Anal. calcd for C<sub>19</sub>H<sub>15</sub>NO<sub>3</sub>: C, 74.74; H, 4.95; Found: C, 74.81; H, 5.02.

*(E)*-5, 7-Dimethoxy-2-(2-methylbenzylidene)-2, 3-dihydro-1H-inden-1-one (**6-12**)

This compound was obtained from 5, 7-dimethoxy-2,3-dihydro-1H-inden-1-one I-2 (0.10g, 0.52 mmol), 2-methylbenzaldehyde (0.07g, 0.57 mmol) and 50% KOH (1ml) as a white solid (56% yield) according to Scheme 2-5: mp: 193 – 195°C; <sup>1</sup>H NMR (DMSO-d<sub>6</sub>, 300MHz): δ 2.39 (s, 3H), 3.87 (s, 3H), 3.88 (s, 3H), 3.92 (s, 2H), 6.52 (s, 1H), 6.72 (s, 1H), 7.30 (d, 3H, J= 2.7 Hz), 7.51 (s, 1H), 7.66 – 7.69 (m, 1H); <sup>13</sup>C NMR (CDCl<sub>3</sub>, 75MHz): δ 20.1, 32.2, 55.8, 55.9, 97.6, 101.5, 120.8, 125.9, 128.4, 128.8, 129.3, 130.7, 134.6, 136.4, 138.9, 154.8, 160.3, 166.8, 190.6; MS (APCI): m/z 295.3 [M+1]<sup>+</sup>; Anal. calcd for C<sub>19</sub>H<sub>18</sub>O<sub>3</sub>: C, 77.53; H, 6.16; Found: C, 77.43; H, 6.12.

*(E)*-5, 7-Dimethoxy-2-(3-methylbenzylidene)-2, 3-dihydro-1H-inden-1-one (**6-13**)

This compound was obtained from 5, 7-dimethoxy-2,3-dihydro-1H-inden-1-one I-2 (0.13g, 0.68 mmol), 3-methylbenzaldehyde (0.09g, 0.75 mmol) and 50% KOH (1ml) as a white solid (65% yield) according to Scheme 2-5: mp: 205 – 207°C; <sup>1</sup>H NMR (CDCl<sub>3</sub>, 300MHz): δ 2.40 (s, 3H), 3.89 (s, 3H), 3.91 (s, 2H), 3.94 (s, 3H), 6.33 (s, 1H), 6.57 (s, 1H), 7.17 (d, 1H, J= 7.2 Hz), 7.32 (t, 1H, J= 7.5 Hz), 7.42 (s, 2H), 7.50 (s, 1H); <sup>13</sup>C NMR (CDCl<sub>3</sub>, 75MHz): 21.5, 32.6, 55.7, 55.8, 97.6, 101.5, 120.6, 127.4, 128.6, 129.9, 131.2, 131.5, 135.3, 135.7, 138.4, 154.5, 160.1, 166.8, 190.8; MS (APCI): m/z 295.3 [M+1]<sup>+</sup>; Anal. calcd for C<sub>19</sub>H<sub>18</sub>O<sub>3</sub>: C, 77.53; H, 6.16; Found: C, 77.60; H, 6.14.

*(E)*-5, 7-Dimethoxy-2-(4-methylbenzylidene)-2, 3-dihydro-1H-inden-1-one (**6-14**)

This compound was obtained from 5, 7-dimethoxy-2,3-dihydro-1H-inden-1-one I-2 (0.10g, 0.52 mmol), 4-methylbenzaldehyde (0.07g, 0.57 mmol) and 50% KOH (1ml) as a white solid (56% yield) according to Scheme 2-5: mp: 196 – 197°C; <sup>1</sup>H NMR (DMSO-d<sub>6</sub>, 300MHz): δ 2.35 (s, 3H), 3.86 (s, 3H), 3.89 (s, 3H), 3.97 (s, 2H), 6.50 (s, 1H), 6.73 (s, 1H), 7.29 (d, 3H, J = 8.1Hz), 7.61 (d, 2H, J = 8.1 Hz); <sup>13</sup>C NMR (CDCl<sub>3</sub>, 75MHz): δ 21.5, 32.7, 55.8, 55.9, 97.6, 101.6, 120.8, 129.6, 130.5, 131.5, 133.0, 134.6, 139.4, 154.5, 160.2, 166.8, 190.9; MS (APCI): m/z 295.3 [M+1]<sup>+</sup>; Anal. calcd for C<sub>19</sub>H<sub>18</sub>O<sub>3</sub>: C, 77.53; H, 6.16; Found: C, 77.35; H, 6.13.

*(E)*-5, 7-Dimethoxy-2-(3, 5-dimethoxybenzylidene)-2, 3-dihydro-1H-inden-1-one (**6-15**)

This compound was obtained from 5, 7-dimethoxy-2,3-dihydro-1H-inden-1-one I-2 (0.10g, 0.52 mmol), 3, 5-dimethoxybenzaldehyde (0.10g, 0.57 mmol) and 50% KOH (1ml) as an orange solid (33% yield) according to Scheme 2-5: mp: 218°C (lit: 194 °C)<sup>165</sup>; <sup>1</sup>H NMR (CDCl<sub>3</sub>, 300MHz): δ 3.84 (s, 3H x 2), 3.90 (s, 3H), 3.93 (s, 2H), 3.96 (s, 3H), 6.35 (s, 1H), 6.49 (t, 1H, J=2.1 Hz), 6.57 (s, 1H), 6.77 (d, 2H, J= 2.1 Hz), 7.45 (s, 1H); <sup>13</sup>C

NMR (CDCl<sub>3</sub>, 75MHz):  $\delta$  32.6, 55.5, 55.8, 55.9, 97.7, 101.3, 101.5, 108.4, 120.6, 131.4, 136.0, 137.5, 154.5, 160.2, 160.9, 167.0, 190.6; MS (APCI):  $m/z$  341.3 [M+1]<sup>+</sup>; Anal. calcd for C<sub>20</sub>H<sub>20</sub>O<sub>5</sub>: C, 70.57; H, 5.92; Found: C, 70.77; H, 5.96.

*(E)*-5, 7-Dimethoxy-2-(3, 5-dihydroxybenzylidene)-2, 3-dihydro-1H-inden-1-one (**6-16**)

This compound was obtained from 5, 7-dimethoxy-2,3-dihydro-1H-inden-1-one I-2 (0.10g, 0.52 mmol), 3,5-bis(tetrahydro-2H-pyran-2-yloxy)benzaldehyde (0.20g, 0.66 mmol) and 50% KOH (1ml) as a pale orange solid (36% yield) according to Scheme 2-5: <sup>1</sup>H NMR (DMSO-d<sub>6</sub>, 300 MHz):  $\delta$  2.99 (s, 3H), 3.01 (s, 3H), 3.03 (s, 2H), 5.41 (s, 1H), 5.64 (s, 1H), 5.68 (d, 2H, J = 1.8 Hz), 5.85 (s, 1H), 6.21 (s, 1H), 8.60 (s, 2H); <sup>13</sup>C NMR (DMSO-d<sub>6</sub>, 75 MHz):  $\delta$  33.1, 56.7, 57.0, 98.6, 103.5, 104.9, 109.5, 120.5, 131.5, 136.6, 137.7, 155.4, 159.7, 160.7, 167.6, 190.2; MS (APCI):  $m/z$  313.2 [M+1]<sup>+</sup>; Anal. calcd for C<sub>18</sub>H<sub>16</sub>O<sub>5</sub>: C, 69.22; H, 5.16; Found: C, 69.31; H, 5.27.

*(E)*-5, 7-Dimethoxy-2-(3-methoxy-4-hydroxy-benzylidene)-2, 3-dihydro-1H-inden-1-one (**6-17**)

This compound was obtained from 5, 7-dimethoxy-2,3-dihydro-1H-inden-1-one I-2 (0.10g, 0.52 mmol), 3-methoxy-4-(tetrahydro-pyran-2-yloxy)benzaldehyde (0.12g, 0.77 mmol), and 50% KOH (1ml) as a pale yellow solid (63% yield) according to Scheme 2-5: mp: 213 - 214°C; <sup>1</sup>H NMR (DMSO-d<sub>6</sub>, 300MHz):  $\delta$  3.84 (s, 3H), 3.85 (s, 3H), 3.87 (s, 3H), 3.95 (s, 2H), 6.48 (s, 1H), 6.73 (s, 1H), 6.87 (d, 1H, J = 8.4 Hz), 7.17 (d, 1H, J = 8.4 Hz), 7.25 (d, 2H, J = 5.7 Hz), 9.63 (s, 1H); <sup>13</sup>C NMR (DMSO-d<sub>6</sub>, 75MHz):  $\delta$  31.9, 55.5, 55.6, 55.9, 97.5, 102.2, 114.2, 115.8, 119.6, 124.4, 126.7, 130.7, 132.7, 147.7, 148.2, 154.3, 159.4, 166.3, 189.3 ppm; MS (APCI):  $m/z$  327.5 [M+1]<sup>+</sup>; Anal. calcd for C<sub>19</sub>H<sub>18</sub>O<sub>5</sub>: C, 69.93; H, 5.56; Found: C, 69.71; H, 5.38.

*(E)*-5, 7-Dimethoxy-2-(3-hydroxy-4-methoxy-benzylidene)-2, 3-dihydro-1H-inden-1-one (**6-18**)

This compound was obtained from 5, 7-dimethoxy-2,3-dihydro-1H-inden-1-one I-2 (0.10g, 0.52 mmol), 4-methoxy-3-(tetrahydro-pyran-2-yloxy)benzaldehyde (0.12g, 0.77 mmol), and 50% KOH (1ml) as a yellow solid (70% yield) according to Scheme 2-5: mp: 220 - 221°C; <sup>1</sup>H NMR (DMSO-d<sub>6</sub>, 300MHz): δ 3.82 (s, 3H), 3.85 (s, 3H), 3.88 (s, 3H), 3.89 (s, 2H), 6.49 (s, 1H), 6.71 (s, 1H), 7.01 (d, 1H, J = 8.1 Hz), 7.13-7.17 (m, 3H), 9.25 (s, 1H); <sup>13</sup>C NMR (DMSO-d<sub>6</sub>, 75MHz): δ 32.0, 55.6, 55.6, 55.8, 97.5, 102.3, 112.2, 116.7, 119.6, 123.2, 128.0, 130.3, 133.3, 146.6, 149.0, 154.2, 159.5, 166.4, 189.2 ppm; MS (APCI): m/z 327.5 [M+1]<sup>+</sup>; Anal. calcd for C<sub>19</sub>H<sub>18</sub>O<sub>5</sub>: C, 69.93; H, 5.56; Found: C, 69.70; H, 5.48.

*(E)*-5, 7-Dimethoxy-2-(3, 4-dihydroxy-benzylidene)-2, 3-dihydro-1H-inden-1-one (**6-19**)

This compound was obtained from 5, 7-dimethoxy-2,3-dihydro-1H-inden-1-one I-2 (0.10g, 0.52 mmol), 3,4-bis(tetrahydro-2H-pyran-2-yloxy)benzaldehyde (0.23g, 0.77 mmol) and 50% KOH (1ml) as a golden solid (72% yield) according to Scheme 2-5: mp: 289 - 290°C; <sup>1</sup>H NMR (DMSO-d<sub>6</sub>, 300MHz): δ 3.85 (s, 3H), 3.88 (s, 5H), 6.49 (s, 1H), 6.71 (s, 1H), 6.83 (d, 1H, J = 8.4 Hz), 7.03 (d, 1H, J = 8.4 Hz), 7.13-7.14 (m, 2H); <sup>13</sup>C NMR (DMSO-d<sub>6</sub>, 75MHz): δ 32.0, 55.5, 55.8, 97.4, 102.3, 115.9, 117.2, 119.6, 123.4, 126.7, 130.7, 132.3, 145.5, 147.3, 154.1, 159.4, 166.2, 189.2; MS (APCI): m/z 313.5 [M+1]<sup>+</sup>; Anal. calcd for C<sub>18</sub>H<sub>16</sub>O<sub>5</sub>: C, 69.22; H, 5.16; Found: C, 69.53; H, 5.03.

*(E)*-5, 7-Dimethoxy-2-(3, 4-dimethoxybenzylidene)-2, 3-dihydro-1H-inden-1-one (**6-20**)

This compound was obtained from 5, 7-dimethoxy-2,3-dihydro-1H-inden-1-one I-2 (0.10g, 0.52 mmol), 3, 4-dimethoxybenzaldehyde (0.14g, 0.77 mmol) and 50% KOH (1ml) as a light beige solid (66% yield) according to Scheme 2-5: mp: 183-185°C; <sup>1</sup>H NMR (DMSO-d<sub>6</sub>, 300MHz): δ 3.81 (s, 3H), 3.85 (s, 6H), 3.88 (s, 3H), 3.98 (s, 2H), 6.49



(s, 1H), 6.74 (s, 1H), 7.04 (d, 1H, J = 8.7 Hz), 7.27-7.29 (m, 3H); <sup>13</sup>C NMR (DMSO-d<sub>6</sub>, 75MHz): δ 31.8, 55.5 (3C), 55.8, 97.6, 102.2, 111.8, 113.3, 119.5, 124.1, 128.0, 130.2, 133.6, 148.7, 149.9, 154.3, 159.5, 166.4, 189.2; MS (APCI): m/z 341.5 [M+1]<sup>+</sup>; Anal. calcd for C<sub>20</sub>H<sub>20</sub>O<sub>5</sub>: C, 70.57; H, 5.92; Found: C, 70.69; H, 5.64.

**(Z)-2-Benzylidene-4,6-dimethoxyindolin-3-one (7-1)**

This compound was obtained from 1-acetyl-4,6-dimethoxy-2,3-dihydro-1H-indole-3-one AZ-2 (0.09g, 0.38mmol), benzaldehyde (0.05g, 0.47 mmol) and 50% KOH (1ml) as a orangy-yellow solid (44% yield) according to Scheme 2-6: mp: 151-153°C (lit: 152-154 °C)<sup>105</sup>; <sup>1</sup>H NMR (Acetone-d<sub>6</sub>, 500MHz): δ 3.86 (s, 3H x 2), 6.02 (d, 1H, J= 2.0Hz), 6.24 (d, 1H, J= 1.5Hz), 6.50 (s, 1H), 7.29 (t, 1H, J= 7.5Hz), 7.41 (t, 2H, J= 8.0 Hz), 7.63 (d, 2H, J= 7.5 Hz), 8.93 (br s, -NH); <sup>13</sup>C NMR (DMSO-d<sub>6</sub>, 75MHz): δ 55.6, 55.8, 88.8, 90.6, 103.1, 107.1, 127.9, 128.9, 129.4, 134.4, 135.4, 157.1, 159.7, 168.1, 181.5; MS (APCI): m/z 282.4 [M+1]<sup>+</sup>; HPLC analyses: t<sub>R</sub>= 16.99 min (96.4% pure at 360nm) on the C<sub>18</sub> analytical column; Mobile phase: solvent system A [70% MeOH and 30% (0.1% HCOOH in H<sub>2</sub>O)] isocratic; t<sub>R</sub>= 6.99 min (99.7% pure at 360nm) on the C<sub>18</sub> analytical column; Mobile phase: solvent system B (CH<sub>3</sub>CN and 0.1% HCOOH in H<sub>2</sub>O) with a gradient of CH<sub>3</sub>CN 40% to 50% from 0 to 7 min and 50% to 70% from 7 to 10 min and then 70% CH<sub>3</sub>CN from 10 to 15 min.

**(Z)-4,6-Dimethoxy-2-(3-methoxybenzylidene)indolin-3-one (7-2)**

This compound was obtained from 1-acetyl-4,6-dimethoxy-2,3-dihydro-1H-indole-3-one AZ-2 (0.10g, 0.43mmol), 3-methoxybenzaldehyde (0.06g, 0.47 mmol) and 50% KOH (1ml) as a orangy-yellow solid (44% yield) according to Scheme 2-6: mp: 112-115°C; <sup>1</sup>H NMR (Acetone-d<sub>6</sub>, 300MHz): δ 3.81 (s, 2 x 3H), 3.84 (s, 3H), 5.99 (d, 1H, J= 1.5Hz), 6.21 (d, 1H, J= 1.5Hz), 6.37 (s, 1H), 6.90 (dd, 1H, J= 2.1, 2.1Hz), 7.19 – 7.24 (m, 2H), 7.35 (t,

<sup>1</sup>H, J= 8.0 Hz), 9.70 (br s, -NH); <sup>13</sup>C NMR (Acetone<sub>d-6</sub>, 75MHz): δ 55.6, 56.0, 56.2, 89.6, 91.6, 104.9, 107.9, 114.2, 115.4, 122.5, 130.7, 137.3, 158.2, 161.0, 161.1, 169.4, 182.4; MS (APCI): m/z 312.3 [M+1]<sup>+</sup>; HPLC analyses: t<sub>R</sub>= 19.53 min (96.0% pure at 360nm) on the C<sub>18</sub> analytical column; Mobile phase: solvent system A [70% MeOH and 30% (0.1% HCOOH in H<sub>2</sub>O)] isocratic; t<sub>R</sub>= 8.39 min (99.5% pure at 360nm) on the C<sub>18</sub> analytical column; Mobile phase: solvent system B (CH<sub>3</sub>CN and 0.1% HCOOH in H<sub>2</sub>O) with a gradient of CH<sub>3</sub>CN 40% to 50% from 0 to 7 min and 50% to 70% from 7 to 10 min and then 70% CH<sub>3</sub>CN from 10 to 15 min.

**(Z)-4,6-Dimethoxy-2-(4-methoxybenzylidene)indolin-3-one (7-3)**

This compound was obtained from 1-acetyl-4,6-dimethoxy-2,3-dihydro-1H-indole-3-one AZ-2 (0.13g, 0.53mmol), 4-methoxybenzaldehyde (0.08g, 0.59 mmol) and 50% KOH (1ml) as a orangy-yellow solid (18% yield) according to Scheme 2-6: mp: 117-120°C; <sup>1</sup>H NMR (Acetone<sub>d-6</sub>, 300MHz): δ 3.83 (s, 3H), 3.86 (s, 6H), 6.00 (d, 1H, J= 1.5Hz), 6.23 (d, 1H, J= 1.5Hz), 6.49 (s, 1H), 6.98 (d, 2H, J= 8.7Hz), 7.60 (d, 2H, J= 8.7 Hz), 8.79 (br s, -NH); <sup>13</sup>C NMR (Acetone<sub>d-6</sub>, 75MHz): δ 55.7, 55.9, 56.1, 89.4, 91.5, 108.5, 115.3, 128.4, 131.8, 135.7, 158.0, 160.4, 161.0, 169.1, 182.4; MS (APCI): m/z 312.4 [M+1]<sup>+</sup>; HPLC analyses: t<sub>R</sub>= 15.45 min (99.0% pure at 360nm) on the C<sub>18</sub> analytical column; Mobile phase: solvent system A [70% MeOH and 30% (0.1% HCOOH in H<sub>2</sub>O)] isocratic; t<sub>R</sub>= 4.82 min (98.0% pure at 360nm) on the C<sub>18</sub> analytical column; Mobile phase: solvent system B (CH<sub>3</sub>CN and 0.1% HCOOH in H<sub>2</sub>O) with a gradient of CH<sub>3</sub>CN 40% to 50% from 0 to 7 min and 50% to 70% from 7 to 10 min and then 70% CH<sub>3</sub>CN from 10 to 15 min.

**(Z)-4,6-Dimethoxy-2-(3-chlorobenzylidene)indolin-3-one (7-4)**

This compound was obtained from 1-acetyl-4,6-dimethoxy-2,3-dihydro-1H-indole-3-one AZ-2 (0.10g, 0.43mmol), 3-chlorobenzaldehyde (0.07g, 0.47 mmol) and 50% KOH (1ml) as a orangy-yellow solid (4% yield) according to Scheme 2-6: mp: 113-116°C; <sup>1</sup>H NMR (Acetone<sub>d-6</sub>, 300MHz): δ 3.86 (2 x 3H), 6.02 (s, 1H), 6.22 (s, 1H), 6.45 (s, 1H), 7.41 (d, 2H, J= 8.1Hz), 7.64 (d, 2H, J= 8.1 Hz), 8.98 (br s, -NH); <sup>13</sup>C NMR (Acetone<sub>d-6</sub>, 75MHz): δ 56.0, 56.2, 89.8, 91.8, 105.8, 128.2, 128.7, 129.3, 131.3, 135.2, 137.8, 138.3, 158.2, 161.3, 169.6 (2C), 182.2; MS (APCI): m/z 316.5 [M+1]<sup>+</sup>; HPLC analyses: t<sub>R</sub>= 17.66 min (95.4% pure at 360nm) on the C<sub>18</sub> analytical column; Mobile phase: solvent system A (MeOH and 0.1% HCOOH in H<sub>2</sub>O) with a gradient of MeOH 50% to 60% from 0 to 3 min, 60% to 70% from 3 to 5 min, 70% to 80% from 5 to 7 min and then 80% MeOH from 7 to 30 min; t<sub>R</sub>= 8.41 min (97.6% pure at 360nm) on the C<sub>18</sub> analytical column; Mobile phase: solvent system B (CH<sub>3</sub>CN and 0.1% HCOOH in H<sub>2</sub>O) with a gradient of CH<sub>3</sub>CN 40% to 50% from 0 to 7 min and 50% to 70% from 7 to 10 min and then 70% CH<sub>3</sub>CN from 10 to 15 min.

**(Z)-4,6-Dimethoxy-2-(4-chlorobenzylidene)indolin-3-one (7-5)**

This compound was obtained from 1-acetyl-4,6-dimethoxy-2,3-dihydro-1H-indole-3-one AZ-2 (0.10g, 0.43mmol), 4-chlorobenzaldehyde (0.07g, 0.47 mmol) and 50% KOH (1ml) as a orangy-yellow solid (18% yield) according to Scheme 2-6: mp: 135-138°C (lit: 146-148 °C)<sup>105</sup>; <sup>1</sup>H NMR (Acetone<sub>d-6</sub>, 300MHz): δ 3.88 (2 x 3H), 6.04 (d, 1H, J=1.5 Hz), 6.21 (d, 1H, J=1.5 Hz), 6.43 (s, 1H), 7.31 (d, 1H, J= 7.8 Hz), 7.43 (t, 1H, J= 7.8 Hz), 7.56 (d, 1H, J=7.8 Hz), 7.65 (s, 1H), 9.05 (br s, -NH); <sup>13</sup>C NMR (Acetone<sub>d-6</sub>, 75MHz): δ 57.2, 57.5, 90.9, 93.0, 106.0, 107.5, 131.0, 132.8, 134.7, 136.2, 138.5, 159.3, 162.4, 170.8, 183.6; MS (APCI): m/z 316.5 [M+1]<sup>+</sup>; HPLC analyses: t<sub>R</sub>= 5.33 min (99.9% pure at 360nm) on the C<sub>18</sub> analytical column; Mobile phase: solvent system A [70% MeOH and

30% (0.1% HCOOH in H<sub>2</sub>O)] isocratic;  $t_R$  = 7.77 min (97.4% pure at 360nm) on the C<sub>18</sub> analytical column; Mobile phase: solvent system B (CH<sub>3</sub>CN and 0.1% HCOOH in H<sub>2</sub>O) with a gradient of CH<sub>3</sub>CN 40% to 50% from 0 to 7 min and 50% to 70% from 7 to 10 min and then 70% CH<sub>3</sub>CN from 10 to 15 min.

**(Z)-4,6-Dimethoxy-2-(3-cyanobenzylidene)indolin-3-one (7-6)**

This compound was obtained from 1-acetyl-4,6-dimethoxy-2,3-dihydro-1H-indole-3-one AZ-2 (0.08g, 0.33mmol), 3-cyanobenzaldehyde (0.05g, 0.37 mmol) and 50% KOH (1ml) as a orangy-yellow solid (5% yield) according to Scheme 2-6: <sup>1</sup>H NMR (Acetone<sub>d-6</sub>, 300MHz):  $\delta$  3.89 (s, 3H), 3.89 (s, 3H), 6.061 (d, 1H, J= 1.5Hz), 6.21 (d, 1H, J= 1.5Hz), 6.47 (s, 1H), 7.36 (s, 1H), 7.60-7.69 (m, 2H), 7.92 (d, 1H, J= 7.5Hz), 9.20 (br s, -NH); MS (APCI): m/z 307.6 [M+1]<sup>+</sup>; HPLC analyses:  $t_R$  = 14.76 min (93.2% pure at 360nm) on the C<sub>18</sub> analytical column; Mobile phase: solvent system A [70% MeOH and 30% (0.1% HCOOH in H<sub>2</sub>O)] isocratic;  $t_R$  = 6.95 min (87.9% pure at 360nm) on the C<sub>18</sub> analytical column; Mobile phase: solvent system B (CH<sub>3</sub>CN and 0.1% HCOOH in H<sub>2</sub>O) with a gradient of CH<sub>3</sub>CN 40% to 50% from 0 to 7 min and 50% to 70% from 7 to 10 min and then 70% CH<sub>3</sub>CN from 10 to 15 min.

**(Z)-4,6-Dimethoxy-2-(3-methylbenzylidene)indolin-3-one (7-7)**

This compound was obtained from 1-acetyl-4,6-dimethoxy-2,3-dihydro-1H-indole-3-one AZ-2 (0.10g, 0.43mmol), 3-methylbenzaldehyde (0.06g, 0.47 mmol) and 50% KOH (1ml) as a orangy-yellow solid (27% yield) according to Scheme 2-6: mp: 104-107°C; <sup>1</sup>H NMR (Acetone<sub>d-6</sub>, 300MHz):  $\delta$  2.35 (s, 3H), 3.87 (2 x 3H), 6.01 (d, 1H, J= 1.8Hz), 6.23 (d, 1H, J= 1.8Hz), 6.48 (s, 1H), 7.12 (d, 1H, J= 7.5Hz), 7.30 (t, 1H, J= 7.7Hz), 7.42 – 7.47 (m, 2H), 8.98 (br s, -NH); <sup>13</sup>C NMR (CDCl<sub>3</sub>, 75MHz):  $\delta$  21.5, 55.8, 55.8, 88.3, 91.2, 105.0, 109.8, 126.3, 129.0, 129.9, 135.0, 136.2, 138.8, 156.5, 160.4, 168.5, 182.4; MS (APCI):

m/z 296.4 [M+1]<sup>+</sup>; HPLC analyses: t<sub>R</sub> = 3.98 min (99.3% pure at 360nm) on the C<sub>18</sub> analytical column; Mobile phase: solvent system A [70% MeOH and 30% (0.1% HCOOH in H<sub>2</sub>O)] isocratic; t<sub>R</sub> = 6.81 min (98.4% pure at 360nm) on the C<sub>18</sub> analytical column; Mobile phase: solvent system B (CH<sub>3</sub>CN and 0.1% HCOOH in H<sub>2</sub>O with a gradient of CH<sub>3</sub>CN 40% to 50% from 0 to 7 min and 50% to 70% from 7 to 10 min and then 70% CH<sub>3</sub>CN from 10 to 15 min.

**(Z)-4,6-Dimethoxy-2-(3-hydrobenzylidene)indolin-3-one (7-8)**

This compound was obtained from 1-acetyl-4,6-dimethoxy-2,3-dihydro-1H-indole-3-one AZ-2 (0.09g, 0.39mmol), 3-(tetrahydro-2H-pyran-2-yloxy)benzaldehyde (0.12g, 0.59 mmol) and 50% KOH (1ml) as a brown solid (7% yield) according to Scheme 2-6: mp: 123-126°C; <sup>1</sup>H NMR (Acetone<sub>d-6</sub>, 300MHz): δ 3.87 (2x 3H), 6.01 (d, 1H, J= 1.5Hz), 6.27 (d, 1H, J= 1.8Hz), 6.43 (s, 1H), 6.79 (dd, 1H, J= 1.5, 1.8 Hz), 7.11 (d, 2H, J= 6.6 Hz), 7.23 (t, 1H, J= 8.1 Hz), 8.92 (br s, -NH); <sup>13</sup>C NMR (Acetone<sub>d-6</sub>, 75MHz): δ 57.0, 57.2, 90.6, 92.6, 105.9, 109.1, 116.8, 117.8, 122.5, 131.7, 138.0, 138.3, 159.2, 159.7, 162.1, 170.4, 183.4; MS (APCI): m/z 298.4 [M+1]<sup>+</sup>; HPLC analyses: t<sub>R</sub> = 7.69 min (98.9% pure at 360nm) on the C<sub>18</sub> analytical column; Mobile phase: solvent system A (MeOH and 0.1% HCOOH in H<sub>2</sub>O) with a gradient of MeOH 50% to 60% from 0 to 3 min, 60% to 70% from 3 to 5 min, 70% to 80% from 5 to 7 min and then 80% MeOH from 7 to 30 min; t<sub>R</sub> = 3.79 min (99.7% pure at 360nm) on the C<sub>18</sub> analytical column; Mobile phase: solvent system B (CH<sub>3</sub>CN and 0.1% HCOOH in H<sub>2</sub>O) with a gradient of CH<sub>3</sub>CN 40% to 50% from 0 to 7 min and 50% to 70% from 7 to 10 min and then 70% CH<sub>3</sub>CN from 10 to 15 min.

#### 4', 6'-Dimethoxy-2'-hydroxychalcone (**11-1**)

This compound was obtained from 2'-hydroxy-4', 6'-dimethoxyacetophenone (0.50g, 2.55mmol), benzaldehyde (0.29g, 2.81 mmol) and 50% KOH (1ml) as a yellow solid (58% yield) according to Scheme 2-7: mp: 84-87°C (lit: 85-86 °C)<sup>165</sup>; <sup>1</sup>H NMR (CDCl<sub>3</sub>, 300MHz): δ 3.80 (s, 3H), 3.89 (s, 3H), 5.94 (d, 1H, J= 2.1), 6.08 (d, 1H, J= 2.4), 7.37 – 7.41 (m, 3H), 7.57- 7. 60 (m, 2H), 7.76 (d, 1H, J= 15.6 Hz), 7.88 (d, 1H, J= 15.6 Hz), 14.32 (s, -OH); <sup>13</sup>C NMR (CDCl<sub>3</sub>, 75MHz): δ 55.5, 55.7, 91.1, 93.7, 106.2, 127.4, 128.3, 128.8, 130.0, 135.5, 142.2, 162.4, 166.2, 168.3, 192.5; MS (APCI): 285.5 [M+1]<sup>+</sup>; Anal. calcd for C<sub>17</sub>H<sub>16</sub>O<sub>4</sub>: C, 71.82; H, 5.67; Found: C, 72.00; H, 5.38.

#### 2'-Hydroxy-3, 4', 6'-trimethoxychalcone (**11-2**)

This compound was obtained from 2'-hydroxy-4', 6'-dimethoxyacetophenone (0.50g, 2.55mmol), 3-methoxybenzaldehyde (0.38g, 2.81 mmol) and 50% KOH (1ml) as a yellow solid (69% yield) according to Scheme 2-7: mp: 94-97°C (lit: 97 °C)<sup>166</sup>; <sup>1</sup>H NMR (CDCl<sub>3</sub>, 300MHz): δ 3.82 (s, 3H), 3.84 (s, 3H), 3.90 (s, 3H), 5.95 (d, 1H, J= 2.4), 6.10 (d, 1H, J= 2.1), 6.93 (dd, 1H, J= 2.1, 2.1) 7.11 (s, 1H), 7.20 (d, 1H, J= 7.5 Hz), 7.3 (t, 1H, J= 8 Hz) 7.72 (d, 1H, J= 15.6 Hz), 7.87 (d, 1H, J= 15.6 Hz), 14.28 (s, -OH); <sup>13</sup>C NMR (CDCl<sub>3</sub>, 75MHz): δ 55.3, 55.6, 55.8, 91.3, 93.8, 106.3, 113.7, 115.6, 120.9, 127.9, 129.8, 137.0, 142.2, 159.9, 162.5, 166.3, 168.4, 192.6; MS (APCI): 315.3 [M+1]<sup>+</sup>; Anal. calcd for C<sub>18</sub>H<sub>18</sub>O<sub>5</sub>: C, 68.78; H, 5.77; Found: C, 68.69; H, 5.40.

#### 2'-Hydroxy-4, 4', 6'-trimethoxychalcone (**11-3**)

This compound was obtained from 2'-hydroxy-4', 6'-dimethoxyacetophenone (0.50g, 2.55mmol), 4-methoxybenzaldehyde (0.38g, 2.81 mmol) and 50% KOH (1ml) as a yellow solid (62% yield) according to Scheme 2-7: mp: 110-112°C (lit: 109-112 °C)<sup>167</sup>; <sup>1</sup>H NMR (CDCl<sub>3</sub>, 300MHz): δ 3.82 (s, 3H), 3.84 (s, 3H), 3.91 (s, 3H), 5.95 (d, 1H, J= 2.1),

6.10 (d, 1H, J= 2.4), 6.92 (d, 2H, J= 8,7) 7.56 (d, 2H, J= 8.7Hz), 7.76 (d, 1H, J= 16.2Hz), 7.81 (d, 1H, J= 15.9Hz), 14.42 (s, -OH); <sup>13</sup>C NMR (CDCl<sub>3</sub>, 75MHz): δ 55.3, 55.5, 55.8, 91.2, 93.8, 106.3, 114.3, 125.1, 128.3, 130.1, 142.4, 161.3, 162.4, 166.0, 168.3, 192.5; MS (APCI): 315.3 [M+1]<sup>+</sup>; HPLC analyses: t<sub>R</sub>= 3.88 min (99.4% pure at 300nm) on the C<sub>18</sub> analytical column; Mobile phase: solvent system A (MeOH and 0.1% HCOOH in H<sub>2</sub>O) with a gradient of MeOH 100% to 70% from 0 to 5 min, 70% to 50% from 5 to 7 min and 50% MeOH from 7 to 10 min; t<sub>R</sub>= 3.82 min (98.4% pure at 300nm) on the C<sub>18</sub> analytical column; Mobile phase: solvent system B (CH<sub>3</sub>CN and 0.1% HCOOH in H<sub>2</sub>O) with a gradient of CH<sub>3</sub>CN 100% to 70% from 0 to 5 min, 70% to 50% from 5 to 7min, 50% to 70% from 7 to 9 min and then 70% to 100% CH<sub>3</sub>CN from 9 min to 12 min.

#### 2'-Hydroxy-3, 4, 4', 6'-tetramethoxychalcone (**11-4**)

This compound was obtained from 2'-hydroxy-4', 6'-dimethoxyacetophenone (0.50g, 2.55mmol), 3,4-dimethoxybenzaldehyde (0.47g, 2.81 mmol) and 50% KOH (1ml) as a yellow solid (49% yield) according to Scheme 2-7: mp: 152-153°C (lit: 151-153°C)<sup>168</sup>; <sup>1</sup>H NMR (CDCl<sub>3</sub>, 300MHz): δ 3.84 (s, 3H), 3.92 (s, 3H), 3.93 (s, 3H), 3.94 (s, 3H), 5.97 (d, 1H, J= 2.4), 6.12 (d, 1H, J= 2.1), 6.90 (d, 1H, J= 8.4 Hz), 7.13 (d, 1H, J= 1.5 Hz), 7.22 (dd, 1H, J= 1.8, 1.8 Hz), 7.75 (d, 1H, J= 15.6 Hz), 7.81 (d, 1H, J= 15.6 Hz), 14.38 (s, -OH); <sup>13</sup>C NMR (CDCl<sub>3</sub>, 75MHz): δ 55.6, 55.8, 55.9, 56.0, 91.3, 93.9, 106.4, 110.5, 111.2, 122.6, 125.5, 128.6, 142.7, 149.2, 151.1, 162.4, 166.1, 168.4, 192.5; MS (APCI): 345.5 [M+1]<sup>+</sup>; Anal. calcd for C<sub>19</sub>H<sub>20</sub>O<sub>6</sub>: C, 66.27; H, 5.85; Found: C, 66.45; H, 5.57.

#### 2'-Hydroxy-3, 5, 4', 6'-tetramethoxychalcone (**11-5**)

This compound was obtained from 2'-hydroxy-4', 6'-dimethoxyacetophenone (0.50g, 2.55mmol), 3,5-dimethoxybenzaldehyde (0.47g, 2.81 mmol) and 50% KOH (1ml) as a yellow solid (36% yield) according to Scheme 2-7: mp: 161-162°C; <sup>1</sup>H NMR (CDCl<sub>3</sub>,

300MHz):  $\delta$  3.83 (s, 3 x 3H), 3.91 (s, 3H), 5.96 (d, 1H, J= 2.1), 6.11 (d, 1H, J= 2.4), 6.51 (s, 1H), 6.75 (d, 2H, J= 1.8 Hz), 7.68 (d, 1H, J= 15.6 Hz), 7.85 (d, 1H, J= 15.6 Hz), 14.25 (s, -OH);  $^{13}\text{C}$  NMR ( $\text{CDCl}_3$ , 75MHz):  $\delta$  55.4 (2C), 55.6, 55.9, 91.3, 93.8, 102.1, 106.4, 128.1, 137.5, 142.2, 161.0, 162.5, 166.3, 168.4, 192.5; MS (APCI): 345.4  $[\text{M}+1]^+$ ; Anal. calcd for  $\text{C}_{19}\text{H}_{20}\text{O}_6$ : C, 66.27; H, 5.85; Found: C, 66.69; H, 5.57.

#### 5, 7-Dimethoxy-2-phenyl-4H-chromen-4-one (**12-1**)

This compound was obtained from 4', 6'-dimethoxy-2'-hydroxychalcone (11-1) (0.20g, 0.71mmol) in DMSO and catalytic amount of iodine as a white solid (45% yield) according to Scheme 2-8: mp: 145-148°C (lit: 147°C)<sup>169</sup>;  $^1\text{H}$  NMR ( $\text{CDCl}_3$ , 300MHz):  $\delta$  3.90 (s, 3H), 3.94 (s, 3H), 6.36 (d, 1H, J= 2.1 Hz), 6.55 (d, 1H, J= 2.1 Hz), 6.66 (s, 1H), 7.45 – 7.50 (m, 3H), 7.84 - 7.87 (m, 2H),  $^{13}\text{C}$  NMR ( $\text{CDCl}_3$ , 75MHz):  $\delta$  55.7, 56.3, 92.7, 96.1, 108.9, 109.2, 125.8, 128.8, 131.1, 131.4, 159.8, 160.5, 160.8, 164.0, 177.5; MS (APCI): 283.5  $[\text{M}+1]^+$ ; HPLC analyses:  $t_{\text{R}}$ = 3.67 min (97.4% pure at 330nm) on the  $\text{C}_{18}$  analytical column; Mobile phase: solvent system A (MeOH and 0.1% HCOOH in  $\text{H}_2\text{O}$ ) with a gradient of MeOH 100% to 70% from 0 to 5 min, 70% to 50% from 5 to 7 min and 50% to 100% MeOH from 7 to 10 min;  $t_{\text{R}}$ = 4.02 min (99.1% pure at 330nm) on the  $\text{C}_{18}$  analytical column; Mobile phase: solvent system B ( $\text{CH}_3\text{CN}$  and 0.1% HCOOH in  $\text{H}_2\text{O}$ ) with a gradient of  $\text{CH}_3\text{CN}$  100% to 70% from 0 to 5 min, 70% to 50% from 5 to 7min, 50% to 70% from 7 to 9 min and then 70%  $\text{CH}_3\text{CN}$  from 9 min to 12 min.

#### 5, 7-Dimethoxy-2-(3-methoxyphenyl)-4H-chromen-4-one (**12-2**)

This compound was obtained from 2'-hydroxy-3, 4', 6'-trimethoxychalcone (11-2) (0.20g, 0.64mmol) in DMSO and catalytic amount of iodine as a white solid (48% yield) according to Scheme 2-8: mp: 142-144°C;  $^1\text{H}$  NMR ( $\text{CDCl}_3$ , 300MHz):  $\delta$  3.88 (s, 3H), 3.91 (s, 3H), 3.95 (s, 3H), 6.37 (d, 1H, J= 2.4 Hz), 6.56 (d, 1H, J= 2.1 Hz), 6.66 (s, 1H),



7.04 (d, 1H, J= 7.8 Hz), 7.37 – 7.46 (m, 3H); <sup>13</sup>C NMR (CDCl<sub>3</sub>, 75MHz): δ 55.4, 55.7, 56.4, 92.8, 96.1, 109.2 (2C), 111.3, 116.8, 118.3, 129.9, 132.8, 159.8, 159.9, 160.4, 160.8, 164.0, 177.6; MS (APCI): 313.5 [M+1]<sup>+</sup>; HPLC analyses: t<sub>R</sub>= 3.72 min (96.9% pure at 330nm) on the C<sub>18</sub> analytical column; Mobile phase: solvent system A (MeOH and 0.1% HCOOH in H<sub>2</sub>O) with a gradient of MeOH 100% to 70% from 0 to 5 min, 70% to 50% from 5 to 7 min and 50% to 100% MeOH from 7 to 10 min; t<sub>R</sub>= 3.96 min (98.8% pure at 330nm) on the C<sub>18</sub> analytical column; Mobile phase: solvent system B (CH<sub>3</sub>CN and 0.1% HCOOH in H<sub>2</sub>O) with a gradient of CH<sub>3</sub>CN 100% to 70% from 0 to 5 min, 70% to 50% from 5 to 7min, 50% to 70% from 7 to 9 min and then 70% CH<sub>3</sub>CN from 9 min to 12 min.

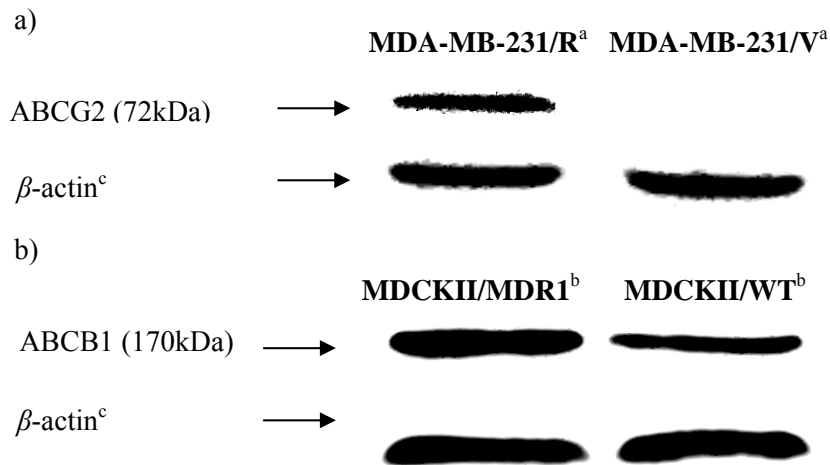
### 5, 7-Dimethoxy-2-(4-methoxyphenyl)-4H-chromen-4-one (**12-3**)

This compound was obtained from 2'-hydroxy-4, 4', 6'-trimethoxychalcone (11-3) (0.20g, 0.64mmol) in DMSO and catalytic amount of iodine as a white solid (32% yield) according to Scheme 2-8: mp: 154-156°C (lit: 153-155 °C)<sup>170</sup>; <sup>1</sup>H NMR (CDCl<sub>3</sub>, 300MHz): δ 3.87 (s, 3H), 3.90 (s, 3H), 3.94 (s, 3H), 6.35 (d, 1H, J= 2.1 Hz), 6.53 (d, 1H, J= 2.1 Hz), 6.57 (s, 1H), 6.98 (d, 2H, J= 8.7 Hz), 7.79 (d, 2H, J= 8.7 Hz); <sup>13</sup>C NMR (CDCl<sub>3</sub>, 75MHz): δ 55.4, 55.6, 56.3, 92.7, 96.0, 107.5, 109.0, 114.2, 123.7, 127.5, 159.7, 160.6, 160.7, 162.0, 163.8, 177.6; MS (APCI): 313.5 [M+1]<sup>+</sup>; HPLC analyses: t<sub>R</sub>= 3.67 min (99.5% pure at 330nm) on the C<sub>18</sub> analytical column; Mobile phase: solvent system A (MeOH and 0.1% HCOOH in H<sub>2</sub>O) with a gradient of MeOH 100% to 70% from 0 to 5 min, 70% to 50% from 5 to 7 min and 50% to 70% MeOH from 7 to 10 min and 70% to 100% MeOH from 10 to 15 min; t<sub>R</sub>= 4.00 min (99.7% pure at 330nm) on the C<sub>18</sub> analytical column; Mobile phase: solvent system B (CH<sub>3</sub>CN and 0.1% HCOOH in H<sub>2</sub>O) with a gradient of CH<sub>3</sub>CN 100% to 70% from 0 to 5 min, 70% to 50% from 5 to 7min, 50% to 70% from 7 to 9 min and then 70% CH<sub>3</sub>CN from 9 min to 12 min.

5, 7-Dimethoxy-2-(3, 5-dimethoxyphenyl)-4H-chromen-4-one (**12-5**)

This compound was obtained from 2'-hydroxy-3, 5, 4', 6'-tetramethoxychalcone (11-5) (0.10g, 0.29mmol) in DMSO and catalytic amount of iodine as a white solid (45% yield) according to Scheme 2-8: mp: 197-198°C (lit: 201-202 °C)<sup>171</sup>; <sup>1</sup>H NMR (CDCl<sub>3</sub>, 300MHz): δ 3.83 (s, 2 x 3H), 3.88 (s, 3H), 3.92 (s, 3H), 6.33 (d, 1H, J= 2.1 Hz), 6.51 (d, 1H, J= 2.1 Hz), 6.55 (t, 1H, J= 2.1 Hz), 6.61 (s, 1H), 6.94 (d, 2H, J= 2.1 Hz); <sup>13</sup>C NMR (CDCl<sub>3</sub>, 75MHz): δ 55.5, 55.7, 56.3, 92.8, 96.1, 103.1, 104.0, 109.2, 109.3, 133.3, 159.8, 160.3, 160.8, 161.0, 164.0, 177.6; MS (APCI): 343.6 [M+1]<sup>+</sup>; HPLC analyses: t<sub>R</sub>= 3.79 min (96.4% pure at 330nm) on the C<sub>18</sub> analytical column; Mobile phase: solvent system A (MeOH and 0.1% HCOOH in H<sub>2</sub>O) with a gradient of MeOH 100% to 70% from 0 to 5 min, 70% to 50% from 5 to 7 min and 50% to 100% MeOH from 7 to 10 min; t<sub>R</sub>= 3.86 min (96.8% pure at 330nm) on the C<sub>18</sub> analytical column; Mobile phase: solvent system B (CH<sub>3</sub>CN and 0.1% HCOOH in H<sub>2</sub>O) with a gradient of CH<sub>3</sub>CN 100% to 70% from 0 to 5 min, 70% to 50% from 5 to 7min, 50% to 70% from 7 to 9 min and then 70% CH<sub>3</sub>CN from 9 min to 12 min.

**Appendix 3-1:** Western blot analyses of ABCG2 and ABCB1 expressions in various cells.



<sup>a</sup>Analyses of ABCG2 expression in MDA-MB-231/R and MDA-MB-231/V cells. The protein loading for each sample was 15 $\mu$ g as determined by protein assay; <sup>b</sup>Analyses of ABCB1 expression in MDCKII/MDR1 and MDCKII/WT cells. The protein loading for each sample was 40 $\mu$ g as determined by protein assay; <sup>c</sup> $\beta$ -actin was used as a positive control for the western blot analyses.

**Appendix 4-1:** Assignment of 19 substructures to test compounds

Compound	pEC <sub>50</sub> <sup>a</sup>	DiOMe <sup>b</sup>	TriOMe <sup>c</sup>	NH <sup>d</sup>	CH2 <sup>e</sup>	ADBCO <sup>f</sup>	OH <sup>g</sup>	B2 <sup>h</sup>	B3 <sup>i</sup>	B4 <sup>j</sup>	B5 <sup>k</sup>	BMeO <sup>l</sup>	BOH <sup>m</sup>	BCH3 <sup>n</sup>	BF <sup>o</sup>
5-1 (ref)	4.523	0	0	0	0	0	0	0	0	0	0	0	0	0	0
1-3	4.973	1	0	0	0	0	0	0	1	0	0	1	0	0	0
2-3	5.266	0	1	0	0	0	0	0	1	0	0	0	0	0	0
3-3	4.523	0	0	0	0	0	1	0	1	1	0	1	1	0	0
4-3	4.523	0	0	0	0	0	1	0	0	1	0	0	0	0	0
5-3	4.523	0	0	0	0	0	0	0	1	0	0	0	1	0	0
6-3	5.353	1	0	0	1	0	0	0	1	0	0	1	0	0	0
7-3	4.301	1	0	1	0	0	0	0	0	1	0	1	0	0	0
8-3	4.301	0	1	0	0	0	0	0	0	1	0	1	0	0	0
9-3	4.523	0	0	0	0	1	1	0	0	0	0	0	0	0	0
10-3 <sup>u</sup>	4.523	0	0	1	0	1	0	0	1	0	1	1	0	0	0
11-3	4.301	1	0	0	0	0	1	0	0	1	0	1	0	0	0
12-3	4.676	1	0	0	0	0	0	0	0	1	0	1	0	0	0

Compound	BCI <sup>p</sup>	BCN <sup>q</sup>	NoDB <sup>r</sup>	NoC5 <sup>s</sup>	NoC <sup>t</sup>
5-1 (ref)	0	0	0	0	0
1-3	0	0	0	0	0
2-3	1	0	0	0	0
3-3	0	0	0	0	0
4-3	1	0	0	0	0
5-3	0	0	0	0	0
6-3	0	0	0	0	0
7-3	0	0	0	0	0
8-3	0	0	1	0	0
9-3	0	0	0	0	0
10-3	0	0	0	0	0
11-3	0	0	0	1	1
12-3	0	0	0	1	0

<sup>a</sup>pEC<sub>50</sub> = -Log (EC<sub>50</sub>) where EC<sub>50</sub> is the concentration of test compound required to increase accumulation of PhA to 50% of the maximum levels obtained with 10 μM PhA; <sup>b</sup>DiOMe = Dimethoxy groups on ring A; <sup>c</sup>TriOMe = Trimethoxy groups on ring A; <sup>d</sup>NH = NH in place of O in ring C; <sup>e</sup>CH<sub>2</sub> = CH<sub>2</sub> in place of O in ring C; <sup>f</sup>ADBCO = Ring A-double bond-C=O motif (to identify isoaurones and indolinones); <sup>g</sup>OH = Hydroxyl groups (1 or more) on ring A; <sup>h-k</sup>B2-B5= Substitution at 2',3',4' and 5' on ring B respectively; <sup>l-q</sup>BMeO, BOH, BCH<sub>3</sub>, BF, BC and BCN = Presence of CH<sub>3</sub>O, OH, CH<sub>3</sub>, F, Cl, CN on ring B respectively; <sup>r</sup>NoDB = Absence of exocyclic double bond (to identify dehydroaurones); <sup>s</sup>NoC5 = Absence of Ring C (to identify chalcones); <sup>t</sup>NoC = Absence of 5 membered ring C (to identify chalcones and flavones); <sup>u</sup>Compound **10-3** as an example would have variables i)NH ii) ADBCO iii) B3 iv) B5 and v)BMeO assigned as "1" and the rest of the variables assigned as "0".

**Appendix 4-2:** Assignment of 13 substructures to test compounds

Compound	pEC <sub>50(BCRP)</sub> <sup>a</sup>	pEC <sub>50(Pgp)</sub> <sup>b</sup>	DiMeO <sup>c</sup>	TriMeO <sup>d</sup>	NH <sup>e</sup>	CH2 <sup>f</sup>	B3 <sup>g</sup>	B4 <sup>h</sup>	B5 <sup>i</sup>	BMeO <sup>j</sup>	BCN <sup>k</sup>	BCl <sup>l</sup>	BOH <sup>m</sup>	NoC5 <sup>n</sup>	NoC <sup>o</sup>
5-1 (reference)	4.523	4.523	0	0	0	0	0	0	0	0	0	0	0	0	0
1-3	4.973	5.325	1	0	0	0	1	0	0	1	0	0	0	0	0
1-14	5.112	5.445	1	0	0	0	1	0	0	0	1	0	0	0	0
1-25 <sup>p</sup>	5.971	5.959	1	0	0	0	1	1	0	1	0	0	0	0	0
1-26	6.041	5.644	1	0	0	0	1	0	1	1	0	0	0	0	0
2-3	5.266	5.000	0	1	0	0	1	0	0	0	0	1	0	0	0
2-7	4.923	5.439	0	1	0	0	0	1	0	1	0	0	0	0	0
2-9	5.344	4.907	0	1	0	0	1	0	0	0	0	0	1	0	0
5-7	4.523	4.520	0	0	0	0	1	0	0	0	1	0	0	0	0
6-3	5.353	5.496	1	0	0	1	1	0	0	1	0	0	0	0	0
6-5	5.754	4.523	1	0	0	1	1	0	0	0	0	0	1	0	0
6-20	5.932	5.597	1	0	0	1	1	1	0	1	0	0	0	0	0
7-2	5.064	5.291	1	0	1	0	1	0	0	1	0	0	0	0	0
7-4	5.336	4.523	1	0	1	0	1	0	0	0	0	1	0	0	0
7-5	5.157	5.009	1	0	1	0	0	1	0	0	0	1	0	0	0
11-4	5.213	4.523	1	0	0	0	1	1	0	1	0	0	0	1	1
11-5	5.539	4.523	1	0	0	0	1	0	1	1	0	0	0	1	1
12-2	5.014	5.088	1	0	0	0	1	0	0	1	0	0	0	1	0
12-4	5.611	5.198	1	0	0	0	1	1	0	1	0	0	0	1	0
12-5	5.635	5.644	1	0	0	0	1	0	1	1	0	0	0	1	0

<sup>a</sup>pEC<sub>50(BCRP)</sub> = -Log (EC<sub>50(BCRP)</sub>) where EC<sub>50(BCRP)</sub> is the concentration of test compound required to increase accumulation of PhA to 50% of the maximum levels obtained with 10 μM PhA; <sup>b</sup>pEC<sub>50(Pgp)</sub> = -Log (EC<sub>50(Pgp)</sub>) where EC<sub>50(Pgp)</sub> is the concentration of test compound required to increase fluorescence readings of accumulated calcein to 50% of the maximum levels (Y<sub>max</sub>) obtained with 3μM cyclosporin A; <sup>c</sup>DiOMe = Dimethoxy groups on ring A; <sup>d</sup>TriOMe = Trimethoxy groups on ring A; <sup>e</sup>NH = NH in place of O in ring C; <sup>f</sup>CH2 = CH2 in place of O in ring C; <sup>g-i</sup>B3-B5= Substitution at 3',4' and 5' on ring B respectively; <sup>j-m</sup>BMeO, BCN, BCl and BOH = Presence of CH<sub>3</sub>O, CN, Cl and OH on ring B respectively; <sup>n</sup>NoC5 = Absence of Ring C (to identify chalcones); <sup>o</sup>NoC = Absence of 5 membered ring C (to identify chalcones and flavones); <sup>p</sup>Compound 1-25 as an example would have variables i)DiMeO ii)B3 iii) B4 and iv)BMeO assigned as "1" and the rest of the variables assigned as "0".

### Appendix 4-3: Descriptors for Auto-QSAR

Compound	mr	logP(o/w)	SlogP	VDW area	VDW volume	TPSA	logS	Weight	b_count	b_rotN	b_1rotN	b_1rotR
1-1	7.907	3.768	3.320	275.538	379.355	44.760	-4.649	282.295	37	3	3	0.130
1-2	8.542	3.722	3.329	307.774	414.446	53.990	-4.700	312.321	41	4	4	0.160
1-3	8.538	3.761	3.329	307.774	414.446	53.990	-4.700	312.321	41	4	4	0.160
1-4	8.538	3.724	3.329	307.774	414.446	53.990	-4.700	312.321	41	4	4	0.160
1-5	8.033	3.458	3.026	285.568	387.877	64.990	-4.287	298.294	38	3	3	0.125
1-6	8.029	3.497	3.026	285.568	387.877	64.990	-4.287	298.294	38	3	3	0.125
1-7	8.029	3.460	3.026	285.568	387.877	64.990	-4.287	298.294	38	3	3	0.125
1-8	8.407	4.358	3.973	293.119	395.311	44.760	-5.384	316.740	37	3	3	0.125
1-9	8.403	4.397	3.973	293.119	395.311	44.760	-5.384	316.740	37	3	3	0.125
1-10	8.403	4.360	3.973	293.119	395.311	44.760	-5.384	316.740	37	3	3	0.125
1-11	8.360	4.064	3.628	292.770	403.784	44.760	-5.123	296.322	40	3	3	0.125
1-12	8.356	4.103	3.628	292.770	403.784	44.760	-5.123	296.322	40	3	3	0.125
1-13	8.356	4.066	3.628	292.770	403.784	44.760	-5.123	296.322	40	3	3	0.125
1-14	8.536	3.465	3.192	299.268	404.785	68.550	-5.000	307.305	38	4	3	0.120
1-15	8.536	3.428	3.192	299.268	404.785	68.550	-5.000	307.305	38	4	3	0.120
1-16	7.976	3.919	3.459	279.947	382.497	44.760	-4.944	300.285	37	3	3	0.125
1-17	7.972	3.958	3.459	279.947	382.497	44.760	-4.944	300.285	37	3	3	0.125
1-18	7.972	3.921	3.459	279.947	382.497	44.760	-4.944	300.285	37	3	3	0.125
1-19	8.480	4.703	4.650	305.997	413.211	44.760	-5.706	350.292	40	4	3	0.111
1-20	8.662	3.451	3.034	317.804	422.968	74.220	-4.338	328.320	42	4	4	0.154
1-21	8.662	3.451	3.034	317.804	422.968	74.220	-4.338	328.320	42	4	4	0.154
1-22	8.155	3.148	2.731	295.598	396.399	85.220	-3.925	314.293	39	3	3	0.120
1-23	8.151	3.187	2.731	295.598	396.399	85.220	-3.925	314.293	39	3	3	0.120
1-24	8.151	3.187	2.731	295.598	396.399	85.220	-3.925	314.293	39	3	3	0.120

<b>1-25</b>	9.171	3.467	3.337	340.009	449.536	63.220	-4.750	342.347	45	5	5	0.185
<b>Compound</b>	<b>mr</b>	<b>logP(o/w)</b>	<b>SlogP</b>	<b>VDW area</b>	<b>VDW volume</b>	<b>TPSA</b>	<b>logS</b>	<b>Weight</b>	<b>b_count</b>	<b>b_rotN</b>	<b>b_IrotN</b>	<b>b_IrotR</b>
<b>1-26</b>	9.168	3.791	3.337	340.009	449.536	63.220	-4.750	342.347	45	5	5	0.185
<b>1-27</b>	8.007	4.109	3.598	284.356	385.639	44.760	-5.239	318.275	37	3	3	0.120
<b>1-28</b>	8.004	4.185	3.598	284.356	385.639	44.760	-5.239	318.275	37	3	3	0.120
<b>2-1</b>	8.546	3.186	3.329	307.774	414.446	53.990	-4.700	312.321	41	4	4	0.160
<b>2-2</b>	9.049	3.776	3.982	325.355	430.401	53.990	-5.434	346.766	41	4	4	0.154
<b>2-3</b>	9.045	3.815	3.982	325.355	430.401	53.990	-5.434	346.766	41	4	4	0.154
<b>2-4</b>	9.045	3.778	3.982	325.355	430.401	53.990	-5.434	346.766	41	4	4	0.154
<b>2-5</b>	9.179	3.140	3.337	340.009	449.536	63.220	-4.750	342.347	45	5	5	0.185
<b>2-6</b>	9.175	3.179	3.337	340.009	449.536	63.220	-4.750	342.347	45	5	5	0.185
<b>2-7</b>	9.175	3.142	3.337	340.009	449.536	63.220	-4.750	342.347	45	5	5	0.185
<b>2-8</b>	9.179	2.883	3.200	331.504	439.876	77.780	-5.051	337.331	42	5	4	0.148
<b>2-9</b>	8.666	2.915	3.034	317.804	422.968	74.220	-4.338	328.320	42	4	4	0.154
<b>2-10</b>	8.995	3.521	3.637	325.006	438.875	53.990	-5.174	326.348	44	4	4	0.154
<b>2-11</b>	8.640	3.201	3.752	313.389	432.151	53.990	-5.413	318.369	47	4	4	0.160
<b>6-1</b>	8.207	3.873	3.526	277.766	393.123	35.530	-4.258	280.323	39	3	3	0.130
<b>6-2</b>	8.845	3.827	3.535	310.002	428.213	44.760	-4.308	310.349	43	4	4	0.160
<b>6-3</b>	8.842	3.866	3.535	310.002	428.213	44.760	-4.308	310.349	43	4	4	0.160
<b>6-4</b>	8.842	3.829	3.535	310.002	428.213	44.760	-4.308	310.349	43	4	4	0.160
<b>6-5</b>	8.336	3.602	3.232	287.796	401.645	55.760	-3.896	296.322	40	3	3	0.125
<b>6-6</b>	8.336	3.565	3.232	287.796	401.645	55.760	-3.896	296.322	40	3	3	0.125
<b>6-7</b>	8.710	4.463	4.180	295.348	409.079	35.530	-4.992	314.768	39	3	3	0.125
<b>6-8</b>	8.706	4.502	4.180	295.348	409.079	35.530	-4.992	314.768	39	3	3	0.125
<b>6-9</b>	8.706	4.465	4.180	295.348	409.079	35.530	-4.992	314.768	39	3	3	0.125
<b>6-10</b>	8.839	3.570	3.398	301.496	418.553	59.320	-4.609	305.333	40	4	3	0.120



6-11	8.839	3.533	3.398	301.496	418.553	59.320	-4.609	305.333	40	4	3	0.120
6-12	8.656	4.169	3.835	294.998	417.552	35.530	-4.732	294.350	42	3	3	0.125
6-13	8.652	4.208	3.835	294.998	417.552	35.530	-4.732	294.350	42	3	3	0.125
6-14	8.652	4.171	3.835	294.998	417.552	35.530	-4.732	294.350	42	3	3	0.125
6-15	9.473	3.896	3.543	342.238	463.304	53.990	-4.358	340.375	47	5	5	0.185
6-16	8.460	3.368	2.937	297.826	410.167	75.990	-3.534	312.321	41	3	3	0.120
6-17	8.971	3.556	3.240	320.032	436.735	64.990	-3.946	326.348	44	4	4	0.154
6-18	8.971	3.556	3.240	320.032	436.735	64.990	-3.946	326.348	44	4	4	0.154
6-19	8.464	3.292	2.937	297.826	410.167	75.990	-3.534	312.321	41	3	3	0.120
6-20	9.477	3.572	3.543	342.238	463.304	53.990	-4.358	340.375	47	5	5	0.185
7-1	8.081	3.540	3.353	278.272	384.981	47.560	-4.075	281.311	38	3	3	0.130
7-2	8.717	3.533	3.362	310.508	420.071	56.790	-4.126	311.337	42	4	4	0.160
7-3	8.717	3.496	3.362	310.508	420.071	56.790	-4.126	311.337	42	4	4	0.160
7-4	8.578	4.169	4.006	295.853	400.937	47.560	-4.809	315.756	38	3	3	0.125
7-5	8.578	4.132	4.006	295.853	400.937	47.560	-4.809	315.756	38	3	3	0.125
7-6	8.681	3.237	3.225	302.002	410.411	71.350	-4.426	306.321	39	4	3	0.120
7-7	8.529	3.875	3.662	295.504	409.410	47.560	-4.549	295.338	41	3	3	0.125
7-8	8.209	3.269	3.059	288.302	393.503	67.790	-3.713	297.310	39	3	3	0.125
11-1	8.103	3.739	3.306	299.188	391.112	55.760	-3.702	284.311	38	5	5	0.227
11-2	8.734	3.732	3.314	331.423	426.202	64.990	-3.753	314.337	42	6	6	0.250
11-3	8.734	3.695	3.314	331.423	426.202	64.990	-3.753	314.337	42	6	6	0.250
11-4	9.366	3.438	3.323	363.659	461.293	74.220	-3.803	344.363	46	7	7	0.269
11-5	9.362	3.762	3.323	363.659	461.293	74.220	-3.803	344.363	46	7	7	0.269
12-1	7.907	3.370	3.320	275.538	379.355	44.760	-4.649	282.295	37	3	3	0.130
12-2	8.538	3.363	3.329	307.774	414.446	53.990	-4.700	312.321	41	4	4	0.160
12-3	8.538	3.326	3.329	307.774	414.446	53.990	-4.700	312.321	41	4	4	0.160

12-4	9.171	3.069	3.337	340.009	449.536	63.220	-4.750	342.347	45	5	5	0.185
12-5	9.168	3.393	3.337	340.009	449.536	63.220	-4.750	342.347	45	5	5	0.185

Compound	b_rotR	a_acc	a_don	a_hyd	a_base	vsa_don	vsa_acc	vsa_hyd	vsa_pol	PM3_HOMO	PM3_LUMO	E	ASA
1-1	0.130	3	0	16	0	0	18.574	236.036	18.574	-9.047	-0.785	75.818	524.701
1-2	0.160	4	0	17	0	0	21.078	264.344	21.078	-8.819	-0.688	90.005	570.823
1-3	0.160	4	0	17	0	0	21.078	264.344	21.078	-8.929	-0.820	84.415	573.425
1-4	0.160	4	0	17	0	0	21.078	264.344	21.078	-8.700	-0.778	85.071	570.883
1-5	0.125	4	1	16	0	0	18.574	228.686	32.141	-8.871	-0.688	78.282	540.352
1-6	0.125	4	1	16	0	0	18.574	228.686	32.141	-8.998	-0.825	72.785	541.929
1-7	0.125	4	1	16	0	0	18.574	228.686	32.141	-8.780	-0.771	73.394	538.579
1-8	0.125	3	0	17	0	0	18.574	254.329	18.574	-9.047	-0.856	79.937	555.337
1-9	0.125	3	0	17	0	0	18.574	254.329	18.574	-9.128	-0.875	74.255	558.335
1-10	0.125	3	0	17	0	0	18.574	254.329	18.574	-8.984	-0.892	75.442	557.111
1-11	0.125	3	0	17	0	0	18.574	251.844	18.574	-9.037	-0.755	80.146	552.336
1-12	0.125	3	0	17	0	0	18.574	251.844	18.574	-8.998	-0.774	78.040	560.423
1-13	0.125	3	0	17	0	0	18.574	251.844	18.574	-8.906	-0.777	78.120	562.558
1-14	0.160	4	0	16	0	0	36.317	222.436	36.317	-9.314	-1.035	79.778	561.409
1-15	0.160	4	0	16	0	0	36.317	222.436	36.317	-9.303	-1.124	81.037	559.387
1-16	0.125	3	0	17	0	0	18.574	241.157	18.574	-9.144	-0.878	77.271	537.457
1-17	0.125	3	0	17	0	0	18.574	241.157	18.574	-9.219	-0.913	73.075	535.724
1-18	0.125	3	0	17	0	0	18.574	241.157	18.574	-9.130	-0.914	74.453	534.203
1-19	0.148	3	0	20	0	0	18.574	267.207	18.574	-9.359	-1.146	85.907	575.523
1-20	0.154	5	1	17	0	0	21.078	256.994	34.645	-8.598	-0.805	90.873	582.935
1-21	0.154	5	1	17	0	0	21.078	256.994	34.645	-8.595	-0.801	90.750	583.902
1-22	0.120	5	2	16	0	0	18.574	221.336	45.708	-8.861	-0.691	76.216	545.688

1-23	0.120	5	2	16	0	0	18.574	221.336	45.708	-8.679	-0.664	75.742	546.514
1-24	0.120	5	2	16	0	0	18.574	221.336	45.708	-8.663	-0.837	71.758	552.801
1-25	0.185	5	0	18	0	0	23.582	292.653	23.582	-8.884	-0.843	101.935	609.859
1-26	0.185	5	0	18	0	0	23.582	292.653	23.582	-8.951	-0.811	91.270	613.121
1-27	0.120	3	0	18	0	0	18.574	246.278	18.574	-9.298	-1.047	75.808	538.238
1-28	0.120	3	0	18	0	0	18.574	246.278	18.574	-9.343	-1.054	67.247	536.172
2-1	0.160	4	0	17	0	0	21.078	264.344	21.078	-9.139	-1.106	98.177	559.948
2-2	0.154	4	0	18	0	0	21.078	282.638	21.078	-9.170	-1.157	102.253	585.538
2-3	0.154	4	0	18	0	0	21.078	282.638	21.078	-9.236	-1.184	96.726	587.338
2-4	0.154	4	0	18	0	0	21.078	282.638	21.078	-9.092	-1.126	97.869	589.274
2-5	0.185	5	0	18	0	0	23.582	292.653	23.582	-8.954	-0.995	111.960	604.850
2-6	0.185	5	0	18	0	0	23.582	292.653	23.582	-9.064	-1.123	106.851	601.305
2-7	0.185	5	0	18	0	0	23.582	292.653	23.582	-8.867	-1.077	107.631	603.294
2-8	0.185	5	0	17	0	0	38.821	250.744	38.821	-9.424	-1.319	102.199	593.822
2-9	0.154	5	1	17	0	0	21.078	256.994	34.645	-9.116	-1.143	95.228	576.035
2-10	0.154	4	0	18	0	0	21.078	280.153	21.078	-9.113	-1.095	100.479	589.812
2-11	0.160	4	0	17	0	0	21.078	264.344	21.078	-9.286	-0.941	81.766	576.742
6-1	0.130	3	0	17	0	0	18.574	239.345	18.574	-9.097	-0.459	76.346	537.712
6-2	0.160	4	0	18	0	0	21.078	267.653	21.078	-9.015	-0.367	90.839	577.371
6-3	0.160	4	0	18	0	0	21.078	267.653	21.078	-9.099	-0.479	84.824	581.969
6-4	0.160	4	0	18	0	0	21.078	267.653	21.078	-8.921	-0.488	85.768	584.882
6-5	0.125	4	1	17	0	0	18.574	231.995	32.141	-9.120	-0.500	73.211	545.779
6-6	0.125	4	1	17	0	0	18.574	231.995	32.141	-8.887	-0.573	73.962	549.103
6-7	0.125	3	0	18	0	0	18.574	257.638	18.574	-9.113	-0.530	80.596	557.196
6-8	0.125	3	0	18	0	0	18.574	257.638	18.574	-9.140	-0.542	74.718	565.153
6-9	0.125	3	0	18	0	0	18.574	257.638	18.574	-9.136	-0.565	76.084	558.479

<b>6-10</b>	0.160	4	0	17	0	0	36.317	225.745	36.317	-9.226	-0.762	80.179	573.738
<b>6-11</b>	0.160	4	0	17	0	0	36.317	225.745	36.317	-9.236	-0.880	81.431	568.571
<b>6-12</b>	0.125	3	0	18	0	0	18.574	255.153	18.574	-9.097	-0.405	80.085	561.944
<b>6-13</b>	0.125	3	0	18	0	0	18.574	255.153	18.574	-9.085	-0.452	78.535	569.792
<b>6-14</b>	0.125	3	0	18	0	0	18.574	255.153	18.574	-9.072	-0.470	78.637	564.922
<b>6-15</b>	0.185	5	0	19	0	0	23.582	295.961	23.582	-9.060	-0.464	92.075	618.908
<b>6-16</b>	0.120	5	2	17	0	0	18.574	224.645	45.708	-9.162	-0.540	69.298	559.322
<b>6-17</b>	0.154	5	1	18	0	0	21.078	260.303	34.645	-8.774	-0.464	91.178	594.788
<b>6-18</b>	0.154	5	1	18	0	0	21.078	260.303	34.645	-8.768	-0.481	90.738	594.942
<b>6-19</b>	0.120	5	2	17	0	0	18.574	224.645	45.708	-8.878	-0.499	72.191	555.047
<b>6-20</b>	0.185	5	0	19	0	0	23.582	295.961	23.582	-9.067	-0.537	102.563	615.932
<b>7-1</b>	0.130	3	1	16	0	5.683	18.574	232.518	24.257	-8.605	-0.672	90.017	536.184
<b>7-2</b>	0.160	4	1	17	0	5.683	21.078	260.826	26.761	-8.600	-0.705	98.590	575.522
<b>7-3</b>	0.160	4	1	17	0	5.683	21.078	260.826	26.761	-8.475	-0.657	99.303	582.774
<b>7-4</b>	0.125	3	1	17	0	5.683	18.574	250.811	24.257	-8.694	-0.766	88.550	560.501
<b>7-5</b>	0.125	3	1	17	0	5.683	18.574	250.811	24.257	-8.658	-0.784	89.826	560.481
<b>7-6</b>	0.160	4	1	16	0	5.683	36.317	218.918	42.000	-8.842	-0.934	94.042	570.563
<b>7-7</b>	0.125	3	1	17	0	5.683	18.574	248.327	24.257	-8.578	-0.665	92.218	564.546
<b>7-8</b>	0.125	4	2	16	0	5.683	18.574	225.168	37.824	-8.629	-0.728	86.965	546.324
<b>11-1</b>	0.227	4	1	16	0	0	18.574	243.386	32.141	-9.157	-0.487	76.527	552.903
<b>11-2</b>	0.250	5	1	17	0	0	21.078	271.694	34.645	-9.027	-0.404	85.170	597.879
<b>11-3</b>	0.250	5	1	17	0	0	21.078	271.694	34.645	-8.774	-0.435	86.090	592.830
<b>11-4</b>	0.269	6	1	18	0	0	23.582	300.003	37.149	-8.965	-0.471	102.837	636.314
<b>11-5</b>	0.269	6	1	18	0	0	23.582	300.003	37.149	-8.986	-0.359	93.660	635.083
<b>12-1</b>	0.130	3	0	16	0	0	18.574	236.036	18.574	-9.199	-0.572	74.239	514.202
<b>12-2</b>	0.160	4	0	17	0	0	21.078	264.344	21.078	-9.203	-0.589	82.205	557.471

<b>12-3</b>	0.160	4	0	17	0	0	21.078	264.344	21.078	-9.077	-0.525	83.581	558.204
<b>12-4</b>	0.185	5	0	18	0	0	23.582	292.653	23.582	-9.204	-0.645	99.900	598.231
<b>12-5</b>	0.185	5	0	18	0	0	23.582	292.653	23.582	-9.194	-0.575	89.298	604.959

<b>Compound</b>	<b>Volume</b>	<b>VSA</b>	<b>ASA_H</b>
<b>1-1</b>	271.000	300.250	410.324
<b>1-2</b>	296.125	331.443	426.051
<b>1-3</b>	296.250	331.436	418.850
<b>1-4</b>	294.875	329.687	416.794
<b>1-5</b>	277.625	308.870	383.835
<b>1-6</b>	275.750	310.152	378.897
<b>1-7</b>	275.250	309.406	374.806
<b>1-8</b>	285.000	317.935	442.295
<b>1-9</b>	285.875	317.861	445.489
<b>1-10</b>	286.125	319.642	443.610
<b>1-11</b>	286.125	323.326	440.250
<b>1-12</b>	289.500	324.148	449.328
<b>1-13</b>	288.625	323.951	451.490
<b>1-14</b>	288.625	324.684	369.621
<b>1-15</b>	289.625	324.545	367.436
<b>1-16</b>	271.625	306.586	425.391
<b>1-17</b>	272.500	308.217	423.189
<b>1-18</b>	272.625	307.117	421.653
<b>1-19</b>	294.750	335.006	360.877
<b>1-20</b>	302.000	342.674	387.423
<b>1-21</b>	302.000	342.211	387.913

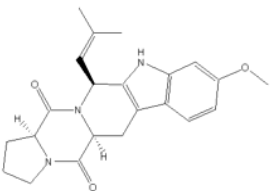
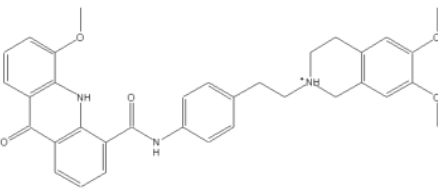
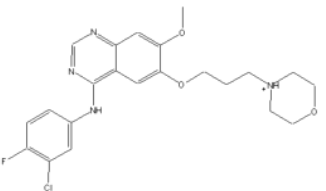
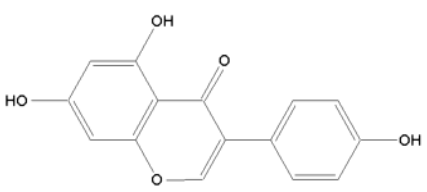
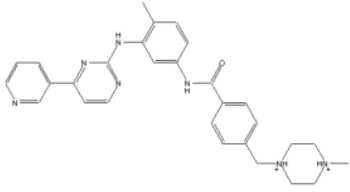
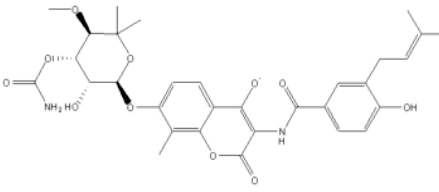
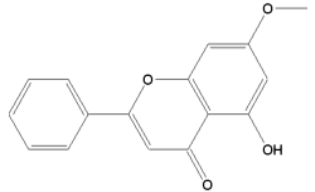
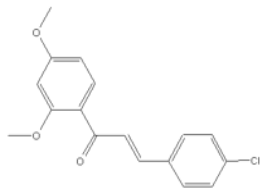
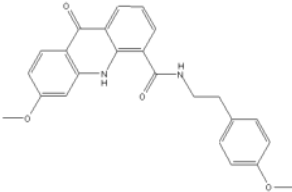
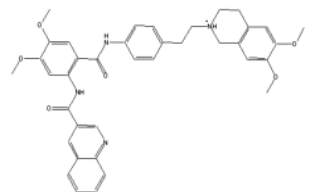
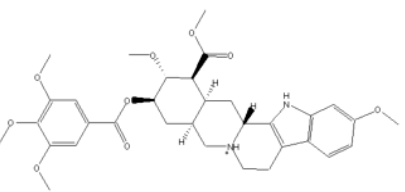
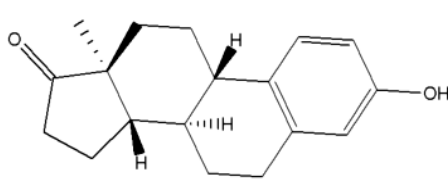
<b>1-22</b>	283.000	317.498	355.967
<b>1-23</b>	281.875	320.005	346.675
<b>1-24</b>	281.875	317.051	352.915
<b>1-25</b>	321.375	360.864	435.944
<b>1-26</b>	321.625	361.708	424.767
<b>1-27</b>	275.750	307.944	428.208
<b>1-28</b>	274.375	308.063	426.142
<b>2-1</b>	295.750	332.916	436.736
<b>2-2</b>	310.500	350.342	460.532
<b>2-3</b>	310.000	349.042	462.281
<b>2-4</b>	312.375	349.259	463.698
<b>2-5</b>	323.125	362.587	449.066
<b>2-6</b>	323.375	362.650	438.699
<b>2-7</b>	322.500	363.766	442.674
<b>2-8</b>	314.875	354.177	388.698
<b>2-9</b>	303.125	342.158	404.122
<b>2-10</b>	314.625	351.653	465.628
<b>2-11</b>	310.000	349.663	443.482
<b>6-1</b>	279.125	309.688	423.997
<b>6-2</b>	305.250	339.544	430.880
<b>6-3</b>	304.875	339.541	432.294
<b>6-4</b>	305.625	339.874	431.573
<b>6-5</b>	287.000	320.235	382.590
<b>6-6</b>	285.875	317.957	386.263
<b>6-7</b>	293.625	329.170	443.072
<b>6-8</b>	295.500	328.161	451.523

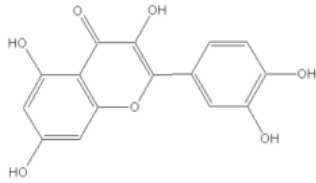
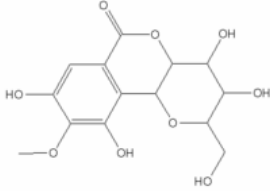
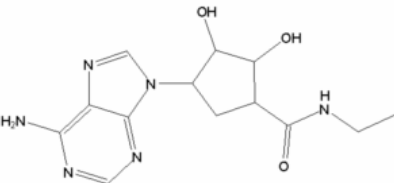
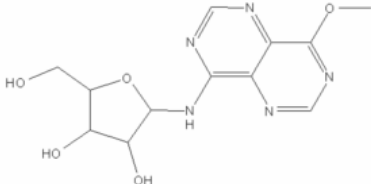
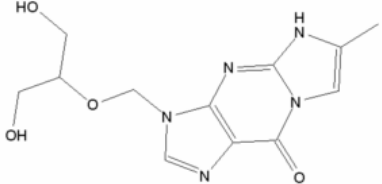
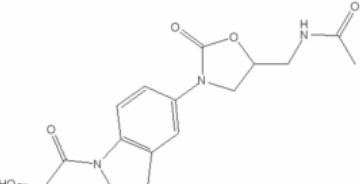
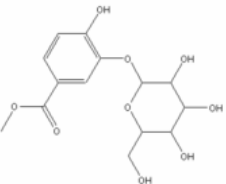
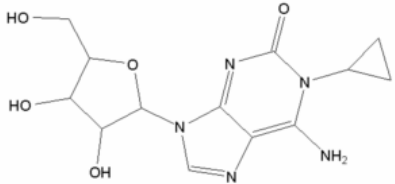
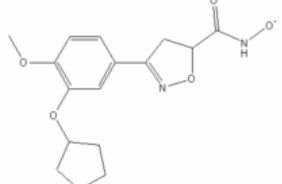
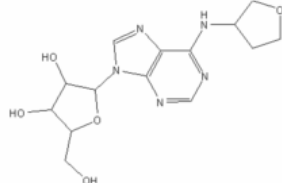
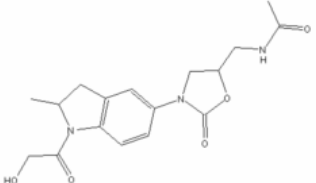
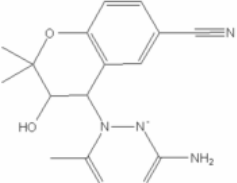
<b>6-9</b>	293.875	327.310	444.991
<b>6-10</b>	297.375	333.237	379.556
<b>6-11</b>	299.125	330.494	373.794
<b>6-12</b>	297.875	330.311	450.419
<b>6-13</b>	297.000	331.706	455.187
<b>6-14</b>	296.250	329.037	451.857
<b>6-15</b>	332.125	370.140	431.832
<b>6-16</b>	290.750	327.627	350.088
<b>6-17</b>	311.125	349.969	399.784
<b>6-18</b>	311.375	348.962	400.239
<b>6-19</b>	292.500	322.918	356.135
<b>6-20</b>	331.250	370.101	440.393
<b>7-1</b>	274.625	305.934	408.015
<b>7-2</b>	299.750	336.293	410.880
<b>7-3</b>	302.375	337.062	415.353
<b>7-4</b>	288.250	324.579	433.903
<b>7-5</b>	290.750	325.635	433.998
<b>7-6</b>	292.750	326.527	364.683
<b>7-7</b>	292.750	328.578	437.456
<b>7-8</b>	281.750	316.686	372.193
<b>11-1</b>	280.125	316.918	412.284
<b>11-2</b>	305.250	345.585	418.763
<b>11-3</b>	307.125	347.100	416.514
<b>11-4</b>	331.250	376.032	432.681
<b>11-5</b>	331.500	375.035	420.697
<b>12-1</b>	268.625	299.500	405.623

<b>12-2</b>	296.875	326.901	409.848
<b>12-3</b>	294.750	329.431	410.424
<b>12-4</b>	322.000	357.174	427.266
<b>12-5</b>	319.875	357.175	418.963

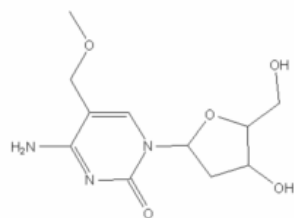


**Appendix 4-4:** Structures of 27 compounds in the external database.

<p>1</p>  <p>Name: Fumitremorgin C</p>	<p>2</p>  <p>Name: Elacridar</p>	<p>3</p>  <p>Name: Gefitinib</p>
<p>4</p>  <p>Name: Genistein</p>	<p>5</p>  <p>Name: Imatinib</p>	<p>6</p>  <p>Name: Novobiocin</p>
<p>7</p>  <p>Name: Tectochrysin</p>	<p>8</p>  <p>Name: 2,4-methoxylated chalcone</p>	<p>9</p>  <p>Name: Methoxylated acridones</p>
<p>10</p>  <p>Name: Tariquidar</p>	<p>11</p>  <p>Name: Reserpine</p>	<p>12</p>  <p>Name: Estrone</p>

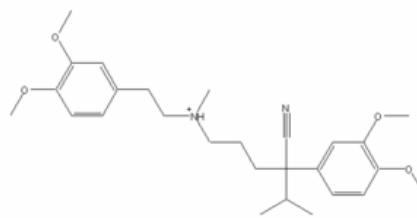
<p>13</p>  <p>Name: Quercetin</p>	<p>14</p>  <p>Name: Unknown_1</p>	<p>15</p>  <p>Name: Unknown_2</p>
<p>16</p>  <p>Name: Unknown_3</p>	<p>17</p>  <p>Name: Unknown_4</p>	<p>18</p>  <p>Name: Unknown_5</p>
<p>19</p>  <p>Name: Unknown_6</p>	<p>20</p>  <p>Name: Unknown_7</p>	<p>21</p>  <p>Name: Unknown_8</p>
<p>22</p>  <p>Name: Unknown_9</p>	<p>23</p>  <p>Name: Unknown_10</p>	<p>24</p>  <p>Name: Unknown_11</p>

25



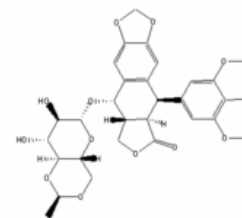
Name: Unknown\_12

26



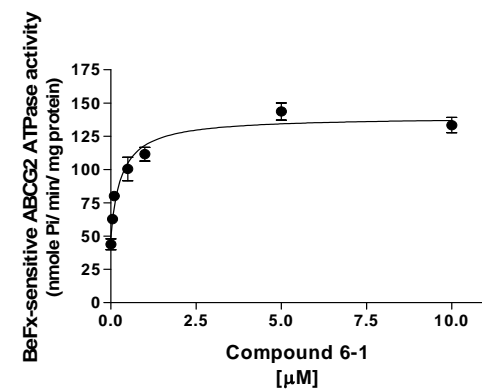
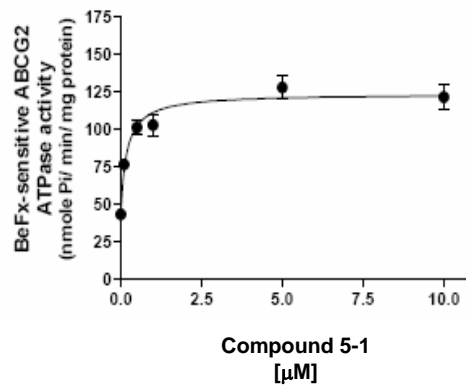
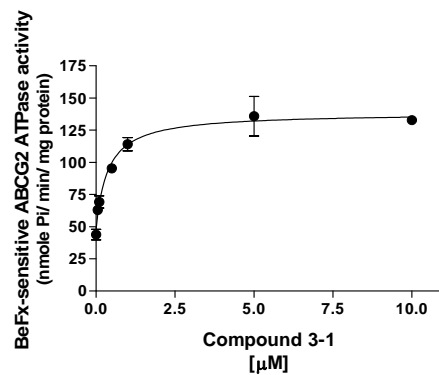
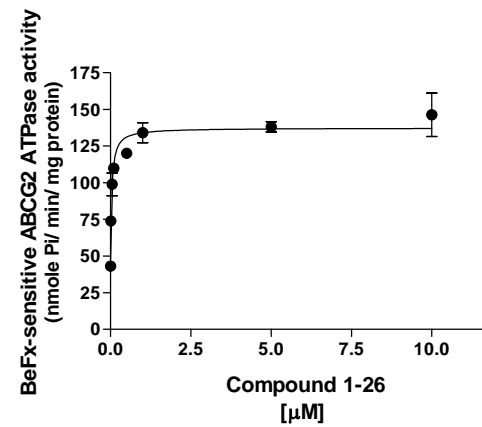
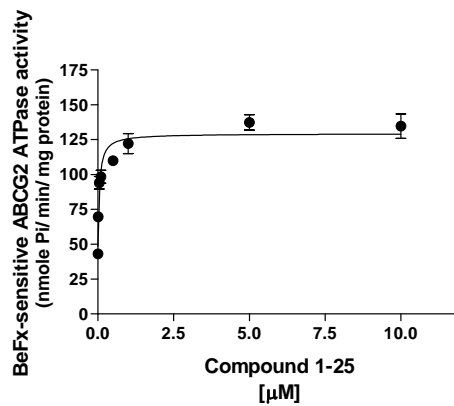
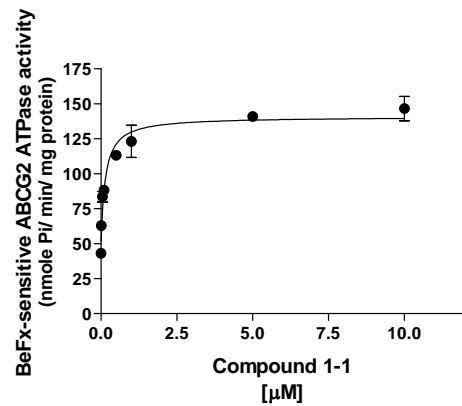
Name: Verapamil

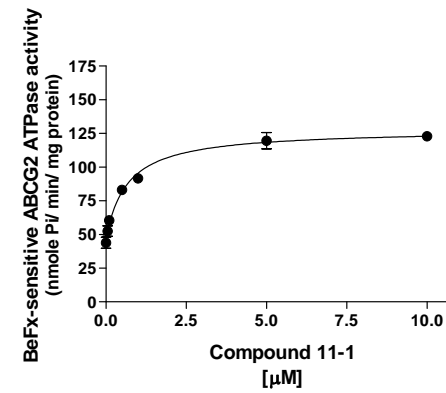
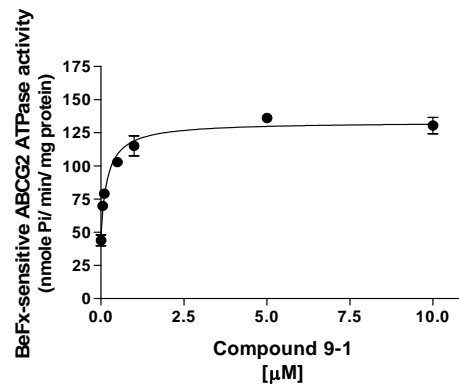
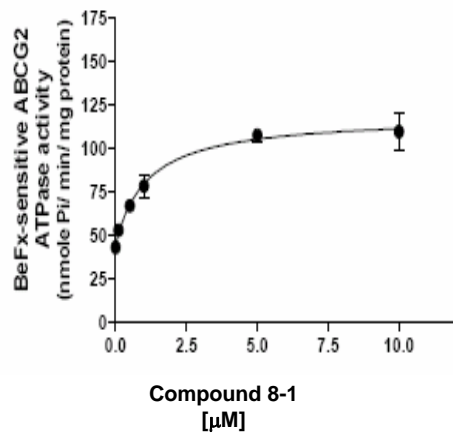
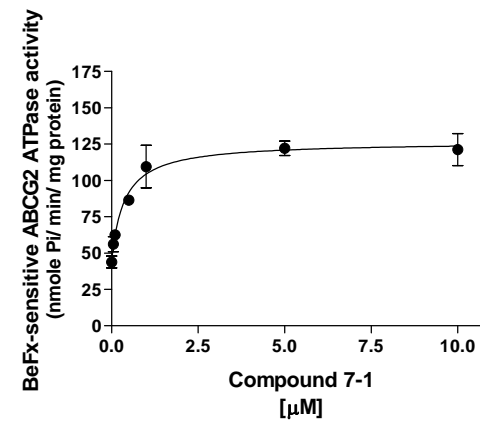
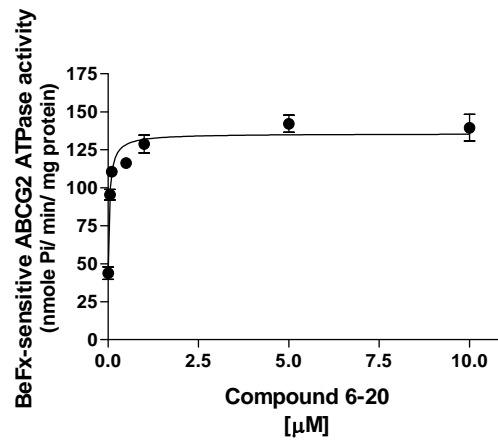
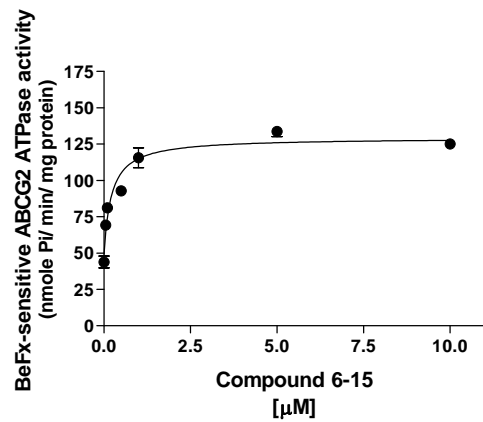
27

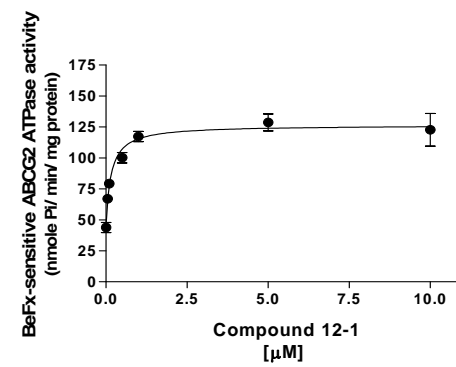
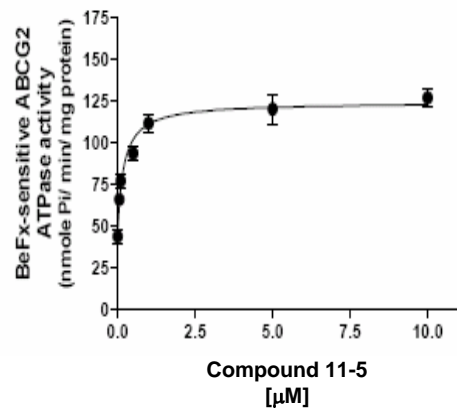
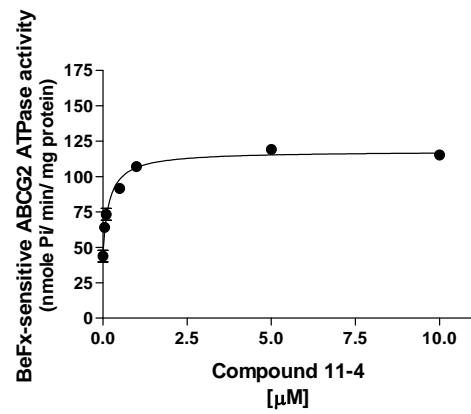


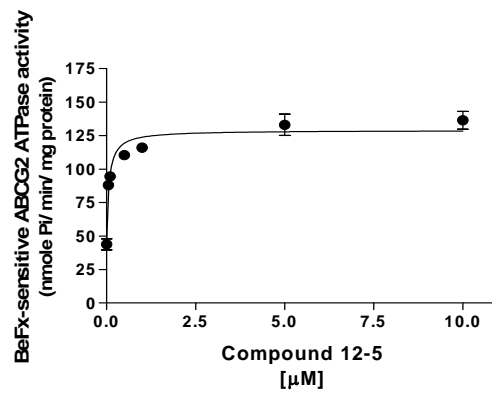
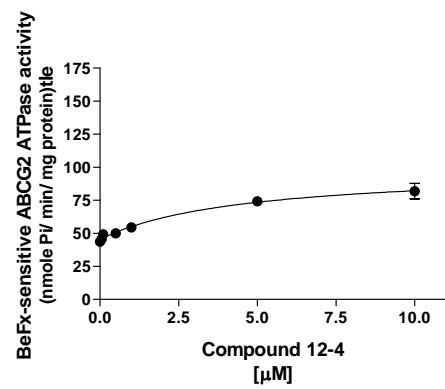
Name: Etoposide

**Appendix 5-1:** Effects of selected test compounds on beryllium fluoride-sensitive ATPase activity in High Five insect cell crude membranes









**Appendix 5-2:** Photoaffinity labelling of ABCG2 with [<sup>125</sup>I]-IAAP in the absence (C, control) or presence of test compounds evaluated at 5 μM in crude membranes of MCF-7 FLV1000 cells

---

Compound	% [ <sup>125</sup> I]-IAAP
Control	100
<b>1-1</b>	32.6
<b>1-25</b>	3.70
<b>1-26</b>	26.2
<b>3-1</b>	15.6
<b>5-1</b>	88.1
<b>6-1</b>	39.9
<b>6-15</b>	25.3
<b>6-20</b>	27.2
<b>7-1</b>	16.2
<b>8-1</b>	49.6
<b>9-1</b>	42.4
<b>11-1</b>	1.09
<b>11-4</b>	0.360
<b>11-5</b>	0
<b>12-1</b>	166
<b>12-4</b>	28.3
<b>12-5</b>	139